Identification of host genes involved in the biotrophic interaction between grapevine and powdery mildew

by

Matthew Allan Hayes
B. Biological Science (Hons.), LaTrobe University

A thesis submitted for the degree of Doctor of Philosophy

at

The University of Adelaide,
School of Agriculture and Wine,
Discipline of Horticulture, Viticulture and Oenology

in collaboration with

CSIRO Plant Industry,
Horticulture Unit

Urrbrae, Adelaide,
January, 2006

Table of contents

Abstract ..... *VI*

Declaration ..... *IX*

Acknowledgements ..... *X*

Abbreviations ..... *XII*

Chapter 1 – General introduction *1*

1.1 Infection process of powdery mildew fungi **3**

1.2 Haustorium structure and function **5**

1.3 Host responses: compatibility and defence **10**

1.4 Host responses: amino acids and carbohydrates **13**

1.5 Carbohydrate distribution in plants **16**

1.6 Pathogen associated changes to host invertase activity **18**

1.7 Induction of sink metabolism in response to pathogens and wounding **18**

1.8 Role of plant growth regulators in biotrophic interactions **20**

1.9 Other signals in biotrophic interactions **23**

1.10 Identification of host susceptibility genes **24**

1.11 Aims of this study **26**

Chapter 2 – General Materials and Methods *28*

2.1 Materials **28**

2.1.1 Solutions, chemicals and growth media 28

2.1.2 Oligodeoxyribonucleotide primers 29

2.1.3 Bacterial and yeast strains 31

2.1.4 Grapevine tissue 32

2.1.5 *Erysiphe necator* culture and maintenance 32

2.1.6 *Plasmopara viticola* culture and maintenance 33

2.2 Methods **33**

2.2.1 Polymerase chain reaction (PCR) 34

2.2.2 Agarose gel electrophoresis 34

2.2.3 Purification of DNA from agarose gel slices 35

2.2.4 Dephosphorylation of DNA 5’ termini 35

2.2.5 Purification of DNA samples following enzymatic reactions 35

2.2.6 DNA ligation 35

2.2.7 Preparation of electro-competent E. coli cells 36

2.2.8 Transformation of bacteria with recombinant plasmids 36

2.2.9 Preparation of plasmid DNA 37

2.2.10 Preparation of bacterial glycerol stocks 37

2.2.11 Preparation of DNA samples for sequencing 38

2.2.12 Preparation of total grape RNA 38

2.2.13 First-strand cDNA synthesis 39

2.2.14 Sequence analysis and manipulation 39

Chapter 3 – Isolation and identification of genes differentially expressed in powdery mildew infected grapevine tissues.....35

3.1 Introduction 35

3.2 Materials and methods..... 36
3.2.1 Microarray analysis of powdery mildew infected berry skin..... 36
3.2.2 Degenerate PCR, analysis and cloning 38
3.2.3 RT-PCR analysis of selected genes in powdery mildew infected grapevine leaves 39

3.3 Results 40
3.3.1 Microarray analysis of powdery mildew infected grape berry skin..... 40
3.3.2 Isolation of partial length grape hexose transporter clones from powdery mildew infected leaves..... 43
3.3.3 Isolation of a partial length grape cell wall invertase clone from powdery mildew infected leaves..... 45
3.3.4 Isolation of partial length grape amino acid permease and proline transporter clones from powdery mildew infected leaves 47
3.3.5 Semi-quantitative RT-PCR analysis of selected genes in powdery mildew infected leaves 50

3.4 Discussion..... 52
3.4.1 Microarray analysis of powdery mildew infected berry skins 53
3.4.2 Isolation of HT, cwINV, AAP and ProT transcripts by degenerate PCR 56
3.4.3 Semi-quantitative RT-PCR analysis of selected genes in powdery mildew infected leaves 58

Chapter 4 - Isolation and functional characterisation of full length hexose transporter and cell wall invertase genes from grapevine 61

4.1 Introduction 61

4.2 Materials and methods..... 62
4.2.1 RACE PCR and amplification of full length cDNAs..... 62
4.2.2 Preparation of DNA constructs for functional characterisation of HTs in yeast..... 64
4.2.3 Lithium acetate yeast transformation..... 64
4.2.4 Functional characterisation of HTs in yeast..... 65
4.2.5 Analysis of GFP-fusion proteins by micro-projectile bombardment 66
4.2.6 Sequence analysis and manipulation..... 67

4.3 Results 68
4.3.1 Analysis of full length VvHT sequences..... 68
4.3.2 Functional characterisation of VvHT1, VvHT3, VvHT4 and VvHT5 in yeast..... 74
4.3.3 Subcellular localization of VvHT3 and VvHT4 proteins..... 78
4.3.4 Analysis of full length *VvcwINV*..... 80

4.4 Discussion..... 84
4.4.1 Isolation of full length *VvHT* cDNAs and functional characterisation..... 84
4.4.2 Isolation of a full length *VvcwINV* cDNA and bioinformatic analysis..... 88

Chapter 5 - Quantitative RT-PCR analysis of sugar transporters and invertases in pathogen infected and wounded grapevine tissues.....90

5.1 Introduction 90

5.2 Materials and methods..... 92
5.2.1 *E. necator* (powdery mildew) inoculation..... 92
5.2.2 Powdery mildew infected and uninfected leaf regions 93
5.2.3 *Plasmopara viticola* (downy mildew) inoculation..... 93
5.2.4 Wounding of leaves 93
5.2.5 RNA extraction, DNase treatment and cDNA synthesis..... 94
5.2.6 Quantitative real-time PCR analysis 94
5.2.7 Measurement of invertase enzyme activity..... 95

5.3 Results **96**
5.3.1 Quantitative RT-PCR analysis of hexose and sucrose transporter expression in powdery mildew infected grapevine tissues 97
5.3.2 Quantitative RT-PCR analysis of invertase expression in powdery mildew infected grapevine tissues 100
5.3.3 Effect of powdery mildew infection on grape leaf acid invertase activity 102
5.3.4 Localisation of VvHT and invertase expression relative to powdery mildew infection sites 103
5.3.5 Changes in expression of VvHTs, SUCTs and invertases in downy mildew infected grape leaves detected by quantitative RT-PCR 104
5.3.6 Effect of wounding on VvHT and invertase expression in grape leaves 106

5.4 Discussion **108**
5.4.1 Powdery mildew infection 109
5.4.2 Specificity of powdery mildew induced transcriptional changes 112
5.4.3 Differential regulation of gene expression in response to powdery and downy mildew infection 114

Chapter 6 – Expression analysis of VvHTs and VvcwINV in grapevine carbohydrate sink tissues *117*

6.1 Introduction **117**

6.2 Materials and methods **118**
6.2.1 Grape berry ripening series 118
6.2.2 Grapevine roots 119
6.2.3 Quantitative RT-PCR analysis 119

6.3 Results **120**
6.3.1 Expression of VvHTs and *VvcwINV* in grape roots 120
6.3.2 Expression of VvHTs and *VvcwINV* during berry ripening 120

6.4 Discussion **123**
6.4.1 Expression of VvHTs and *VvcwINV* in grapevine carbohydrate sink tissues during normal growth and development 123
6.4.2 Role of *VvHT*s and *VvcwINV* in grape berry development 125

Chapter 7 - Hormonal regulation and analysis of promoters of VvHT and invertase genes *130*

7.1 Introduction **130**

7.2 Materials and Methods **131**
7.2.1 Exogenous application of ABA, ethylene and methyl jasmonate 131
7.2.2 Isolation of BAC DNA and direct sequencing 132
7.2.3 Promoter analysis 133
7.2.4 Quantitative RT-PCR analysis of ABA biosynthetic genes 133
7.2.5 Measurement of bulk leaf ABA concentration 134

7.3 Results **134**
7.3.1 Expression of VvHTs and invertases in grapevine leaves exogenously supplied with ethylene and methyl jasmonate 134
7.3.2 Expression of VvHTs and invertases in grapevine leaves exogenously supplied with ABA 135
7.3.3 Promoter analysis 137
7.3.4 Induction of ABA biosynthetic genes in mildew infected and wounded grapevine leaves 140
7.3.5 ABA concentration in powdery mildew infected grapevine leaves 143

7.4 Discussion **145**

Chapter 8 – Summary and concluding remarks *151*

Reference list 156

Appendix 1- sequences isolated during this project 173
Appendix 2- Expression of control genes 180
Appendix 3- List of cDNAs on grape berry Microarray.....184

Abstract

Grapevine powdery mildew is caused by *Erysiphe necator*, an Ascomycete fungus and an obligate biotroph restricted to growth on its grapevine host. Biotrophic pathogens form a stable association with host cells without directly causing cell death, and take up nutrients from, in the case of powdery mildew (PM), host epidermal cells (Rumbolz et al., 2000). As the fungus grows, its increasing biomass becomes a strong nutrient sink capable of altering assimilate flow and storage in the host.

To identify host genes that may mediate nutrient delivery to powdery mildew infected tissues and therefore may contribute to disease susceptibility, a candidate gene approach using degenerate and RT-PCR, and a non-targeted approach using microarray analysis was instigated. Once identified, "susceptibility genes" could be targeted for manipulation to provide alternative resistance strategies based on reduced susceptibility in the future. In addition to genes encoding pathogenesis and stress related proteins, microarray analysis revealed that transcript levels of a putative metal transporter and a cell wall structural protein were elevated in infected berry skin, while aquaporin water channels and genes associated with photosynthesis were generally repressed. Degenerate PCR was used to isolated new cell wall invertase, monosaccharide and amino acid transporter genes and initial RT-PCR revealed that expression of genes involved in sugar mobilisation were the most significantly modulated by powdery mildew infection.

Previously unreported hexose transporters (HTs), (*VvHT3*, *VvHT4* and *VvHT5*) and a cwINV (*VvcwINV*) had been isolated from cDNA prepared from powdery mildew infected grapevine leaves. Full length clones of grapevine HTs and cwINV were obtained by RACE PCR. Heterologous expression of the three new

HTs in yeast confirmed that VvHT4 and VvHT5 mediated glucose uptake, while VvHT3 did not function in the yeast system. However, transient expression of a translational fusion of the VvHT3 protein with green florescence protein in onion epidermal cells indicated that it is targeted to the plasma membrane of plant cells.

Quantitative RT- PCR analysis of these new genes, together with previously reported grapevine HTs and cytoplasmic and vacuolar invertases, indicated that expression of *VvcwINV* and *VvHT5*, were significantly up-regulated by PM infection, while a vacuolar invertase was strongly down-regulated by PM infection. Invertase activity assays were in agreement with these findings, showing elevated sucrolytic activity in insoluble fractions and reduced sucrolytic activity in soluble fractions. These results suggest that apoplasmic phloem unloading of sucrose in the infected leaf is elevated and that *VvHT5* is induced to recover the additional hexoses from the apoplasm. Basic localisation studies indicated that *VvHT5* and *VvcwINV* are not induced specifically in powdery mildew infected leaf regions, but are induced in a more diffuse distribution within infected leaves.

To determine if induction of *VvHT5* and *VvcwINV* is specific to PM infection or if other stimuli may also mediate these responses, leaves were inoculated with downy mildew or stressed by wounding. Transcript levels of *VvHT5* and *VvcwINV* were elevated by wounding and downy mildew infection, suggesting that the induction of these genes may be part of a general stress response.

To explore the signalling pathways that may underlie these responses, leaves were treated with the plant growth regulators ethylene, jasmonate and abscisic acid. Exogenous application of ethylene and methyl jasmonate only marginally affected the expression of the genes studied, however foliar application of abscisic acid (ABA) induced gene expression changes similar to those observed in response to powdery mildew infection and wounding. Promoter sequences of *VvHT3*, *VvHT4*,

VvHT5 and *VvcwINV* were isolated and analysed for the presence of regulatory elements. Compared with the promoters of VvHTs that were not induced by pathogen infection or wounding, the *VvHT5* and *VvcwINV* promoters contained numerous motifs associated with induction by ABA including ABRE, Myc and Myb binding elements.

The path of sugar loading into the mesocarp of grape berries during ripening is still poorly understood and few molecular components associated with this process have been described. Quantitative RT-PCR was used to monitor the expression of five HTs and *VvcwINV* during Cabernet sauvignon and Shiraz berry development and ripening. Of the three new HTs reported here, the expression of *VvHT3* is most consistent with a potential role in sugar loading, while *VvHT5* is induced late in this process. *VvcwINV* transcript levels were high pre-ripening and also during the later stages of ripening, therefore based on this expression pattern, a role for this enzyme during ripening is not clearly evident. These results are discussed in terms of an apoplasmic step in phloem unloading in ripening grape berries.

This study has provided new insights into the molecular and biochemical processes associated with the formation of carbohydrate sink metabolism in response to stress stimuli, and sugar delivery to grape berries during ripening. ABA-dependant pathways may mediate the stress-associated induction of *VvcwINV* and *VvHT5*, presumably to recruit additional carbohydrates to the affected organ to energise repair and defence responses. At this stage it is unknown if this response is beneficial to pathogen nutrition, however potentially, modification of genes associated with carbohydrate sink metabolism could provide an alternative way to engineer resistance to this pathogen.

Declaration

This work contains no material that has been accepted for the award of any other degree or diploma in any university or other tertiary institution and to the best of my knowledge and belief, contains no material previously published or written by another person, except where due reference has been made in the text.

I give consent to this copy of my thesis, when deposited in the University Library, being available for loan and photocopying.

Matthew Hayes

January 2006

Acknowledgements

I would first like to acknowledge the late Robyn Van Heeswijck who convinced me through her enthusiasm, intelligence and warmth to move to Adelaide and commence study under her guidance. Unfortunately, after a short period of time, Robyn needed to focus on her health and was unable to continue as my supervisor, however, in the generous and composed fashion that was typical of all interaction I had with Robyn, she identified potential supervisors and continued to take an interest in my studies until her passing. Thank you Robyn, I will always be grateful for the brief time our paths crossed and wish you peace and happiness.

Due to Robyn's' advice, I was amazingly fortunate to meet Ian Dry who quickly accepted the responsibility to become my supervisor and provided me with a stimulating project. I cannot thank Ian enough for the enthusiasm, dedication and unbounded support that he has given to me during the last 3.5 years. He has been the best supervisor imaginable and has become a friend for whom I care and respect deeply. I also thank my co-supervisor, Steve Tyerman, for always taking time to discuss my work and providing physiological insights that are sometimes lacking in gene-jockey's like me.

Thanks to Claire Barker, Karina Swan and Dale Godfrey, who compose the Fungal pathology group at CSIRO in Adelaide. Claire allowed me access to and provided pertinent advice regarding working with the genomic BAC library. Karina managed to keep the powdery mildew inoculum available whenever needed and organised almost everything around the lab that myself and other staff were too busy (read lazy) to do. Many thanks to Dale who taught me how to wrestle RNA out of grapevine tissue, along with other techniques, and with whom I collaborated to perform the GFP studies and hormonal treatments. More broadly, I would like to

thank all the staff at CSIRO Plant Industry in Adelaide for being very generous with their time and resources. Specifically I would like to mention Chris Davies who donated Cabernet Sauvignon berry cDNA samples and always found time for a chat or to read drafts. Also, thanks to the administrative staff for all their efforts, especially Julie Powell who did everything in her powder to ensure I had the components necessary for my work.

I am grateful to the University of Adelaide for awarding me an Australian Post Graduate Award and the Cooperative Research Centre for Viticulture (CRCV) for providing a top-up scholarship and a generous operating budget. Peter Mansfield from the CRCV was particularly generous with his time.

I thank my family, particularly Mum and Dad, for always supporting my decisions and providing love and the financial means that have allowed me to become who I am today. Thanks to friends around Adelaide and back in Melbourne, for happy distractions and life beyond the laboratory.

Finally I want to thank my wonderful partner Rebecca Burtt who has suffered life as a PhD widow, particularly during the last 6 months, and who has shown boundless love, support and understanding during our 5 years together. I could not have done this without Rebecca and am humbled by her devotion to me.

Abbreviations

ATP	adenosine triphosphate
ATPase	adenosine triphosphatase
BLAST	basic local alignment search tool
bp	base pairs
cDNA	complementary DNA
cwINV	cell wall invertase
DNA	deoxyribonucleic acid
dNTP	deoxynucleotide triphosphate
DPI	days post-inoculation
dsDNA	double-stranded DNA
EDTA	ethylenediamine-*tetra*-acetic acid
ER	endoplasmic reticulum
EST	expressed sequence tag
FD	Faraday(s)
FW	fresh weight
g	gram(s)
g	relative centrifugal force
GFP	green fluorescent protein
h	hour(s)
HT	Hexose (monosaccharide) transporter
IPTG	*Iso*-propyl-β-D-thiogalactopyranoside
kb	kilobase pairs
L	litre(s)

LB	Luria broth
M	molar
min	minute(s)
MOPS	3-N-Morpholinopropanesulfonic acid
mRNA	messenger RNA
MPa	Mega Pascals
nINV	neutral (cytoplasmic) invertase
nt	nucleotide(s)
ORF	open reading frame
PCR	polymerase chain reaction
PM	powdery mildew
RACE	rapid amplification of cDNA ends
RNA	ribonucleic acid
rpm	revolutions per minute
RT-PCR	reverse transcription-PCR
s	second(s)
Ssynth	Sucrose synthase
SUCT	sucrose transporter
SDS	sodium dodecyl sulphate
TBE	tris-borate-EDTA
Tm	temperature of DNA disassociation (melt)
Tris	tris(hydroxymethyl)aminomethane
V	volt(s)
vINV	vacuolar invertase

Page numbers do not correspond with the print copies.

Chapter 1 – General introduction

Powdery mildew is a costly and widespread fungal disease to which all commercially important European cultivars of *Vitis vinifera* are susceptible. The viticultural industry is highly dependant on the use of fungicides to manage powdery mildew. A recent report commissioned by the European Union indicated that while grapevine plantings comprised only 8% of the total crop production area in member states, grapevine cultivation accounted for approximately 70% of the total fungicide volume applied to all crops (Montgomery and Hansen, 2000). Without the use of fungicides, and particularly in mild weather conditions that favour growth of the pathogen, outright crop loss can occur (Savocchia et al., 2004).

The most heavily used fungicides in Australia are sulphur and the sterol demethylation inhibiting fungicides (DMIs). Sulphur has been in use for more than 100 years and continues to be generally effective for powdery mildew control. DMIs were first introduced in the 1970's and initially offered excellent control. However, pathogen resistance to DMIs is now widespread in North America (Erickson and Wilcox, 1997) and powdery mildew strains with reduced sensitivity to DMIs have been isolated from Australian vineyards, indicating the development of resistance to these chemicals in Australia also (Savocchia et al., 2004).

The most commonly observed symptom of powdery mildew disease is powdery white to ash-grey growth on leaf surfaces (Fig. 1.1 A). Leaf infections cause a generalised reduction in vine vigour and are a major source of inoculum for infection of young fruit, which is responsible for most of the economic losses. Uneven maturation and cracking of the fruit results in fruit rot (Ough and Berg, 1979; Fig. 1.1B). Even low levels of fruit infection reduces the quality of the final

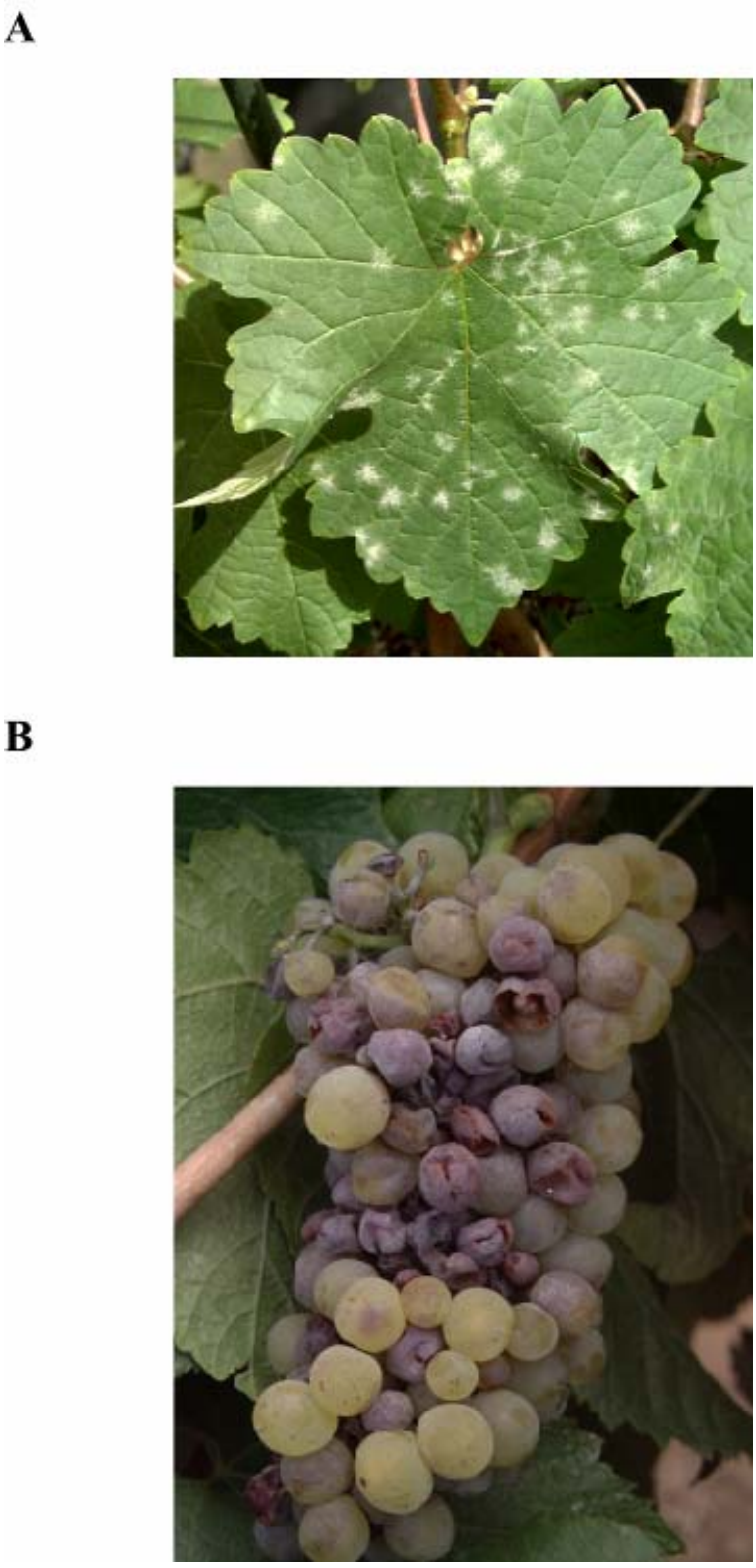

Figure 1.1. Powdery mildew infected grapevine tissues

(A) Powdery mildew colonies on the adaxial surface of an infected *V. vinifera* cv. Cabernet Sauvignon leaf. (B) Mature *V. vinifera* cv. Chardonnay bunch showing damage caused by early season powdery mildew infection

wine product by introducing negative sensory characteristics such as unpalatable flavours and aromas and an unpleasant mouth-feel (Ough and Berg, 1979; Stummer et al., 2005).

The causative agent of grapevine powdery mildew, *Erysiphe necator* (syn. *Uncinula necator*), is an Ascomycete fungus and an obligate biotroph restricted to growth on grapevine. Unlike necrotrophic pathogens such as *Botrytis cinerea* which degrade plant cells and absorb nutrients from dead tissue, biotrophic pathogens associate with host cells without directly causing host cell death and obtain all their nutrients in this manner (Rumbolz et al., 2000). Nutrient transfer from host to fungus is facilitated by the haustorium, a specialised feeding structure that develops only during plant-pathogen interaction and is formed from both fungal and host components (Rumbolz et al., 2000; Hahn and Mendgen, 2001).

1.1 Infection process of powdery mildew fungi

The infection process typical of *E. necator* is illustrated in Figures 1.2 and 1.3. Conidia are dispersed by wind or physical contact between infected and healthy plant parts. A conidium attaches to the surface of a plant tissue where it germinates and extends a primary hyphae (Fig. 1.2. A and B; Fig. 1.3. A). The primary hyphae differentiates into a lobed structure called an appressorium (Fig. 1.2 B; Fig. 1.3 B) which, via the generation of turgor pressure and enzymes that digest the cuticle and cell wall barrier, forces a penetration peg through the surface cuticle and the cell wall of the epidermal cell below. Appressoria of the wheat powdery mildew pathogen *Blumeria graminis* developes tugor pressure between 2.1 to 4.1 MPa, while appressoria of *Magnaporthe grisea* produced turgor pressure that reached eight MPa (Howard *et al*., 1991; Pryce-Jones et al., 1999). Various hydrolytic

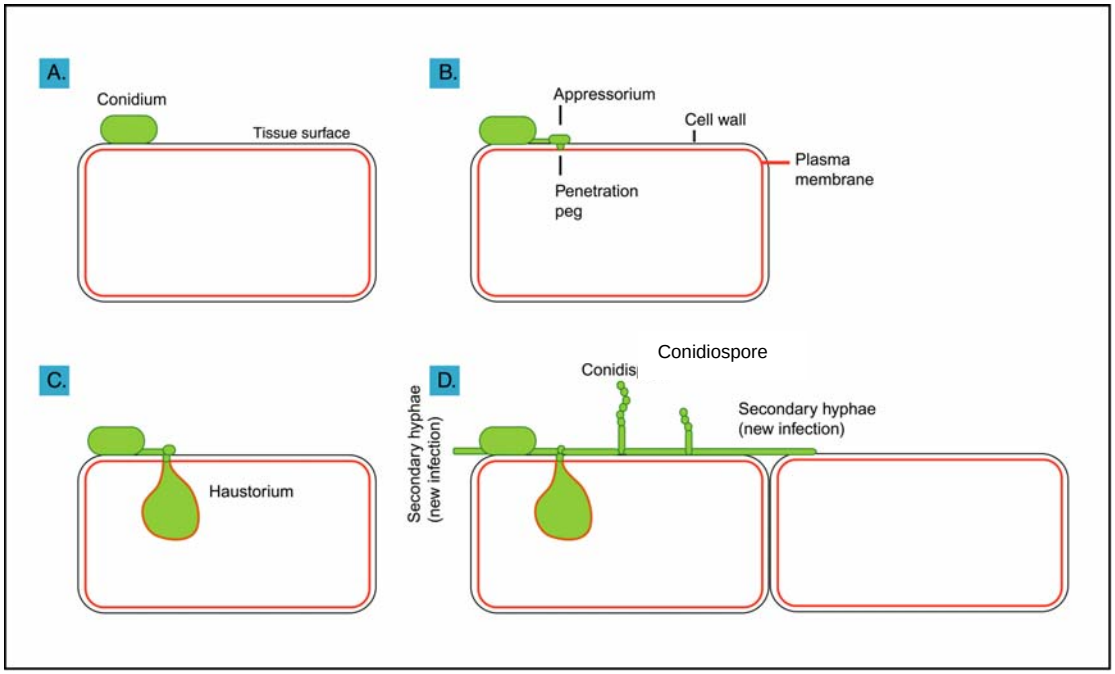

Figure 1.2. Stylised diagram of the grapevine powdery mildew infection process. For details refer to text.

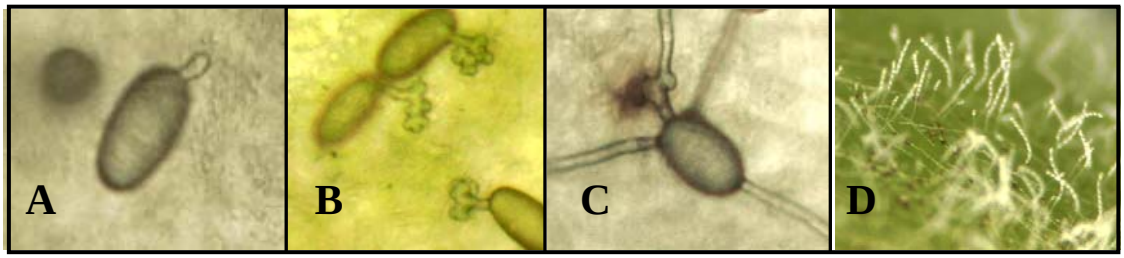

Figure 1.3. Infection structures of *E. necator* growing on *V. vinifera* leaves Cv. Chardonnay. (A): germination and hyphae extension; (B): appressorium formation; (C): secondary hyphae extension; (D): conidiophores on leaf surface. A, B, C: 40x magnification, D: 10x magnification.

enzymes have been detected in association with germinated *B. graminis* condia including esterase, protease and amylase while immunofluorescence microscopy localised cellulose enzymes to appressoria of *Trichoderma reesei* (Fric and Wolf, 1994; Pryce-Jones et al., 1999). After cuticle and cell wall penetration the fungus begins to invade into the cell but does not pierce the plasma membrane of the epidermal cell; instead the plasma membrane invaginates and expands to surround the fungal body (Fig. 1.2. C). At this point the haustorium feeding structure is complete and the fungus draws nutrients from the plant allowing continuation of the infection cycle: extension of secondary hyphae, infection of additional cells and production of conidiophores bearing new conidia (Fig. 1.2 D, Fig. 3. C and D). Germination, appressorium formation, penetration and haustorium formation occur within 24 h after inoculation and conidiophore production is observed within eight to ten days post innoculation.

1.2 Haustorium structure and function

Biotrophic fungi of several genera are pathogens of a diverse range of agriculturally important plant species. The powdery mildews (Ascomycetes), downy mildews (Oomycetes) and the rusts (Basidiomycetes) all form haustoria within host cells to gain nutrition, however the site of infection and method of host invasion differ (Voegele et al., 2001). The powdery mildews infect epidermal cells with mycelial growth on the tissue surface, therefore the haustorium is the only fungal structure inside plant tissue during these infections. The downy mildews and rusts infect mesophyll cells reached initially by penetration through stomata, with infection spreading to other mesophyll cells via intercellular mycelial growth (Green et al., 2002). Haustoria generated by members of these different genera have a range of morphologies from simple to extensively lobed in appearance, however the basic

structure and mechanism of function is presumably quite similar (Harrison, 1999). While there is a paucity of information defining the infection structures of grapevine powdery mildew, much can be inferred from data collected from the study of closely related powdery mildew haustoria of barley (*Blumeria graminis* on *Hordeum vulgare*) and pea (*Erysiphe pisi* on *Pisum sativum*), and rust haustoria (*Uromyces fabae* on *Vicia fabae*).

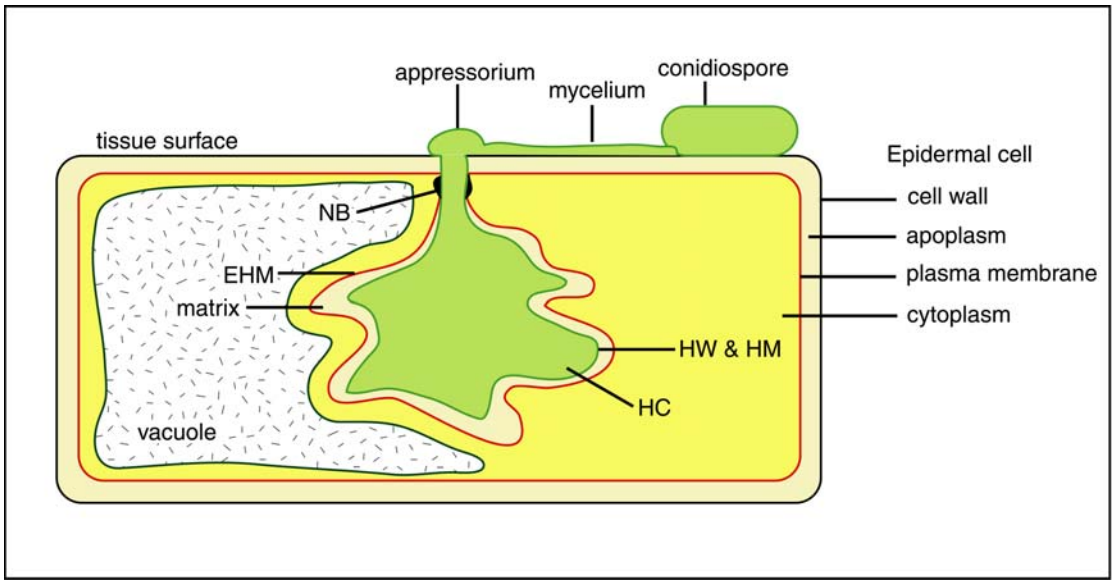

Figure 1.4. General structure of a powdery mildew haustorium. NB: neck bands; EHM: extrahaustorial membrane; HC: haustorial cytoplasm; HW: haustorial wall; HM: haustorial membrane.

A stylized diagram of a powdery mildew haustorium is shown in Figure 1.4. Haustoria are located within the cell, but are not in direct contact with the cytoplasm, because the invaginated and expanded plant plasma membrane surrounds the fungal body and isolates it from the cytoplasm. During fungal invasion, the distribution of host cell organelles becomes altered. Nuclei position shifts from the usual location at the bottom of the cell, adjacent to the mesophyll layer below, and

migrates towards the haustorium, while its volume was observed to be approximately twice that of uninfected cells (Koh et al., 2005). The endoplasmic reticulum is observed to envelop the haustorium in a mesh-like structure, while golgi, mitochondria and peroxisomes aggregate at the developing haustorium, potentially contributing to membrane synthesis and assembly for expansion of the host plasma membrane (Koh et al., 2005; Leckie et al., 1995; Aist and Bushnell, 1991). The invaginated plasma membrane of the host that surrounds the fungal body is called the extra-haustorial membrane (EHM) and it features a range of structural and compositional differences, when compared to the normal plant cell plasma membrane, that may cause altered functional properties that potentially benefit fungal nutrient acquisition (Perfect and Green, 2001). For example, antibodies raised against pea powdery mildew haustoria and pea leaf plasma membranes recognised epitopes unique to the EHM but absent from pea leaf plasma membranes, while others recognised epitopes present on leaf plasma membranes that were absent from EHM (Roberts et al., 1993). Using *Arabidopsis thaliana* lines expressing plasma membrane proteins tagged with green fluorescent protein (GFP), labelling in four lines was restricted to the host cell plasma membrane and neck band regions while completely absent from the EHM (Koh et al., 2005). Furthermore, the EHM of pea and barley powdery mildew haustoria were shown to lack the ATPase activity typical of the plasma membrane surrounding the epidermal cell cytoplasm, indicating that the membrane potential of the EHM is probably depolarised (Manners and Gay, 1982). All these observations are consistent with the hypothesis that the composition and therefore function of the EHM is distinct from the plasma membrane. Reduced ATPase activity suggests the EHM is not actively transporting nutrients but rather may be leaky, allowing deregulated solute flux into the intervening matrix between the EHM and the fungal haustorial

membrane (Fig. 1.4; Manners and Gay, 1982). The matrix is enclosed from the general apoplasm by electron dense neck bands located at the haustorial neck where the fungal and plant cell plasma membranes are fused (Koh et al., 2005). Therefore, solutes that arrive in the matrix from the host cell cytoplasm are confined to this compartment from which the fungus draws nutrients and cannot re-enter the general apoplasm (Harrison, 1999).

The fungal side of the matrix is bounded by the haustorial wall and haustorial membrane that are derived from the fungal wall and plasma membrane respectively and both appear to be differentiated from the membranes and walls associated with other fungal structures. Antibodies raised against isolated pea powdery mildew haustoria and flax rust haustoria reacted with glycoprotein and oligosaccharide epitopes on haustorial membranes and walls that were absent from other fungal structures (Green et al., 1994; Murdoch et al., 1998). Recent molecular studies on the interaction between the rust fungus *Uromyces fabae* and its broad bean host *Vicia fabae* have clearly demonstrated that the haustorial membrane, relative to the plasma membrane of other fungal structures, is uniquely differentiated to facilitate active uptake of hexoses and amino acids from the matrix into the fungal body. Screening of a cDNA library of rust fungus *in planta* induced genes (PIGs) identified putative hexose (*UfHXT1*) and amino acid (PIG2/*AAT2* and PIG27/*AAT1*) transporters and a plasma membrane H^+-ATPase (Hahn and Mendgen, 1997; Voegel et al., 2001). Detailed localisation studies demonstrated that *UfHXT1* and *AAT2* were localised specifically to the haustorial plasma membrane and, relative to other fungal membranes, high ATPase activity is a characteristic of the haustorial membrane (Struck et al., 1996; Hahn et al., 1997; Voegele et al., 2001).

The cytoplasm of the rust haustorial body does not become vacuolated like hyphae from which they differentiate and seems to be the site of biosynthetic

processes important for growth of the pathogen. Continued investigation of other rust haustorial-expressed genes has identified thiamine and mannitol biosynthetic proteins as active and localised specifically within this site but not in other fungal structures (Sohn et al., 2000; Voegele et al., 2005). Thiamine diphosphate is a cofactor of carbon and amino acid biosynthetic enzymes and a satisfactory supply of this cofactor is essential for fungal growth (Sohn et al., 2000). Specific biosynthesis of thiamine in haustoria suggests that it is either not synthesised in other fungal structures, is not available in adequate concentrations from the host or cannot be retrieved due to lack of an appropriate transporter (Sohn et al., 2000). In infected *V. fabae* leaves the concentration of mannitol increases while expression of a fungal mannitol:NADP+ 2-oxidoreductase in haustoria coincides with this accumulation (Voegele et al., 2005). Mannitol is a polyol that is not usually synthesised nor can be utilised by *V. fabae*, suggesting that its biosynthesis may be catalysed by the fungal mannitol dehydrogenase which would convert fructose obtained from the host via the haustorial expressed transporter *UfHXT1* (Voegel et al., 2001). Conversion of fructose to mannitol would potentially provide the pathogen with a carbohydrate store that is inaccessible to this host plant. Secondly, mannitol may protect the fungus from reactive oxygen species produced by the host as part of a defence response, contributing to the stability that is characteristic of biotrophic interactions (Voegele et al., 2005). These observations suggest that in addition to nutrient acquisition, haustoria play a role in biosynthetic processes essential for normal growth of the fungus.

Although only limited information is available regarding the nature and functionality of the EHM, the excellent investigations of Mendgen and co-workers provide a molecular basis for a model of haustorium function which is summarised below in the following text and Figure 1.5. The depolarisation of the EHM may

allow a deregulated flux of solutes from the host cell cytoplasm to the matrix. An electrochemical gradient across the haustorial membrane is established by H^+-ATPase activity, providing energy for active uptake of hexoses and amino acids by specific transporters localised on this membrane. Sealing of the matrix from the plant apoplasm at the haustorial neck means that solutes will not remix with apoplasmic fluids and that the electrochemical gradient across the haustorial membrane can be maintained. In the haustorial body, a mannitol dehydrogenase converts fructose into mannitol providing a carbon source that may not be utilised by the host and additionally is a factor that suppresses the host defence response. The biosynthesis of thiamine also occurs in the haustorial body, possibly because adequate amounts cannot be retrieved from the host.

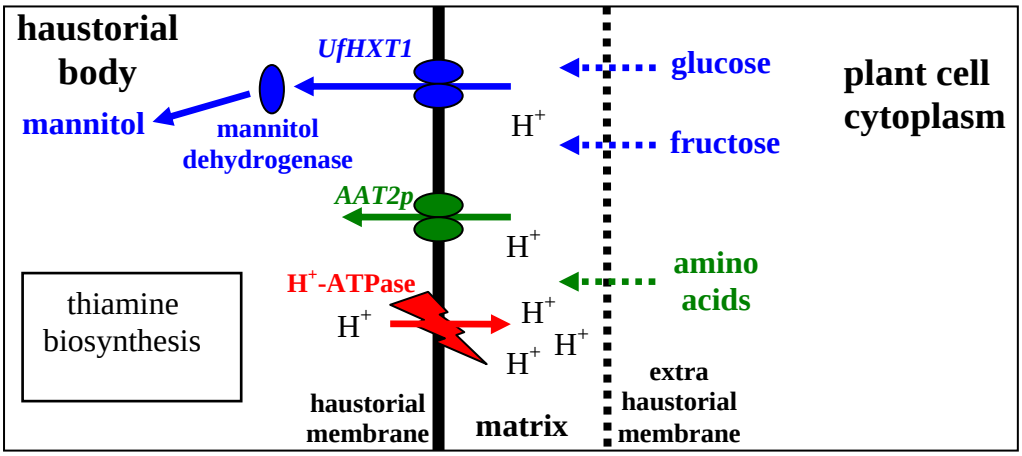

Figure 1.5. Proposed transport events and biosynthetic reactions at the haustorium interface. Refer to text above for details.

1.3 Host responses: compatibility and defence

V. vinifera is a compatible host for *E. necator* in that the pathogen is able to successfully penetrate epidermal cells and establish haustoria, enabling it to obtain sufficient nutrition to complete its asexual life cycle. However, *E. necator* is unable

to infect other plant species for example *Nicotiana tobaccum*, *Chenopodium album* and *Ricinus communis* (Boubals, 1961) that employ a range of innate defences to resist penetration and subsequent infection. These so-called 'non-host' resistance determinants may be pre-formed or induced and confer broad-spectrum resistance against the vast majority of pathogens (Heath, 2000). However, most commercially cultivated plants are susceptible to a few specific fungal pathogens that avoid or are immune to these generalised defence mechanisms, and subsequently initiate a compatible interaction with the host and establish infections.

The reasons underlying compatibility between a host plant and the few pathogens it tolerates remain obscure. Compatible pathogens may tolerate a pre-formed antimicrobial chemical produced by its host, while an incompatible pathogen may be sensitive to it (Papadopoulou et al., 1999). Host recognition and monitoring for pathogen molecules plays a part in the inducible sphere of non-host resistance responses because pathogens may lose a factor and gain susceptibility, however only to a narrow range of hosts (Kamoun et al., 1998). Furthermore, with relevance to the powdery mildews and rusts, host-specific chemical or architectural cues are perceived by a compatible fungal pathogen and influence morphogenesis of the fungal penetration organ, which initiates the whole infection process (Heath, 1976; Tsuba et al., 2002). Clearly, establishment of a compatible interaction requires a complex interplay of correctly timed cues perceived by host and pathogen, and avoidance of the non-host factors that prohibit infection by the vast majority of pathogens.

Compatible interactions are also sanctioned, or not, by 'host' resistance pathways which may be activated in subpopulations of a typically susceptible host species. Relative to the broad spectrum resistance conferred by the non-host scheme, this form of resistance is usually only effective against a single pathogen

species or race of that species. Host resistance is often controlled by single receptor-like host genes that physically interact with an avirulence factor produced by the pathogen: this interaction initiates a signal transduction cascade and activates an array of defence responses that often results in death of the infected cell via a hypersensitive response (Hammond-Kosack and Jones, 1996). This form of resistance has frequently been used by plant breeders to introduce disease resistance into otherwise susceptible cultivars. Currently, a map-based cloning approach is being used to isolate a powdery mildew resistance gene from the North American vine *Muscadinia rotundifolia*, with the eventual intention to introduce the gene into elite wine grape cultivars (Barker et al., 2005).

Although *V. vinifera* is a compatible host for *E. necator*, some typical defence responses are observed during the progression of grapevine powdery mildew disease. Expression of pathogenesis-related proteins such as chitinases and glucanases, and corresponding enzymatic activities, are induced by powdery mildew infection (Jacobs et al., 1999). In barley and *A. thaliana* infected with compatible powdery mildew fungi, induction of equivalent pathogenesis related proteins is also observed (Boyd et al., 1994; Reuber et al., 1998). Gregersen *et al*. (1997) identified additional powdery mildew induced transcripts from barley including several oxalate oxidase homologues, associated with papillae formation and penetration resistance, and putative flavonoid biosynthesis genes, which potentially contribute to phytoalexin synthesis. An oxalate oxidase gene family consisting of seven members has been identified in grapevine and two members are induced by powdery mildew infection (Godfrey and Dry, unpublished data). Ongoing analysis of this gene family is designed to determine if these genes may be used to engineer novel resistance to powdery mildew infection of grapevine. Taken together, these observations indicate that defence responses are initiated during these interactions,

but the response is not effective in halting disease progression. The defence may not be strong enough, may be too slow or may not be directed to the appropriate site at the appropriate time.

1.4 Host responses: amino acids and carbohydrates

After a pathogen has successfully avoided or suppressed all components of the plant defence network, infection is established. In the case of biotrophic fungal pathogens haustoria are formed, which retrieve nutrients from the host and allow the fungal biomass to expand and eventually reproduce via conidiospores. Several lines of evidence indicate that rust and powdery mildew infection alters amino acid composition and metabolism in host organs. Elevated lysine, proline and asparagine, and decreased glutamine levels were observed in powdery mildew infected barley leaves (Butters et al., 1985; Murray and Ayres, 1986; Jackson et al., 1995). In musk melon (*Cucumis melo* L.) infected with the powdery mildew pathogen *Sphaerotheca fuliginea*, gradual decreases in aspartic acid, glutamic acid, threonine, gamma-amino butyric acid, methionine and arginine were recorded, while cysteine and phenylalanine concentrations increased (Jindal et al., 1979). Powdery mildew infected pea leaf discs were found to have a greater capacity for amino acid uptake when compared with discs cut from uninfected leaves, and glutamine was rapidly taken up by suspensions of powdery mildew mycelia (Clarke and Hall, 1998).

Molecular studies have identified host genes involved in amino acid metabolism and transport that are induced during rust infection. For example, in rust infected broad bean, genes encoding an asparagine synthase (*VfAS1*) and an amino acid transporter (*VfAAPc*), were up regulated compared with uninfected samples (Wirsel et al., 2001). In flax infected with the rust pathogen *Melampsora lini*, *fis1*,

a gene that probably encodes a protein involved in the catabolism of proline, is strongly induced (Roberts and Pryor, 1995). Homologues of *fis1* from maize and barley are also induced by compatible rust pathogens, indicating the activity of this host gene product may serve an important role during pathogen infection (Ayliffe et al., 2002).

Changes to host carbohydrate composition and metabolism have also been observed in response to infection by biotrophic pathogens. In oak (Hewitt and Ayres, 1976), barley (Hwang and Heitefuss, 1986), pea (Aked and Hall, 1993), grapevine (Brem et al., 1986) and cucumber (Abood and Lösel, 2003) infected with compatible powdery mildew pathogens, the concentrations of glucose and fructose were found to be elevated when compared with uninfected samples, whilst sucrose concentrations declined or were unchanged. Concurrent with the rise in hexose levels of infected host tissues, net assimilation or photosynthetic activity is reduced in infected tissue. By measuring the rate of $^{14}CO_2$ fixation by grapevine leaves, Brem *et al*. (1986) showed that powdery mildew and downy mildew infection reduced net assimilation by 40% and 85% respectively. Scholes *et al*. (1994) found that the activities of three key photosynthetic enzymes; stromal fru-1,6-P_2ase, Rubisco and NADP-GAPDH, declined by approximately 50% five days after inoculation with powdery mildew in parallel with large increases in glucose, fructose and sucrose concentrations in infected tissue. The authors postulated that the high sugar levels cause a gradual decline in Calvin cycle activity which in turn inhibits photosynthetic activity.

Considered together, the dual observations of elevated carbohydrate content and reduced photosynthetic activity in diseased leaves suggests that the additional sugars may be sourced from otherwise healthy leaves or other sources and imported into the infected organ. Consistent with this idea, powdery mildew infected oak and

barley leaves showed abnormal patterns of translocation, whereby infected leaves exported less, and imported more photosynthate from uninfected healthy leaves (Hewitt and Ayres, 1976; Hwang and Heitefuss, 1986). Alternatively, in *A. thaliana* infected with white blister rust, starch was degraded from infected leaf regions in parallel with increased glucose concentrations, indicating that metabolism of carbohydrate stores may also contribute to the increased sugar levels observed in infected host tissue (Chou et al., 2000). However, starch content in uninfected leaf regions was greater than in controls, indicating that starch degradation may only occur within discreet regions and that other parts of the leaf may compensate by producing additional starch (Chou et al., 2000). In barley leaves infected with powdery mildew, total starch content increased during the period two to seven days after inoculation, indicating that infected leaves may actually contain increased levels of insoluble carbohydrate, in addition to greater amounts of soluble sugars such as glucose and fructose (Scholes et al., 1994).

The association between powdery mildew infection and increased carbohydrate content in infected tissues is further supported by studies indicating that glucose is the main carbon source transferred from the host to the fungal mycelium. Mendgen and Nass (1988) used a potentiometric fluorescent dye to estimate the membrane potential across mitochondria in haustoria of barley powdery mildew. Feeding the infected host cells with D-glucose induced an immediate reduction of fluorescence in haustorial mitochondria, indicating the D-glucose had been taken up by the haustorium. Feeding infected cells with sucrose induced a similar reaction, but the response was delayed by 20 min. Other sugars produced either smaller reductions of fluorescence or none at all. It was concluded that glucose is taken up by haustoria from host cells immediately, whereas other sugars such as sucrose, require time to be metabolised before they reach the haustorium and

mitochondria within (Mendgen and Nass, 1988). Consistent with this proposal, pea leaf disks infected with powdery mildew and mycelial suspensions acquired glucose more rapidly than fructose and sucrose, and the uptake was sensitive to chemical inhibitors of energy dependant membrane transporters (Clarke and Hall, 1998). Using asymmetrically labelled sucrose to investigate powdery mildew infected wheat, Sutton *et al*. (1999) also concluded that sucrose is hydrolysed in the host cell before being taken up by the fungus as glucose.

1.5 Carbohydrate distribution in plants

Changes to carbohydrate metabolism and translocation in host tissue infected with pathogens have been more rigorously studied than equivalent alterations to amino acid metabolism or distribution. In the following section, physiological aspects of carbohydrate distribution are discussed, however in general, the concepts also apply to amino acids (Patrick, 1997).

Plants are a mixture of autotrophic, photosynthetically active source tissues such as mature leaves, and heterotrophic sink organs such as roots, seeds and fruits. Carbohydrate assimilate synthesized in source tissues is loaded into the phloem network as sucrose in the majority of plant species, and is distributed to the various sinks where it is utilised or converted for storage. In non-leguminous plants, nitrate reductase activity in roots and leaves converts nitrate into ammonium; subsequent synthetic reactions yield amino nitrogen compounds which are also distributed by the phloem (Patrick et al., 2001). As plants develop, there are changes in both the level of supply and the numbers and sizes of sinks competing for assimilate, triggering distributive modulations to balance the carbohydrate budget. In addition to these developmental changes, exogenous factors such as environmental

conditions and pathogen challenge may retard assimilate production or apply additional carbohydrate demands, and therefore modify allocation within the plant (Roitsch et al., 2000).

Phloem unloading of sucrose at sink organs may occur within the symplasm, mediated by direct plasmodesmatal connection between the terminal sink cell cytoplasm and the end of the phloem path. Alternatively, phloem unloading may occur via efflux into the apoplasm and subsequent carrier-mediated uptake from the apoplasm by the terminal sink cells, or cells of the sink path. Apart from the relatively poorly understood control of phloem unloading mediated by the various methods of modification of plasmodesmatal conductance, metabolism and compartmentation of sucrose at the sink play delimiting roles in both routes and provide a direct connection between supply and demand (Patrick et al., 2001). Via the symplasmic path, cytoplasmic or neutral invertase (nINV) and sucrose synthase activity metabolise sucrose arriving in the sink cell cytoplasm, while uptake of sucrose into the vacuole and subsequent vacuolar invertase (vINV) activity, also contributes to the maintenance of a sucrose gradient between the sink cell cytoplasm and the phloem (Patrick, 1997). Apoplasmic unloading is driven by cell wall invertase (cwINV), which cleaves sucrose transported from the phloem to the apoplasm, thereby maintaining a sucrose gradient to support further efflux. Sucrose, and its monosaccharide cleavage products are then taken up from the apoplasm by transporters on the plasma membranes of sink cells. Thus symplasmic supply is modulated by the action of nINV, sucrose synthase and vINV, whereas apoplasmic supply is mainly regulated by cwINV and sugar transporters.

1.6 Pathogen associated changes to host invertase activity

Elevated invertase activity is commonly associated with the increased sugar concentrations observed in powdery mildew infected tissue, and most studies have concluded that the increased activities are due to invertases of host origin. Early studies on barley, grapevine and wheat reported that soluble acid invertase activity, contributed mainly by vINV forms, was elevated in powdery mildew infected tissue (Hwang and Heitefuss, 1986; Brem et al., 1986; Storr and Hall, 1992). In barley at least, most of the additional activity was confined within the mesophyll cell layer below the infected epidermis, indicating some signal is passed from the site of infection to the cells below (Scholes et al., 1994; Wright et al., 1995).

Subsequent analysis of pea leaves infected with powdery mildew showed that isolated apoplasmic fluids contained approximately 2.5 times more glucose and fructose and nearly four fold higher invertase activity than healthy leaves, indicating that most of the increase may be due to additional cwINV activity (Clarke and Hall, 1998). In powdery mildew infected wheat, all forms of invertase activity are elevated, however the biggest increase observed was in cwINV activity, consistent with the proposal that apoplasmic sucrose cleavage is an important step in sugar import to mildew infected tissues (Hall and Williams, 2000).

1.7 Induction of sink metabolism in response to pathogens and wounding

Molecular studies provide additional evidence that cwINV induction is a common element in host responses to pathogen infection and more broadly, to abiotic stresses such as wounding. In carrot storage roots, infection with the bacterial pathogen *Erwinia carotovora* strongly induced cwINV transcript one hour after inoculation before subsequently declining, while wounding induced cwINV by

a similar degree, but not until 12 hours after the wound event (Sturm and Chrispeels, 1990). Addition of fungal elicitors to suspension cultures of *Chenopodium rubrum* and tomato induced transcription of specific cwINV genes, as did mechanical wounding of source leaves of both plants (Roitsch et al., 2000). Studies on *A. thaliana* leaves infected with two different biotrophic pathogens indicated that one specific member of the cwINV gene family was induced. In leaves infected with the white blister rust pathogen *Albugo candida*, transcript levels of the cwINV *AtβFRUCT1* were found to be induced approximately ten fold, eight days after inoculation and reached levels of more than 40 fold higher than uninfected control samples 13 days after inoculation (Chou et al., 2000). Similarly, powdery mildew infected *A. thaliana* leaves displayed elevated *AtβFRUCT1* transcript levels, however only approximately four fold higher than control leaves (Fotopoulos et al., 2003).

As previously discussed, apoplasmic phloem unloading is regulated by the combined activities of cwINV, sucrose transporters and monosaccharide transporters, and genes encoding these proteins are often expressed in sink tissues. Expression of the sucrose transporter *AtSUC3* is limited to phloem cells and sink tissues such as root tips and pollen grains in *A. thaliana*. Additionally, wounding caused a strong induction of this gene within three hours and then subsequently declined (Meyer et al., 2004). Expression of the monosaccharide transporter *AtSTP4* is also induced by wounding, however by a greater amount and over a longer time period than *AtSUC3* (Truernit et al., 1996; Meyer et al., 2004). Like *AtSUC3*, *AtSTP4* expression is also usually restricted to sink organs such as roots and flowers. Fotopoulos *et al*. (2003) recently demonstrated that *AtSTP4* expression is also induced in response to powdery mildew infection in coordination with the cwINV gene *AtβFRUCT1*. Similar to the predominantly mesophyll localised induction of

invertase activity in powdery mildew infected wheat, *AtSTP4* expression was localised throughout the mesophyll and vascular tissue below areas of infected epidermis (Fotopoulos et al., 2003; Scholes et al., 1994).

In a physiological context, the induction of cwINV and sugar transporters observed in response to pathogen colonisation suggests the formation of an additional carbohydrate sink at the site of infection. cwINV and sugar transporters were also found to be induced in cells not directly infected by pathogens indicating that multiple cell layers, and potentially the whole organ, may revert to sink metabolism (Fotopoulos et al., 2003; Benhamou et al., 1991). Because wounding, in addition to pathogen infection, can induce similar gene expression modulations, it seems most likely that sink strength is increased to deliver additional carbohydrate to provide energy for defence and repair. However, in carrot storage tissues at least, the dynamics of induction of the cwINV in response to wounding and pathogen infection were quite different, suggesting that factors associated with pathogen infection may trigger more potent responses in the host (Sturm and Chrispeels, 1990). Whether or not these metabolic changes are actually beneficial for fungal nutrition has not been demonstrated.

1.8 Role of plant growth regulators in biotrophic interactions

Plants continuously interact with the biotic environment throughout their development, sanctioning some beneficial mutualistic associations, while the vast majority of pathogenic organisms are kept at bay via defence responses. Somewhere between these two outcomes is the response of plants to a select group of compatible biotrophic pathogens which manage to avoid defence responses, establish feeding sites and acquire host assimilate, which is ultimately detrimental to the plant. Plant growth regulators are thought to mediate plant-microbe interactions and many

agriculturally significant microbes, mutualistic and pathogenic alike, are capable of synthesising cytokinins and auxins, or inducing production of these regulators in infected host tissue. The pathogenesis of gall forming bacteria such as *Agrobacterium tumefaciens* and *Pseudomonas syringae* pv. s*avastanoi* is in part mediated by auxin and cytokinin biosynthetic genes encoded on specific plasmids borne by these bacteria (Jameson, 2000). Biotrophic and hemibiotrophic fungal pathogens synthesise cytokinins *in vitro* whereas necrotrophic pathogens do not, suggesting that maintenance of the biotrophic lifestyle, characterised by stable interaction between host and pathogen, may involve plant growth regulators (Murphy et al., 1997).

Elevated concentrations of plant hormones are found in infected plant tissue. During legume-rhizobia symbiosis and subsequent root nodulation that is characteristic of this association, elevated auxin and cytokinin concentrations are apparent in root cortical cells that divide and initiate nodule formation, whereas ethylene is described as a negative regulator of nodulation (Mathesius et al., 1998; Lohar et al., 2004). Interestingly, cytokinins and auxin have also been implicated in the establishment of root-knot nematode (genus *Meloidogyne*) feeding sites, also characterised by discrete regions of cell division (Lohar et al., 2004; Bird, 2004). Biotrophic and hemibiotrophic pathogens of barley, oilseed rape and apple are associated with the formation of green 'islands': infected or surrounding regions of host tissue where senescence is retarded and biosynthetic and metabolic activity is maintained (Coglan and Walters, 1990; Angra and Mandahar, 1991; Murphy et al., 1997; Cooper and Ashby, 1998). Green islands in powdery mildew and *Helminthosporium teres* I infected barley leaves contained elevated concentrations of cytokinins and polyamines, and reduced ethylene production (Coghlan and Walters, 1990; Angra and Mandahar, 1991). Furthermore, exogenous application of

cytokinins induced formation of similar zones (Angra and Mandahar, 1991). Molecular studies using *Chenopodium rubrum* suspension cultures demonstrated that cytokinins induce expression of a cwINV and a monosaccharide transporter, suggesting an induction of sink metabolism (Ehneß and Roitsch, 1997). Furthermore, a recent study by Lara *et al*. (2004) elegantly demonstrated that extracellular invertase is an essential component of cytokinin mediated delayed senescence, unequivocally proving the importance of cwINV and carbohydrate delivery in overriding usual programs of cell death.

Abscisic acid (ABA) is widely implicated in regulating responses to abiotic stresses such as drought and salinity (Zhu, 2002). More recently ABA has been found to regulate plant-microbe interactions, however the nature of its contribution to resistance and susceptibility remains unclear. Treatment of an incompatible soybean cultivar with ABA during infection with the oomycete *Phytophthora sojae* allowed the development of a compatible interaction (McDonald and Cahill, 1999). Typically, the incompatible interaction is characterised by a sharp rise in phenylalanine ammonia lyase (PAL) activity within eight h after inoculation, however this response was abolished by ABA treatment. Conversely, application of the ABA biosynthesis inhibitor norflurazon to a compatible soybean cultivar converted the interaction into an incompatible one, featuring a burst of PAL activity (McDonald and Cahill, 1999). Similar findings were observed in *A. thaliana* in response to infection by the bacterial pathogen *Pseudomonas syringae* and the downy mildew pathogen *Peronospora parasitica*. ABA application and drought stress induced susceptibility to an avirulent strain of *P. syringae*, while the ABA-deficient *A. thaliana* line *aba1-1* displayed reduced susceptibility to virulent strains of *P. parasitica* (Mohr and Cahill, 2003). These studies indicate that the endogenous ABA concentration contributes to the development of susceptibility

when plants are infected with biotrophic and other pathogens. This effect may involve down regulation of salicylic acid dependant defence pathways, as was attributed to the increased susceptibility of tomato to *Botrytis cinerea* observed after exogenous ABA application (Audenaert et al., 2002).

1.9 Other signals in biotrophic interactions

The association between legumes and Rhizobial bacteria is one of the most intensively studied plant-microbe interactions. Initiation of infection and subsequent nodule formation requires a complex procession of signals between both partners of the association, many of which are not carried by hormones. Initially, Rhizobia perceive phenolic signals such as flavonoids, secreted by legume roots, which attract bacteria and prime them for production of the various lipochitooligosaccharide symbiotic signals known as Nod factors (Long, 1996). Nod factor perception by host root cells mediates the formation of the infection thread which lines the root hair with plant derived substances such as pectins, xyloglucans and cellulose and forms a path for bacteria to invade into the root cortex where cellular division initiates nodule formation (Rae et al., 1992; Oldroyd, 2001). Although nodulation is ultimately beneficial for plant nutrition, hosts are observed to regulate the frequency of nodule initiation by means similar to the hypersensitive response observed during plant defence against many pathogens (Vasse et al., 1993).

The bacterial pathogen of bean, *Pseudomonas syringae* pv. *phaseolicola* secretes 'effector' molecules during host infection, of which three were shown to allow the bacterium to evade hypersensitive responses associated with the plant defence network (Tsiamis et al., 2000). An effector from *P. syringae* pv. *tomato* called AvrPtoB, acts as a negative regulator of programmed cell death in plants

which undermines the hosts hypersensitive response, and thus induces susceptibility to infection (Abramovitch et al., 2003). Fungal biotrophic pathogens are known to produce defence suppressing molecules, for example the soluble glucans secreted by the oomycete *Phytophthora infestans* during initial stages of infection (Doke, 1975). The tomato leaf spot fungus *Septoria lycopersici* produces tomatinase, an enzyme which degrades saponins which are antimicrobial factors and part of the preformed defence system in the host. Although tomatinase is described as a pathogenicity factor due to its role in undermining defence, the saponin degradation products were found to suppress the hypersensitive response associated with induced defence, and can therefore be considered signalling molecules (Bouarab et al., 2002).

1.10 Identification of host susceptibility genes

Host genes that contribute to susceptible pathogen interactions could be novel targets for modification to engineer resistance based on reduce susceptibility. Vogel and Somerville (2000) initiated a methane sulfonic ethyl ester mutant screen of *A. thaliana* and identified 32 lines that displayed reduced susceptibility to powdery mildew. Because the authors aimed to identify loci involved in powdery mildew susceptibility, lines which showed elevated defence activity were set aside, leaving 20 *pmr* (powdery mildew resistant) mutants. Only a few of the *pmr* loci have been mapped and cloned: *PMR5* and *PMR6* encode genes probably involved in pectin metabolism (Vogel et al., 2002; Vogel et al., 2004). Analysis of the epidermal cell walls of *pmr5* and *pmr6* plants suggested that both contained elevated pectin content, and that the pectin had altered chemical properties relative to wild type plants (Vogel et al., 2004). Contrary to the phenotype that would be predicted of plants carrying mutations in *PMR4*, the loci was found to encode a pathogen-induced callose synthase gene implicated in penetration resistance via the production

of cell wall appositions, also known as papillae (Nishimura et al., 2003). The basis of *pmr4* reduced susceptibility was found to be hyper-activation of salicylic acid defence pathways. Importantly, two of the three *PMR* genes identified up to this point do not encode proteins proposed to be involved with resistance responses, indicating that manipulation of susceptibility determinants can reduce pathogen infection. Identification of the other *PMR* genes will provide important insights into host factors involved in powdery mildew susceptibility.

Microarray analysis has also revealed novel aspects of the host response to pathogen infection. Zimmerli *et al*. (2004) monitored *A. thaliana* transcriptional responses to inoculation with compatible and incompatible powdery mildew isolates and found that overall, the responses overlapped substantially. Genes encoding putative defence factors such as a β-1, 3-glucanase like protein, a TIR-NBS class resistance protein and a thioredoxin were induced by both pathogens. However, inoculation with the incompatible pathogen *B. graminis* f. sp. *hordei* induced expression of defensin genes via a jasmonate/ethylene dependant pathway, while inoculation with two compatible pathogens did not initiate this response (Zimmerli et al., 2004). This observation is consistent with the hypothesis that compatible pathogens avoid host recognition, do not activate specific defence pathways and therefore establish disease. Commencing with microarray analysis to identify genes responsive to chitin treatment, Ramonell *et al*. (2005) identified three *A. thaliana* T-DNA mutants that were more susceptible to powdery mildew infection. Although the genes encoded at the loci probably encode proteins involved in defence responses, this investigation highlights the usefulness of microarray analysis to identify novel genes that participate in host responses to powdery mildew infection.

Candidate gene approaches have been successful in identifying genes that may contribute to the metabolic changes observed in tissue infected with various

biotrophic organisms. Examples include genes that encode proteins involved in carbohydrate and amino acid metabolism, and transporters of sugars, amino acids and phosphates (Roberts and Pryor, 1995; Chou et al., 2000; Wirsel et al., 2001; Harrison et al., 2002; Fotopoulos et al., 2003; Hoth et al., 2005). Potentially the induction of these genes in response to infection may contribute to host susceptibility.

1.11 Aims of this study

Grapevine powdery mildew is a prevalent and costly disease. Current management practices are heavily reliant on the use of fungicides which have detrimental health and overall ecological implications, and which are not compatible with the viticultural industries desire to progress towards sustainable production methods. The overall aim of this project is to investigate host (grapevine) genes that may mediate nutrient delivery to powdery mildew infected tissue and therefore can be considered susceptibility factors. Susceptibility genes could be targets for future manipulation to provide alternative disease control strategies based on reduced susceptibility rather than the introduction of traditional resistance determinants currently under investigation (Barker et al., 2005).

The specific objectives of the work described in this thesis were:

1. Identification and isolation of host genes associated with nutrient metabolism or transport that are induced by powdery mildew infection by degenerate PCR, RT-PCR and microarray analysis. In addition to enhancing current knowledge of the grapevine-powdery mildew interaction, isolation of new metabolic and transporter genes from grapevine may provide greater understanding of grape berry development.

2. Functional characterisation of novel host genes by:

    (i) sequence analysis

    (ii) heterologous expression of transporters in yeast

    (ii) determination of subcellular localisation

3. Investigation of the signalling network(s) involved in the regulation of powdery mildew responsive host genes by:

    (i) investigation of exogenous and endogenous stimuli

    (ii) isolation and analysis of promoter regions

    (iii) investigation of the hormonal regulation of these genes

Chapter 2 – General Materials and Methods

2.1 Materials

2.1.1 Solutions, chemicals and growth media

Solutions and growth media used in this project are shown in Table 2.2. All chemicals were analytical or molecular biology grade and obtained from BDH or Sigma. Solutions were prepared with nanopure or deionised water and autoclaved as necessary. Restriction endonucleases were obtained from Fermentas and Roche Diagnostics. The sources of all other supplies used in this project are indicated in the relevant methods section.

Table 2.1. Suppliers of chemicals, enzymes, growth media and other miscellaneous consumables.

Amersham Biosciences	Castle Hill, NSW, Australia
BDH	Kilsyth, Vic., Australia
Becton Dickinson (BD)	North Ryde, NSW, Australia
Bioline	Alexandria, NSW, Australia
Bio 101 Systems	distributed by Integrated Sciences
Fermentas	distributed by Quantum Scientific
Integrated Sciences	Willoughby, NSW, Australia
Invitrogen	Mount Waverley, Vic., Australia
Promega	Annandale, NSW, Australia
Qiagen	Clifton Hill, Vic., Australia
Quantum Scientific	Paddington, QLD, Australia
Roche Diagnostics	Castle Hill, NSW, Australia
Sigma-Aldrich	Castle Hill, NSW, Australia

Table 2.2. General solutions and growth media.

Solution	Composition
DNA loading dye (10x)	78% (w/v) glycerol, 0.25% (w/v) bromophenol blue, 0.25% (w/v) xylene cyanol, 10 mM EDTA
RNA loading dye (5x)	90% (v/v) deionised formamide, 10% DNA loading dye (10x))
DNSA-reagent	1% (w/v) 3,5-dinitrosalicylic acid, 0.5M KOH, 1M K/Na-tartrate
LB (liquid growth media)	1% (w/v) bacto-tryptone, 0.5% (w/v) yeast extract, 1% (w/v) NaCl pH 7.0
LB agar (solid growth media)	1% (w/v) bacto-tryptone, 0.5% (w/v) yeast extract, 1% (w/v) NaCl, 1.2% (w/v) bacto-agar, pH 7.0
Murashige and Skoog (MS) salts	4.33 g MS basal salt mixture (complete) L^{-1}
RNA extraction buffer	5 M sodium perchlorate, 0.3 M TrisHCl (pH 8.3), 1% (w/v) SDS, 1% (v/v) β-mercaptoethanol, 8.5% (w/v) PVPP, 2% (w/v) PEG 4000
RNA extraction buffer (modified)	5 M sodium perchlorate, 0.3 M TrisHCl (pH 8.3), 1% (w/v) SDS, 1% (v/v) β-mercaptoethanol
5 x SSC	750 mM NaCl, 75 mM tri-sodium citrate, pH 7.0
STET buffer	8% (w/v) sucrose, 5% (w/v) triton X-100, 50 mM EDTA (pH8.0), 50 mM Tris (pH8.0)
TBE buffer	90 mM Tris-HCl, 90 mM borate, 2 mM EDTA, (pH 8.3)
TE buffer (pH 7.6)	10 mM Tris-HCl (pH 7.6), 1 mM EDTA (pH 8.0)
YT1	10 mM Tris-HCl (pH 8.0), 1 mM EDTA (pH 8.0), 100 mM lithium accetate
YT2	10 mM Tris-HCl (pH 8.0), 1 mM EDTA (pH 8.0), 100 mM lithium accetate, 45% (v/v) PEG-4000
YPM (Liquid yeast media)	1% (w/v) yeast extract, 2% (w/v) peptone, 2% (w/v) maltose
YPM agar (Solid yeast media)	1% (w/v) yeast extract, 2% (w/v) peptone, 2% (w/v) maltose, 1.2% (w/v) bacto-agar
Uracil drop out media	0.17% (w/v) Difco yeast nitrogen base without amino acids (BD), 0.5 % (w/v) ammonium sulfate, 0.08% (w/v) CSM -uracil (Bio101 systems), 2% (w/v) maltose
Uracil drop out media agar	0.17% (w/v) Difco yeast nitrogen base w/o amino acids (BD), 0.5% (w/v) ammonium sulfate, 0.08% (w/v) CSM-uracil (Bio101 systems), 2% (w/v) maltose, 1.2% (w/v) bacto-agar

2.1.2 Oligodeoxyribonucleotide primers

All oligodeoxyribonucleotide primers were obtained from GeneWorks (Hindmarsh, SA, Australia) and their sequences are shown in Table 2.3. Degenerate oligodeoxyribonucleotide primers were designed with the assistance of CODEHOP: Consensus-Degenerate Hybrid Oligonucleotide Primers (Rose *et al.* 1998; http://blocks.fhcrc.org/blocks/codehop.html/). All other primers were designed

manually and with the assistance of Oligo Calculator (http://mbcf.dfci.harvard.edu/docs/oligocalc.html) to estimate Tm.

Table 2.3. Oligonucleotide primers used in this study. Underlined sequences correspond to specific restriction enzyme sites.
Mixed base codes: R(AG) Y(CT) K(GT) S(GC) W(AT) H(ACT) B(GCT) V(AGC) D(AGT) N(AGCT)
I(deoxyinosine)

Primer	Description	Sequence (5'-3')
AAPDEGF1	Degenerate PCR	CAGTTACCGGAAAGAGGAACTAYACNTAYAT
AAPDEGR1	Degenerate PCR	GTGGGGACTTAACGGTATCYTGDATYTC
AAPF1	Quantitative RT-PCR	GGAGGACAGTTGGAGTGGA
AAPR1	Quantitative RT-PCR	CCAACACAACCGCATAGGAC
AAP	5' RACE PCR	GGCCACGCGTCGAACTAGTACGGGIIGGGIIGGGIIG
B26	3' RACE PCR	GACTCGAGTCGACATCGATTTTTTTTTTTTTTTTT
BQ794584 fwd	Quantitative RT-PCR	CTATGGCTTCTTCGCCTTTG
BQ794584 rev	Quantitative RT-PCR	AGTCCACATCCCTTCTCCAC
BQ794584rev.2	5' RACE PCR	ATGTCAGTTAGACCAGCTCCAT
BQ794584rev.3	5' RACE PCR	GACAATGCAGCCAGCATAAAC
BQ794584FLF	Clone full length cDNA	GTGAATTCAAAAACATGGAAACTGAGCTG
BQ794584FLR	Clone full length cDNA	CACTCGAGCTTCCTCTATGAAGCC
CWINVDEGF1	Degenerate PCR	AAATACCGGAATGTGGGARTGYCC
CWINVDEGR1	Degenerate PCR	AAGCGAAAGTCATCAGTCCRAANGGNCC
CWINV fwd	Quantitative RT-PCR	ATGAATCATCTAGYGTGGAGCAC
CWINV rev	Quantitative RT-PCR	CTTAAACGATATCTCCACATCTGC
CWINVrace fwd	3' RACE PCR	GTGCATCAGTAAAAGGTGGG
CWINVrace rev	5' RACE PCR	GTATCCTTCTCACGGTTGTAGC
CWINVrace rev	5' RACE PCR	TCCAATCGTGTAGTAGTCATGC
CWINVFL fwd	Clone full length cDNA	GTGAATTCAAAGCCATCATGGCCAC
CWINVFL rev	Clone full length cDNA	GTCAAGCTTCACTCACAACTCTACATAC
CWINVBS 1	Promoter sequencing	GATCATTCATCCAGTTCTTGCG
CWINVBS 2	Promoter sequencing	GGGATTGGCCAAAAAGCTCC
CWINVBS3	Promoter sequencing	GAAAATAAACACTGCAAGTGTGCC
CWINVBS4	Promoter sequencing	CAGAGGAATCTTGGAAAATTTGTCAG
GIN1fwd	Quantitative RT-PCR	CCATCTCCATCCCATCGTAACC
GIN1rev	Quantitative RT-PCR	GGCTATCCAAGTTTCCAACCAACC
GIN2fwd	Quantitative RT-PCR	GAGCACAGTTCCAGTAATCAAAGG
GIN2rev	Quantitative RT-PCR	GTGAGGCGTAGTTTTAGGACTCC
HT1 fwd	Quantitative RT-PCR	TCGGAGTGGATGGAGAACCTTG
HT1 rev	Quantitative RT-PCR	GACATCACCACCACAAAGAAGGC
HT1FL fwd	Clone full length cDNA	CTGGATCCATGCCGGCTGTCGGAGGC
HT1FL rev	Clone full length cDNA	GACTCGAGTCATACATTCTTAACAGGGTAGTTTTCC
HT2 fwd	Quantitative RT-PCR	GTTGCCGTCAACTTCGCAAC
HT2 rev	Quantitative RT-PCR	GAAGGAATTTAGCTATGGCAGAG
HTDEGF1	Degenerate PCR	TCCACTGTACCTGTCCGARATGGCNCC
HTDEGR1	Degenerate PCR	TCCCAGTGGTCCCCANSWCCA
HT3 fwd	Quantitative RT-PCR	TAATCGAACGGGGATCAAG
HT3 rev	Quantitative RT-PCR	CCCCCAGAAATCAATAAAACTC
HT3race fwd	3' RACE PCR	GCTAGTGAGCCTGCAAACTCA
HT3race rev	5' RACE PCR	ATGAGGGGAGCTTTGCAGTT
HT3race rev	5' RACE PCR	TCCCCGTCGTAGTTGCTAAC
HT3FL fwd	Clone full length cDNA	GTAGAATTCAGAAGAGGAACTATGGAGG
HT3FL rev	Clone full length cDNA	TCAAGCTTGGCTCATGATAGGAGC
HT3GFP fwd	Translational fusion to GFP	GCTCGAGGAAGAAGAGGAACTATGGAG
HT3GFP rev	Translational fusion to GFP	CTCTAGAGCTGCCTAGCTTTGTCTTTTCAC
HT3BS1	Promoter sequencing	GTCATTGTACTTGCAGTAGTGG
HT3BS2	Promoter sequencing	GTCATAGCCGAAAATTGCACCC
HT3BS3	Promoter sequencing	CTGCTATGTCTGCATTCCTCC

Table 2.3. (continued).

Primer	Description	Sequence (5'-3')
HT4 fwd	Quantitative RT-PCR	CCTACTTTGTCGACAGAGTAGACG
HT4 rev	Quantitative RT-PCR	GGAGGCCATACCAACTACG
HT4race fwd	3' RACE PCR	GGTAGGAGGAATATTGGCAGC
HT4race rev	5' RACE PCR	AGCCAATGCTAGAGAAACTCG
HT4race rev	5' RACE PCR	TAATAAGGTTAGCTGATAGAGCC
HT4FL fwd	Clone full length cDNA	GTAGAATTCAGAGCCATGGCAGTG
HT4FL rev	Clone full length cDNA	ACAAGCTTAGAGGAGGATGCTGTTG
HT4GFP rev	Translational fusion to GFP	CGTCTAGAGGCTGTCTCCATTTTAGG
HT4BS 1	Promoter sequencing	AGGGAGGATGTGAATGAGGTC
HT4BS2	Promoter sequencing	CCATGGCTTGTTACTGCAATTCC
HT4BS3	Promoter sequencing	GAAACAAAATCGCATTTATACCATTGC
HT5 fwd	Quantitative RT-PCR	GTCGCTTGGAAGAAGGAAAG
HT5 rev	Quantitative RT-PCR	CCTACTTTGTCGACAGAGTAGACG
HT5race fwd	3' RACE PCR	GGTAATTGCAATCATACTAGGCAT
HT5race rev	5' RACE PCR	CCAGCCAACCCCAATGATAC
HT5race rev	5' RACE PCR	TAGTGACGTTAAGTTGGAACAGT
HT5FL fwd	Clone full length cDNA	CTGAATTCCATCATGCCTGCTGGA
HT5FL rev	Clone full length cDNA	ACAAGCTTTCCCTCCCCATACAC
HT5BS 1	Promoter sequencing	CTGTAGCCCTTGGTTGTCG
HT5BS2	Promoter sequencing	GATGTCACCACCTACAAAGTCC
HT5BS3	Promoter sequencing	GATGTCACCACCTACAAAGTCC
HT5BS4	Promoter sequencing	GTCAGAGTTGATGGCATCGAG
HT5BS5	Promoter sequencing	GGTCATTCAACTAAAATAGATAAAACAATCC
PhT1F	Quantitative RT-PCR	CTTTGCAGGTGGACATTGAG
PhT1R	Quantitative RT-PCR	GAGCAATAAGCGTTTGCGC
PhT2F	Quantitative RT-PCR	AGATATGTCTAAAGTTCTCCACCTT
PhT2R	Quantitative RT-PCR	CTGCAGAGGGCTATGAGAGT
PIP1A fwd	Quantitative RT-PCR	TCCTGTTCTGGCACCTCTTC
PIP1A rev	Quantitative RT-PCR	CCTGAATGACCCAAGAGCC
ProTDEGF1	Degenerate PCR	ATACTCCGGTACCATTATGGTNCCNYT
ProTDEGR1	Degenerate PCR	TCGTACATTGGGGAAGCRAADATRTG
ProTF1	Quantitative RT-PCR	CAGGAACAGAAGCAAGCAAGG
ProTR1	Quantitative RT-PCR	AACCAAACTGGACCAGAGAC
SP6	Screening & sequencing	TTAGGTGACACTATAGAATACTC
SUC11 fwd	Quantitative RT-PCR	AAACCAAATGAAGGGCAGAA
SUC11 rev	Quantitative RT-PCR	TCAGTGCAGCAATCACAACA
SUC12 fwd	Quantitative RT-PCR	CGGATTGGATGGGTAGAGAA
SUC12 rev	Quantitative RT-PCR	CATGCAGGCAAACACAATAAA
SUC27 fwd	Quantitative RT-PCR	GGGGCTGATGCTGAACTCT
SUC27 rev	Quantitative RT-PCR	AAGCCAGAGCAAATGGAATG
TC11451fwd	Quantitative RT-PCR	GATGCAGAGAAGAGGCTCGC
TC11451rev	Quantitative RT-PCR	CCGTCCAGTTTTGCTGAGGTC
TC11207fwd	Quantitative RT-PCR	GCCAGAATACTATGATGGAAAGCTC
TC11207rev	Quantitative RT-PCR	CCGAATACAGAATACAAACTACCTGC
TIP3 fwd	Quantitative RT-PCR	GTATGCCACAGCAGTGGATCC
TIP3 rev	Quantitative RT-PCR	GAAGATGTGATCGTAGATGATGGC
TC7206fwd	Quantitative RT-PCR	CGAAATGGGCGGTTCATAGGC
TC7206rev	Quantitative RT-PCR	CCACCATGCTCTTCCTCGTG
UBQ fwd	Quantitative RT-PCR	AGTAGATGACTGGATTGGAGGT
UBQ rev	Quantitative RT-PCR	GAGTATCAAAACAAAAGCATCG
T7	Clone screening, sequence	GTAATACGACTCACTATAGGG

2.1.3 Bacterial and yeast strains

Escherichia coli strain XL1-Blue (Stratagene; Cedar Creek, TX) was used for all cloning procedures. Yeast strain *EBY.VW4000* (Wierkzork *et al*., 1999) was used for heterologous expression of putative HTs.

2.1.4 Grapevine tissue

The various grapevine tissues used in this study were sampled from the Coombe vineyard and from potted glasshouse vines on the Waite Campus of Adelaide University (Adelaide, South Australia, latitude 34° 56' south, longitude 138° 36' east). Grapevines were propagated from dormant Cabernet Sauvignon and Chardonnay cuttings obtained from the Riverland Vine Improvement Committee (Monash, South Australia), stored at 4ºC before use. To strike, the base of each cutting was cut and scored, dipped in Clonex Hormone Rooting Gel (Growth Technology, Western Australia) and transferred to pots containing potting mix of sand : composted pine bark (1:2 v/v) supplemented with 1 g L^{-1} ferrous sulphate and 4 g L^{-1} Osmocote slow release fertilizer (Yates, Australia). Pots were incubated on a 25°C heat-bed containing Perlite for three weeks following striking and watered lightly at two-day intervals. During this period rooting and bud-burst occurred, and pots were transferred to temperature-controlled glasshouses with a minimum air temperature of 23ºC and a maximum temperature of 25ºC. Each pot was irrigated with a single drip emitter with two irrigations per day.

2.1.5 *Erysiphe necator* culture and maintenance

E. necator was maintained on a detached leaf inoculation system as previously reported (Donald et al., 2002) with some modifications. Young, glossy *V. vinifera* leaves, typically 3 to 8 cm in diameter, were sterilised for 3 min in 50% (v/v) Milton Solution (Procter and Gamble, NSW, Australia) containing 0.01% (v/v) Tween 20 with gentle agitation, followed by four times in sterile water. Sterilised leaves were laid on to four sterile toothpicks placed across the surface of agar plates containing 1% (w/v) agar and 400µl L^{-1} Pimaricin (Sigma) and petioles embedded in the agar with tweezers. Spores from powdery mildew-infected leaves were applied

to leaves prepared as above by vigorously tapping the infected leaf above the recipient leaf allowing spores to fall onto the surface. Plates were sealed with Parafilm and incubated at 24.5°C under a 16 h light and 8 h dark cycle. Leaves were examined for sporulation after 8 d using a Stemi 2000 microscope (Zeiss, North Ryde, Australia).

2.1.6 *Plasmopara viticola* culture and maintenance

P. viticola was maintained on glasshouse-grown potted vines. Infected leaves (7 to 10 DPI) were removed and incubated upside down on moist filter paper in large petri dishes overnight at 22°C to facilitate sporulation. To collect spores, leaves were placed in a 50 ml Falcon tube containing 5 mL water and agitated to displace the spores and a haemocytometer used to estimate the spore concentration. The spore solution was diluted to a concentration of 1 $x10^6$ spores per ml before being sprayed on the abaxial surface of leaves on glasshouse-grown potted vines. Inoculated leaves were enclosed in plastic bags overnight to maintain humidity.

2.2 Methods

This section outlines general methods used throughout this project and are essentially as described by Sambrook and Russell (2001) or according to the manufacturer's instructions. Methods significantly modified from their published form are outlined. Other methods specific to experiments carried out in one chapter only are outlined in the materials and methods section of the relevant chapter.

2.2.1 Polymerase chain reaction (PCR)

Typical components of a PCR reaction were as follows: DNA template (cDNA 2 μl, genomic DNA 10 ng), oligonucleotide primers (200-500 nM), 1× PCR buffer (Bioline), 200 μM dATP, dCTP, dGTP, and dTTP (Invitrogen), 1.5 μM $MgCl_2$, and 1 unit of recombinant BioTaq Red DNA polymerase (Bioline), in a 20 μl reaction volume.

For amplification of full-length cDNAs for functional characterisation and for sub cellular localization (Chapter 4), Platinum Taq DNA Polymerase High Fidelity (Invitrogen) was used according to the manufacturer's instructions and with supplied buffer. Thermal cycling generally consisted of: 3 min at 95°C (one cycle); 30 s at 94°C, 30 s at 52-57°C, 30 - 90 s at 72°C (30-40 cycles); 7 min at 72°C (1 cycle).

2.2.2 Agarose gel electrophoresis

EasyCast horizontal minigel tanks (OWL Scientific Inc., Cambridge, UK) were used for electrophoresis of DNA. Agarose gels, 0.7-2.0% (w/v) were prepared with TBE buffer (Table 2.1), and contained 0.5 μg ml^{-1} (w/v) ethidium bromide. Before application to wells, DNA loading dye (Table 2.1) was added to each sample to a final concentration of 2×. Gels were electrophoresed at approximately 100 V in TBE running buffer before being visualized and photographed using a short wavelength UV transilluminator.

Electrophoresis of RNA was essentially the same as that described for DNA except that gel tanks, trays, and combs were treated with 0.2 M NaOH for approximately 1 h prior to use, an RNA loading dye (Table 2.1) was added and each

sample was heated at 65°C for five min and then chilled on ice for two min before loading into wells.

2.2.3 Purification of DNA from agarose gel slices

Purification of specific DNA species from agarose gels after visualization with ethidium bromide was achieved using a QIAquick Gel Extraction Kit (Qiagen) according to the manufacturer's instructions.

2.2.4 Dephosphorylation of DNA 5' termini

The 5' phosphate groups were removed from restricted vector DNA fragments prior to ligation with insert DNA fragments using calf intestinal alkaline phosphatase (Roche). The enzyme was inactivated by addition of 20 mM EDTA and incubation at 65°C for 15 min.

2.2.5 Purification of DNA samples following enzymatic reactions

Extraction of DNA samples after restriction enzyme digestion (Section 2.2.1), PCR (Section 2.2.4) and dephosphorylation (Section 2.2.5) reactions was achieved using a QIAquick PCR Purification Kit (Qiagen).

2.2.6 DNA ligation

Purified PCR products were ligated into the T-tailed vectors pGEM T-Easy (Promega) or pDRIVE (Qiagen) using the pGEM T-Easy Vector System I (Promega) and the PCR Cloning Kit (Qiagen) according to the manufacturer's instructions.

All other ligations were carried out in 10 μl reaction volumes containing an insert: vector ratio of approximately 6:1, 10 units of T4 DNA ligase (Fermentas) in the supplied buffer and incubated overnight at 16°C.

2.2.7 Preparation of electro-competent E. coli cells

LB (500 ml) was inoculated with a five ml overnight culture of XL1-Blue and grown at 37°C with vigorous shaking to an optical density (OD_{600}) of 0.5. Cells were chilled on ice for 10 min and centrifuged for 15 min at 4°C at 5000 *g*. The cells were resuspended in 500 ml of sterile ice-cold water and centrifuged again. The cells were washed and centrifuged again with 250 ml sterile ice-cold water and resuspended in 10ml of sterile ice-cold 10% (v/v) glycerol. The cells were transferred to a new 50 ml falcon tube and centrifuged again. The cells were finally resuspended in 2 ml of ice-cold glycerol. Aliquots of 40 μl were placed into ice-cold eppendorf tubes, snap-frozen in liquid nitrogen, and stored at -80°C.

2.2.8 Transformation of bacteria with recombinant plasmids

Electro-competent *E. coli* XL1-Blue were transformed by electroporation using a Gene-Pulser apparatus (Bio-Rad, CA, USA). Approximately 10 ng of plasmid or 1 μl ligation reaction was mixed with a 40 μl aliquot of cells and transferred to an ice-cold electroporation cuvette (path length = 1mm; Invitrogen). This was then given a single pulse in the Gene-Pulser (1.8 kV, 125 μFD, 200 Ohms), and immediately resuspended in 600 μl of LB (Table 2.1). After incubation at 37°C for 1 h to allow expression of antibiotic-resistance genes, the transformed cells were spread on 1.2% LB agar plates (Table 2.1) with appropriate antibiotic selection and incubated at 37°C overnight.

2.2.9 Preparation of plasmid DNA

High quality plasmid DNA for vector preparation, DNA sequencing, yeast transformation and for transient expression in onion cells was prepared from 1-5 ml of overnight culture using a QIAprep Spin Miniprep Kit (Qiagen) according to the manufacturers instructions. Large-scale (20-50 ml cultures) preparation of plasmid DNA was achieved using a Plasmid Midi Kit (Qiagen).

For general screening purposes, plasmid DNA was prepared using a miniprep boiling method (Holmes and Quigley, 1981). Briefly, 1 ml of overnight culture was centrifuged at 16,000 *g* for 1 min at room temperature. The supernatant was discarded and the pellet resuspended in 350 µl STET (Table 2.1) buffer. After adding 12.5 µl of 20 mg ml^{-1} lysozyme, the cells were placed in boiling water for one min and centrifuged at 16,000 *g* for 20 min. The pellet was removed with a sterile toothpick and 40 µl of 3 M sodium acetate and 220 µl isopropanol added to the supernatant. This mixture was centrifuged at 16,100 *g* for 10 min. The resulting pellet was washed with 70% (v/v) ethanol, dried briefly under vacuum, and resuspended in 50 µl of sterile water.

2.2.10 Preparation of bacterial glycerol stocks

Bacterial glycerol stocks were prepared by adding 1 volume of 40% (v/v) sterile glycerol to overnight culture, snap-freezing in liquid nitrogen, and storing at -80°C.

2.2.11 Preparation of DNA samples for sequencing

DNA sequencing reactions were carried out using an ABI PRISM BigDye Terminator Cycle Sequencing Ready Reaction Kit (PE Applied Biosystems, Norwalk, CT, USA) according to the manufacturer's instructions using plasmid DNA prepared with the QIAprep Spin Miniprep Kit (Qiagen). Extension products were precipitated by adding 80 µl of 75% (v/v) isopropanol, incubating for 20 min at room temperature, and centrifuging at 16,000*g* for 20 min. After discarding the supernatant and adding another 250 µl of 75% (v/v) isopropanol, the tubes were centrifuged at 16,000*g* for 5 min. The samples were then aspirated, dried under vacuum for 15 min, and sent to the Institute of Medical and Veterinary Science (Adelaide, Australia) for analysis.

2.2.12 Preparation of total grape RNA

Total RNA was isolated from grape tissues using a sodium perchlorate method (Rezaian and Krake, 1987) with modifications. Plant material (0.5 to 4 g FW), was ground in liquid nitrogen in a mortar and pestle, the powder added to 20 ml of RNA extraction buffer (Table 2.2) and mixed by shaking at 200 rpm on an orbital shaker at room temperature for 30 min. The homogenate was then centrifuged at 80 *g* for 10 min at 4°C through a crude separation apparatus consisting of a 20 ml disposable syringe plugged with approximately 2 cm^3 of silane-treated glass wool (Alltech, Baulkam Hills, NSW, Australia) wrapped in Miracloth (Calbiochem, Croydon, Vic., Australia) and secured into a 250 ml centrifuge tube (Corning, Acton, USA). Modified extraction buffer (Table 2.2), was added to the crude separation apparatus and centrifuged as before. The combined eluate was mixed with 2.5 vol of cold absolute ethanol and stored at -20°C

overnight. The precipitate was pelleted via centrifugation at 10,000 *g* for 20 min at 4°C and the resulting pellet was dried under vacuum and resuspended in 1 mL of TE Buffer (Table 2.1) containing 0.2% (v/v) *β*-mercaptoethanol. The suspension was extracted 3 times with an equal volume of phenol:chloroform:isoamyl alcohol (25:24:1 v/v) and once with an equal volume of chloroform:isoamyl alcohol (24:1 v/v). The upper aqueous phase was retained, mixed with 2.5 vol of cold absolute ethanol and 0.1 vol of 3 M sodium acetate (pH 5.2) and then stored at -20°C overnight to precipitate RNA. The RNA precipitate was pelleted at 16,000 *g* for 10 min at 4°C, dried under vacuum, rinsed with cold 70% (v/v) ethanol and resuspended in 50 to 200 µl of sterile water. RNA was quantified spectrophotometrically and integrity checked by agarose gel electrophoresis.

2.2.13 First-strand cDNA synthesis

Before reverse transcription, 100 µg of total RNA was further purified and DNase treated using an RNeasy Mini Kit (Qiagen) and an RNase-Free DNase Set (Qiagen) according to the manufacturer's instructions. DNase-treated RNA (2 µg) was reverse transcribed using the SuperScript III First-Strand Synthesis System for RT-PCR (Invitrogen) using the Oligo $(dT)_{20}$ primer according to the manufacturer's instructions. Before use in RT-PCR experiments, cDNA reactions were diluted 10-fold to 200 µl with 10 mM Tris-HCl, pH 7.6.

2.2.14 Sequence analysis and manipulation

DNA sequences were analysed using various basic local alignment search tools (BLAST) served at the National Centre for Biotechnology Information (NCBI) website (http://www.ncbi.nlm.nih.gov/BLAST/) and the GCG WebAngis Wisconsin

software package operated by the Australian National Genomic Information Service (http://www.angis.org.au/). Multiple sequence alignments were drawn by Pile Up or ClustalW (both served at ANGIS) and displayed and further manipulated using GeneDoc (www.psc.edu/biomed/genedoc). Potential signal peptides of deduced amino acid sequences were mapped using SignalP v. 3.0 (http://www.cbs.dtu.dk/services/SignalP/). Transmembrane domains and membrane topology was predicted using TMHMM v 2.0 (http://www.cbs.dtu.dk/services/TMHMM; Krogh et al., 2001) and theoretical isoelectric points were calculated using Iep, also served at ANGIS (http://www.angis.org.au/).

Chapter 3 – Isolation and identification of genes differentially expressed in powdery mildew infected grapevine tissues

3.1 Introduction

Biotrophic pathogens, such as powdery mildew, form a stable association with host epidermal cells to acquire nutrients from the host plant. Nutrient transfer from plant to fungus is facilitated by a specialised structure called the haustorium, a biotrophic interface that develops only during this interaction, formed from fungal and host components (Hahn & Mendgen, 2001). As the fungus grows, its increasing biomass becomes a strong nutrient sink capable of altering assimilate flow and storage in the host (Brem et al., 1986; Murray & Ayres, 1986; Jackson et al., 1995; Clarke and Hall, 1998). Two approaches were initiated to identify grapevine genes that are responsive to powdery mildew infection and may mediate these changes.

To identify differentially expressed grapevine transcripts, a grape microarray was screened with probes generated from powdery mildew infected Chardonnay berry skin and probes produced from healthy uninfected berry skin. This array consists of approximately 1,200 ESTs isolated from grape berries spotted in duplicate, allowing calculation of the standard error of expression of each gene via comparison of these technical replicates. Microarray analyses of powdery mildew infected *A. thaliana* and wheat have identified previously unreported host genes that are induced by infection with these pathogens (Zimmerli et al., 2004; Ramonell et al., 2005). By using microarray analysis to compare gene expression in powdery

mildew infected and healthy grapevine tissue samples, novel powdery mildew responsive grapevines genes may be identified.

Molecular studies in broad bean and *A. thaliana* have identified host carbohydrate and amino acid transporters, and metabolic enzymes that are induced in response to infection with biotrophic fungal pathogens (Wirsel et al., 2001; Fotopoulos et al., 2003). Specifically in powdery mildew infected grapevine leaves, hexose concentrations and invertase activity were increased, while net assimilation was repressed, suggesting additional carbohydrate is imported to the infection site (Brem et al., 1986). Based on these published observations a second screening approach was initiated to target genes that may contribute to these metabolic changes. To isolate new grapevine and powdery mildew responsive transcripts a degenerate PCR cloning approach using cDNA prepared from powdery mildew infected leaves as template was employed. It should be noted that at the time this project commenced, the sequences of only two grapevine HTs (*VvHT1* and *VvHT2*; Fillion et al., 1999) and two vacuolar invertases (vINVs) (GIN1 and GIN2; Davies and Robinson, 1996) had been reported.

3.2 Materials and methods

3.2.1 Microarray analysis of powdery mildew infected berry skin

The *V. vinifera* cDNA microarray slide (kindly donated by Dr Mark R. Thomas, CSIRO Plant Industry, Adelaide, Australia) contained 1,220 unique sequences, (now part of the grapevine Unigene set at http://www.ncbi.nlm.nih.gov/) plus 12 non-*V. Vinifera* control sequences. All genes were printed in duplicate within the array and are subsequently referred to as technical replicates. Total RNA was extracted as described (Section 2.2.12) from healthy and powdery mildew

infected Chardonnay berry skins collected 10 DPI, and then treated with DNase using the RNase free DNase Set (Qiagen) in combination with the RNeasy mini kit (Qiagen). Microarray probes were prepared from the total RNA using a method modified from Schenk *et al*. (2000). RNA (60 μg) was reverse transcribed using Superscript II (Invitrogen) with an oligo(dT) 23mer anchored primer (Invitrogen) at 42°C for one h. The cDNA was treated with 2 U of RNase H (Invitrogen) at 37°C for 30 min and then purified and concentrated to 8 μl in TE (pH 8.0) using YM-30 Microcon centrifugal columns (Millipore). Half of the resulting concentrate was used for each labelling reaction as described in Schenk *et al*. (2000) except that 10 U of Klenow enzyme was used for each labelling reaction. Probes produced from total RNA extracted from powdery mildew infected berry skins were labelled with Cyanine 5 and probes prepared from RNA extracted from healthy Chardonnay berry skins were labelled with Cyanine 3.

Cyanine 5-labelled probe was combined with an equal amount of Cyanine 3-labelled probe, the mix purified and concentrated using YM-30 Microcon columns, and then resuspended with 10 μg single stranded salmon sperm DNA in 25 μl hybridization solution (25% (w/v) formamide, 5x SSC, 0.1% (w/v) SDS). After heat denaturation at 65°C for 5 min, the denatured probe was added to the array and hybridized overnight in a sealed hybridization chamber at 42°C. After hybridization, slides were washed with 0.1x SSC, 0.1% SDS, and then rinsed in 0.1x SSC and water, and finally dried by centrifugation.

The microarray slides were scanned using a GenePix Scanner 4000A (Molecular Devices Corporation, Sunnyvale, Ca., USA) to measure the fluorescence intensity at 635 nm and 532 nm of each spot. The fluorescence intensity was corrected using local background measurements surrounding each spot using

GenPixPro Version 3 (Molecular Devices Corporation). A GenePixPro *gpr* file, which included all fluorescent intensity measurements, was generated for the array and this file was imported into GeneSpring Version 5 (Agilent Technologies, Forest Hill, Vic., Australia) for statistical analysis to determine which genes were differentially expressed between the powdery mildew infected and healthy samples. The fluorescent intensity values were adjusted using the values obtained for 10 negative control sequences and corrected for dye incorporation biases using Intensity Dependent Normalisation of 100% of the data. When the value of intensity at 532 nm was less than 10, the data point was removed from the analysis. The ratio of normalised Cyanine 5: Cyanine 3 intensity was calculated for each gene, and values greater than 2 or less than -2 were considered to be differentially expressed.

3.2.2 Degenerate PCR, analysis and cloning

HT, cwINV, ProT and AAP degenerate PCR products were PCR amplified (Section 2.2.) from cDNA prepared from total RNA extracted from powdery mildew infected grapevine leaves using BioTaq Red DNA polymerase (Bioline) and the PCR conditions as described (Section 2.2.) Degenerate primer sequences are listed in Table 2.3.

Amplified products were cloned using the pGEM T-Easy Vector System I (Promega) and transformed into XL1-Blue (Stratagene). To screen transformants, inserts were amplified using SP6 and T7 primers which bind left and right of the pGEM T-Easy polylinker, and these products subsequently restricted with *Rsa*I. Analysis of the restriction pattern of individual transformants allowed identification of different insert species which were then DNA sequenced as described (Section 2.2.11).

3.2.3 RT-PCR analysis of selected genes in powdery mildew infected grapevine leaves

Expression analysis was done by real-time PCR using a SYBR green method on a Rotor-Gene 3000 thermal cycler (Corbett Research, Mortlake, Australia). Reactions were run in triplicate and each 15 µl reaction contained: 333 nM of each primer, 3 µl of diluted cDNA (Section 2.2.15), 1 x ABsolute^{TM} QPCR SYBR$^{®}$ Green ROX Mix (Integrated Sciences) and water. The thermal cycling conditions used were 95°C for 15 min followed by 40 cycles of: 95°C for 30 s, 56°C or 58°C for 30 s, and 72°C for 30 s, followed by a melt cycle of 1°C increments from 55 to 96°C. All primer pairs amplified a single product of the expected size and sequence, which was confirmed by melt-curve analysis, agarose gel electrophoresis and DNA sequencing. A set of standards, consisting of isolated PCR product from each primer pair diluted in a 10 fold dilution series (usually 10^{-4} to 10^{-8} dilutions), was used to draw a standard curve from which the target concentration, corresponding to each primer pair, was estimated in each cDNA sample analysed. The concentration of actin was used to normalise the target concentration in each sample. To calculate the change in gene expression, a ratio of normalised target concentration in powdery mildew infected leaves to the target concentration in control leaves was made (infected:control). For negative changes the opposite ratio was calculated. This method was used to estimate the difference in target concentration in powdery mildew infected leaves compared with control leaves to determine if any selected genes are induced or repressed by powdery mildew infection. The change in gene expression does not reflect the level of expression of each gene relative to the others tested. Primer sequences are listed in Table 2.3.

For this analysis, control and powdery mildew infected detached Cabernet Sauvignon leaves were prepared as described (Section 2.1.5). RNA was prepared (Section 2.2.12) from control and infected leaves two days after detachment and inoculation and cDNA synthesised (Section 2.2.13). Under the conditions used, more than 90% of powdery mildew conidia germinate and have established haustoria, as indicated by secondary mycelial extension, within 24 h. At the time sampled, considerable mycelial coverage of the leaf surface was observed using a Stemi 2000 microscope (Zeiss).

3.3 Results

3.3.1 Microarray analysis of powdery mildew infected grape berry skin

RNA was extracted from healthy control and powdery mildew infected (collected 10 DPI) Chardonnay berry skins and Cy3 (control) and Cy5 (infected) labeled probes synthesized. Microarray analysis indicated that 75 (6.1%) of the transcripts on the *V. vinifera* cDNA microarray grape array were differentially expressed more than two fold in powdery mildew-infected berry skins compared with uninfected control samples (Table 3.1). Thirty five of these transcripts were up regulated in response to powdery mildew infection. The largest class of differentially expressed transcripts, which comprised approximately 60% of the up regulated genes, encode typical pathogenesis related and other stress responsive proteins. Members of this class accounted for 17 of the 20 most strongly up regulated transcripts in the powdery mildew infected sample. A group of seven transcripts encoding cell wall and structural proteins such as expansin and peptidylprolyl isomerase homologues were generally down regulated in the infected sample. However, *GRIP 13* (AJ237983), a grape berry ripening-induced gene

Table 3.1. Powdery mildew induced changes to gene expression in grape berry skins determined by microarray analysis. Probes from powdery mildew infected berry skin were labelled with Cy5 and control probes were labelled with Cy3. The array consisted of 1,225 ESTs isolated from grape berries. The array was scanned using a GenePix Scanner 4000A and GenPixPro Version 3 software. Data were analysed using GeneSpring Version 5.

Rank	EST ID	Normalised Ratio LogCy5:LogCy3	StdDev	Best blast match or description
Pathogenesis and stress related				
+1	1414	10.20	0.20	PR-13 cDNA
+2	1432	10.19	0.04	Germin-like gene (VvGLP3)
+3	1422	10.11	0.14	(Y109920) PR5-type Thaumatin-like protein (VvTL2)
+4	1429	9.13	0.90	Stilbene synthase
+5	1433	8.04	2.22	Germin-like gene (VvGLP4)
+6	1417	7.89	0.27	(AF053750) PR2-type basic glucanase (VvGlub)
+7	1430	7.64	0.06	Germin-like gene (VvGLP1)
+8	1412	7.26	0.06	Prl-7 cDNA
+9	1416	7.14	0.17	(U68144) PR2-type basic glucanase (VvGlua)
+10	1415	6.01	0.35	Prl-5 cDNA
+11	1421	5.49	0.60	(Z68123) PR3-type ClassIII basic chitinase (VvChi3)
+12	1413	5.30	0.37	Prl-4 cDNA
+13	1406	4.51	0.90	(AF003007) thaumatin-like protein
+15	1121	4.42	0.44	GLUCAN ENDO-1,3-BETA-GLUCOSIDASE PRECURSOR
+18	1407	3.82	0.46	(AF061329) VVPR-4A cDNA PR-4 type protein
+19	185	3.37	0.13	(X94995) naringenin-chalcone synthase [Juglans nigra x Juglans regia]
+20	1410	3.33	0.21	chalcone isomerase
+28	549	2.67	0.12	(AJ236913) metallothionein-like protein [Elaeis guineensis]
+33	1431	2.29	0.21	Germin-like gene (VvGLP2)
-12	1066	-3.64	0.83	(ABB02395) temperature-induced lipocalin, Vitis vinifera
Cell wall and structural proteins				
+14	1441	4.45	0.21	(AJ237983) Grip 13, Cell wall associated
-24	814	-2.75	0.25	(AAC27459) cellulase, Arabidopsis thaliana
-19	1102	-3.01	0.29	(BAD09075) putative fiber protein Fb14, Oryza sativa
-14	1367	-3.20	0.77	(AAC27459) cellulase (EC 3.2.1.4) F16B22.6 - Arabidopsis thaliana
-7	1453	-3.91	0.71	Expansin 3 (Exp3-4)
-6	1112	-4.08	0.26	(AB015468) peptidylprolyl isomerase [Arabidopsis thaliana]
-2	1246	-5.31	0.26	(AF248055) proline-rich protein [Glycine max]

Rank	EST ID	Normalised Ratio LogCy5:LogCy3	StdDev	Best blast match or description
Membrane channels and transporters				
+17	1265	3.91	0.61	(AAS00691) metal-nicotianamine transporter YSL1 [Arabidopsis thaliana]
+23	526	3.22	0.23	(AF200713) inwardly rectifying potassium channel Kir7.1 [Cavia porcellus]
+24	33	3.10	0.74	(Z70524) PDR5-like ABC transporter [Spirodela polyrrhiza]
-29	1375	-2.60	0.47	(AP002818) putative peptide transporter-like protein [Oryza sativa]
-20	1042	-2.98	0.62	(AAF80557) plasma membrane aquaporin, Vitis vinifera
-4	710	-4.22	0.31	(AF271660) putative aquaporin TIP3 [Vitis berlandieri x Vitis rupestris]
General metabolism				
+16	740	4.14	0.53	(AC004473) Arabidopsis thaliana Similar to red-1 (related to thioredoxin)
+26	314	2.92	0.26	(S71580) GLUTAMINE SYNTHETASE CYTOSOLIC ISOZYME 2
-25	756	-2.73	0.66	(AF044204) lipid transfer protein precursor - upland cotton
-3	1292	-4.63	0.00	cryptogene protein G4 - Leishmania tarentolae (strain LEM125)
Secondary metabolism				
+30	393	2.56	0.39	(AJ238754) phenylalanine-ammonia lyase [Citrus clementina x Citrus reticulata]
+35	510	2.23	0.00	(AF194174) alcohol dehydrogenase 2 [Vitis vinifera]
-35	755	-2.28	0.06	(AC015446) Similar to Allinase [Arabidopsis thaliana]
-15	385	-3.12	0.73	(AAB87126) mannose-1-phosphate guanylyltransferase, Arabidopsis thaliana
Photosynthesis				
-38	1220	-2.16	0.10	(AF139468) photosystem I reaction center subunit III [Vigna radiata]
-30	650	-2.55	0.35	(AF139470) chlorophyll a/b-binding protein CP24 precursor [Vigna radiata]
-18	1154	-3.04	0.48	(AB012639) light harvesting chlorophyll a/b-binding protein [Nicotiana sylvestris]
-16	71	-3.08	0.24	(CAD37939) photosystem I subunit O, Arabidopsis thaliana
-11	1293	-3.76	0.17	(CAB44683) cytochrome P450 homolog F23K16.110 - Arabidopsis thaliana

Rank	EST ID	Normalised Ratio LogCy5:LogCy3	StdDev	Best blast match or description
Transcription factors				
+21	538	3.28	0.07	(AJ237992) putative ripening-related bZIP protein [Vitis vinifera]
+22	476	3.23	0.39	(AF200322) putative glycine-rich RNA binding protein 3 [Catharanthus roseus]
+31	290	2.50	0.13	(AAM65129) putative DNA-binding protein [Arabidopsis thaliana]
-33	1215	-2.34	0.18	(AAA23712) transcription activator of D-serine dehydratase - Escherichia coli
Protein turnover				
+25	213	3.07	0.44	(AB033601) polyubiquitin [Cucumis melo]
+29	607	2.65	0.44	(M62431) nonstructural protein; putative helicase/protease
+32	246	2.45	0.16	(U66264) ubiquitin [Nicotiana tabacum]
-27	1322	-2.68	0.25	(AAT08675) ubiquitin-conjugating enzyme, Hyacinthus orientalis
Heat shock proteins				
-34	265	-2.30	0.29	(AAB63310) small heat-shock protein class I, 18.6K - common sunflower
-21	570	-2.95	0.40	(U13949) AtHSP101 HEAT SHOCK PROTEIN 101, Arabidopsis thaliana
-13	548	-3.34	0.08	(AJ297951) p23 co-chaperone [Arabidopsis thaliana]
Hormone signalling and development				
-31	1274	-2.53	0.14	(AF136539) YABBY2 [Arabidopsis thaliana]
-28	1007	-2.65	0.26	S-ADENOSYLMETHIONINE SYNTHETASE 1 (ethylene production)
-26	634	-2.71	0.48	(T09782) 3-HYDROXY-3-METHYLGLUTARYL-COENZYME A REDUCTASE 1
Unknown or miscellaneous				
+27	397	2.73	0.39	(D84126) leptin receptor(short cytoplasmic form) [Rattus norvegicus]
+34	558	2.24	0.25	(AAC17693) hypothetical protein, Caenorhabditis elegans
-40	324	-2.13	0.03	(CAB36531) hypothetical protein F10M23.190 - Arabidopsis thaliana
-37	281	-2.21	0.15	(AAD18971) ct565 hypothetical protein - Chlamydia pneumoniae
-36	833	-2.27	0.25	No match

Rank	EST ID	Normalised Ratio LogCy5:LogCy3	StdDev	Best blast match or description
Unknown or miscellaneous (continued)				
-32	176	-2.44	0.22	(CAA99759) hypothetical protein SENU1, senescence up-regulated - tomato
-23	1321	-2.75	0.20	(AAC49369) (U34333) proline-rich 14 kDa protein, kidney bean
-22	1200	-2.91	0.03	(AF228877) unknown [Strongylocentrotus purpuratus]
-17	1319	-3.04	0.00	conserved hypothetical protein CP1049, Chlamydophila pneumoniae
-10	1342	-3.77	0.90	(AF090446) unknown [Zea mays]
-9	1223	-3.88	0.23	(CAA49341) ADR11-2 protein - soybean auxin down regulated (X69640)
-5	421	-4.10	0.31	No match
-1	540	-5.53	0.00	(A38958) TRANSLATIONALLY CONTROLLED TUMOR PROTEIN HOMOLOG

proposed to be involved with cell wall modification was 4.45 times more highly expressed in the infected berry skin than in the control sample. *GRIP 55* (AJ237992), another grape ripening induced gene which encodes a bZIP transcription factor, was also elevated in the powdery mildew infected berry skins.

Grape genes encoding membrane channels and transporters were also differentially expressed in response to powdery mildew infection. Thus, a putative tonoplast aquaporin (AF271660) and one plasma membrane aquaporin (AAF80557) were down regulated in the powdery mildew infected sample whereas a metal-nicotianamide YSL transporter homologue (CF403181), an inwardly rectifying potassium channel homologue (CV179380), and an ABC transporter homologue

(CF403138), were induced more than three fold in the infected berry skins. Transcript levels of five photosynthesis related genes and three heat shock proteins were significantly reduced in powdery mildew-infected grape berry skin compared to control samples. Expression of individual members of other functional classes of genes did not change in a consistent manner. A complete list of the ESTs on the array can be found in the Appendix section.

3.3.2 Isolation of partial length grape hexose transporter clones from powdery mildew infected leaves

Multiple sequence alignments of plant HT peptide sequences identified a number of absolutely conserved regions within this family. Using CODEHOP (Rose et al., 1998), a pair of degenerate primers were designed (Table 2.3) to the plant HT family at the conserved residues 'SEMAP' (HTDEGF1) and 'WSWGP' (HTDEGR1) as indicated in Figure 3.1 A.

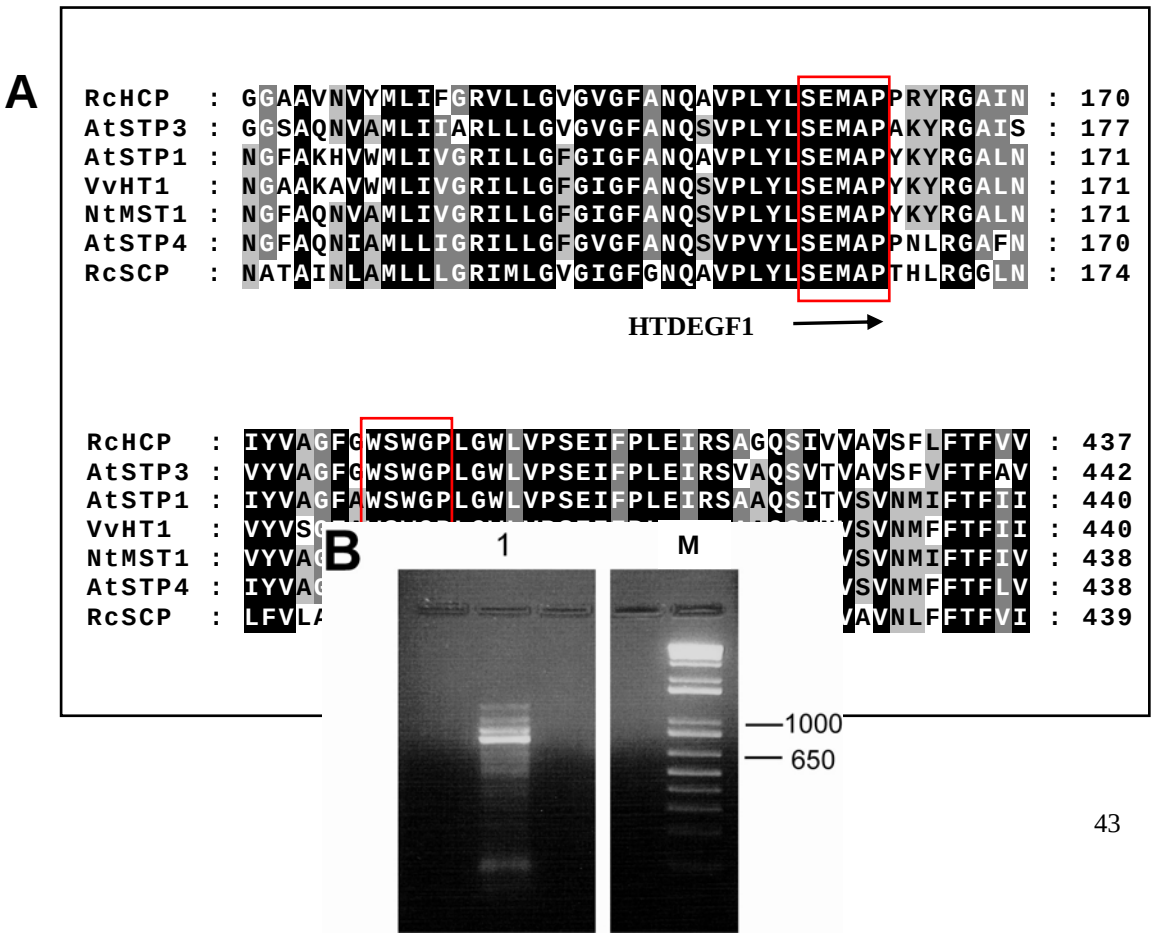

Table 3.2. Homology between predicted translation products of grapevine degenerate HT clones and previously reported plant HT peptides. The percentage identity and similarity (in brackets) between protein sequences as determined by the BestFit algorithm. Bolded values indicate the highest BestFit values. Database accession numbers of the sequences used in the comparison are: VvHT1 (CAA70777), VvHT2 (AY663846), AtSTP7 (AJ344331), AtSTP13 (AJ344338), RcHex6 (AAA79857), AtSTP4 (BAB01308).

	VvHT4	**VvHT5**	**VvHT1**	**VvHT2**	**AtSTP7**	**AtSPT13**	**RcHex6**	**AtSTP4**
VvHT3	61 (74)	56 (73)	56 (66)	53 (64)	**80 (87)**	61 (74)	52 (65)	55 (66)
VvHT4		51 (64)	57 (66)	56 (66)	53 (64)	57 (67)	**80 (89)**	56 (67)
VvHT5			58 (68)	53 (63)	55 (70)	**84 (91)**	50 (64)	52 (65)
VvHT1				57 (56)	57 (66)	61 (69)	58 (70)	59 (69)
VvHT2					52 (62)	54 (64)	54 (65)	53 (65)
AtSTP7						62 (73)	57 (69)	56 (67)
AtSPT13							56 (67)	55 (67)
RcHex6								59 (67)

PCR using the HT degenerate primers HTDEGF1, HTDEGR1 and cDNA template prepared from RNA isolated from powdery mildew infected leaves, amplified two major products around the expected size of 750 bp and other products of different sizes in less abundance (Fig. 3.1 B). Products of the expected size were cloned, inserts amplified using SP6 and T7 primers and these products fingerprinted using *Rsa*I, a restriction enzyme with a four base-pair recognition site, to detect sequence differences. After representative clones of each species were sequenced and analysed using Blast and BestFit analysis, three different HT-like sequences

were obtained. The predicted peptides encoded by the three partial length grape HT degenerate products were observed to share 80-84% amino acid identity with HT proteins from *A. thaliana* and *Ricinus communis* (Table 3.2) and were designated as *VvHT3, VvHT4* and *VvHT5*. These three VvHT sequences share approximately 60% amino acid identity with each other and with the previously reported grapevine sequences *VvHT1* (CAA70777) and *VvHT2* (AY663846) (Table 3.2).

3.3.3 Isolation of a partial length grape cell wall invertase clone from powdery mildew infected leaves

Multiple sequence alignment of cwINV protein sequences identified a number of absolutely conserved regions within this family, however many motifs are also present in vINV protein sequences. In order to avoid amplification of the highly expressed grape vINV genes *GIN1* and *GIN2* (Davies and Robinson, 1996), the cwINVDEGF1 degenerate primer targeted the motif 'WECP' that is conserved within the cwINV family but which is substituted with 'WECV' in vacuolar invertase forms (Fig. 3.2 A). The reverse degenerate primer, cwINVDEGR1, targeted the motif 'GPFG' which is common to both cwINV and vINV forms. The nINV family of cytoplasmic-localised proteins is not homologous at these targeted motifs.

Amplification with cwINV degenerate primer combination cwINVDEGF1 / cwINVDEGR1 produced a single, clean band of approximately the expected size of 650 bp from powdery mildew infected leaf cDNA (Fig. 3.2 B). Cloning and sequencing indicated that degenerate PCR targeting the cwINV family had amplified a single species with homology to the targeted family.

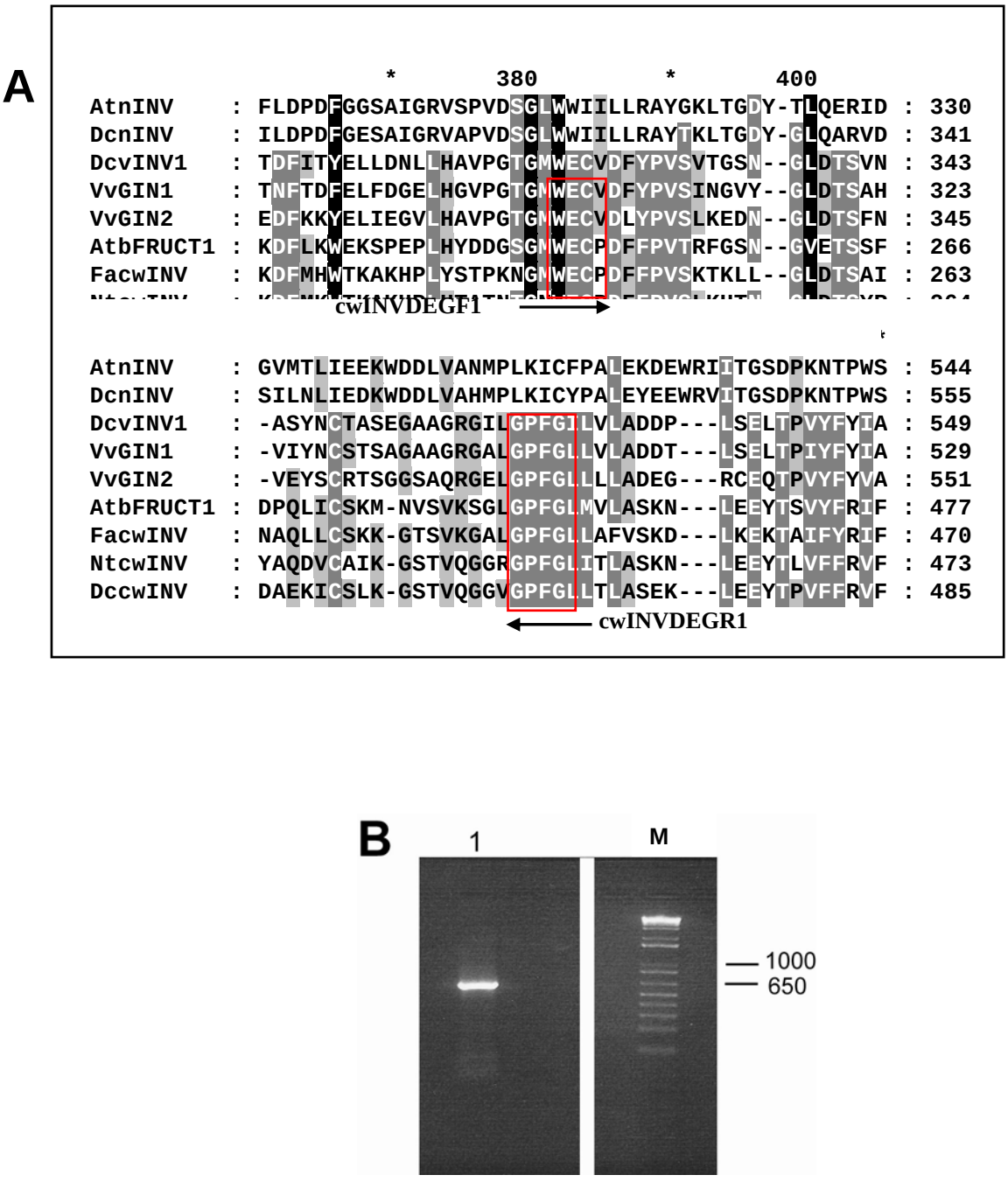

Figure 3.2. Degenerate PCR targeting grapevine cell wall invertase (cwINV). (A) Conserved motifs targeted by degenerate primers. (B) Amplification products generated by PCR using these primers with cDNA template prepared from powdery mildew infected grapevine leaves. Lane 1: degenerate PCR product, M: DNA size markers, in bp. ClustalW was used to make the multiple sequence alignment, only part of which is shown. Accession numbers of the sequences used in the alignment are: AtnINV (AAP40464), DcnINV (CAA76145), DcvINV (P80065), VvGIN1 (AAB47171), VvGIN2 (AAB47172), AtbFRUCT1 (CAA52620), FacwINV (AAD10959), DccwINV (AAA03516), NtcwINV (X81834). Primer sequences are in Table 2.3.

Table 3.3. Homology between the predicted translation product of the grapevine cwINV degenerate clone, two previously reported plant cwINV proteins and the two grapevine vacuolar invertase proteins (VvGIN1 and VvGIN2). The percentage identity and similarity (in brackets) between protein sequences as determined by the BestFit algorithm. Database accession numbers of the sequences used in the comparison are: AtcwINV (NP_566464), BvcwINV (CAB95010), VvGIN1 (AAB47171), VvGIN2 (AAB47172).

	AtcwINV	**BvcwINV**	**VvGIN1**	**VvGIN2**
VvcwINV	65 (75)	69 (74)	46 (54)	48 (53)
AtcwINV		66 (74)	42 (51)	45 (52)
BvcwINV			44 (54)	44 (53)
VvGIN1				62 (70)

Blast analysis and local alignment using BestFit of the predicted peptide encoded by the cwINV degenerate product indicated that it shares approximately 75% amino acid similarity with cwINV sequences from *A. thaliana* (NP_566464) and *Beta vulgaris* (CAB95010) and less than 55% amino acid similarity with the grapevine vINVs GIN1 and GIN2 (Table 3.3).

3.3.4 Isolation of partial length grape amino acid permease and proline transporter clones from powdery mildew infected leaves

Alignment of plant proline transporter (ProT) and amino acid permease (AAP) protein sequences identified conserved regions within these peptide families. Forward and reverse degenerate primers were designed with the assistance of CODEHOP to two of these motifs within each family. In AAPs the conserved peptides targeted were “TYMD” by the forward primer AAPDEGF1 and “EIQD” by the reverse primer AAPDEGR1 (Figure 3.3 A). In ProTs the motifs targeted were

A

```
StAAP1 : FSFITYFTSTLLADCYRSPGPISGKRNYTYMDVVRSHLGGVKVTLCGIAQY :  83
AtAAP1 : FSFITYFTSTMLADCYRAPDPVTGKRNYTYMDVVRSYLGGRKVQLCGVAQY : 129
AtAAP2 : FSLVTLYSSTLLSDCYRTGDAVSGKRNYTYMDAVRSILGGFKFKICGLIQY : 138
RcAAP1 : FSLVTYYTSTLLSACYRSGDPVNGKRNYTYMDAVRTNLGGAKVKLCGFVQY :  67
RcAAP2 : FSLVTYYTSTLLSACYRSGDPVNGKRNYTYMDAVRTNLGGAKVKLCGFVQY : 131
AtAAP3 : FSAVTYFTSSLLAACYRSGDPISGKRNYTYMDAVRSNLGGVKVTLCGIVQY : 122
RcAAP3 : FSLVTYYTSTLLSACYRTGDPVNGKRNYTYMDAVRSNLGGAKFKICGYVQY : 110
AtAAP5 : FSFVTFYTSTLLCSCYRSGDSVTGKRNYTYMDAIHSNLGGIKVKVCGVVQY : 120
                                          ──►
                                          AAPDEGF1

StAAP1 : TGVVVGV-----DVSGTEKVWRSFQAIGDIAFAYAYSTVLIEIQDTLK-SS : 228
AtAAP1 : TGTAVGV-----DVTAAQKIWRSFQAVGDIAFAYAYATVLIEIQDTLR-SS : 273
AtAAP2 : TGISIGT------VTQTQKIWRTFQALGDIAFAYSYSVVLIEIQDTVR-SP : 281
RcAAP1 : TGISIGA-----NVTPTQKIWRSFQALGDIAFAYSYSIILIEIQDTVR-SP : 211
RcAAP2 : TGISIGA-----NVTPTQKIWRSFQALGDIAFAYSYSIILIEIQDTVR-SP : 275
AtAAP3 : TGISIGA------VTETQKIWRTFQALGDIAFAYSYSIILIEIQDTVK-SP : 265
RcAAP3 : TGISIGT------VTETQKIWRSFQALGDIAFAYSYSLILIEIQDTIR-SP : 255
AtAAP5 : TGVTVGTVTLSGTVTSSQKIWRTFQSLGNIAFAYSYSMILIEIQDTVK-SP : 269
                                          ◄──
                                          AAPDEGR1
```

B

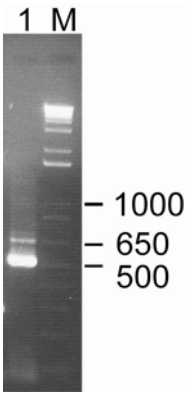

Figure 3.3. Degenerate PCR targeting the grapevine amino acid permease (AAP) gene family. (A) Conserved motifs targeted by degenerate primers. (B) Amplification products generated by PCR using these primers with cDNA template prepared from powdery mildew infected grapevine leaves. Lane 1: degenerate PCR product, M: DNA size markers, in bp. ClustalW was used to make the multiple sequence alignment (A), only part of which is shown. Accession numbers of the sequences used in the alignment are: StAAP1 (CAA70968.2), AtAAP1 (AAB87674), AtAAP2 (CAA50672), RcAAP1 (ABA96629), RcAAP2 (CAA07563), AtAAP3 (CAA54630), RcAAP3 (CAA10608), AtAAP5 (CAA54632). Primer sequences are in Table 2.3.

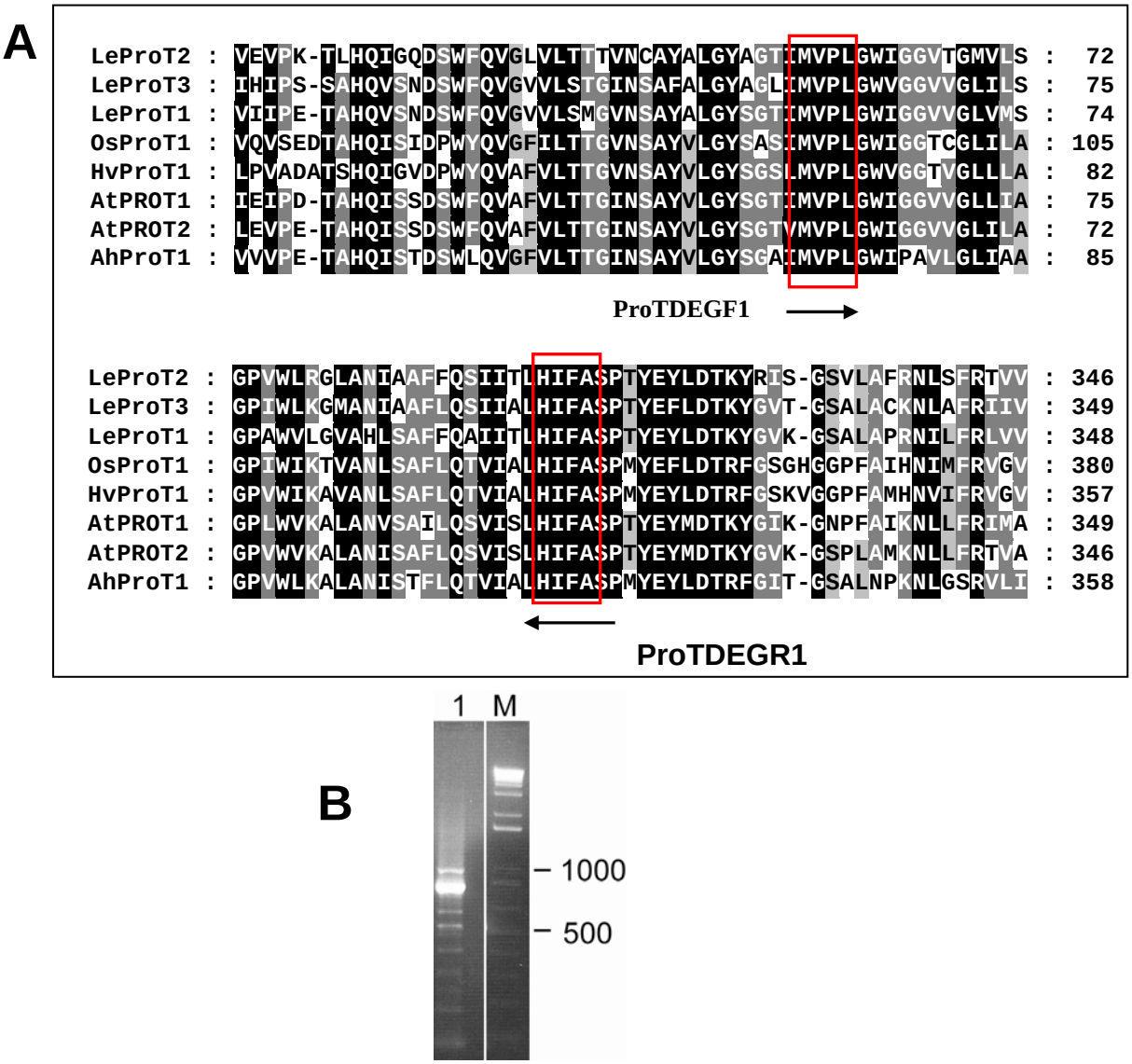

Figure 3.4. Degenerate PCR targeting the grapevine proline transporter (ProT) gene family. (A) Conserved motifs targeted by degenerate primers. (B) Amplification products generated by PCR using these primers with cDNA template prepared from powdery mildew infected grapevine leaves. Lane 1: degenerate PCR product, M: DNA size markers, in bp. ClustalW was used to make the multiple sequence alignment (A), only part of which is shown. Accession numbers of the sequences used in the alignment are: LeProT2 (AAD25161), LeProT3 (AAD25162), LeProT1 (AAD25160), OsProT1 (BAA93437), HvProT1 (BAB69951), AtProT1 (AAB95274), AtProT2 (CAA65053), AhProT1 (AAF7897); Primer sequences are in Table 2.3.

"MVPL" by the forward primer ProTDEGF1 and "FQFT" by the reverse primer ProTDEGR1 (Figure 3.4 A).

PCR with AAP and ProT degenerate primers amplified products of the expected sizes of approximately 520 bp (Fig. 3.3 B) and 850 bp (Fig. 3.4 B) respectively, which were cloned and transformants screened using *Rsa*I fingerprinting as described previously. After sequencing, degenerate PCR targeting AAP and ProT families were found to have amplified a single species with homology to the targeted families. Blast analysis revealed that the AAP and ProT partial sequences encode predicted peptides that share 92% and 89% identity with RcAAP2 (CAA07563) from *Ricinus communis* and AtProT1 (AAB95274) from *A. thaliana* respectively (data not shown).

3.3.5 Semi-quantitative RT-PCR analysis of selected genes in powdery mildew infected leaves

To determine if any of the genes isolated by degenerate PCR were induced during powdery mildew infection, gene-specific primers were designed to each of the partial cDNAs, and to sequences of previously reported HTs (VvHT1 and VvHT2), SUCTs (SUC11, SUC12, SUC27) and vINVs (GIN1 and GIN2). Primers were also designed to two partial grape sequences homologous to plant phosphate transporters, *VvPi1* (AY463369) and *VvPi2* (AY463367) which had been recently cloned in the CSIRO Plant Industry laboratory (Malone and Dry, unpublished data). Additionally, in early 2003 a grapevine EST sequence database became publicly accessible at http://www.tigr.org/tigr-scripts/tgi/T_index.cgi?species=grape. Primers were designed based on grape EST sequences homologous to three neutral (cytoplasmic) invertases (nINVs) (TC7206, TC11451 and TC11207) and two

Table 3.4. Semi quantative RT-PCR analysis of changes in gene expression in response to powdery mildew infection. Detached leaves were inoculated with powdery mildew and sampled two days later. Change in gene expression is the ratio, infected : control expression (induction), or the ratio, control : infected expression (repression). All values were normalised by the level of actin expression in each sample and each value is the average of three replicates. * indicates the gene was isolated in this study.

	Transcript	Accession number	Change transcript amount (fold)
Hexose transporters	VvHT1	CAA70777	1.6
	VvHT2	AY663846	2.17
	VvHT3	*	-1.13
	VvHT4	*	1.5
	VvHT5	*	7.1
Sucrose transporters	VvSUC11	AAF08329	-1.13
	VvSUC12	AAF08330	1.2
	VvSUC27	AAF08331	2.48
Invertases	VvcwINV	*	12.8
	VvGIN1	AAB47171	-1.5
	VvGIN2	AAB47172	2.47
	TC7206	TC7206	2.02
	TC11451	TC11451	1.7
	TC11207	TC11207	1.2
Sucrose synthases	TC4408	TC4408	1.6
	TC5103	TC5103	-1.3
Phosphate transporters	VvPi1	AY463369	-2.6
	VvPi2	AY463367	3
Amino acid transporters	VvAAP	*	1.1
	VvProT	*	1.82

sucrose synthases (SSynth) (TC4408 and TC5103). Semi-quantitative real-time PCR using a Sybr green method was used to measure abundance of the selected transcripts in cDNA prepared from control and powdery mildew infected detached Cabernet Sauvignon leaves sampled two days after detachment and inoculation. The housekeeping gene actin was used as the reference for normalisation of the samples being compared. After normalisation using actin, the ratio of infected:control expression was calculated for each transcript to determine the fold-change in transcript abundance (Table 3.4). Negative changes were calculated using the opposite ratio.

Transcripts of *VvHT5* and *VvcwINV* were 7.1 and 12.8 fold more abundant in powdery mildew infected leaves compared to control samples, respectively (Table 3.4). Expression of the four other putative HTs did not change significantly, but tended to be higher in the infected sample. Similarly, expression of the other invertase forms did not change significantly and, with the exception of the vINV *GIN1*, transcript levels of each tended to be elevated in the powdery mildew infected sample. The putative grapevine phosphate transporters responded differentially to powdery mildew infection with one induced 2.6 fold and one repressed three fold compared to the control, whereas transcript levels of the ProT and AAP degenerate clones were not significantly different in the samples measured.

3.4 Discussion

The general aim of this project is to identify and characterise host genes that might contribute to the metabolic changes observed in powdery mildew infected tissue and thus mediate nutrient delivery to the site of infection. To achieve this goal, two approaches were instigated. Firstly, a general, non-targeted analysis of

gene expression in powdery mildew infected berry skins was conducted using a grapevine microarray consisting of 1,225 ESTs isolated from grape berries at various stages of development. Secondly, based on evidence that indicates changes to carbohydrate and amino acid metabolism in host tissue are associated with powdery mildew infection, a candidate gene approach was initiated using degenerate PCR was used to isolated new grapevine transcripts encoding putative HT, cwINV, AAP and ProT proteins. Subsequent RT-PCR analysis was then used to determine if the abundance of any of these transcripts changed in powdery mildew infected leaves, relative to controls. Additionally, RT-PCR was used to measure expression of previously reported HTs, SUCTs, vINVs and ESTs homologous to nINV and SSynth in powdery mildew infected leaves.

3.4.1 Microarray analysis of powdery mildew infected berry skins

The microarray screen indicated that 75, or 6.1% of the total 1,225 ESTs comprising the array, were differentially expressed (Table 3.1). The largest and most strongly up regulated group encode typical PR and stress induced proteins. Enhanced expression of pathogenesis-related proteins such as chitinases, glucanases and thaumatins has been previously reported in grapevine and in *A. thaliana* infected with powdery mildew, and is taken in the current study as molecular evidence of a host defence response to fungal pathogenesis (Jacobs et al., 1999; Boyd et al., 1994; Reuber et al., 1998). Expression of the secondary metabolism gene phenylalanine-ammonia lyase (PAL) was also increased by PM infection of grape, and elevated PAL expression and enzyme activity in response to pathogen infection is another typical host defence response (McDonald and Cahill, 1999). Recent microarray analysis of *A. thaliana* responses to inoculation with the powdery mildew species

Erysiphe cichoracearum reported induction of a few defence genes only, however in this study probes were prepared from samples collected only 24 h after inoculation, therefore infection and probably host defence responses may have only just commenced (Zimmerli et al., 2004).

Only 3 of the 20 most strongly induced genes do not encode pathogenesis related proteins. Transcripts of *GRIP 13* were 4.45 fold more abundant in powdery mildew infected samples compared to controls and it was the 14th most induced transcript. *Grip 13* encodes a proline rich cell wall associated protein proposed to be involved in cell wall modification and repair during the ripening phase of berry development (Davies and Robinson, 2000). Considering that cell wall penetration is required for powdery mildew infection, the induction of GRIP 13 may be associated with defence and repair in response to this injury.

A member of the ubiquitous thioredoxin gene family (CF403952) was also up-regulated more than 4 fold and was the 16th most strongly induced gene in powdery mildew infected grape berries, relative to controls. In addition to a protective role against oxidative damage, specific thioredoxins have been implicated in the host response to exogenous stress stimuli. For example, expression of a thioredoxin from *A. thaliana, AtTRXh5,* is strongly and rapidly induced in response to pathogen infection and wounding while another related gene did not respond (Laloi et al., 2004).

Interestingly, a putative metal-nicotianamine transporter, or YSL homologue, was identified by the microarray to be induced 3.9 fold in response to powdery mildew infection and was the 17th most strongly induced gene. The *Arabidopsis* genome contains a family of eight YSL proteins and two of these have been shown to transport iron and copper complexed with nicotianamine (DiDonato

et al., 2004). YSLs are expressed in vascular associated cells of roots, leaves and shoots (DiDonato et al., 2004) indicating that nicotianamine-complexed metals are transported throughout plants. Microarray analysis showed that *YSL3* from *A. thaliana* was down regulated in root-knot nematode infected roots (Hammes et al., 2005), however no other data regarding the expression of this family of transporters in response to pathogen infection is currently available. YSL peptides are grouped within the oligopeptide transporter (OPT) family, and expression of another grapevine OPT homologue was repressed in the powdery mildew infected berry skins approximately 2.6 fold compared with controls. The array study of Hammes *et al*. (2005) reported that expression of two additional OPT genes declined during root-knot nematode infection, however the identity of these genes is not available.

Grapevine aquaporins, one homologous to tonoplast membrane intrinsic proteins (TIP) and one homologous to plasma membrane intrinsic proteins (PIP), were observed to be down regulated in powdery mildew infected grapevine tissue (Table 3.1). A family of at least 8 TIP and PIP aquaporins have been identified in grapevine (Baiges et al., 2001). Specific members are expressed in most grapevine tissues and some are developmentally regulated (Baiges et al., 2001; Picaud et al., 2003). Recent studies indicate that expression of two PIPs are up regulated in water stressed grapevine roots and homologues from other plant species are differentially responsive to stress stimuli (Vandeleur and Tyerman, unpublished data). Individual TIPs and PIPs expressed in *A. thaliana* roots were down or up regulated in response to treatment with 100 mM NaCl, drought and exogenous ABA application (Boursiac et al., 2005; Jang et al., 2004). In tomato, expression of *LeAqp2* is induced within 6 h after inoculation with an incompatible pathogen while expression of *TRAMP*, a closely related gene, was not altered (Werner et al., 2001). Specific aquaporins have

also been shown to be strongly induced in the Rhizobial, arbuscular mycorrhizal and root-knot nematode biotrophic interfaces, further indicating that individual members of the aquaporin gene family are regulated by diverse stimuli (Miao and Werma, 1993; Roussel et al., 1997; Opperman et al., 1994).

Genes associated with photosynthesis were down regulated in the powdery mildew infected berry skins (Table 3.1). At the developmental stage when these berries were sampled, they are green and photsynthetically active and have not yet proceeded into the ripening phase where colour development and sugar accumulation occurs. Reduced activity of key photosynthetic enzymes was measured in barley leaves infected with powdery mildew, while net CO_2 fixation declined in powdery mildew infected grapevine leaves by approximately 50% (Scholes et al., 1994; Brem et al., 1986). Scholes *et al*. (1994) suggested that elevated sugar levels associated with pathogen infection may cause a gradual decline in the Calvin cycle which, in turn, inhibits photosynthetic activity.

3.4.2 Isolation of HT, cwINV, AAP and ProT transcripts by degenerate PCR

Using a degenerate PCR approach new grapevine transcripts that encode putative HT, cwINV, AAP and ProT proteins were isolated. Fillion *et al*. (1999) had previously reported two grapevine HT sequences: *VvHT1* and *VvHT2*. In the current study, three new partial sequences homologous to plant HT peptides were isolated (*VvHT3, VvHT4, VvHT5*), indicating that a family with at least five HT genes is encoded in the grapevine genome: in *A. thaliana* the STP family contains approximately 12 members (Büttner and Sauer, 2000). The TIGR grape gene index (http://www.tigr.org/tigr-scripts/tgi/T_index.cgi?species=grape) contains one EST identical to *VvHT3* (TC47882), however ESTs of *VvHT4* and *VvHT5* were not

identified in the database. Obviously, isolation of the full length cDNAs of *VvHT3*, *VvHT4* and *VvHT5*, and subsequent analysis, will establish if these transcripts do encode functional HT proteins.

Degenerate cloning targeting the cwINV family isolated one transcript homologous to each group, and other non-related sequences. Blast and BestFit analysis of the predicted peptide encoded by cwINV showed that it shares most homology with cwINV peptides from other plant species and considerably less with vINV peptides such as those reported by Davies and Robinson (1996). The TIGR grape gene index contains one EST (TC42830) that shares 96% amino acid identity with the predicted peptide encoded by the cwINV degenerate clone.

As was observed with the cwINV degenerate cloning, one sequence homologous to the AAP and ProT families were isolated amongst other unrelated transcripts. The TIGR grape gene index contains at least four ESTs homologous to the AAP family (TC39577; CF213995; CB342010, CB344631), although none shares more than 60% identity with the predicted AAP peptide encoded by the sequence isolated by degenerate PCR, indicating this clone represents a different form. Furthermore, this suggests there are multiple AAP genes in grapevine, which is consistent with the multi-member AAP family identified in *A. thaliana* (Fischer et al., 1998). In contrast, the TIGR index contains two ESTs identical to the putative ProT partial cDNA isolated by degenerate PCR, but no other sequences that encode peptides that are homologous to ProT proteins.

There are several possible scenarios that would explain why only one sequence belonging to the cwINV, AAP and ProT families were isolated while three HT sequences were identified. Firstly, the species amplified may be the most prevalent forms of the targeted families represented in the template cDNA and

therefore other species may have been amplified at a relatively low frequency. This seems a likely explanation for the ProT and cwINV clones because only one member of these families is found on the TIGR EST database. Alternatively, despite designing the cwINV, AAP and ProT degenerate primers to include the majority of nucleotide possibilities at the conserved motifs targeted, these primers may have some innate bias towards the forms amplified and therefore may not have primed amplification of other related species as efficiently.

3.4.3 Semi-quantitative RT-PCR analysis of selected genes in powdery mildew infected leaves

Semi-quantitative RT-PCR was used to measure the change in abundance of 20 selected transcripts in cDNA prepared from powdery mildew infected leaves compared with cDNA prepared from uninfected control leaves. The largest changes observed were 12.8 fold and 7.1 fold increases in *VvcwINV* and *VvHT5* transcripts in the infected sample, respectively. Both genes are previously unreported in grapevine, however in other plants species, pathogen infection and other stress stimuli are known to induce expression of homologous genes. For example, the expression or enzyme activity of cwINV from *Daucus carota*, *Pisum sativum, C. rubrum* and *A. thaliana* is observed to increase in response to infection by a diverse range of pathogen species, and the carrot and *C. rubrum* homologues are also induced by wounding (Sturm and Chrispeels, 1990; Clarke and Hall, 1998; Roitsch et al., 2000; Chou et al., 2000). The two previously reported HTs from grapevine, *VvHT1* and *VvHT2* are developmentally regulated during grape berry ripening, however their expression pattern in pathogen infected or other stressed tissues has not been documented (Fillion et al., 1999; Vignault et al., 2005). The family of

approximately 12 HTs from *A. thaliana* (called STPs for Sugar Transport Proteins) contains two pathogen or wound induced members, *AtSTP4* and *AtSTP3*. *AtSTP4* is rapidly and strongly induced by wounding while *AtSTP3* responds more slowly and by a smaller amount (Truernit et al., 1996; Büttner et al., 2000). A recent study of powdery mildew infected leaves showed that expression of *AtSTP4* and one of four cwINV genes, *AtβFRUCT1*, are co-ordinately induced (Fotopoulos et al., 2003). The proposed physiological significance of the induction of cwINV and HTs in response to pathogen infection suggests the formation of a new carbohydrate sink via elevated phloem unloading of sucrose (Patrick, 1997). Additional carbohydrate may provide energy for host defence or repair, or in terms of the biotrophic interface, increased availability of carbohydrate for pathogen nutrition (Truernit et al., 1996; Fotopoulos et al., 2003). In grapevine leaves infected with powdery mildew, the specific induction of one of eight sucrose cleaving enzymes and one of five HTs indicates that these particular genes contain unique qualities that mediate this responsiveness, or that the localisation of the gene products may be of particular significance during infection.

The other significant change identified by RT-PCR analysis was the differential response of the host phosphate transporters *VvPi1* and *VvPi2*. In leaves, *VvPi1* is constitutively expressed while *VvPi2* expression increases during leaf expansion (J. Malone and I.B. Dry, unpublished data). Interestingly, powdery mildew infection strongly repressed *VvPi1* expression and simultaneously elevated *VvPi2* transcript levels. Expression of specific phosphate transporters from *Medicago truncatula* were also repressed or up-regulated in response to infection with Arbuscular Mycorrhizal (AM) fungi (Liu et al., 1998; Harrison et al., 2002). These fungi associate with a diverse range of plant species and contribute to plant

phosphorus nutrition in exchange for reduced carbon in a mutualistic relationship. *MtPT1* and *MtPT2* are down regulated during the development of the association while *MtPT4* is expressed exclusively in AM infected cells (Liu et al., 1998; Harrison et al., 2002). Furthermore, MtPT4 protein co-localises with the peri-arbuscular membrane, consistent with a role in retrieving fungal released phosphate (Harrison et al., 2002).

Chapter 4 - Isolation and functional characterisation of full length hexose transporter and cell wall invertase genes from grapevine

4.1 Introduction

In *A. thaliana*, rice and tomato, molecular studies and genome sequencing have established that monosaccharide transporters are encoded by multi-member gene families (Büttner and Sauer, 2000; Gear et al., 2000; Toyofuku et al., 2000). In the plant kingdom, the best characterised family is from *A. thaliana*: it contains 14 members which are differentially expressed in response to spatial, temporal and exogenous cues, but are predominantly expressed in sink organs such as roots and reproductive structures (Büttner and Sauer, 2000). All plant monosaccharide transporters characterised range in size from approximately 510 to 560 amino acids and hydrophobicity profiles indicate the presence of 12 membrane-spanning domains with a large cytoplasm-located loop between domains six and seven (Büttner and Sauer, 2000). Using the yeast heterologous expression system, the function of HTs from a range of plant species has been successfully demonstrated. In yeast, plant HT function is sensitive to external pH and the addition of proton ionophores, consistent with proton-symport energetics (Boorer et al., 1992; Gear et al., 2000). Most plant HTs appear to have a strong preference for glucose as substrate, but are capable of transporting other monosaccharides such as fructose, galactose and mannose at lower rates (Weber et al., 1997; Scholz-Starke et al., 2003).

At the commencement of this project, two putative grapevine monosaccharide transporters (*VvHT1* and *VvHT2*) had been reported by Fillion *et al*.

(1999) and more recently, *VvHT1* has been demonstrated to be functional by heterologous expression in yeast (Vignault et al., 2005). In Chapter 3, three partial length cDNAs homologous to plant monosaccharide transporters were cloned from powdery mildew infected leaves. In this chapter, the isolation of full length *VvHT* cDNAs is described and the function and sub-cellular localization of the encoded proteins analysed.

Plant invertases are also encoded by multi-member gene families and their expression and activity is subject to extensive regulation (Tymowska-Lalanne and Kreis, 1998). The encoded proteins are localized to three cellular compartments: the vacuole, cytoplasm and apoplasm, where they catalyse the hydrolysis of sucrose into the hexose monomers, glucose and fructose. In grapevine, Davies and Robinson (1996) reported the isolation of two vacuolar (vINV) isoforms from grapevine, *GIN1* and *GIN2*, however a cell wall invertase (cwINV) has not been previously reported. In Chapter 3, a partial cwINV clone was isolated from powdery mildew infected leaves and in this Chapter the cloning and analysis of a full length cwINV clone is described.

4.2 Materials and methods

4.2.1 RACE PCR and amplification of full length cDNAs

After cloning and sequencing of partial cDNA fragments (Section 3.3.2), full-length cDNA sequences and clones were obtained using RACE PCR techniques (Frohman et al., 1988). For amplification of 3' cDNA ends, target cDNA was amplified using 25 ng of a target-specific forward primer and 25 ng of the oligodT-adapter B26 primer, using grapevine leaf cDNA as template. All target specific

primers were designed to produce approximately 100 nt overlaps with the partial cDNA fragments from Chapter 3 to facilitate unambiguous alignment.

For amplification of 5' cDNA ends, first-strand cDNA was synthesized using 25 ng of a target-specific reverse primer, 1 µg of DNase-treated total RNA and the SuperScript III First-Strand Synthesis System for RT-PCR (Invitrogen) according to the manufacturer's instructions. The cDNA was then purified using the QIAquick PCR purification kit (Qiagen) and resuspended in a final volume of 20 µl. Half of the cDNA reaction was treated with 1 µl of Terminal deoxynucleotide transferase (TdT; Invitrogen) in the buffer supplied and supplemented with 200µM dCTP to add homopolymeric tails of dCTP to the 3'-ends of the cDNAs. C-tailed cDNAs were purified again using the QIAquick PCR purification kit and resuspended in a final volume of 20 µl. Target molecules were amplified from 2 µl of C-tailed cDNA using 25 ng of the AAP (Oligo-dG^{14}) forward primer, which anneals to the homopolymeric tail at the 3'-ends of the cDNAs, and 25 ng of a target-specific reverse primer.

For both 3' and 5' RACE, standard PCR techniques (Section 2.2.1) using 1 unit of recombinant BioTaq Red DNA polymerase (Bioline) were used to amplify the targets. Target DNA was cloned into pGEM T-Easy or pDRIVE vectors and sequenced using T7 and SP6 primers (Table 2.3) as described in Chapter 2.

The RACE sequences were aligned with the degenerate products isolated in Chapter 3 manually using GeneDoc (www.psc.edu/biomed/genedoc) and ORFs and translation products predicted using ORF Finder (http://bioinformatics.org/sms/orf_find.html). After sequence coverage of complete mRNA molecules, new oligonucleotide primers were designed incorporating the predicted initiation and termination codons. Using these primers, full-length cDNAs

were amplified from grapevine powdery mildew infected leaf cDNA with HiFi *Taq* High Fidelity DNA polymerase (Invitrogen) in the buffers supplied and according to the protocols of the manufacturer. These products were cloned into pGEM T-Easy or pDRIVE vectors as described in Chapter 2. All oliognucleotide primers are listed in Table 2.3.

4.2.2 Preparation of DNA constructs for functional characterisation of HTs in yeast

The yeast expression vector p426Met25 (Mumberg et al., 1994), which contains the *URA3* gene for uracil prototrophy and the Met25 promoter for constitutive expression of a trans-gene, was used for heterologous expression of grapevine HTs. Full length cDNAs of *VvHT3*, *VvHT4* and *VvHT5* were sub-cloned from pGEM T-Easy or pDRIVE vectors into p426Met25 via *Eco*RI and *Hind*III restriction sites designed into the forward and reverse primers respectively. After PCR amplification and cloning into pGEM T-Easy, the *VvHT1* full length cDNA was subcloned into p426Met25 via *Bam*HI and *Eco*RI sites designed into the primers. Primer sequences are listed in Table 2.3.

4.2.3 Lithium acetate yeast transformation

Yeast cultures, in 5 ml of YPM, were incubated at 30°C overnight with shaking. The following day, 50 ml of YPM was inoculated with the overnight culture to an OD_{600} of 0.2 - 0.3 and grown at 30°C with shaking for 4 h. Cells were pelleted by centrifugation at 1000 *g* for 5 min, resuspended in 20 ml sterile water, pelleted again, and resuspended in 1.5 ml of YT1. For transformation, 200 ng of

plasmid DNA, 100 μg of denatured salmon sperm DNA, 100 μl of resuspended cells and 600 μl of YT2 were mixed in microcentrifuge tubes. After vortexing, tubes were incubated at 30°C with gentle shaking for 30 min. A 70 μl volume of DMSO was added and the tubes mixed by gentle inversion and incubated at 42°C for 15 min. After cooling on ice for 2 min, cells were pelleted at 16,000 *g* for 15 s and resuspended in 0.4 ml TE buffer. Aliquots of 200 μl of transformation mix was spread on 90 mm plates, and incubated at 30°C for 2 days.

4.2.4 Functional characterisation of HTs in yeast

After selection for uracil prototrophy on minimal media uracil drop-out plates, 5 ml cultures of transformants of strain *EBY.VW4000* carrying p426Met25-*VvHT1*, p426Met25-*VvHT3*, p426Met25-*VvHT4*, p426Met25-*VvHT5* and p426Met25 vector alone, were grown in uracil drop-out media (Table 2.2) overnight at 30°C with shaking. The following day, 100 ml of uracil drop-out medium was inoculated with the overnight culture to an OD_{600} of 0.2 - 0.3 and grown at 30°C with shaking for 4 h or until an OD_{600} of 1.0 - 1.2 was reached. Cells were pelleted by centrifugation, washed twice with 25mM $NaHPO_4/NaH_2PO_4$ (pH 5.0) and resuspended in this buffer at a final concentration of 10 OD_{600} units per ml.

For each measurement, one OD_{600} unit (100 μl) of cell suspension was incubated at 30°C on a shaking water bath for 2 min prior to addition of 100 μl of D-[U-^{14}C]glucose (specific activity: 185 KBq μmol^{-1}; Amersham Biosciences) at the specified concentration in 25mM $NaHPO_4/NaH_2PO_4$ (pH 5.0) and incubated for 30 min. Duplicate samples of 100 μl were pipetted directly into 10ml cold water, filtered onto GF/C filters (Whatman, #1822021) followed by two washes with 15ml

cold water. Filters were removed, placed into scintillant and incorporation of radioactivity determined using a Beckman LS3801 liquid scintillation counter. For competitor and inhibitor studies, D-[U-^{14}C]glucose concentration was 100μM, competing sugars were at 500μM and CCCP was at 50μM. Transport activity was determined per FW of yeast cells.

4.2.5 Analysis of GFP-fusion proteins by micro-projectile bombardment

The pART7 vector (Gleave, 1992) was modified to produce pART7-C'gfp which contains the full length *GFP* ORF (lacking the start codon) downstream of the multiple cloning site (T. Franks, unpublished results), and used to transiently express VvHT3:GFP and VvHT4:GFP fusion proteins in onion epidermal strips. Full length *VvHT3* and *VvHT4* cDNAs were amplified using primers HT3GFPfwd/HT3GFPrev, HT4FLfwd/HT4GFPrev with HiFi *Taq* High Fidelity DNA polymerase and cloned into pART7-C'gfp using *Xho*I and *Xba*I (VvHT3:GFP) or *Eco*RI and *Xba*I (VvHT4:GFP) sites within the primers (Table 2.3). Also used in this experiment was pART7-ATG:GFP (T. Franks, unpublished results) which expresses free GFP. The localization of GFP fusion proteins was determined by bombardment of GFP constructs into onion epidermal strips and subsequent visualization using confocal microscopy.

The internal surface of onion epidermal peels were placed facing up on agar plates containing Murashige and Skoog (MS) Salt Mixture (Invitrogen) and bombarded with the vectors. For four shots, 400 μg of gold particles in 100 μl ethanol were vortexed for 2 min, spun down for 10 s in a microfuge, drained, washed twice with sterile water, and resuspended in 25 μl of 40% glycerol. While gently vortexing, 4 μl of the plasmid solutions (400 ng μl^{-1}), 10 μl of cold 0.1 M

spermidine and 25 µl 2.5 M $CaCl_2$ were added drop-wise and this mixture incubated on ice for 10 min. The particles were spun down, washed with 70% ethanol, resuspended in 24 µl cold absolute ethanol and 6 µl aliquots were placed onto sterile filter holders. After sterilising the gun chamber with 70% (v/v) ethanol, plates containing onion strips on MS media were placed inside, covered with a sterile mesh, and bombarded with a pressure of 650 kPa after evacuating the chamber to 90 kPa. After bombardment, tissue was stored in the dark for 48 h and GFP fluorescence visualised using a Bio-Rad Radiance 2100 Confocal Laser Scanning Microscope System (The Hanson Institute Detmold Family Trust Cell Imaging Centre, Institute for Medical and Veterinary Science, Adelaide, Australia). The excitation wavelength used for GFP detection was 488nm.

4.2.6 Sequence analysis and manipulation

DNA sequences were analysed using various basic local alignment search tools (BLAST) served at the National Centre for Biotechnology Information (NCBI) website (http://www.ncbi.nlm.nih.gov/BLAST/) and the GCG WebAngis Wisconsin software package operated by the Australian National Genomic Information Service (http://www.angis.org.au/). Multiple sequence alignments were drawn by Pile Up or ClustalW (both served at ANGIS), displayed and further manipulated using GeneDoc (www.psc.edu/biomed/genedoc) and after RACE sequences were joined, open reading frames (ORFs) were predicted using ORF Finder (http://bioinformatics.org/sms/orf_find.html). Cellular location and potential signal peptides of deduced amino acid sequences were predicted using PSORT (http://psort.nibb.ac.jp/form.html; Nakai and Horton, 1999), WoLFPSORT (http://wolfpsort.seq.cbrc.jp/; Horton, Park, Obayashi and Nakai, manuscript in

preparation), PLOC (http://www.genome.jp/SIT/plocdir/; Park and Kinehisa, 2003), SignalP 3.0 (http://www.cbs.dtu.dk/services/SignalP/; Bendtsen et al. 2004), IPSORT (http://hc.ims.u-tokyo.ac.jp/iPSORT/; Bannai et al., 2002) and ChloroP (http://www.cbs.dtu.dk/services/ChloroP/; Emanuelsson et al., 1999). Transmembrane helices were mapped using TMHMM Server v.2.0 (http://www.cbs.dtu.dk/services/TMHMM/ ; Krogh et al. 2001) and theoretical isoelectric points were calculated using Iep, served at ANGIS (http://www.angis.org.au/).

4.3 Results

4.3.1 Analysis of full length VvHT sequences

Based on the sequences of the partial clones isolated in section 3.3.2, RACE PCR methods were used to isolated full length cDNAs of *VvHT3*, *VvHT4* and *VvHT5*. The target specific oligos used to amplify 5' and 3' cDNA ends, primed products with approximately 100 bp sequence overlap with the partial clones. Over these overlapping regions, RACE and degenerate clones were observed to share 100% sequence identity and therefore concluded to be fragments from the same transcript (data not shown). These sequences were joined and ORFs predicted using ORF Finder, which identified a single ORF in each sequence between 5' and 3' untranslated regions. New primers were designed to incorporate predicted start and stop codons and these used to amplify full length cDNAs using a high fidelity polymerase. The sequences of full length *VvHT3*, *VvHT4* and *VvHT5* cDNAs were

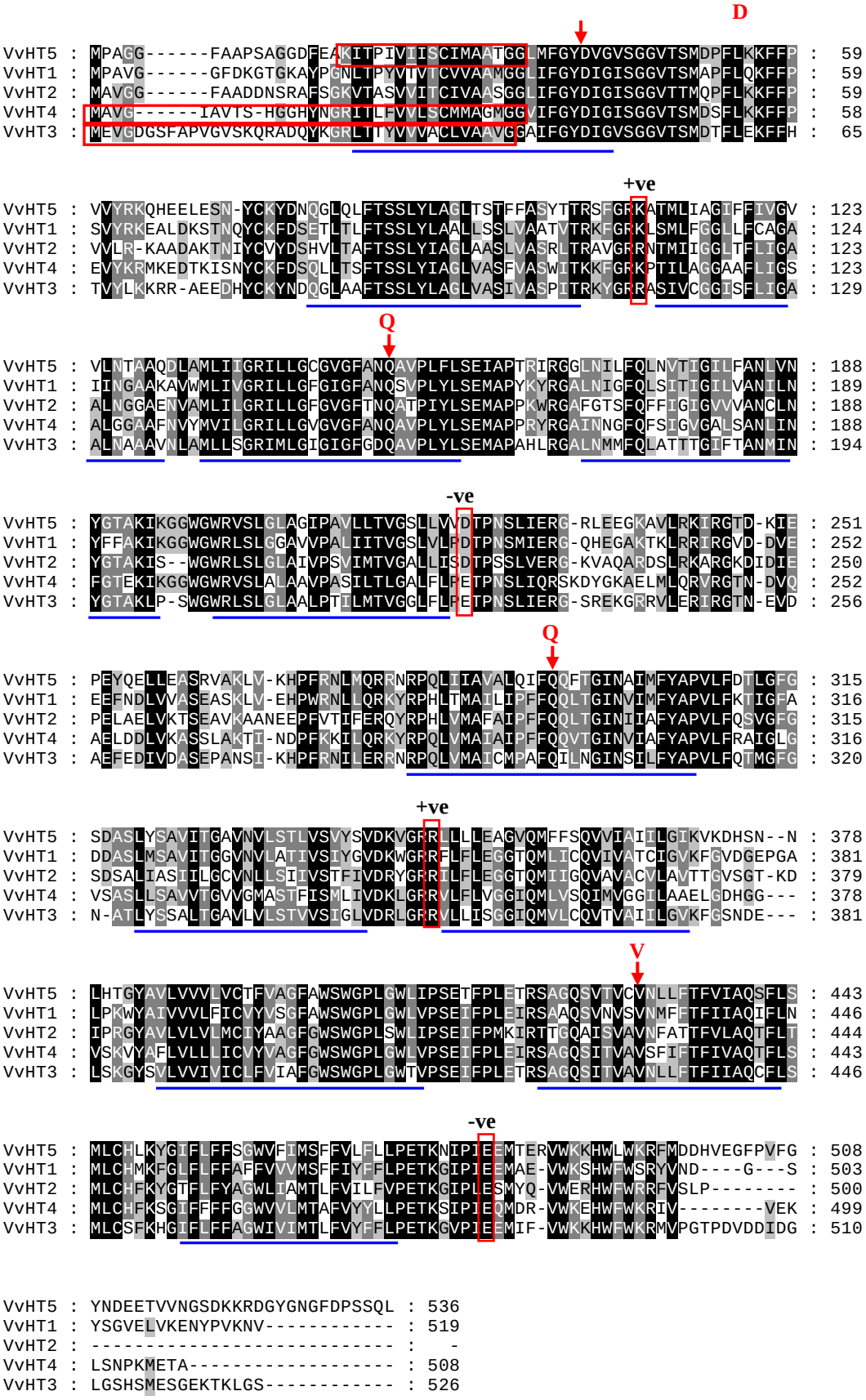


```
VvHT5 : MPAGG------FAAPSAGGDFEAKITPIVIISCIMAATGGLMFGYDVGVSGGVTSMDPFLKKFFP :  59
VvHT1 : MPAVG------GFDKGTGKAYPGNLTPYVTVTCVVAAMGGLIFGYDIGISGGVTSMAPFLQKFFP :  59
VvHT2 : MAVGG------FAADDNSRAFSGKVTASVVITCIVAASGGLIFGYDIGISGGVTTMQPFLKKFFP :  59
VvHT4 : MAVG------IAVTS-HGGHYNGRITLFVVLSCMMAGMGGVIFGYDIGISGGVTSMDSFLKKFFP :  58
VvHT3 : MEVGDGSFAPVGVSKQRADQYKGRLTTYVVVACLVAAVGGAIFGYDIGVSGGVTSMDTFLEKFFH :  65

VvHT5 : VVYRKQHEELESN-YCKYDNQGLQLFTSSLYLAGLTSTFFASYTTRSFGRKATMLIAGIFFIVGV : 123
VvHT1 : SVYRKEALDKSTNQYCKFDSETLTLFTSSLYLAALLSSLVAATVTRKFGRKLSMLFGGLLFCAGA : 124
VvHT2 : VVLR-KAADAKTNIYCVYDSHVLTAFTSSLYIAGLAASLVASRLTRAVGRRNTMIIGGLTFLIGA : 123
VvHT4 : EVYKRMKEDTKISNYCKFDSQLLTSFTSSLYIAGLVASFVASWITKKFGRKPTILAGGAAFLIGS : 123
VvHT3 : TVYLKKRR-AEEDHYCKYNDQGLAAFTSSLYLAGLVASIVASPITRKYGRRASIVCGGISFLIGA : 129

VvHT5 : VLNTAAQDLAMLIIGRILLGCGVGFANQAVPLFLSEIAPTRIRGGLNILFQLNVTIGILFANLVN : 188
VvHT1 : IINGAAKAVWMLIVGRILLGFGIGFANQSVPLYLSEMAPYKYRGALNIGFQLSITIGILVANILN : 189
VvHT2 : ALNGGAENVAMLILGRILLGFGVGFTNQATPIYLSEMAPPKWRGAFGTSFQFFIGIGVVVANCLN : 188
VvHT4 : ALGGAAFNVYMVILGRILLGVGVGFANQAVPLYLSEMAPPRYRGAINNGFQFSIGVGALSANLIN : 188
VvHT3 : ALNAAAVNLAMLLSGRIMLGIGIGFGDQAVPLYLSEMAPAHLRGALNMMFQLATTTGIFTANMIN : 194

VvHT5 : YGTAKIKGGWGWRVSLGLAGIPAVLLTVGSLLVVDTPNSLIERG-RLEEGKAVLRKIRGTD-KIE : 251
VvHT1 : YFFAKIKGGWGWRLSLGGAVVPALIITVGSLVLPDTPNSMIERG-QHEGAKTKLRRIRGVD-DVE : 252
VvHT2 : YGTAKIS--WGWRLSLGLAIVPSVIMTVGALLISDTPSSLVERG-KVAQARDSLRKARGKDIDIE : 250
VvHT4 : FGTEKIKGGWGWRVSLALAAVPASILTLGALFLPETPNSLIQRSKDYGKAELMLQRVRGTN-DVQ : 252
VvHT3 : YGTAKLP-SWGWRLSLGLAALPTILMTVGGLFLPETPNSLIERG-SREKGRRVLERIRGTN-EVD : 256

VvHT5 : PEYQELLEASRVAKLV-KHPFRNLMQRRNRPQLIIAVALQIFQQFTGINAIMFYAPVLFDTLGFG : 315
VvHT1 : EEFNDLVVASEASKLV-EHPWRNLLQRKYRPHLTMAILIPFFQQLTGINVIMFYAPVLFKTIGFA : 316
VvHT2 : PELAELVKTSEAVKAANEEPFVTIFERQYRPHLVMAFAIPFFQQLTGINIIAFYAPVLFQSVGFG : 315
VvHT4 : AELDDLVKASSLAKTI-NDPFKKILQRKYRPQLVMAIAIPFFQQVTGINVIAFYAPVLFRAIGLG : 316
VvHT3 : AEFEDIVDASEPANSI-KHPFRNILERRNRPQLVMAICMPAFQILNGINSILFYAPVLFQTMGFG : 320

VvHT5 : SDASLYSAVITGAVNVLSTLVSVYSVDKVGRRLLLEAGVQMFFSQVVIAIILGIKVKDHSN--N : 378
VvHT1 : DDASLMSAVITGGVNVLATIVSIYGVDKWGRRFLFLEGGTQMLICQVIVATCIGVKFGVDGEPGA : 381
VvHT2 : SDSALIASIILGCVNLLSIIVSTFIVDRYGRRILFLEGGTQMIIGQVAVACVLAVTTGVSGT-KD : 379
VvHT4 : VSASLLSAVVTGVVGMASTFISMLIVDKLGRRVLFLVGGIQMLVSQIMVGGILAAELGDHGG--- : 378
VvHT3 : N-ATLYSSALTGAVLVLSTVVSIGLVDRLGRRVLLISGGIQMVLCQVTVAIILGVKFGSNDE--- : 381

VvHT5 : LHTGYAVLVVVLVCTFVAGFAWSWGPLGWLIPSETFPLETRSAGQSVTVCVNLLFTFVIAQSFLS : 443
VvHT1 : LPKWYAIVVVLFICVYVSGFAWSWGPLGWLVPSEIFPLEIRSAAQSVNVSVNMFFTFIIAQIFLN : 446
VvHT2 : IPRGYAVLVLVLMCIYAAGFGWSWGPLSWLIPSEIFPMKIRTTGQAISVAVNFATTFVLAQTFLT : 444
VvHT4 : VSKVYAFLVLLLICVYVAGFGWSWGPLGWLVPSEIFPLEIRSAGQSITVAVSFIFTFIVAQTFLS : 443
VvHT3 : LSKGYSVLVVIVICLFVIAFGWSWGPLGWTVPSEIFPLETRSAGQSITVAVNLLFTFIIAQCFLS : 446

VvHT5 : MLCHLKYGIFLFFSGWVFIMSFFVLFLLPETKNIPIEEMTERVWKKHWLWKRFMDDHVEGFPVFG : 508
VvHT1 : MLCHMKFGLFLFFAFFVVVMSFFIYFFLPETKGIPIEEMAE-VWKSHWFWSRYVND----G---S : 503
VvHT2 : MLCHFKYGTFLFYAGWLIAMTLFVILFVPETKGIPLESMYQ-VWERHWFWRRFVSLP-------- : 500
VvHT4 : MLCHFKSGIFFFFGGWVVLMTAFVYYLLPETKSIPIEQMDR-VWKEHWFWKRIV--------VEK : 499
VvHT3 : MLCSFKHGIFLFFAGWIVIMTLFVYFFLPETKGVPIEEMIF-VWKKHWFWKRMVPGTPDVDDIDG : 510

VvHT5 : YNDEETVVNGSDKKRDGYGNGFDPSSQL : 536
VvHT1 : YSGVELVKENYPVKNV------------ : 519
VvHT2 : ---------------------------- :   -
VvHT4 : LSNPKMETA------------------- : 508
VvHT3 : LGSHSMESGEKTKLGS------------ : 526
```

Figure 4.1. Amino acid sequence alignment of putative grapevine hexose transporters. The full length sequence of *VvHT3*, *VvHT4* and *VvHT5* were cloned by RACE PCR and the ORF and amino acid sequence was predicted using ORF Finder. Signal peptides are marked with horizontal red boxes, conserved and functionally important residues are marked with arrows, and conserved charged residues are marked with vertical red boxes. Residues predicted to form transmembrane helices are underlined with a blue line. The alignment was made with ClustalX (Thompson et al., 1997). The accession numbers used in the alignment are *VvHT1* (CAA70777), *VvHT2* (AY663846).

found to be identical to the full length sequence obtained by joining the initial partial and RACE cDNA clones.

The predicted ORFs of *VvHT3*, *VvHT4* and *VvHT5* encode peptides of 508, 526 and 536 amino acids respectively (Fig. 4.1) which share approximately 60% amino acid identity with predicted peptides of the previously reported grapevine HT genes *VvHT1* and *VvHT2* (Table 4.1). Most of the homology between the VvHT peptides is located within discrete regions predicted to form twelve transmembrane helices in these proteins (Fig. 4.1 and Fig. 4.2). All three VvHT predicted proteins also show the presence of an approximate 60 amino acid cytoplasmic-exposed loop between transmembrane helices six and seven (Fig. 4.2; residues 220 to 290) which is another typical secondary structural element of plant HTs (Büttner and Sauer, 2000). According to SignalP 3.0, VvHT3 and VvHT4 peptides contain predicted *N*-terminal sorting signals: VvHT3 has an uncleaved signal anchor while VvHT4 has a signal peptide cleaved between resides 32 and 33 (Fig. 4.1). SignalP analysis suggested VvHT5 does not contain a *N*-terminal sorting signal, however it is homologous to VvHT3 around the signal peptide cleavage site predicted by SignalP. Conserved charged residues and other functionally important residues (Will et al.,

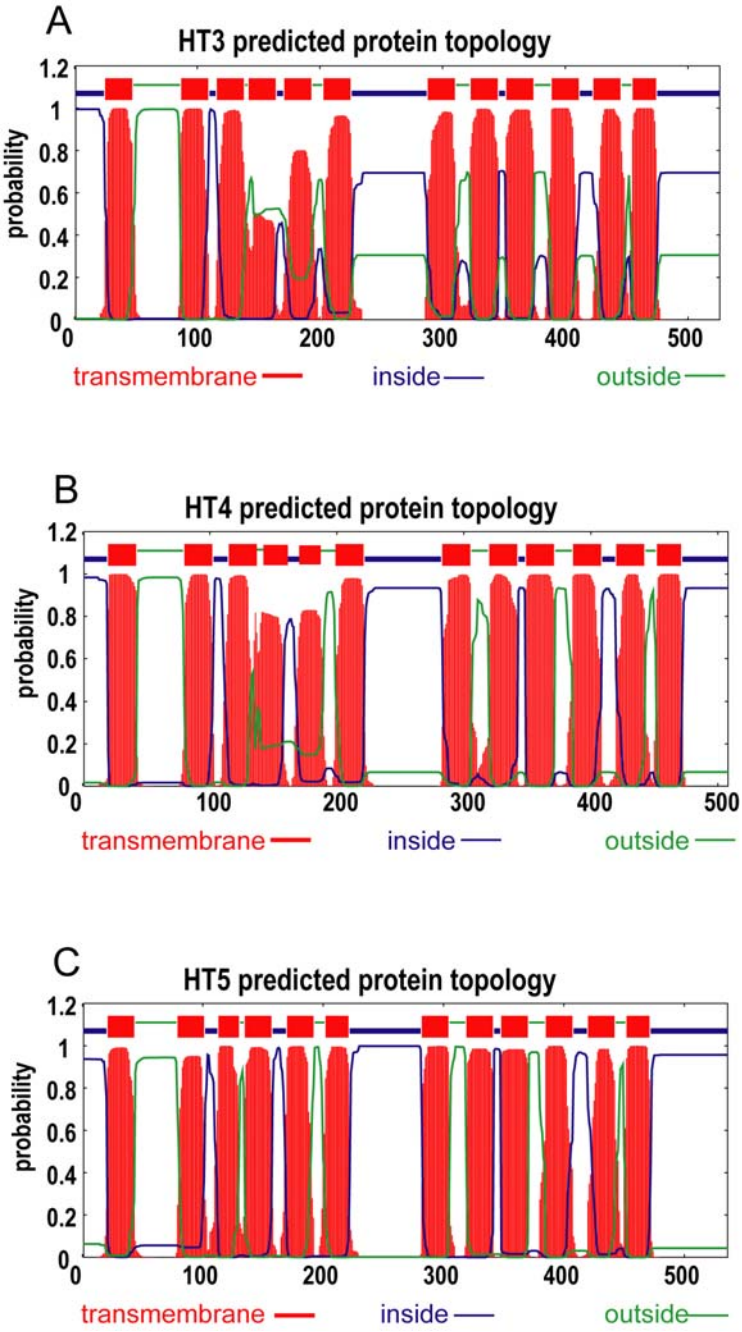

Figure 4.2. Protein topology predicted for VvHT3 (A), VvHT4 (B) and VvHT5 (C) indicates the presence of 12 transmembrane helices and a large cytoplasm-located loop between helices six and seven. THMMH Server v. 2.0 (Krogh et al., 2001) was used to predict transmembrane helices and location of intervening loops.

Table 4.1. Homology between plant hexose transporters. The accssion numbers of the sequecnes used can be found in Figure 4.3. Bolded numbers indicate sequences with the highest level of homology with VvHT3, VvHT4 and VvHT5. The percentage identity and similarity (in brackets) as determined by the Gap algorithm are shown.

	VvHT2	VvHT3	VvHT4	VvHT5	VvHT6	AtSTP1	AtSTP4	AtSTP7	AtSTP8	AtSTP13	CkHUP1	LeHT2	MtST1	NtMST1	RcHex6
VvHT1	57 (66)	56 (64)	58 (66)	58 (68)	26 (35)	83 (88)	62 (72)	56 (64)	51 (63)	59 (67)	46 (56)	57 (67)	82 (87)	81 (87)	57 (67)
VvHT2		53 (64)	56 (66)	53 (63)	25 (35)	57 (66)	53 (65)	52 (62)	48 (60)	54 (64)	43 (53)	52 (63)	56 (65)	56 (67)	54 (65)
VvHT3			58 (67)	56 (68)	24 (32)	56 (65)	54 (64)	**78 (84)**	51 (61)	59 (69)	47 (56)	59 (69)	54 (65)	59 (69)	56 (67)
VvHT4				56 (68)	24 (33)	57 (66)	57 (67)	56 (66)	50 (60)	57 (66)	45 (56)	58 (68)	58 (66)	60 (68)	**80 (88)**
VvHT5					25 (35)	57 (67)	57 (64)	59 (71)	57 (66)	**84 (89)**	47 (57)	**83 (88)**	59 (68)	56 (68)	56 (66)
VvHT6						26 (36)	24 (35)	26 (36)	26 (36)	26 (36)	25 (33)	23 (34)	24 (34)	26 (36)	24 (33)
AtSTP1							62 (71)	56 (65)	51 (64)	58 (66)	46 (56)	55 (65)	80 (85)	80 (85)	58 (67)
AtSTP4								55 (66)	50 (61)	54 (65)	45 (55)	53 (64)	62 (71)	63 (72)	58 (67)
AtSTP7									51 (62)	61 (72)	48 (58)	60 (72)	55 (65)	57 (68)	56 (67)
AtSTP8										58 (67)	47 (58)	60 (68)	51 (62)	53 (66)	50 (60)
AtSTP13											48 (57)	82 (87)	60 (68)	59 (69)	54 (65)
CkHUP1												50 (61)	47 (57)	46 (58)	47 (57)
LeHT2													57 (66)	57 (67)	56 (66)
MtST1														80 (86.	58 (66)
NtMST1															59 (68)

1994) are also present in the grapevine HT peptides and these map to various transmembrane helices and cytoplasm-located loops (Fig. 4.1).

A sixth putative HT sequence from grapevine, *VvHT6* (AAX47312) has also recently appeared on the GenBank database. This transcript encodes a predicted ORF of 740 amino acids, suggested to form 11 transmembrane helices with an approximate 250 amino acid insertion between transmembrane helices six and seven (data not shown). On either side of this insertion, VvHT6 shares significant homology with the other putative grapevine HTs, however overall it is only 30% homologous with these peptides. VvHT6 is homologous to sequences from *A. thaliana* (AAM19835) and rice (XP_464773) however no putative HTs of this type have been functionally demonstrated.

In phylogenetic analysis the grapevine sequences fall into different nodes, indicating that they share more homology with sequences from other plant species than with those from grapevine (Fig. 4.3). VvHT3 shares approximately 80% amino acid identity with AtSTP7 (CAB80698) from *A. thaliana* while VvHT4 shares approximately 80% amino acid identity with RcHex6 (AAA79857; Weig et al., 1994) from *R. communis* (Table 4.1). VvHT5 is most homologous to AtSTP13 (CAC69074) and LeHT2 (AJ132224; Gear et al., 2000) from *A. thaliana* and *Lycopersicon esculentum* respectively. Interestingly, *VvHT1* groups in a node

containing the first HTs isolated from *A. thaliana* (AtSTP1; Sauer et al., 1990), *Medicago truncatula* (Harrison, 1996), *Vicia faba* (VfSTP1; Weber et al., 1997) and *Nicotiana tabacum* (NtMST1; Sauer and Stadler, 1993), while *VvHT2* and *VvHT6* are separated from the other sequences analysed.

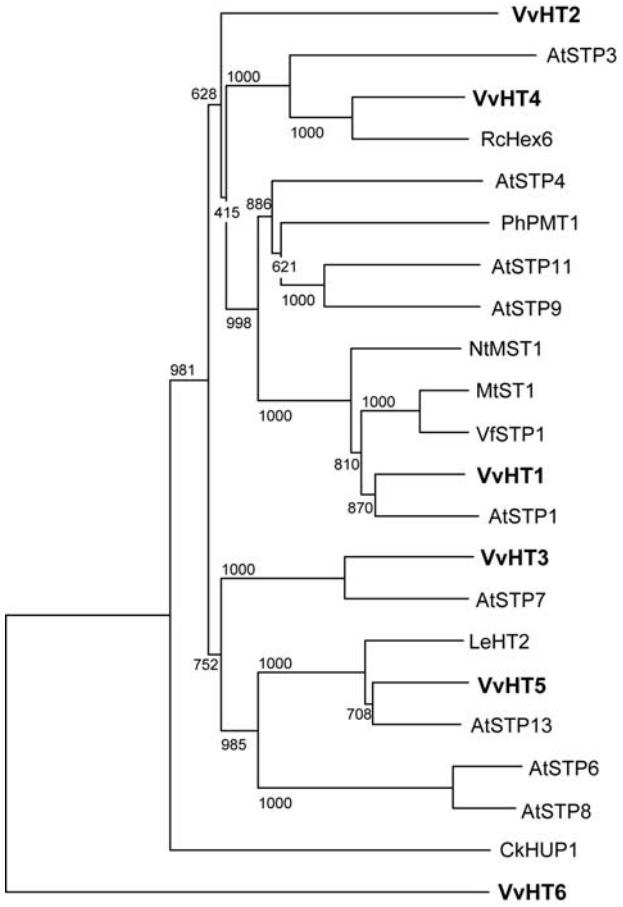

Figure 4.3. Phylogenetic analysis of monosaccharide transporter like sequences from grapevine and other plant species. Multiple sequence alignment was made with ClustalX (Thompson et al., 1997) and phylogenetic analysis was done by the parsimony method with Protpars (Felsenstein, 1989) using VvHT6 as the outgroup. Bootstrap analysis was performed with ClustalX (Thompson et al., 1997), and values shown at internal nodes indicate the occurance of these nodes in 1000 replicates. Database accession numbers of the sequences used are: VvHT6 (AAX47312), VvHT2 (AY663846), AtSTP3 (AJ012399), RcHex6 (AAA79857), AtSTP4 (AB025631), PhPMT1 (AF061106), AtSTP11 (AJ001664), AtSTP9 (AJ001662), NtMST1 (X66856), MtST1 (U38351), VfSTP1 (Z93775), VvHT1 (CAA70777), AtSTP1 (AC007259), AtSTP7 CAB80698), LeHT2 (AJ132224), AtSTP6 (AJ001659), AtSTP13 (CAC69074), AtSTP8 (AF077407), CkHUP1 (X55349).

4.3.2 Functional characterisation of VvHT1, VvHT3, VvHT4 and VvHT5 in yeast

Analysis of the full length sequences of *VvHT3*, *VvHT4* and *VvHT5* suggested that they encode HTs. To demonstrate functionality, each was expressed in the hexose transport-impaired *Saccharomyces cerevisiae* mutant *EBY.VW4000* (Wiezorke et al., 1999) and the rate of D-[U-^{14}C]glucose transport measured. This strain has a very low rate of hexose uptake due to concurrent knockout of 20 endogenous transporter genes, and has been used in recent studies to functionally characterise monosaccharide transporters (Scholz-Starke et al., 2003; Vignault et al., 2005). The functionality of VvHT1 was also tested in this system, and *EBY.VW4000* expressing empty vector was used as a measure of the innate rate of glucose uptake by this strain.

Yeast expressing VvHT1, VvHT4 and VvHT5 accumulated radio-labelled glucose at faster rates than the empty vector control, indicating that they were functional glucose transporters (Fig. 4.4A). In yeast, VvHT1 facilitated the highest rate of glucose transport, estimated to be in excess of 1 μmol min^{-1} g FW^{-1} (Fig. 4.4 A). The rates of glucose transport mediated by VvHT4 and VvHT5 were approximately 10 and 20 fold less than VvHT1 respectively, or approximately 0.1 μmol min^{-1} g FW^{-1} for VvHT4 and 0.04 μmol min^{-1} g FW^{-1} for VvHT5. Glucose uptake into yeast facilitated by VvHT1, VvHT4 and VvHT5 was also sensitive to the pH of the external medium, with uptake rates significantly higher at pH 5.0 than at pH7.0 (Fig. 4.4 B, C and D).

Yeast expressing VvHT3 accumulated radio-labelled glucose at a similar rate to the empty vector control, indicating that VvHT3 was not functioning as a hexose transporter. Even after re-sequencing of the VvHT3 construct, repeat transformation

of yeast and finally re-synthesis of the expression construct and transformation, functionality was not observed.

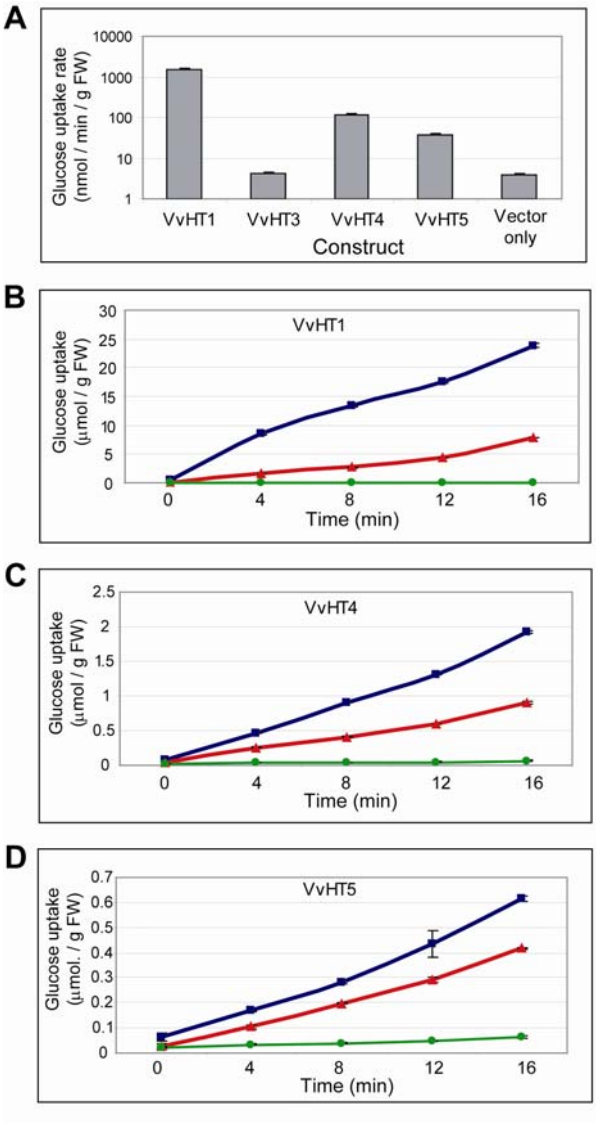

Figure 4.4. Glucose uptake assays in yeast. (A) Relative rates of glucose uptake in yeast expressing grapevine HTs (Note: log scale). (B) Effect of pH on glucose uptake in yeast expressing grapevine HTs. Glucose uptake was measured using 200 µM [^{14}C]-D-glucose in phosphate buffer pH 5.0 (A) or pH as indicated (B, C and D). Yeast strain *EBYVW4000* was transformed with expression constructs containing *VvHT1*, *VvHT3*, *VvHT4* and *VvHT5* ORFs, or empty vector only as a control. Data are means of one transformant tested in duplicate and are representative of two transformants tested. Error bars represent standard errors. pH 5.0, pH 7.0, vector only control .

Each of the functional transporters exhibited concentration-dependant rates of D-[U-^{14}C] glucose uptake (Fig. 4.5 A, C, E). The Lineweaver-Burk double-reciprocal plot of the data displayed a linear relationship, indicating that the glucose transport mediated by these proteins conforms to typical Michaelis-Menten kinetics (Fig. 4.5 B, D, F). Of the three hexose transporters analysed, VvHT1 had the highest affinity for glucose with an estimated K_m for glucose of 67 μM (+/-12.2). VvHT4 and VvHT5 displayed lower affinities for glucose with K_m's of 137 μM (+/-25.5) and 89 μM (+/-12.1) respectively.

To test if VvHT1, VvHT4 and VvHT5 may have affinity for, and therefore potentially transport other sugars, the rate of D-[U-^{14}C]glucose transport was measured in the presence of fructose, galactose, mannose and sucrose supplied at five-fold higher concentrations in an uptake competition assay (Fig. 4.6). Glucose transport by yeast expressing VvHT1 was inhibited more than 60% and 50% by galactose and mannose respectively, and these values were significantly different to controls at the 95% confidence level, as calculated with the student's t-Test. Glucose transport mediated by VvHT4-expressing yeast was slightly inhibited by galactose and mannose, however the students t-Test indicated these values were not significantly different from controls at the 90% confidence level. In contrast, glucose transport facilitated by VvHT5 was not significantly inhibited in the presence of galactose and mannose but was reduced approximately 25% by fructose, significantly different from controls at the 90% confidence level.

The effect of the proton ionophore cyanide *m*-chlorophenylhydrazone (CCCP) on glucose uptake was also tested. CCCP addition ablated transport activity in all yeast lines tested (Fig. 4.6), indicating that a pH gradient across the plasma membrane is essential for VvHT1, VvHT4 and VvHT5 mediated glucose uptake.

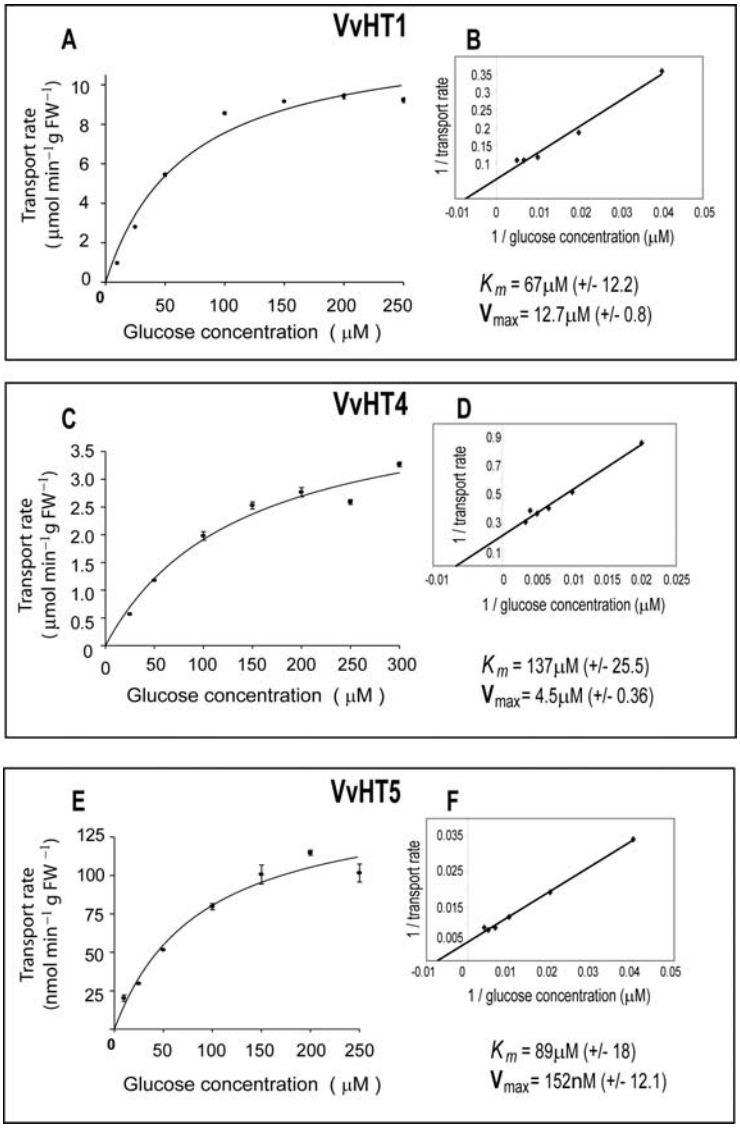

Figure 4.5. Concentration-dependant [^{14}C]-D-glucose uptake by yeast strain *EBY.VW4000* expressing grapevine hexose transporters. (A and B): VvHT1, Michaelis-Menton curve (A), double reciprocal plot (B) and estimate of Km and Vmax.
(C and D): VvHT4, Michaelis-Menton curve (C), double reciprocal plot (D) and estimate of Km and Vmax.
(E and F): VvHT5, Michaelis-Menton curve (E), double reciprocal plot (F) and estimate of Km and Vmax.
Uptake was determined in phosphate buffer pH 5.0. Data are means of one transformant tested in duplicate and are representative of two transformants tested. Error bars represent standard errors. FW= fresh weight.

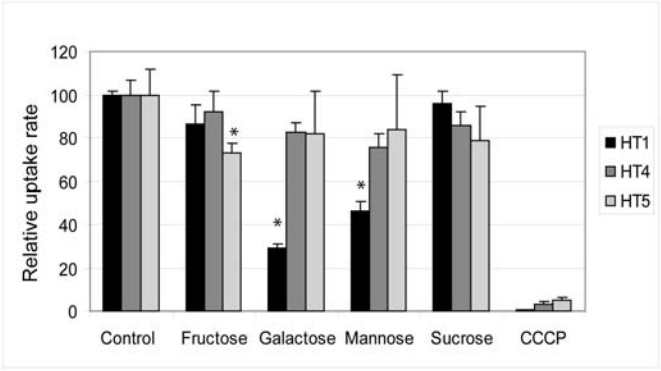

Figure 4.6. Substrate specificity of grapevine hexose transporters. Competitive inhibition of C-glucose uptake by yeast expressing VvHT1, VvHT4 and VvHT5. C-glucose was supplied at 100 mM, competing sugars were supplied at 500 mM and CCCP was supplied at 50 mM. Values are expressed as the percentage of the control without competing sugar and are means of two transformants. Asterix indicates signifcant differences at 90% confidence level. Error bars are standard deviations.

4.3.3 Subcellular localization of VvHT3 and VvHT4 proteins

To be functional in the yeast heterologous expression system, transporters must be targeted to the plasma membrane. To try and gain further information regarding the subcellular localization of VvHT3, which would provide additional information regarding its function and physiological role *in planta*, additional bioinformatic analysis was made. PSORT suggested that VvHT3 may be targeted to the chloroplast or the plasma membrane, while WoLFPSORT and PLOC predicted it is directed to the plasma membrane (Table 4.2). Analysis for potential *N-terminal* sorting signals was more unclear. ChloroP suggested that VvHT3 peptide does not contain a chloroplast transit peptide, while SignalP v 3.0 suggested it may contain an uncleaved signal anchor. Conversely, iPSORT did not detect an *N-terminal* sorting signal in the VvHT3 peptide. The ambiguous results from these bioinformatic analyses were not restricted to VvHT3: WoLFPSORT suggested VvHT4 may be localized to the vacuole membrane, whereas VvHT1 and VvHT4 were predicted by

all three programs to be localized to the plasma membrane. Analysis for *N-terminal* sorting sequences were also unclear, in that the three programs used gave conflicting results.

Table 4.2. Subcellular localisation and *N*-terminal sorting sequences in *VvHT1*, *VvHT3*, *VvHT4* and *VvHT5* peptides, predicted using various bioinformatic tools.

	VvHT1	VvHT3	VvHT4	VvHT5
Subcellular localisation				
PSORT [a]	PM	Chloroplast/PM	PM	PM
Wolf PSORT [b]	PM	PM	PM/Vac	PM
PLOC [c]	PM	PM	PM	PM
N-terminal sorting sequences				
SignalP v 3.0 [d]	Signal anchor	Signal anchor	Signal peptide	Non secretory
iPSORT [e]	Mitochnondrial	No signal	Chloroplast	Chloroplast
ChloroP 1.1 [f]	not present	not present	not present	not present

[a] Nakai and Horton (1999). Predicts subcellular location of proteins.

[b] Updated version of PSORT (Horton, Park, Obayashi and Nakai, in preparation).

[c] Park and Kinehisa (2003). Predicts subcellular location of proteins.

[d] Bendtsen *et al.* (2003). Predicts presence of *N*-terminal sorting sequences and cleavage sites.

[e] Bannai *et al.* (2002). Predicts presence of *N*-terminal sorting sequences.

[f] Emanuelsson *et al.* (1999). Predicts presence of chloroplast transit peptides.

To directly investigate the subcellular localization of VvHT3, the full length cDNA was cloned upstream and in-frame with GFP and downstream of the CaMV 35S promoter. As an example of likely plasma membrane targeting, a C-terminal GFP fusion construct with *VvHT4* was also prepared. The fusion proteins VvHT3:GFP and VvHT4:GFP, together with a native GFP construct, were transiently expressed in onion epidermal cells following biolistic delivery of vector DNA and cellular localization analysed by confocal microscopy.

Free GFP was found to be distributed in both the cytoplasm and nucleus of bombarded onion cells (Fig. 4.7 A). In contrast, VvHT4:GFP and VvHT3:GFP were localized exclusively to the periphery of bombarded cells (Fig. 4.7 B, C and D). Careful analysis of serial optical-sections of both VvHT4:GFP and VvHT3:GFP bombarded cells, established that these fusion proteins were only associated with the cell periphery and were never observed around the inner edge of nuclei, suggesting a likely plasma membrane localization (data not shown).

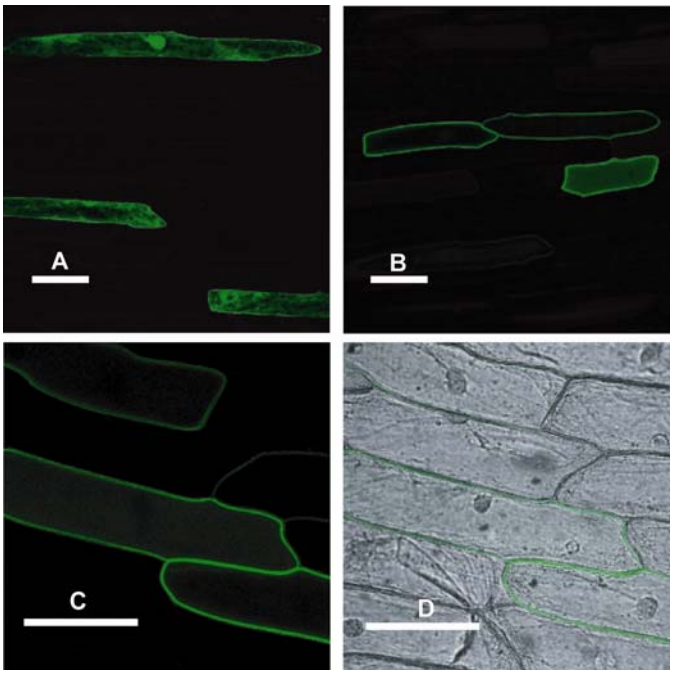

Figure 4.7. Analysis of the cellular targeting of VvHT3:GFP and VvHT4:GFP fusion proteins in onion epidermal cells. GFP alone (A), VvHT4:GFP (B) and VvHT3:GFP (C and D) were expressed in onion epidermal cells using the CaMV 35S promoter following biolistic delivery of vector DNA. VvHT4:GFP was a positive control for plasma membrane localisation. Cells were analysed for GFP fluorescence (A, B and C) by confocal microscopy and false colour applied. Differential phase contrast (DIC) and GFP fluorescence image were merged (D). Bar = 100 mm.

4.3.4 Analysis of full length *VvcwINV*

Using the sequence of the partial cwINV clone isolated in section 3.3.3 by degenerate PCR, RACE PCR methods were used to isolate a full length cDNA. Target specific oligos for 5' and 3' RACE were designed to amplify products with approximately 100 bp sequence overlap with the partial clone isolated earlier. Over the overlapping regions, RACE and degenerate clones shared 100% sequence identity and were concluded to be fragments from the same transcript (data not shown). These sequences were joined, ORFs predicted using ORF Finder, new primers designed incorporating predicted start and stop codons and these used to

amplify a full length cDNA using a high fidelity polymerase. The sequence of full length *VvcwINV* was identical to the full length sequence obtained by joining the initial and RACE cDNA clones (data not shown).

The full length grapevine *VvcwINV* ORF is predicted to encode a peptide of 576 amino acids and contains the proposed active site and other motifs characteristic of invertase enzymes (Fig. 4.8). The first motif, DPNG, is conserved in all invertase isoforms. The second, WECPDFFPV, contains a Cysteine considered important for sucrose catalysis along side other conserved residues (Sturm and Chrispeels 1990). In vINV peptides, this motif is typically WECVDF/LYPV, with the substitution of Valine for Proline characteristic of vINV isoforms (Roitsch et al., 1995). Grapevine VvcwINV shares between 55 - 69% amino acid identity with cwINV sequences from other plant species, less than 50% identity with vINV sequences and only low identity with neutral invertase (nINV) isoforms (Table 4.3).

Phylogenetic analysis of invertase peptides shows that VvcwINV forms a distinct group with cwINV and fructan exohydrolase (FEH) peptides from a range of plant species (Fig. 4.9). Vacuolar INV and nINV sequences group in separate branches. FEH and cwINV sequences share considerable homology and these functionally distinct enzymes cannot be separated for function based on sequence comparison alone. FEH have acidic theoretical isoelectric point (pI) values whilst true VvcwINV have basic pI values (De Conninck et al., 2005). The theoretical pI of VvcwINV, as estimated using the computer program IeP, is 9.7, well within the basic range, suggesting that it does encode a cwINV enzyme and is the first isolated from grapevine (Fig. 4.10 A).

The predicted translation product of *VvcwINV* contains a signal peptide that is predicted to target the protein for secretion to the extracellular space. The signal

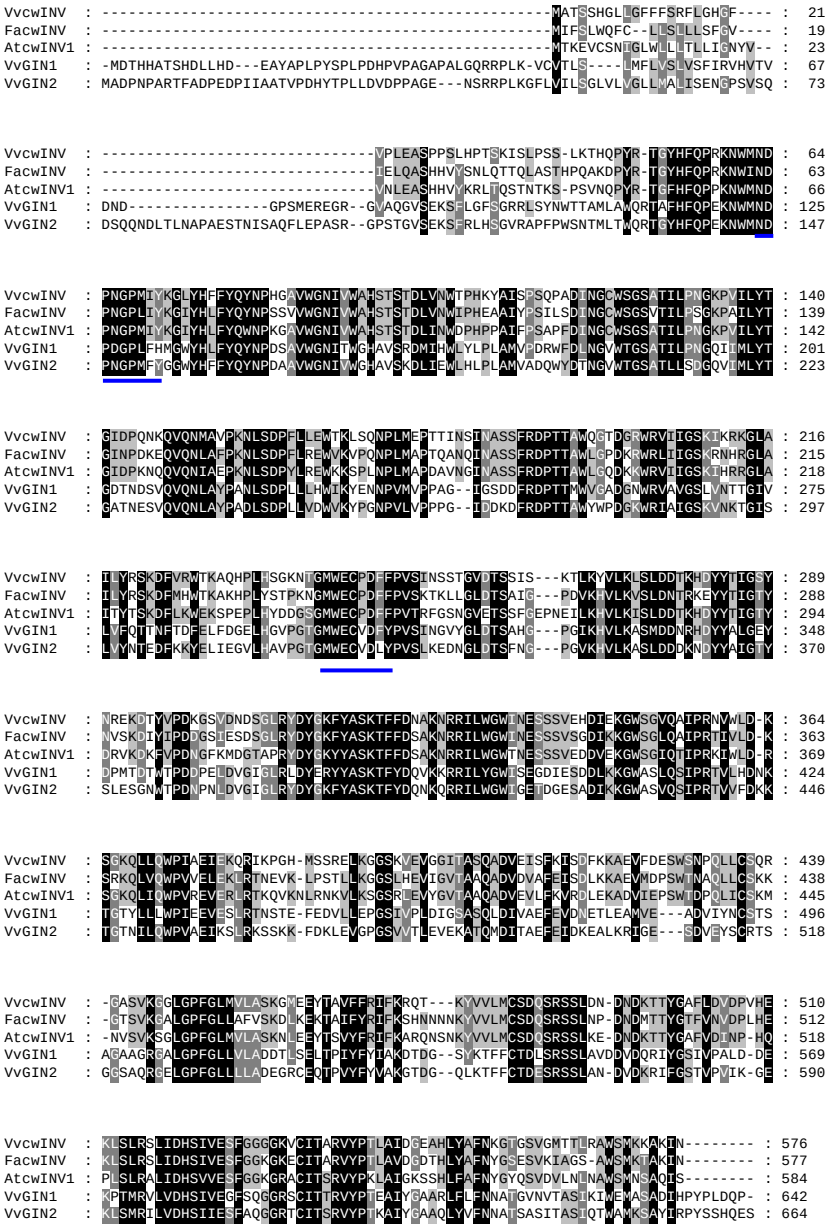

Figure 4.8. Alignment of the full length predicted peptide encoded by *VvcwINV* with grapevine vacuolar invertases (*VvGIN1* and *VvGIN2*) and cwINVs from other plants species. Underlined motifs are conserved in all invertase sequences. Full length *VvcwINV* was cloned by RACE PCR and the ORF and amino acid sequence was predicted using ORF Finder. The alignment was made with ClustalX (Thompson et al., 1997). The accession numbers used are: FacwINV (AF000521), AtcwINV1 (X74514), VvGIN1 (AAB47171), VvGIN2 (AAB47172).

peptide, predicted using SignalP v.3.0, is 26 amino acids in length and contains a prevalence of hydrophobic residues (Met, Ala, Leu, Phe, Val, Trp and

Pro), characteristic of the signal peptides encoded by cwINV sequences from other plants (Fig. 4.10 B). The grapevine VvcwINV signal peptide is predicted to be cleaved inside a motif that is found in cwINV peptides from several plant species which is located approximately 25 residues after the start Methionine.

Table 4.3. Homology between plant invertase peptide sequences. The accession numbers used can be found in Figure 5.8. The percentage identity and similarity (in brackets) as determined by the Gap algorithm are shown. cwINV for cell wall invertase, vINV for vacuolar invertse and nINV for neutral invertase.

	FacwINV	ZmcwINV	AtcwINV1	NtcwINV	VvGIN1	VvGIN2	DcvINV	AtnINV	DcnINV
VvcwINV	69 (74)	55 (62)	66 (73)	57 (63)	46 (53)	47 (54)	47 (56)	14 (29)	50(50)
FacwINV		55 (62)	65 (73)	59 (66)	44 (52)	46 (53)	47 (55)	14 (29)	43 (43)
ZmcwINV			54 (61)	59 (66)	44 (51)	46 (53)	47 (55)	27 (33)	43 (43)
AtcwINV1				60 (68)	44 (51)	45 (52)	47 (55)	43 (52)	42(42)
NtcwINV					43 (51)	45 (52)	45 (52)	25 (33)	16 (33)
VvGIN1						62 (70)	68 (73)	32 (41)	8 (8)
VvGIN2							63 (70)	43 (43)	20(20)
DcvINV								21 (26)	17 (20)
AtnINV									53 (64)

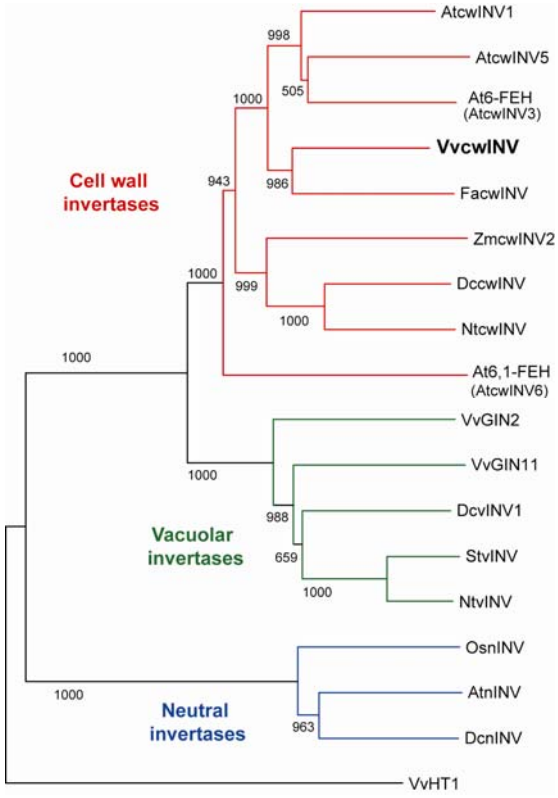

Figure 4.9. Phylogenetic analysis of the predicted amino acid sequences of invertases from grapevine and other plant species. Multiple sequence alignment was made with ClustalX (Thompson et al., 1997) and phylogenetic analysis was done by the parsimony method with Protpars (Felsenstein, 1989) using VvHT1 as the outgroup. Bootstrap analysis was performed with ClustalX (Thompson et al., 1997), and values shown at internal nodes indicate the occurance of these nodes in 1000 replicates. cwINV for cell wall

invertase, vINV for vacuolar invertase and nINV for neutral invertase. Database accession numbers of the sequences used are: VvHT1 (CAA70777), AtcwINV1 (X74514), AtcwINV5 (AP001307), AtcwINV3 (AB029310), FacwINV (AF000521), ZmcwINV2 (AF050128), DccwINV (M58362), NtcwINV (X81834), AtcwINV6 (Ay060553), VvGIN2 (AAB47172), VvGIN1 (AAB47171), DcvINV1 (P80065), StvINV (AAQ17074), NtvINV (CAC83577), OsnINV (BAD53496), AtnINV (AAP40464), DcnINV (CAA76145).

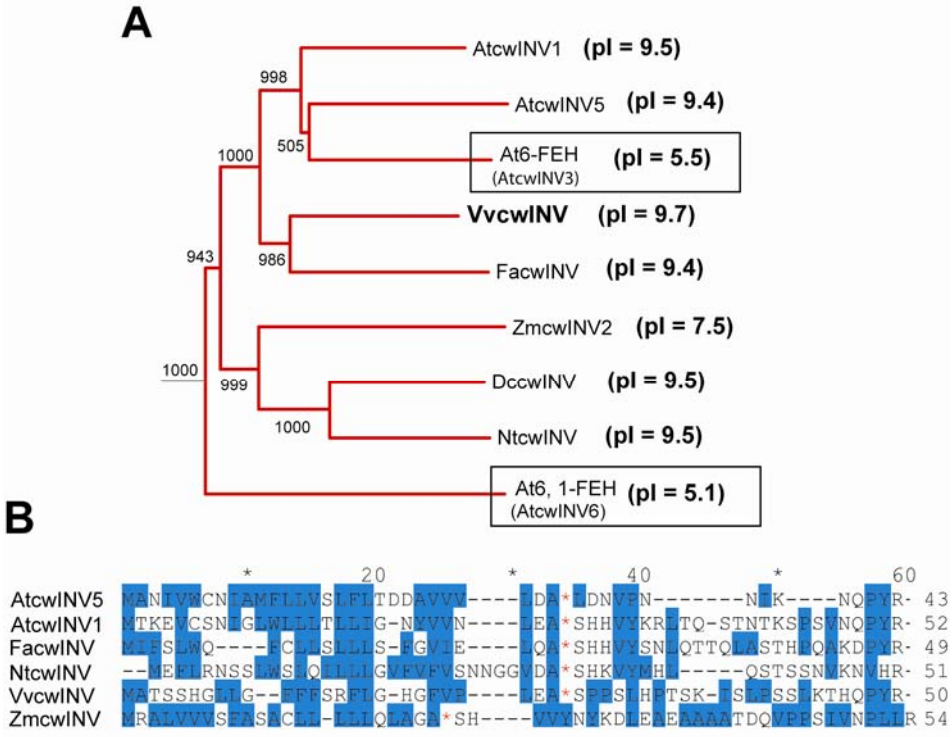

Figure 4.10. (A) The cwINV sub-tree from the phylogenetic analysis preseneted in Figure 4.9. The theoretical isoelectric point (pI) is indicated in brackets and was calculated using the computer program IeP. Fructan exohydrolases from *A. thaliana* are boxed. The accession numbers used can be found in Figure 4.9. (B) Alignment of the first fifty amino acids of cwINV peptide sequences. Hydrophobic non-polar residues are highlighted in blue and predicted signal peptide cleaveage sites are indicated by red asterix. Hydrophobic residues were identified using GeneDoc (Nicholas et al., 1997) and signal peptide cleavage sites were mapped with SignalP v. 3.0 (Bendtsen et al., 2004).

4.4 Discussion

4.4.1 Isolation of full length *VvHT* cDNAs and functional characterisation

In this chapter, full length cDNAs of each of the three partial HT cDNAs isolated in section 3.3.1 were cloned, analysed and functionally tested by expression

in yeast. The inferred peptide products of the three *VvHT* cDNAs are predicted to form secondary structures with 12 transmembrane helices and a large cytoplasmic loop located between helices six and seven. All plant HTs isolated to date have this secondary structure in common and this is a typical feature of members of the major facilitator superfamily (MFS) of uniporter, symporter and antiporter proteins (Büttner and Sauer, 2000). Functionally important conserved residues identified by site-directed mutagenesis and K_m mutant screening of a monosaccharide transporter from *Chlorella kessleri* (CkHUP1) are also present in predicted translation products of *VvHT3*, *VvHT4* and *VvHT5* (Fig. 4.1; Will et al., 1994). The full length sequences isolated in the current study share approximately 60% amino acid identity with the other grapevine HTs excluding *VvHT6*, but up to 80 % identity with HTs from other plant species (Table 4.1). This suggests that the evolutionary ancestors of plants already had several HT genes, theoretically allowing differential regulation and cell-specific monosaccharide uptake, as observed in the higher plants of today (Büttner and Sauer, 2000).

To demonstrate functionality of VvHT3, VvHT4 and VvHT5, each was expressed in a hexose transport-impaired yeast strain (*EBY.VW4000*; Wiezorke et al., 1999) and the rate of D-[U-^{14}C]glucose transport measured. Initially, a complementation assay was employed, however yeast expressing VvHT3, VvHT4 and VvHT5 did not exhibit enhanced growth rates on glucose media indicating that these transporters did not enable sufficient glucose transport to support yeast growth (M. Hayes and I.B. Dry, unpublished data). Subsequently it was decided to attempt a more sensitive assay to determine if these transporters did mediate glucose uptake. Using radio-labelled glucose, yeast expressing VvHT4, VvHT5 and VvHT1 (Fillion et al., 1999) accumulated glucose at faster rates than yeast transformed with the

empty vector suggesting they are functional glucose transporters, however, VvHT3 did not increase this rate and is therefore not functional in yeast. Glucose transport facilitated by VvHT4, VvHT5 and VvHT1 was sensitive to external pH (Fig. 4.4) and the proton ionophore CCCP (Fig. 4.6), indicating that these transporters are energized by the plasma membrane electrochemical gradient and therefore are likely to be H^+/glucose symporters.

VvHT4 shares 80% amino acid identity with RcHex6, one of six putative HT sequences isolated from *R. communis*, however, RcHex6 has not been further investigated (Weig et al., 1994). Phylogenetic analysis (Fig 4.3) grouped VvHT4 and RcHex6 with a third transporter, AtSTP3, which shares 65% amino acid identity (74% similarity) with VvHT4. Of the three grapevine HTs examined, VvHT4 had the lowest affinity for glucose (K_m 137 μM; Fig. 4.5 C). Functional characterisation of AtSTP3 in yeast indicated that this transporter also has a low affinity for glucose, however in this case, the estimated K_m for glucose was 2 mM, approximately 20 fold higher than the K_m of VvHT4 and far higher than the K_m range of 15-80 μM estimated for other plant HTs (Büttner et al., 2000; Büttner and Sauer, 2000). Thus, despite the significant homology between AtSTP3 and VvHT4 peptides, there are major functional differences suggesting that substrate affinity may be determined by a few important amino acid residues. This idea is supported by mutational analysis of CkHUP1, where mutation of amino acids at positions D44, Q179, Q298 and V433 increased K_m values by 10 to 500 fold (Will et al., 1994). It should also be noted that these particular residues are conserved in AtSTP3 and all other functionally determined plant HTs, (including VvHT1, VvHT4 and VvHT5; Fig. 4.1), which suggests there may be additional amino acid residues that determine substrate affinity that have not yet been identified.

VvHT5 is most closely related to the hexose transporters AtSTP13 and LeHT2 (Fig. 4.3) and shares approximately 80% amino acid identity with these peptides (Table 4.1). When expressed in yeast, VvHT5 mediated glucose uptake with a K_m for glucose of 89 μM (Fig. 4.5 E), similar to the K_m estimated for RcHex3 (80 μM) but almost double the K_m estimated for its close homologue LeHT2 (Weig et al., 1994; Gear et al., 2000). The rate of glucose uptake facilitated by VvHT5 was reduced in competition with fructose suggesting glucose and fructose may be potential substrates for this transporter. Initial studies using [^{14}C]fructose indicated that VvHT5 can transport fructose, but at less than half the rate observed for glucose (data not shown).

VvHT1 was the first HT isolated from grapevine (Fillion et al., 1999) and shares more than 80% amino acid identity with AtSTP1, MtST1 and NtMST1, the first HTs isolated from *A. thaliana*, *M. truncatula*, and *N. tabacum* respectively. VvHT1 also mediated glucose transport in yeast with a K_m for glucose of 67 μM (Fig. 4.5 A), which is in close agreement with the report of Vignault *et al*. (2005) where the K_m of VvHT1 was estimated at 70 μM. In competition assays, galactose and mannose strongly inhibited uptake of radio-labelled glucose suggesting they may also be substrates for VvHT1. Vignault *et al*. (2005) also observed this inhibition in competition assays, however expression of VvHT1 only marginally increased the rate of radio-labelled mannose uptake relative to untransformed yeast cells, suggesting that mannose may compete for the active site in VvHT1, but may not transported.

Despite numerous attempts, and observation of all HT-associated hallmarks in the predicted peptide of *VvHT3*, glucose transport activity was never observed in yeast. Bioinformatic analysis of VvHT3 using several software prediction tools

gave ambiguous predictions of its subcellular targeting. However, VvHT3:GFP fusion proteins were localized to the plasma membrane of onion epidermal cells indicating that, at least in plant cells, VvHT3 is targeted to the plasma membrane, and additionally suggesting that targeting problems in yeast may not explain its non-functionality. However, the localisation of VvHT3 in yeast was not determined, therefore it is possible that aberrant targeting may have prevented functionality in this particular heterologous expression system.

The likelihood that a particular HT will function in yeast is unpredictable due to numerous potential problems (N. Sauer, personal communication). It is possible that VvHT3 might facilitate transport of a substrate other than glucose, although all functionally defined plant HTs transport glucose to some degree (Büttner and Sauer, 2000). Alternatively, improper protein folding or a low rate of translation or transcription may have impeded the functional activity of VvHT3 in yeast, however these possibilities were not investigated.

4.4.2 Isolation of a full length *VvcwINV* cDNA and bioinformatic analysis

RACE PCR was also successfully used to obtain the full length cDNA sequence of a grapevine cwINV, the first reported from this plant species. The predicted ORF of *VvcwINV* displays a number of features typical of cwINV enzymes isolated from other plants including an isoform specific active site motif (Sturm and Chrispeels, 1990; Roitsch et al., 1995), a high theoretical pI value (Fig. 4.10A) and a predicted N-terminal signal peptide (Fig. 4.10 B).

Phylogenetic analysis grouped VvcwINV with functionally characterised cwINV peptides and with two functionally distinct fructan exohydrolase (FEH) enzymes from *A. thaliana* (Fig. 4.10 A). Although sequence homology alone is

insufficient to determine if *VvcwINV* encodes a true invertase enzyme, the theoretical pI value can be used to distinguish between cwINV and FEH peptides and thus provide additional evidence (De Conninck et al., 2005). True cwINV enzymes have high pI values whereas FEH enzymes (and vINV isoforms) have low, acidic pI values. VvcwINV was estimated to have a high pI value, suggesting it is a cwINV enzyme and not an FEH.

The first 26 residues encoded by the grapevine cwINV peptide were predicted by Signal P v. 3.0 (Bendtsen et al., 2004) to function as a signal peptide that directs the protein for secretion to the cell wall space. The N-terminal signal sequence of cwINV peptides from grapevine and other plants feature a run of approximately ten hydrophobic residues and a conserved motif that marks the peptidase cleavage site (Fig. 4.10 B; Bendtsen et al., 2004).

Chapter 5 - Quantitative RT-PCR analysis of sugar transporters and invertases in pathogen infected and wounded grapevine tissues

5.1 Introduction

Investigations on powdery mildew infected grapevine and barley leaves have described elevated soluble carbohydrate concentrations, increased invertase activity and decreased assimilation or photosynthetic activity (Brem et al., 1986; Scholes et al., 1994). Investigators have proposed that additional sugars are probably imported from adjacent non-infected and otherwise healthy leaves due to increased phloem unloading mediated, in part, by the elevated invertase activity. More recently, studies employing molecular biology techniques have shown that pathogen infection and wounding elevates expression of specific cwINV and HT genes suggesting that apoplasmic phloem unloading of sucrose is enhanced by these biotic and abiotic stress stimuli (Truernit et al., 1996; Roitsch et al., 2000; Fotopoulos et al., 2003).

In Chapter 3, semi-quantitative RT-PCR analysis indicated that transcript levels of *VvHT5* and *VvcwINV* were elevated 12.8 and 7.1 fold respectively, in powdery mildew infected leaves relative to controls. These leaves were detached from vines, a subset inoculated with spores and incubated for two days under conditions that facilitate maximal infection rates and therefore would be expected to produce a strong host response. To confirm that the gene expression changes reported in Chapter 3 were due to powdery mildew infection and were not an artefact of detachment from the plant and subsequent incubation, expression of sugar transporters and invertases was measured in three additional powdery mildew infected samples and controls. Leaf samples from cv. Cabernet Sauvignon and cv.

Chardonnay vines grown under glasshouse conditions, and berry skin samples from cv. Chardonnay vines grown in a local vineyard were assessed.

The experimental procedures and analysis method were improved from Chapter 3 to yield more informative and robust data by following the quantitative RT-PCR strategy described by Muller *et al*. (2002). In addition to quantifying differences in transcript amounts of a single gene in several cDNA samples, as achieved in Chapter 3, this method can estimate transcript abundance of one gene relative to the abundance of another. This additional layer of information is of importance when quantifying transcript levels of several members of a gene family that may be expressed within the same tissue, as may be the case with the sugar transporter and invertase gene families. Furthermore, this method incorporates vigorous statistical analysis to estimate means and standard errors ensuring validity of the final data.

The specificity of powdery mildew-associated gene expression responses was investigated in several ways. Firstly, transcript levels were measured in discrete powdery mildew infected regions and compared to levels observed in uninfected areas of the same leaf. This comparison was made to determine if gene expression changes were restricted to infected leaf regions as a preliminary experiment to indicate if more time consuming localisation studies by *in situ* hybridisation may be justified. Secondly, to establish if powdery mildew induced gene expression changes were specific to this pathogen or if they may be part of a more general response, the expression of sugar transporters and invertases was monitored in downy mildew infected and wounded leaves. Like powdery mildew, downy mildew is a biotrophic pathogen, however, it infects mesophyll cells while powdery mildew infection is restricted to the epidermis. Wounding was tested as it is an abiotic

stimulus which has been shown in *A. thaliana* and carrot to induce expression of sugar transporters and invertases, reflecting responses observed in pathogen infected tissue (Sturm and Chrispeels, 1990; Truernit et al., 1996; Fotopoulos et al., 2003; Meyer et al., 2004).

5.2 Materials and methods

5.2.1 *E. necator* (powdery mildew) inoculation

E. necator spores grown on detached leaves (section 2.1.5) were transferred to leaves of glasshouse grown *V. vinifera* cultivars Cabernet Sauvignon and Chardonnay using a fine paintbrush. Powdery mildew infected leaves were sampled eight to 10 days after inoculation. Healthy control leaves were sampled from vines grown in a separate glasshouse compartment but maintained under identical temperature and irrigation conditions. Healthy and powdery mildew infected leaves were of similar developmental ages and always sampled at the same time of day.

Young Chardonnay bunches consisting of berries two to four days post flowering were tagged and inoculated with *E. necator* spores grown on detached leaves and suspended in water at a concentration of 1×10^6 spores per ml. Berries were visually inspected for infection and severely infected and healthy berries sampled two weeks after inoculation. Berry skin, seeds and pulp were separated by hand and stored at -80^{o}C before RNA extraction.

5.2.2 Powdery mildew infected and uninfected leaf regions

Discrete powdery mildew infected regions of Cabernet Sauvignon leaves were excised from uninfected leaf areas using a scalpel and these infected regions and the remaining leaf tissue were stored at -80^{o}C until RNA was extracted as described previously. Microscopic observation using a Stemi 2000 microscope (Zeiss, North Ryde, Australia) was used to view leaf surfaces to establish that areas beyond the excised powdery mildew colonies were free of surface mycelia.

5.2.3 *Plasmopara viticola* (downy mildew) inoculation

P. viticola was maintained as described (section 2.1.6). A spore solution containing 1 x10^{6} spores per ml was sprayed on to the abaxial surface of fully expanded leaves on glasshouse-grown potted vines. Inoculated leaves and water-sprayed controls were enclosed in plastic bags overnight to maintain humidity and infected and control leaves sampled 10 DPI and stored at -80°C before RNA was extracted.

5.2.4 Wounding of leaves

The adaxial surface of glasshouse-grown Cabernet Sauvignon leaves were gently rubbed with fine sandpaper and two control and two wounded leaves sampled at 0, 1, 2, 4, 8 and 24 h post-wounding. Leaves were immediately frozen in liquid nitrogen and stored at -80°C before RNA was extracted independently from each leaf.

5.2.5 RNA extraction, DNase treatment and cDNA synthesis

Total RNA was extracted following the method of Rezaian and Krake (1987) and DNase treated as described (section 2.2.12). RNA (2 μg) was reverse transcribed using the SuperScript III First-Strand Synthesis System for RT-PCR (Invitrogen) as described (section 2.2.13).

5.2.6 Quantitative real-time PCR analysis

Expression analysis was carried out by real-time PCR using a SYBR green method on a Rotor-Gene 3000 (Corbett Research, Mortlake, Australia) thermal cycler. Each 15 μl PCR reaction contained: 330 nM of each primer, 3 μl of diluted cDNA (Section 2.2.15), 1 x ABsolute^{TM} QPCR SYBR$^{®}$ Green ROX Mix (Integrated Sciences) and water. The thermal cycling conditions used were 95°C for 15 min followed by 40 cycles of: 95°C for 30 s, 56°C or 58°C for 30 s, and 72°C for 30 s, followed by a melt cycle of 1°C increments from 55 to 96°C. All primer pairs amplified a single product of the expected size and sequence, which was confirmed by melt-curve analysis, agarose gel electrophoresis (section 2.2.2) and DNA sequencing (Section 2.2.11). After testing the suitability of actin (TC45156), ubiquitin (TC38636) and β-tubulin (TC39826) for use as reference genes, actin was selected for normalisation of all pathogen infected and wounded comparisons, while β-ubiquitin expression was used as the reference for the analysis of the grape berry developmental series (see Chapter 6). The expression of each target gene was calculated relative to the expression of actin in each cDNA tested using Rotor-Gene 6.0 software (Corbett Research, Mortlake, Australia) to calculate CT values, observe melt profiles and to measure primer pair amplification efficiencies. Q-Gene software (Muller et al., 2002) was used to calculate the mean normalized expression

level (and the standard error) of each gene in each cDNA tested relative to actin using method two (Equation 3 in Table 2; Muller et al., 2002). The expression of genes belonging to a single gene family were analysed together to produce data representative of the relative expression of these genes. For example, the expression of five hexose transporters were analysed as a group, and six invertases were analysed as a separate group. All primer sequences are described in Table 2.3. The un-normalized expression of actin in pathogen infected and wounded samples is shown in Appenidx 2, Figures A2.1 through A2.4.

5.2.7 Measurement of invertase enzyme activity

Invertase was extracted from grape leaves and enzyme activity measured using the method of Ruffner *et al*. (1995), with some modifications from Tang *et al*. (1996). Briefly, 0.5 g tissue was ground under liquid nitrogen, 1.8 ml of extraction buffer added (0.25 M MES, 20 mM cysteine/HCl, 20 mM DTT, 3 mM EDTA, 5% (w/v) PEG 4000, pH 6.5) followed by further grinding. The semi-thawed slurry was transferred to a 2ml microcentrifuge tube and centrifuged at 10,500 rpm for 10min at 4°C. The supernatant was collected and stored on ice and used as the soluble invertase extract. The pellet was washed three times by resuspending in 1.8 ml ice-cold extraction buffer and subsequent centrifugation as above, before finally resuspending in 1ml acetate buffer (0.2 M Na acetate, 0.2 M acetic acid, pH 4).

To measure invertase activity, 50 µl of cell wall pellet suspension or soluble extract was mixed with 200 µl acetate buffer (pH 4) and 200 µl 0.225 M sucrose and incubated on a rotating wheel for 40 min at 30°C. To stop the reaction, 500 µl of DNSA-reagent (1% (w/v) 3,5-dinitrosalicylic acid, 0.5M KOH, 1M K/Na-tartrate) was added and this mixture placed in a boiling water bath for 10min and then on ice

for 5min. Before the insoluble extract was boiled, tissue debris was removed by centrifugation at 13,000 rpm for 3 min and the supernatant decanted to a new tube and then boiled. Absorbance was read at 560 nm. Protein concentration in extracts was determined using a D_C protein assay kit (Biorad) according to the manufacturer's instructions using bovine serum albumin standards (Fermentas) to make a standard curve.

5.3 Results

Semi-quantitative RT-PCR analysis in Chapter 3 indicated that expression of *VvHT5* and *VvcwINV* is up regulated by powdery mildew infection. To confirm and extend these observations, sugar transporter and invertase transcript levels were measured using a quantitative RT-PCR analysis in additional powdery and downy mildew infected samples, and in leaves wounded with sandpaper.

Selection of a reference gene to normalise the cDNAs being compared is a critical component of any quantitative RT-PCR analysis. In this study ubiquitin (TC38636) and actin (TC45156) transcripts were selected as reference genes after also testing β-tubulin (TC39826). The expression of actin was the most stable of the three candidates in the pathogen infection and wounded treatments and was selected as the reference for these comparisons. Microarray analysis (section 3.3.1; Table 3.1) indicated that transcript levels of ubiquitin were 2.45 fold higher in powdery mildew infected berry skin than control samples. However, actin was found to be more variable when comparing tissues at different developmental stages or from different organs, therefore, ubiquitin was used for comparisons across grape berry developmental series' and for comparing gene expression in different organs

(Chapter 6). β-Tubulin was not a good candidate as it was expressed at a relatively low level and gave inconsistent results. The sequences were obtained from the TIGR Grape Gene Index (http://www.tigr.org/tigr-scripts/tgi/T_index.cgi?species=grape).

5.3.1 Quantitative RT-PCR analysis of hexose and sucrose transporter expression in powdery mildew infected grapevine tissues

Glasshouse-grown Chardonnay and Cabernet Sauvignon grapevine leaves were inoculated with powdery mildew and control (healthy) and infected leaves collected 10 DPI. Additionally, young field-grown Chardonnay berries approximately seven days after flowering were inoculated with powdery mildew and control and infected berries collected 14 DPI. Total RNA was extracted from these samples, genomic DNA removed by DNase treatment and the expression of *VvHT1* and *VvHT2* (Fillion et al., 1999), and *VvHT3*, *VvHT4* and *VvHT5* (Chapter 3) measured using quantitative RT-PCR.

Similar changes to HT transcript levels were observed in powdery mildew infected leaves of Cabernet Sauvignon and Chardonnay, when compared with controls (Fig. 5.1 A and B). In healthy grapevine leaves, a low level of constitutive expression of all *VvHT* genes was observed with *VvHT1* having the highest expression. However, in powdery mildew infected leaf samples, *VvHT*5 transcript levels were strongly elevated by approximately 12 fold and 20 fold, relative to controls, in Cabernet Sauvignon and Chardonnay leaves respectively (Fig. 5.1 A & B). *VvHT1* was also induced in response to powdery mildew infection but to a much smaller degree, approximately 3-4 fold compared to healthy leaves. In contrast, the

expression of *VvHT2* and *VvHT3* and *VvHT4* showed little or no response to PM infection.

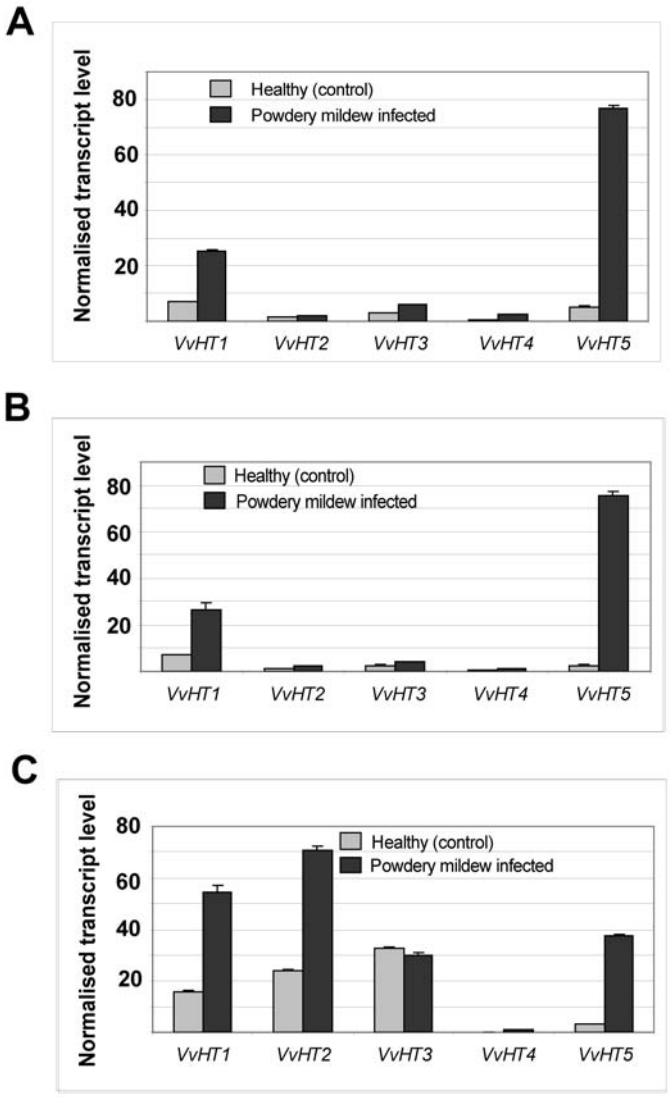

Figure 5.1. Quantitative RT-PCR analysis of HT expression in powdery mildew infected grape tissues.
(A) Cabernet Sauvignon leaves
(B) Chardonnay leaves
(C) Chardonnay berry skin

All values were normalised to the expression of actin and each is the average of one sample tested in triplicate. Analysis was performed using the method of (Muller et al., 2002) which allows comparison of expression level between the genes in each figure. Error bars represent the standard error, primer sequences are in Table 2.3.

A somewhat different *VvHT* expression pattern was observed in Chardonnay berry skin samples (Fig. 5.1 C). In the skin of healthy berries, *VvHT1*, *VvHT2* and *VvHT*3 were expressed considerably more than *VvHT4* and *VvHT5*. As in leaves, powdery mildew infection of Chardonnay berries resulted in a marked increase of *VvHT5* transcript levels in skin tissue (~12 fold) and a lower induction of *VvHT1* (~ 3 fold). However, *VvHT2* expression was also up regulated by approximately 3 fold and was therefore the most highly expressed *VvHT* gene in infected berry skin. As was observed in grapevine leaves, *VvHT4* was the least expressed of the VvHTs.

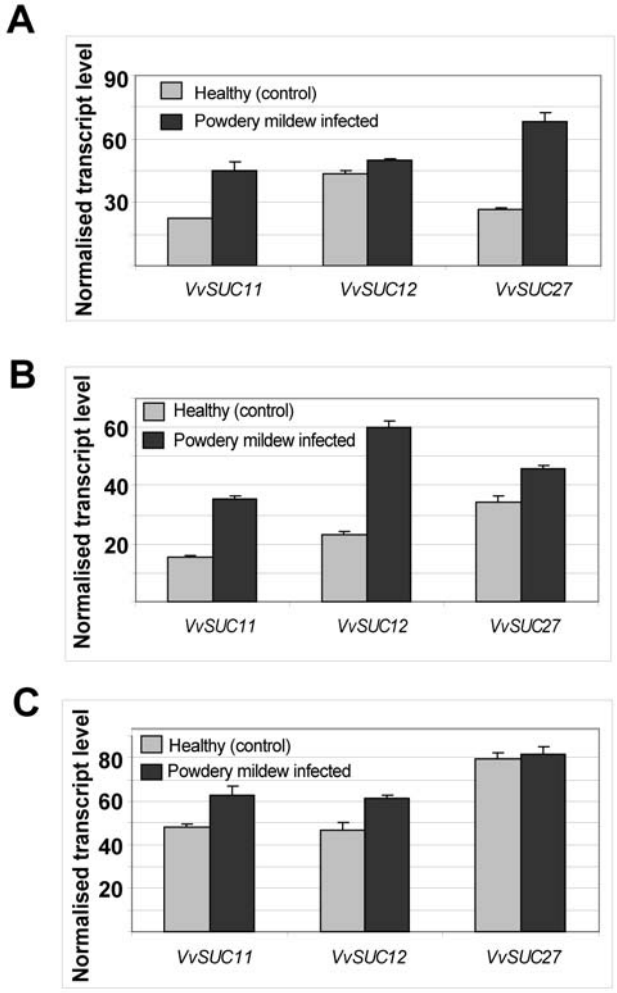

Figure 5.2. Quantitative RT-PCR analysis of sucrose transporter expression in powdery mildew infected grapevine tissues.
(A) Cabernet Sauvignon leaves
(B) Chardonnay leaves
(C) Chardonnay berry skin

All values were normalised to the expression of actin and each is the average of one sample tested in triplicate. Analysis was performed using the method of (Muller et al., 2002) which allows comparison of expression level between the genes in each figure. Error bars represent the standard error, primer sequences are in Table 2.3.

The expression of three sucrose transporters reported by Davies *et al*. (1999) was also monitored in powdery mildew infected and control leaf and berry samples (Fig. 5.2 A-C). It can be seen that while there was a general trend for the expression of these sucrose transporter genes to be up regulated in response to powdery mildew infection, the size of the response was much smaller than observed for *VvHT1* and especially *VvHT5*, and no common trend was apparent between the different samples.

5.3.2 Quantitative RT-PCR analysis of invertase expression in powdery mildew infected grapevine tissues

Transcript levels of *VvcwINV* were measured in the powdery mildew infected and control samples described above and compared with levels of two vacuolar invertases, (*VvGIN1* and *VvGIN2;* Davies and Robinson, 1996) and three grape ESTs (TC7206, TC11451, TC11207; retrieved from the TIGR Grape Gene Index) which share between 84% and 87% identity with nINV homologues from carrot (CAA76146) and *A. thaliana* (CAB45447). With the exception of TC11207 which is expressed at a low level in the samples measured, all of the invertase genes investigated were constitutively expressed in healthy leaves of both grape cultivars examined. The only major difference was that in healthy Cabernet Sauvignon leaves, *VvGIN1* transcript levels were significantly higher compared with transcript levels of the other invertases tested, while in Chardonnay, this difference was smaller (Fig. 5.3 A and B). In the powdery mildew infected Cabernet Sauvignon

and Chardonnay leaf samples, *VvcwINV* expression was elevated more than 9 and 4 fold respectively. In contrast, transcript levels of *VvGIN1* were strongly reduced more than 10 fold in both leaf samples. Also worth noting, expression of TC7206, one of three nINV-homologous ESTs was up regulated approximately 3 fold in powdery mildew infected leaf samples from both cultivars. To summarise, in the powdery mildew infected leaf samples *VvcwINV* transcripts are significantly more abundant than any of the other invertase transcripts measured.

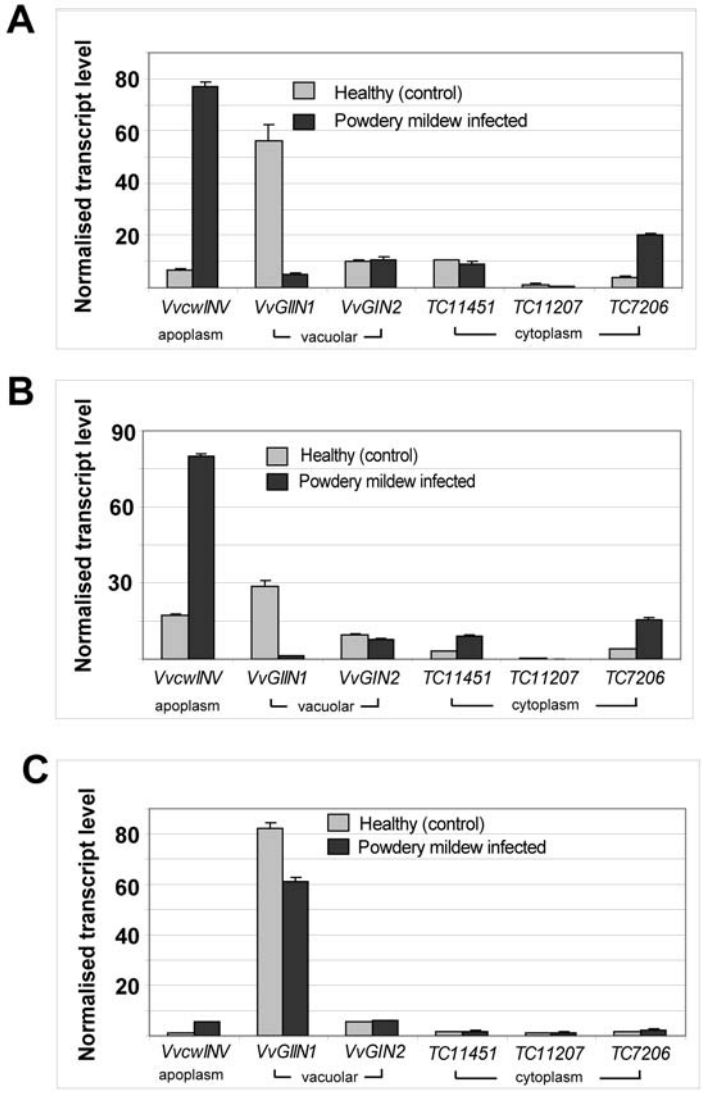

Figure 5.3. Quantitative RT-PCR analysis of invertase expression in powdery mildew infected leaves and berry skin.
(A) Cabernet Sauvignon leaves
(B) Chardonnay leaves
(C) Chardonnay berry skin

All values were normalised to the expression of actin and each is the average of one sample tested in triplicate. Analysis was performed using the method of (Muller et al., 2002) which allows comparison of expression level between the genes in each figure. TC numbers correspond to sequences on the TIGR grape gene index. Error bars represent the standard error, primer sequences are in Table 2.3.

As observed in the leaf samples, *VvGIN1* showed the highest levels of gene expression in healthy Chardonnay berry skin (Fig. 5.3 C). However, in contrast to the response of powdery mildew infected leaf samples, *VvGIN1* expression was only slightly reduced in the powdery mildew infected berry skin sample. Furthermore, while *VvcwINV* was induced approximately 4 fold in the powdery mildew infected sample, the level of *VvcwINV* expression was approximately 10 fold less than the amount of *VvGIN1* transcripts in the powdery mildew infected sample. The other invertase transcripts quantified were expressed at relatively low levels in Chardonnay berries and were not significantly altered by powdery mildew infection.

5.3.3 Effect of powdery mildew infection on grape leaf acid invertase activity

The relative sucrolytic activity of soluble and insoluble extracts obtained from healthy and powdery mildew infected leaves are shown in Figure 5.4. The rate of sucrose hydrolysis is expressed on a h^{-1} g FW^{-1} basis to allow comparison with previous reports of invertase activity in grapevine tissues (Ruffner et al., 1990). In the buffer (pH 4) used for the assay, *VvcwINV* activity is measured in the insoluble pellet suspension and mainly vINV activity contributes to the soluble sucrolytic activity. In the healthy Cabernet Sauvignon leaf samples, the average rate of invertase activity in the soluble fraction was 82.5 μmol sucrose hydrolysed h^{-1} g FW^{-1} while in the insoluble pellet suspension the average rate of invertase activity was 23.9 μmol sucrose hydrolysed h^{-1} g FW^{-1} or approximately 3.5 fold less. These rates

are similar to those published by Ruffner *et al*. (1990) where soluble and cell wall associated activities were approximately 72 and 25 μmol sucrose hydrolysed h^{-1} g FW^{-1} respectively. In contrast, in powdery mildew infected leaf samples, the soluble activity was decreased by 55% to 45.9 μmoles sucrose hydrolysed h^{-1} g FW^{-1} while the insoluble invertase activity was found to be increased by 2.5-fold to 61.6 μmol sucrose hydrolysed h^{-1} g FW^{-1} which is in agreement with the observed increase in *VvcwINV* transcript levels (Fig. 5.3 A).

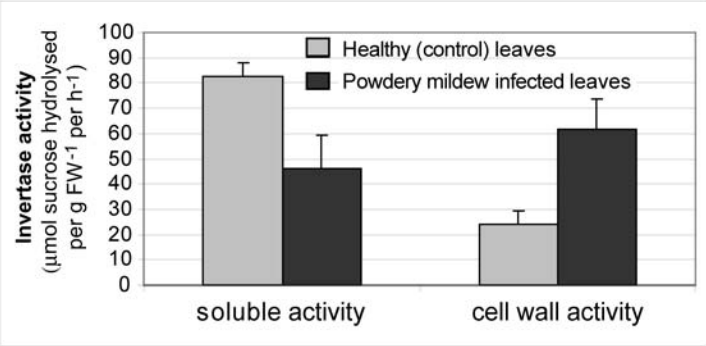

Figure 5.4. Acid invertase activity assays on soluble (vINV) and insoluble (cwINV) extracts from healthy and powdery mildew infected leaves. Invertase assays were performed in 0.1M accetate buffer, pH4.0. The values plotted are the averages of two independant extractions of 0.5 g leaves, each extraction tested in triplicate. Error bars represent one standard deviation.

5.3.4 Localisation of VvHT and invertase expression relative to powdery mildew infection sites

To investigate if powdery mildew induced gene expression changes were restricted to infected leaf regions and therefore may be specific to infected cells, transcript levels of *VvHT1*, *VvHT5*, *VvcwINV* and *VvGIN1* were measured in discrete powdery mildew infected regions and compared to levels observed in uninfected areas of the same leaf. As an infection-specific positive control, expression of a powdery mildew induced grapevine germin-like protein homologue (*VvGLP3*; AY298727) was measured in these samples. Unpublished RT-PCR analysis and

localisation studies using transgenic *A. thaliana* plants expressing the GUS reporter gene under control of the *VvGLP3* promoter indicate that expression of this gene is induced specifically in powdery mildew infected epidermal cells (D. Godfrey and I. B. Dry, manuscript in preparation). Relative to uninfected leaf regions, *VvGLP3* transcript levels were more than five fold higher in powdery mildew infected areas, consistent with previous data regarding its specificity (Fig. 5.5). In contrast, *VvHT1*, *VvHT5*, *VvcwINV* and *VvGIN1* transcript levels were reasonably similar in infected areas and in uninfected regions indicating that powdery mildew induced expression of these genes is not highly specific for the infection site.

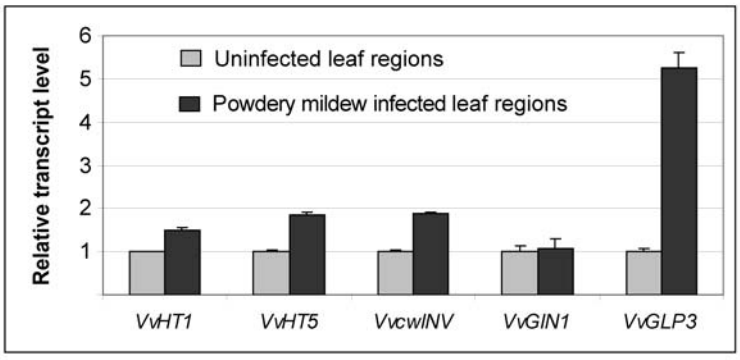

Figure 5.5. Localisation of transcripts of powdery mildew responsive genes by semi-quantitative RT-PCR. cDNA was synthesised from powdery mildew infected leaf regions and from uninfected areas of the same leaf. The ratio of transcript levels in infected areas : uninfected areas was caluclated using semi-quantative RT-PCR. All values were normalised to the expression of actin and each is the average of one sample tested in triplicate. Error bars represent the standard error, primer sequences are in Table 2.3.

5.3.5 Changes in expression of VvHTs, SUCTs and invertases in downy mildew infected grape leaves detected by quantitative RT-PCR

Leaves were inoculated with grapevine downy mildew (*P. viticola*) by spray application to the under dermis of fully expanded leaves. Control and infected leaves were sampled 10 days post inoculation. Leaf age was matched by size and node position. Relative transcript levels of VvHT genes in control leaves were similar to those observed in Figure 5.1 A with *VvHT1*, *VvHT3* and *VvHT5* expressed

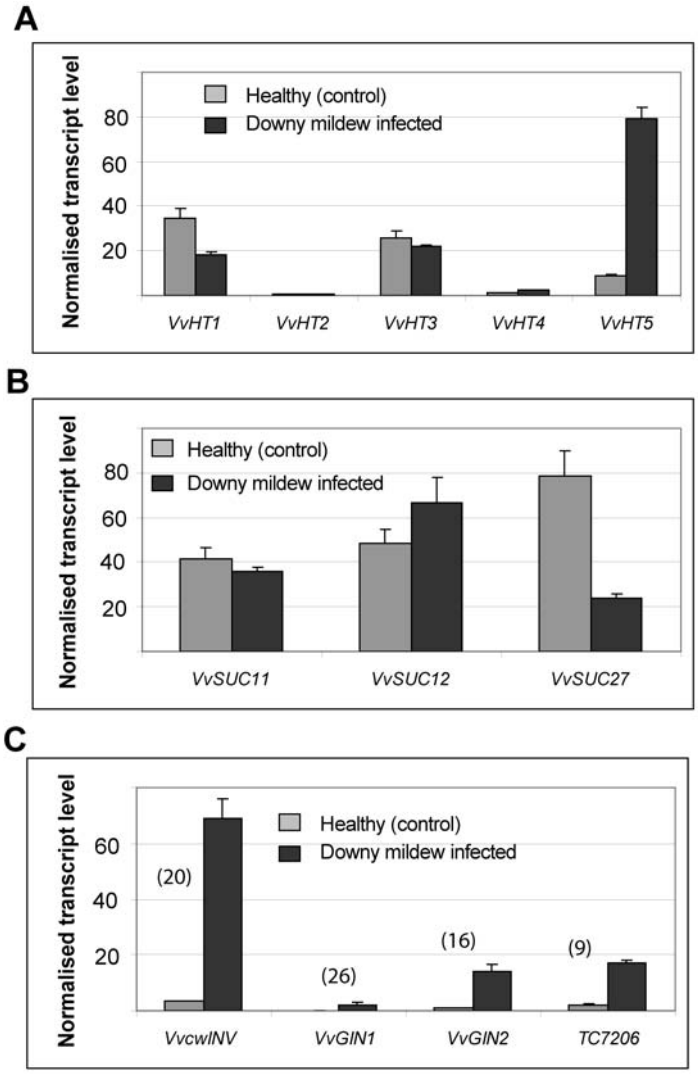

Figure 5.6. Quantitative RT-PCR analysis of HTs (A), sucrose transporters (B) and invertases (c) downy mildew infected Cabernet Sauvignon leaves. All values were normalised to the expression of actin, each value is the average of three replicates and are representative of two infected and control samples tested. Numbers in brackets are the fold change in expression between the control and infected samples. Analysis was performed using the method of (Muller et al., 2002) which allows comparison of expression level between the genes in each figure. Error bars represent the standard error, primer sequences are in Table 2.3.

more than *VvHT2* and *VvHT4* (Fig. 5.6 A). In downy mildew infected samples, transcript levels of *VvHT*5 increased more than 6-fold relative to the control sample and became the most highly expressed *VvHT* in the downy mildew infected leaf by approximately 4 fold. Expression of the other *VvHT*s was only moderately affected

or not altered by downy mildew infection. Interestingly, while expression of *VvHT1* was induced approximately 4 fold in powdery mildew infected leaves (Fig. 5.1A), it was slightly repressed in response to downy mildew infection (Fig. 5.6 A). Expression of the sucrose transporter genes *VvSUC11* and *VvSUC12* in the downy mildew sample was not significantly different from the control sample, however, *VvSUC27* transcript levels were approximately three fold lower in infected samples (Fig. 5.6 B).

Invertase transcript levels were very low in downy mildew control samples in comparison to the levels observed in powdery mildew control samples (Fig. 5.3). In downy mildew infected samples, expression of all invertase genes examined was dramatically elevated (Fig. 5.6 C). *VvcwINV* transcript levels increased by more than 20 fold, *VvGIN1* and *VvGIN2* expression was enhanced 26 fold and 16 fold respectively, while the nINV EST homologue TC7206 was induced 9 fold. However compared to the level of *VvcwINV* expression in downy mildew infected samples, these transcript levels were relatively low.

5.3.6 Effect of wounding on VvHT and invertase expression in grape leaves

Leaves were wounded by abrasion of the upper surface with sandpaper and wounded and control leaves collected at 1 h, 2 h, 4 h, 8 h and 24 h after the wound event. Two wounded and two control leaves of similar age, (as defined by node position and size), were collected at each time point. Quantitative RT-PCR analysis revealed that both *VvHT5* and *VvHT1* were significantly induced within 1-2 h following the wounding treatment (Fig. 5.7 A). *VvHT5* transcript levels were approximately 4 fold higher than controls 1 h after wounding and approximately 10 fold higher after 2 h. Expression levels then appeared to gradually decline over the

next 4-24 h but remained significantly higher than in control leaves during this period. The response of *VvHT1* to the wounding treatment was more transient and less pronounced than *VvHT5*. Expression was elevated approximately 2 fold compared to control leaves 2 h after wounding and had declined back to control levels within 8 h after wounding. There were no significant differences in *VvHT4* transcript levels between the wounded and control samples. *VvHT*2 which was expressed at a relatively low level, was slightly but consistently down regulated in the 2 h, 4 h and 8 h wounded samples. Similarly, transcript levels of *VvHT*3 were also lower than controls in the 2 h, 4 h and 8 h wounded samples.

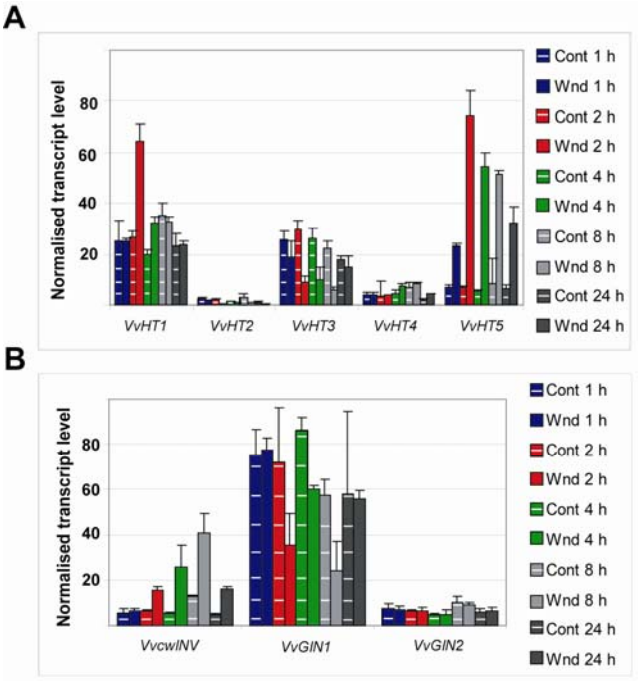

Figure 5.7. Quantitative RT-PCR analysis of VvHTs (A) and invertases (B) in wounded Cabernet Sauvignon leaves over a 24 h time period. All values were normalised to the expression of actin and each is the average of two biological replicates tested in triplicate. Analysis was performed using the method of (Muller et al., 2002) which allows comparison of expression level between the genes in each figure. Cont = control, Wnd = wounded. Error bars represent the standard error, primer sequences are in Table 2.3.

Transcript levels of *VvcwINV* were also higher in wounded samples compared to controls, but the timing of induction was delayed relative to *VvHT5*

(Fig. 5.7 B). *VvcwINV* expression was not elevated in the 1 h wounded sample but gradually increased over the 2 h, 4 h and 8 h period. Transcripts of *VvcwINV* were still considerably higher than controls in the 24 h wounded sample. *VvGIN1* expression appeared to be repressed in the 2 h, 4 h and 8 h wounded leaves compared to controls, but returned to the control level after 24 h. In contrast, *VvGIN2* transcript levels were not significantly different in control and wounded samples.

5.4 Discussion

Invertase, and sucrose and monosaccharide transporter activities, contribute to carbohydrate sink metabolism and the genes that encode these proteins are regulated by numerous endogenous and exogenous cues. Infection with fungal pathogens such as powdery or downy mildew elicits alterations to normal host carbohydrate distribution which result in elevated soluble carbohydrate concentrations and repressed photosynthetic activity (Brem et al., 1986; Scholes et al., 1994 Abood and Losel, 2003). A candidate gene approach was commenced to identify new grapevine genes that may mediate these carbohydrate changes. Based on a review of literature concerning host responses to biotrophic pathogen infection, the monosaccharide and cwINV gene families were targeted. In Chapters 3 and 4, cDNAs encoding three new HTs and a new cwINV were isolated from cDNA prepared from powdery mildew infected leaves, while preliminary RT-PCR analysis suggested *VvHT5* and *VvcwINV* transcript levels are elevated in infected leaves, compared to controls. To confirm and extend these observations, quantitative RT-PCR methods have been used to measure invertase and sugar transporter gene expression in additional powdery mildew infected samples, and in downy mildew

infected and wounded leaves. Together, these studies indicate that expression of specific invertase and sugar transporter genes are induced in pathogen infected and wounded tissues.

5.4.1 Powdery mildew infection

Gene expression studies carried out on leaves from two different grapevine cultivars showed that powdery mildew infection was accompanied by a strong increase of *VvcwINV* transcripts and reduced expression of the vacuolar invertase *VvGIN1* (Fig 5.3). *VvcwINV* expression was also enhanced in infected berry skin, however, relative to *VvGIN1* expression, this gene was expressed at a low level. As *VvcwINV* was cloned as part of this study, there is no pre-existing data concerning the expression of this gene in grapevine. However, previous research on carrot (Sturm and Chrispeels, 1990), *A. thaliana* (Chou et al., 2000; Fotopoulos et al., 2003) and *C. rubrum* (Roitsch et al., 2000), has shown that exogenous stimuli such as pathogen infection and wounding can elevate cwINV transcript levels and activity. *VvGIN1* is one of two vINV genes cloned from grape berries by Davies and Robinson (1996) who showed that *VvGIN1* transcript levels are much higher than *VvGIN2* levels in expanding leaves and in berries. The quantitative RT-PCR analysis presented in this chapter is consistent with these observations.

Although the magnitude of the changes to soluble and insoluble invertase enzyme activity were not as large as those observed in *VvcwINV* and *VvGIN1* gene expression, enzyme assays were in agreement with the transcriptional analysis, indicating that infected leaves contained reduced vINV activity and approximately two fold increased cwINV activity (Fig. 5.4). In reference to the soluble enzyme, the apparent stability of grapevine vacuolar invertase activity may underlie the

discrepancy between gene expression and enzyme activity, because in grape berries soluble acid activity remains strong six weeks after expression of *VvGIN1* and *VvGIN2* has stopped (Davies and Robinson, 1996).

Initial studies on powdery mildew infected barley, grapevine and pea leaves concluded that acid invertase activity was elevated compared with healthy tissue, however, these investigations did not examine the potential contribution of cell wall associated forms to the elevated sucrolytic activities observed (Hwang and Heitefuss, 1986; Brem et al., 1986; Storr and Hall, 1992). By measuring invertase activity in apoplasmic washing fluids prepared from control and powdery mildew infected pea leaves, Clarke and Hall (1998) demonstrated that extracts from infected leaves contained nearly four fold more invertase activity and also, higher concentrations of glucose and fructose. Fotopoulos *et al*. (2003) also observed a similar increase in cell wall associated invertase activity and gene expression in powdery mildew infected *A. thaliana* leaves. According to Hall and Williams (2000), all forms of invertase activity are elevated in powdery mildew infected wheat, however the biggest increase is observed in cwINV activity. Thus, the results obtained in the current study support previous observations indicating an important role for apoplasmic sucrose cleavage in the establishment of powdery mildew infection.

In coordination with the powdery mildew induced elevation of *VvcwINV* expression and enzyme activity, was increased expression of specific grapevine monosaccharide transporters. Of the five studied, expression of *VvHT5* and *VvHT1* was significantly enhanced in powdery mildew infected leaves while the other three transporters did not respond. In berry skin, expression of *VvHT1* and *VvHT5* was also higher than controls, however, transcript levels of *VvHT2* were also greater,

suggesting some tissue specific responses to infection (Fig. 5.1 C). The enhanced expression of a subset of *VvHT* genes in response to powdery mildew infection is in agreement with studies in *A. thaliana,* where expression of two members of the STP family is elevated by powdery mildew infection. *AtSTP4* transcript levels were strongly elevated while expression of *AtSTP3* was increased by a relatively small amount (Fotopoulos et al., 2003).

Elevated expression of *VvHT5, VvHT1* and *VvcwINV,* and increased cwINV activity may have significant effects on carbohydrate distribution in the host. Apoplasmic phloem unloading of sucrose is driven by cwINV activity which cleaves sucrose desorbed from the phloem to the apoplasm, thereby maintaining a sucrose gradient to support further efflux (Patrick, 1997). Sucrose and the hexose cleavage products are then taken up from the apoplasm by sucrose and monosaccharide transporters localised on the plasma membranes of sink cells. In light of these physiological roles, increased *VvcwINV* activity would increase apoplasmic phloem unloading of sucrose, and also reduce phloem loading of sucrose produced in the infected tissue, while elevated *VvHT5* and *VvHT1* expression would enhance the monosaccharide uptake capacity of sink cells. Powdery mildew infected grapevine leaves showed elevated sucrose, glucose and fructose concentrations when compared with healthy control leaves, and because photosynthetic ^{14}C-fixation was reduced, it is likely that the additional sugars are the result of enhanced import (Brem et al., 1986). Coordinate induction of cwINV and HT expression was correlated with elevated glucose and sucrose uptake capacity in *C. rubrum* suspension cultures treated with cytokinins and in powdery mildew infected *A. thaliana* leaves, suggesting a direct link between cwINV and HT expression in sink tissues and the rate of sugar import (Ehneß and Roitsch 1997; Fotopoulos et al., 2003).

Furthermore, additional cwINV activity can delay leaf senescence and inhibit activation of usual cell death programs (Lara et al., 2004), which in terms of biotrophic fungi, would prolong the viability of the host-pathogen association by providing a continued supply of nutrients.

Reduced vINV expression and activity may also mediate changes to carbohydrate allocation via regulation of the symplasmic path of phloem unloading. In addition to regulation by plasmodesmatal conductance, symplasmic unloading is controlled by sucrolytic activity and sucrose compartmentation at the sink cells (Patrick, 1997). The powdery mildew associated reduction in vINV expression and activity, in terms of sink physiology, implies reduced vacuolar compartmentation of sucrose at the sink cells which may in turn retard the symplasmic unloading of sucrose at the sink tissue. However, sucrose hydrolysing enzymes localised in the cytoplasm such as nINVs and sucrose synthases, also regulate the rate of symplasmic unloading (Patrick, 1997). Therefore, without investigation of these alternative sucrolytic possibilities, a diagnosis of the activity of the symplasmic route in powdery mildew infected leaves cannot be established.

5.4.2 Specificity of powdery mildew induced transcriptional changes

The broad aim of this project was to isolate and characterise grapevine transporter or metabolic genes induced by powdery mildew infection. To establish if these genes might be good targets for modification to form the basis of alternative resistance to powdery mildew via reduced susceptibility, the specificity of powdery mildew-associated induction of *VvHT1*, *VvHT5* and *VvcwINV* was explored. Firstly, the spatial specificity was investigated by quantitative RT-PCR. Transcript levels of *VvHT1*, *VvHT5* and *VvcwINV* were less than 2 fold higher in powdery mildew

infected leaf regions compared with uninfected areas of the same leaf, suggesting that expression of these genes is modulated in cells remote from infection sites (Fig. 5.5). This observation is in agreement with previous studies on powdery mildew infected leaves. Using transgenic *A. thaliana* plants expressing the glucuronidase reporter gene under control of the *AtSTP4* promoter, Fotopoulos *et al*. (2003) showed that this promoter drives expression in the mesophyll and vasculature in cells not in direct contact with the infected epidermis. Furthermore, in powdery mildew infected barley leaves, the additional invertase activity was predominantly associated with the mesophyll cell layer and not specifically with infected epidermal cells (Scholes et al., 1994). Due to the lack of spatial specificity indicated by the results presented in Figure 5.5, additional localisation studies were not performed.

To determine if other exogenous stimuli might elicit the powdery mildew-associated responses discussed above, expression of invertases and sugar transporters was measured in downy mildew infected and in wounded grapevine leaves. Quantitative RT-PCR analysis of *VvHT1*, *VvHT5* and *VvcwINV* indicated that expression of these genes was elevated by downy mildew infection (Fig. 5.6) and by wounding (Fig. 5.7), indicating that biotic and abiotic stimuli may elicit a common signal in the host that up regulates expression of these genes. Taken together, these observations are consistent with the hypothesis that induction of *VvHT1*, *VvHT5* and *VvcwINV* expression represents a generalised stress response that may be important to provide energy for repair and the initiation of defence mechanisms in the host. In terms of biotrophic pathogens such as powdery and downy mildew fungi, additional carbohydrate import to infected organs may also contribute to pathogen nutrition and may extend the host-pathogen association by repression of senescence (Lara et al., 2004).

Overall, sucrose transporters were not responsive to pathogen infection, however, their response to wounding was not investigated. At least one sucrose transporter from *A. thaliana*, (*AtSUC3*), is strongly and rapidly induced by wounding (Meyer et al., 2004). This suggests that in pathogen infected tissue, when phloem unloading of sucrose occurs via the apoplasm, sucrose is rapidly hydrolysed to hexoses which are subsequently retrieved by *VvHT*s.

5.4.3 Differential regulation of gene expression in response to powdery and downy mildew infection

Of the invertase transcripts measured in powdery mildew infected tissues, only *VvcwINV* expression was significantly elevated by powdery mildew infection, while in contrast, downy mildew infection elevated expression of all invertase genes tested (Fig 5.6). As powdery mildew infection is limited to the epidermis and downy mildew infects mesophyll cells, these contrasting host responses may relate to distinctive properties of the specific cell types infected. For example, epidermal cells contain predominantly anticlinal positioned plasmodesmata and therefore relatively little symplasmic interconnection with the cell layers below, suggesting that the epidermal cell layer forms an isolated symplasmic domain (Vasil'ev, 1999; Ma and Peterson, 2001). In contrast, downy mildew infects the mesophyll which is comprised of phototrophic cells symplasmically integrated with the phloem via plasmodesmatal connection (Haupt et al., 2001; Blackman and Overall, 2001). The induction of vacuolar (*VvGIN1* & *VvGIN2*) and cytoplasmic (TC7206) invertase genes, as observed in response to downy mildew infection, may alter the source-sink status of infected cells and mediate symplasmic unloading of sucrose at infected cells and reduce phloem loading (Patrick, 1997).

Alternatively, the differential responsiveness of invertase gene expression to powdery and downy mildew infection may be associated with differences in the metabolic status and age of leaves used for powdery and downy mildew inoculations. Powdery mildew studies used expanding leaves, approximately two weeks post emergence, in which transcript levels of invertase genes were considerably higher than in the fully expanded mature leaves used for the downy mildew expression analysis (compare healthy control levels in Fig. 5.3 and 5.6). The decrease in vacuolar invertase expression during leaf development is consistent with observations by Davies and Robinson (1996) who showed that expression of *VvGIN*1 and *VvGIN2*, and soluble acid invertase enzyme activity, declined sharply once leaves had fully matured. Koch (2004) suggested that invertase activity mediates sink formation and expansion while the developmental transition to mature status is marked by a shift from invertase to sucrose synthase cleavage paths. Thus, in mature leaves downy mildew infection may cause leaf metabolism to revert from a mature carbohydrate "source" status to an importing "sink" state characteristic of younger growing tissues. This metabolic environment would presumably provide energy for host defences and repair, and may favour nutrient delivery to and acquisition by the pathogen.

Another notable difference in the response of carbohydrate metabolism genes between powdery and downy mildew infection was the expression of the sucrose transporter *VvSUC27* which was repressed in downy mildew infected leaves (Fig. 5.6) but appeared to increase slightly in response to powdery mildew infection. Again, this differential response may reflect the different site of infection or the age of the leaves tested as discussed in relation to *VvGIN1* expression. Additionally, if *VvSUC27* has a role in phloem loading, its down regulation may be associated with

reduced carbohydrate export and elevated soluble carbohydrate concentrations observed in leaves infected with fungal pathogens (Hewitt and Ayres, 1976; Brem et al., 1986; Hwang and Heitefuss, 1986). Consistent with this proposal is the finding that antisense repression of *NtSUT1* in tobacco leaves led to an accumulation of soluble carbohydrates and reduced export of fixed $^{14}CO_2$ (Burkle et al., 1998). Relative to the other two reported grapevine sucrose transporters, the expression profile of *VvSUC27* is quite different. During berry development, Vv*SUC27* expression is limited to the green phase which precedes the period of rapid sugar import while *VvSUC11* and *VvSUC12* expression is elevated during the sugar accumulation phase (Davies et al., 1999). Furthermore, *VvSUC27* is expressed more highly in mature leaves than in young leaves, but is also strongly expressed in roots, indicating expression in sink and source tissues (Davies et al., 1999). Phloem localised ZmSUT1 from maize was recently shown to mediate both sucrose efflux and uptake dependant on the direction of the sucrose gradient and membrane potential, providing a physiological explanation for the role of sucrose transporters in source and sink tissues (Carpaneto et al., 2005).

Chapter 6 – Expression analysis of VvHTs and *VvcwINV* in grapevine carbohydrate sink tissues

6.1 Introduction

Plants are an assortment of photosynthetically active source organs and heterotrophic sink tissues. Mature leaves produce carbohydrate in surplus of their needs and export it to organs that obtain all, or at least part of their carbohydrate requirements by importation. Variation in supply and demand is a function of the normal life cycle of the plant. Leaves initiate as carbohydrate importers and mature into net exporters. Roots and other sites of vegetative growth require a constant supply of carbohydrate, while other sink tissues such as reproductive organs, tubers and fruit exert demand during tightly regulated periods of development. Additionally, exogenous biotic or abiotic stimuli can influence supply and demand for carbohydrate, contributing further complexity to the problem of establishing a dynamic equilibrium between source and sink organs (Chou et al., 2000).

In Chapter 5, pathogen infection and wounding of grapevine leaves was observed to co-ordinately induce expression of *VvcwINV*, *VvHT1* and *VvHT5* and to repress expression of *VvGIN1*. The aim of the experiments described in this Chapter were to investigate the potential involvement of these stress induced hexose transporter and invertase genes in carbohydrate metabolism associated with sugar importing (sink) tissues of grapevine during normal growth and development. In particular, the research focussed on the regulation of expression of these genes in roots and in ripening berries.

Sugar import into grape berries is of considerable commercial significance because during wine making fermentation of sugar by yeasts produces alcohol and

augments the flavour and aroma profile of the final wine product. Grape berry development can be essentially divided into two stages. During the first phase, imported carbohydrate is utilized for several processes including seed development, cell proliferation and expansion, and the synthesis of organic acids (Davies and Robinson, 1996). The inception of the second or "ripening" phase, between 8-14 weeks after flowering, is termed véraison. After véraison berries accumulate sugar, soften, and in the case of red varieties, accumulate anthocyanins (Davies and Robinson, 1996). During ripening, imported carbohydrate is loaded into the vacuoles of berry pericarp cells which expand significantly in size and, at ripeness, contain approximately 1 M glucose and fructose concentrations (Vignault et al., 2005). Previous studies have identified vINVs, HTs and SUCTs expressed during various stages of grape berry ripening (Davies and Robinson, 1996; Davies et al., 1999; Fillion et al., 1999; Terrier et al., 2005). In this context, the expression of *VvHT1*, *VvHT2*, *VvHT3*, *VvHT4*, *VvHT5* and *VvcwINV* was examined in ripening V. Vinifera cv. Cabernet Sauvignon and cv. Shiraz berries sampled at two week intervals.

6.2 Materials and methods

6.2.1 Grape berry ripening series

The Shiraz berry series was collected from the Coombe vineyard at the Waite Campus of Adelaide University (Adelaide, South Australia, latitude 34° 56' south, longitude 138° 36' east) during the 2002/2003 growing season. Flowering was defined as the date on which 50 % of flowers within an individual bunch had undergone capfall. All subsequent samplings were conducted at two week intervals

after this date. Berries were skinned and deseeded before RNA extraction of the sugar-loading pulp cells and cDNA synthesis as described in sections 2.2.12 and 2.2.13. Sugar concentration of a subset (12 berries) of sampled berries was estimated by the total soluble solids determined with a refractometer (Reichart, Vienna). The Cabernet Sauvignon berry cDNAs and associated developmental data were kindly provided by Dr Chris Davies (CSIRO Plant Industry, Adelaide).

6.2.2 Grapevine roots

Young roots were removed from glasshouse-grown Cabernet Sauvignon plants, soil removed by gentle washing and the roots frozen in liquid nitrogen and then RNA extracted and cDNA synthesized as described in sections 2.2.12 and 2.2.13.

6.2.3 Quantitative RT-PCR analysis

Quantitative RT-PCR was conducted according to the methods outlined in section 5.2.6 using ubiquitin (TC38636) instead of actin as the reference gene for normalization. The level of actin expression was found to be more stable than ubiquitin in pathogen infected and wounded samples, however in grape berry developmental series ubiquitin was more stable than actin (M. Hayes and C. Davies, unpublished data). The un-normalized expression of ubiqutin during Cabernet Sauvignon and Shiraz berry development is shown in Appenidx 2, Figure A2.5 and Figure A.2.6.

6.3 Results

6.3.1 Expression of VvHTs and *VvcwINV* in grape roots

The expression of *VvHT*s and *VvcwINV* was also examined in roots, to investigate if these genes contribute to the importation of carbohydrate into this sink tissue. *VvHT5* was found to be the most highly expressed HT of those examined in roots (Fig. 6.1). It was expressed approximately 8 fold more than *VvHT3* and more than 50 fold more than *VvHT1* and *VvHT4*. *VvcwINV* was also strongly expressed in roots.

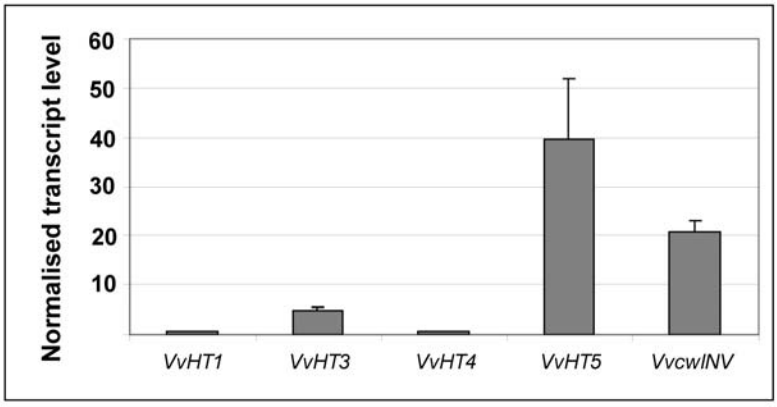

Figure 6.1. Quantitative RT-PCR analysis of HTs and cwINV in Shiraz roots. Values are relative to the expression of ubiquitin and the analysis performed allows comparison of expression level of genes within the figure (Muller et al., 2002). Data are the mean of one sample tested in triplicate. Error bars are the standard error, primer sequences are described in Table 2.3.

6.3.2 Expression of VvHTs and *VvcwINV* during berry ripening

The expression of *VvHT1*, *VvHT2*, *VvHT3*, *VvHT4*, *VvHT5* and *VvcwINV* was measured across ripening in Cabernet Sauvignon and Shiraz berries sampled at two week intervals to investigate if these genes may contribute to the accumulation of sugar that occurs during berry ripening.

Figure 6.2 shows changes in the weight and sugar concentration of Shiraz and Cabernet Sauvignon berries sampled over the growing season. At ripeness,

Shiraz berries weighed approximately 1.2 g, almost double the weight of Cabernet Sauvignon berries. Both cultivars commence a rapid increase in sugar concentration at 8 weeks post flowering which continues to increase to almost 25% total soluble solids after 14 weeks. Berries are usually considered ripe and are harvested between 22 - 25% (w/v) total soluble solids.

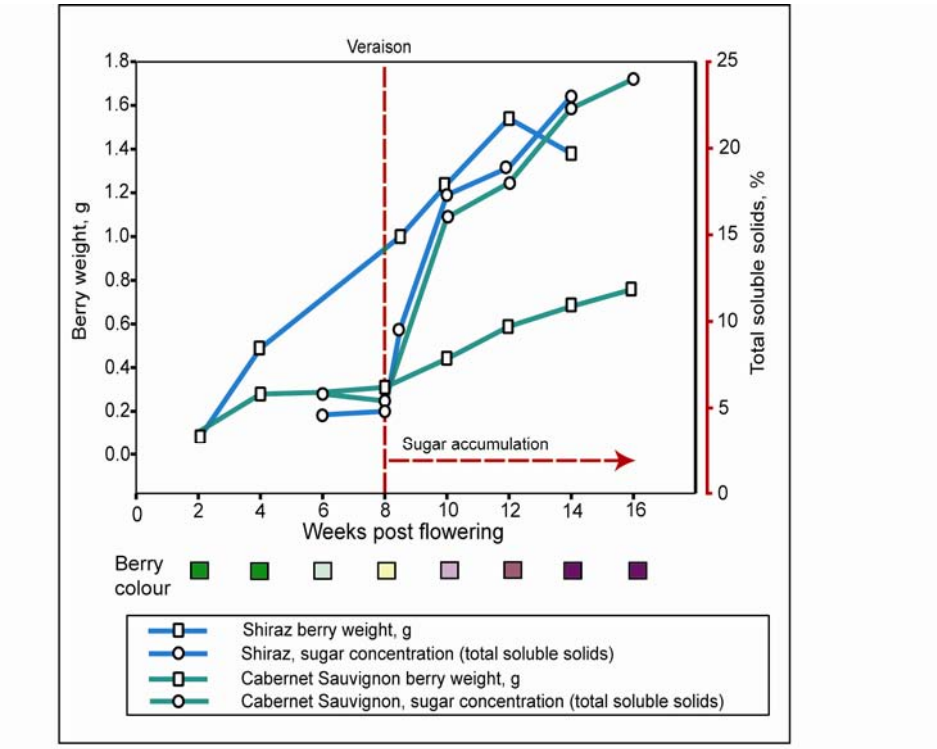

Figure 6.2. Weight and sugar concentration of Shiraz and Cabernet Sauvignon grape berries sampled over development until ripeness. Sugar concentration was measured using a refractometer to estimate total soluble solids. All values are means of multiple berries tested. Veraison marks the inception of ripening.

Figure 6.3 shows that *VvHT1*, *VvHT2* and *VvHT3* were much more highly expressed than *VvHT4* and *VvHT5* in berries of both Shiraz and Cabernet Sauvignon across the developmental period. In Shiraz, *VvHT1* was expressed more highly pre-véraison than post-véraison (Fig. 6.3 A). This trend was also observed in Cabernet Sauvignon berries (Fig. 6.3 B), however, a second increase in the amount of *VvHT1* transcript post-véraison was apparent in this cultivar whereas in Shiraz *VvHT1* expression declined sharply after the 6 weeks post flowering sample.

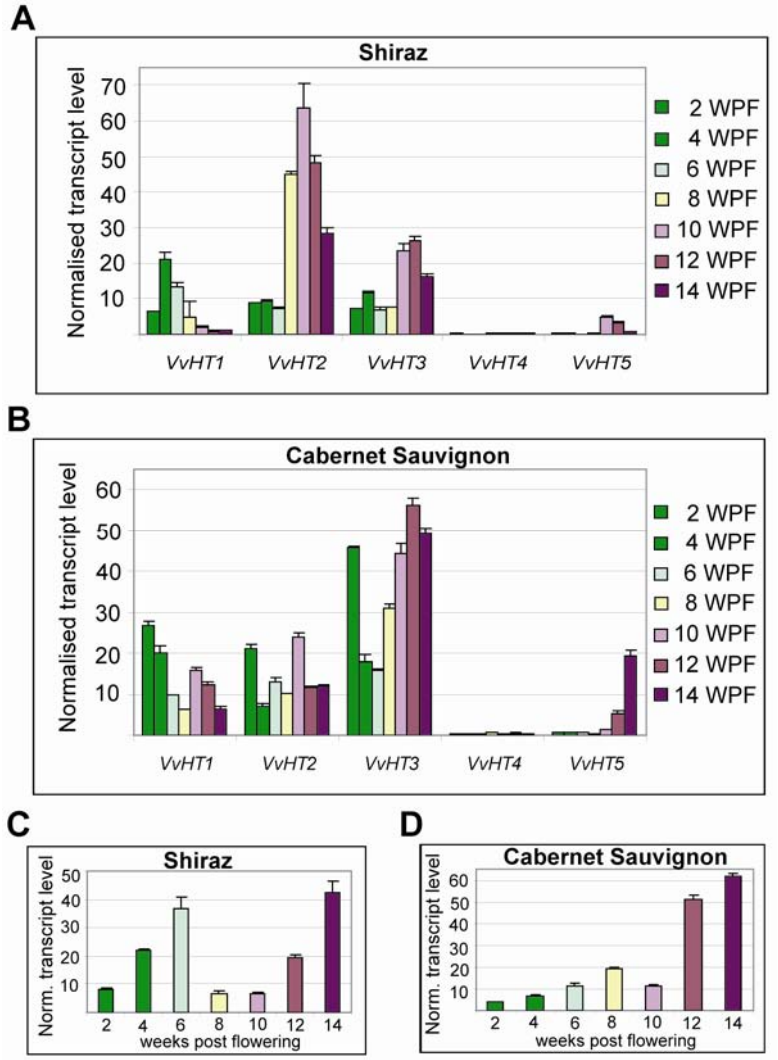

Figure 6.3. Quantitative RT-PCR analysis of VvHTs (A and B) and *VvcwINV* (C and D) during Shiraz (A and C) and Cabernet Sauvignon (B and D) berry ripening. All values were normalised to the expression of ubiquitin and each is the average of three replicates. Analysis was performed using the method of (Muller et al., 2002) which allows comparison of expression level between the genes in each figure. Error bars represent the standard error, primer sequences are described in Table 2.3.

In the initial stages of Shiraz berry development, the level of *VvHT2* expression was low before an approximate 10 fold increase between 6 and 10 weeks after flowering (Fig. 6.3 A). *VvHT2* was the most highly expressed HT post-véraison in Shiraz. In contrast, there was no clear trend in *VvHT2* expression in Cabernet Sauvignon berries.

VvHT3 expression in Shiraz also appeared to increase during the period of sugar accumulation post-véraison (Fig. 6.3 A), but did not reach the expression level of *VvHT2*. In contrast, *VvHT3* was by far the most highly expressed VvHT in post-véraison Cabernet Sauvignon berries with transcript levels increasing significantly in the 8, 10 and 12 week samples, before declining slightly in the 14 week sample.

Relative to the other VvHTs, *VvHT4* and *VvHT5* were only expressed at relatively low levels in both Shiraz and Cabernet Sauvignon berries (Fig. 6.3 A and B). *VvHT4* expression was barely detectable throughout berry development in both cultivars whereas *VvHT5* transcript levels increased in post-véraison berries of both cultivars. In Shiraz, *VvHT5* expression increased 10 fold between the 8 - 10 week samples before declining in subsequent samples. *VvHT5* expression in Cabernet Sauvignon berries increased strongly during the final 4 weeks of berry development.

In general, the expression profile of *VvcwINV* in both cultivars was reasonably similar (Fig. 6.3 C and D). Significantly, *VvcwINV* expression increased markedly during the period of sugar accumulation following véraison at week 8.

6.4 Discussion

6.4.1 Expression of VvHTs and *VvcwINV* in grapevine carbohydrate sink tissues during normal growth and development

Roots represent one of many heterotrophic tissues in plants reliant on carbohydrate import to support normal function and growth. Studies on plasmodesmata frequency and dye tracer experiments in roots indicate that phloem unloading and subsequent distribution via the symplasm can deliver carbohydrate to most root zones (Ma and Peterson, 2001). However, cwINV and HT genes are

expressed in roots (Truernit et al., 1996; Tymowska-Lalanne et al., 1998; Meyer et al., 2004), indicating an apoplasmic supply may also be active. The importance of apoplasmic carbohydrate supply in roots was previously well demonstrated in carrot roots where antisense repression of cwINV expression drastically reduced tap root size (Tang et al., 1999).

In grapevine roots, *VvHT5* and *VvcwINV* were relatively highly expressed suggesting these genes may be preferentially expressed in sink tissues (Fig. 6.1). Previous studies have shown that vacuolar invertase expression in grapevine roots is low (Davies and Robinson, 1996). Taken together, these observations indicate that the apoplasm may be an important carbohydrate supply path to root sink cells, consistent with studies on other plants. For example, in *A. thaliana* roots, the cell wall invertase gene *AtβFRUCT1*, and the sugar transporter genes *AtSTP4* and *AtSUC3* are expressed relatively strongly compared with other members of these particular gene families (Truernit et al., 1996; Tymowska-Lalanne et al., 1998; Meyer et al., 2004). Interestingly, these genes are also induced by wounding and/or pathogen infection, indicating these genes encode proteins that regulate the formation of sink metabolism in response to both developmental and stress-associated cues (Truernit et al., 1996; Chou et al., 2000; Meyer et al., 2004).

Expression of *VvHT5* and *VvcwINV* was also induced in grape berries during the phase of rapid sugar accumulation (Fig. 6.3 A-D) consistent with the idea that these genes are predominantly expressed in sink tissue. In berries, however, other sugar transporter and invertase proteins are likely to play a more significant role in sugar delivery to this particular sink organ (see section 6.4.2 below).

The induction of *VvHT5* and *VvcwINV* at relatively late stages during berry ripening may be mediated by stress-associated signals rather than developmental

cues. Differential screening and northern analysis has previously shown that genes involved in defence responses are amongst the most highly induced during grape ripening (Davies and Robinson, 2000). Structural modifications to permit changes in cell volume, and induction of proteins to manage increased osmotic potential in the sugar accumulating cells, are proposed explanations of these initial observations which have now been confirmed in subsequent publications (Sarry et al., 2004; Terrier *et al*., 2005; Goes da Silva et al., 2005). Potentially, *VvcwINV* and *VvHT5* may be induced as part of this grape berry stress response.

6.4.2 Role of *VvHT*s and *VvcwINV* in grape berry development

Analysis of *VvHT1-5* and *VvcwINV* expression during grape berry development has also provided new insights into the mechanism of sugar import and storage into berries during ripening. Because of the commercial importance of sugar accumulation into grape berries, there is a significant amount of interest in understanding the biochemistry and genetic regulation of this process. (Davies and Robinson, 2000).

In Shiraz and Cabernet Sauvignon berries, *VvHT1*, *VvHT2* and *VvHT3* transcript levels were generally higher than the levels of *VvHT4* and *VvHT5* transcripts. *VvHT1* was most highly expressed pre-véraison in both cultivars, however a small induction at véraison was observed in Cabernet Sauvignon berries (Fig. 6.3). This expression pattern for *VvHT1* is consistent with the biphasic expression pattern observed during the development of *V. vinifera* cv. Ugni Blanc berries in which there was a decrease in transcript levels during an approximate five week period around véraison (Fillion et al., 1999). Interestingly, there was no similar increase in *VvHT1* transcript levels post-véraison in Shiraz berries, which

may indicate cultivar differences in the expression of this gene during berry ripening. Alternatively, these differences may reflect contrasting environmental conditions or different management practices used in the vineyards from where these berries were sampled.

Recently, *VvHT1* transcript and protein was localized to phloem-associated cells in berries rather than the sugar accumulating cells of the pulp, while expression of *VvHT1* was found to be mainly confined to the pre-véraison period of berry development (Vignault et al., 2005). These observations are consistent with a role for VvHT1 in hexose retrieval by cells of the conducting complex during the early phase of berry development, when sugars are utilized for cell proliferation and growth (Vignault et al., 2005).

The expression pattern of *VvHT2* during Shiraz berry ripening was correlated with the period of rapid sugar accumulation, however in Cabernet Sauvignon this correlation was not evident (Fig. 6.3). This cultivar difference in *VvHT2* expression during berry ripening was also noted in the oligo array analysis of Terrier *et al.* (2005). Their analysis indicated that *VvHT2* expression in Shiraz was strongly induced during berry ripening, while in Chardonnay and Cabernet Sauvignon, the increase in *VvHT2* expression was not significant. *VvHT3* expression profiles in Shiraz and Cabernet Sauvignon were also found to be different. In post-véraison Shiraz berries, *VvHT2* transcript levels were significantly greater than *VvHT3*, whereas in Cabernet Sauvignon, the opposite was observed (Fig. 6.3). *VvHT2* expression did not strictly correlate with the phase of sugar accumulation, while *VvHT3* expression was elevated post-véraison and maintained at the highest level of the VvHTs measured. These results suggest that sugar loading into ripening berries of different *V. vinifera* cultivars may not be mediated by common carriers.

Alternatively, cultivar differences in the efficiency of translation of *VvHT2* and *VvHT3* transcripts, or differences in the activity of the respective proteins, could mean these transcriptional differences might not reflect the level of active protein found in the berry.

The amount of *VvHT4* transcript was consistently low during grape berry development, indicating that this gene is not involved in sugar importation during berry ripening, while as discussed above, VvHT5 was induced during the late stages of ripening.

The transcript levels of *VvcwINV* during berry development exhibited a biphasic profile with two peaks in expression, one preceding or approximately at the time of véraison, and another at the ripe stage (Fig. 6.3). Consistent with this biphasic expression profile, proteomic and immunohistochemistry studies have shown the presence of cwINV peptides in berries at early and late stages of berry development. Famiani *et al*. (2000) reported that cwINV epitopes, identified using a cwINV specific antibody, were associated with berry palisade cells associated with developing seeds and vasculature, and with cells underlying the berry epidermis. As berry development proceeded towards véraison, cwINV epitopes were lost from palisade cells. Unfortunately, due to technical limitations, berries after véraison were not analysed in this study (Famiani et al., 2000). Using a proteomic approach, Sarry *et al*. (2004) identified a cwINV degradation product at relatively high concentrations in extracts isolated from ripe berries, however berries at earlier developmental stages, still rapidly accumulating sugars, were not analysed.

Previous studies in grape indicate that transcripts of two vINVs, *GIN1* and *GIN2*, are found at high levels in grape pulp until ten weeks after flowering, and a high level of soluble acid invertases activity is maintained, at least on a per berry

basis, until berries are ripe (Davies and Robinson, 1996). Immunohistochemistry indicated that high levels of vINV protein is localized throughout the sugar-accumulating pulp cells up to the time of véraison (Famiani et al., 2000), while enzymatic studies suggest that vINV activity accounts for the vast majority of invertase activity in berries and cwINV activity represents only 4% of the total activity (Ruffner et al., 1995). Considered together, these observations suggest that sucrose may not be cleaved in the apoplasm before it is loaded into pulp cells.

The actual path of sugar delivery to grape pulp cells, apoplasmic or symplasmic, is yet to be fully resolved, but an apoplasmic step is commonly observed in fruits and seeds where sugars are accumulated to high concentrations (Patrick et al., 2001). Furthermore, after véraison in grapes, enhanced phloem transport is accompanied by reduced xylem flow (Greenspan et al., 1994). Bondada *et al*. (2005) hypothesized that increased apoplasmic solute concentrations may elevate the hydrostatic potential of this compartment, and thus be responsible for the elimination of xylem inflow to ripening berries.

Although a role for cwINV during berry ripening is not clearly supported by current evidence, sugar transporters are expressed by berry pulp cells, indicating that sugars may be retrieved from the apoplasm. In the current study, the expression profiles of *VvHT2* and *VvHT3* during berry ripening were found to be consistent with this role. Monosaccharide transporters from *A. thaliana* (*AtSTP11*; Schneidereit et al., 2005), tomato (*LeHT3*; Gear et al., 2000) and apple (Zhang et al., 2004) are expressed by sink cells where they are proposed to be important for carbohydrate acquisition. Also, transcript levels of two grapevine sucrose transporters, *VvSUC11* and *VvSUC12*, increase significantly after véraison and remain highly expressed through-out the period of sugar accumulation (Davies et al.,

1999). Sucrose transporters isolated from plants other than grapevine have been localized to phloem cells where they are proposed to contribute to sucrose loading, unloading or re-absorption along the phloem path (Stadler et al., 1995; Barth et al., 2003; Carpaneto et al., 2005). Other sucrose transporters are expressed in sink cells, such as *DcSUT2* which is expressed on storage parenchyma cells of *Daucus carota* L. roots, and *AtSUC3* which is expressed on a range of *A. thaliana* sink cells, for example root tips, trichomes and pollen grains (Shakya and Sturm, 1998; Meyer et al., 2004). Although expression of *VvSUC11* and *VvSUC12* has not been localized at the cellular level, the induction of these genes in berry pulp in coordination with the commencement of sugar loading, suggests they may mediate the import of sucrose into berry pulp cells. Vacuolar compartmentation of sucrose, supported by the high rate of vacuolar invertase activity (Davies and Robinson, 1996), would support retrieval of sucrose from the apoplasm by VvSUC11 and VvSUC12, as the inward activity of these transporters is probably dependant on the sucrose concentration gradient between the apoplasm and the sink cell cytoplasm (Carpaneto et al., 2005). However, it must be acknowledged that the pulp of grapes does represent a heterogenous mixture of cell types at different stages of development (Famiani et al., 2000), therefore alternative roles for VvHT2, VvHT3, VvSUC11 or VvSUC12 cannot be ruled out. Potentially, VvSUC11 or VvSUC12 may be localised to the phloem and mediate phloem unloading, rather than sink cell loading. Similarly, VvHT2 or VvHT3 may be localized to phloem-associated cells and as has been proposed for VvHT1 (Vignault et al., 2005), VvHT2 and VvHT3 may contribute to hexose retrieval in the conducting complex.

Chapter 7 - Hormonal regulation and analysis of promoters of VvHT and invertase genes

7.1 Introduction

Plant hormones such as ethylene, jasmonate and abscisic acid (ABA), are important regulators of stress responsive pathways. Ethylene and jasmonate are commonly associated with defence pathways activated by pathogen infection and wounding (Zimmerli et al., 2004) while ABA is well known to regulate responses to abiotic factors such as salinity and drought (Zhou, 2002). More recently, ABA has also been implicated in the establishment of compatible interactions between fungal pathogens and host plants (McDonald and Cahill, 1999; Mohr and Cahill, 2003). Exogenous application of ethylene (Jacobs et al., 1999), jasmonate (Zimmerli et al., 2004) and ABA can elicit aspects of the host response to stress stimuli.

Genomic DNA upstream of protein coding regions, or promoters, contain short (approximately 6-12 bp) nucleotide motifs, or *cis*-acting regulatory elements, that contribute to the transcriptional regulation of the gene downstream. Many stress-associated *cis*-elements that activate transcription in response to salinity, drought, wounding and pathogen infection have been identified in plants (Korfhage et al., 1994; Mihiri et al., 1997; Choi et al., 2000). Web-based databases such as PLACE DB (Higo et al., 1999) provide a convenient way to search for these previously identified promoter motifs in DNA sequences.

In Chapter 5 expression of *VvHT1*, *VvHT5* and *VvcwINV* was observed to be induced by pathogen infection and wounding, while *VvGIN1* expression was repressed by wounding and powdery mildew infection but induced by downy mildew infection. To investigate the potential regulatory factors that may contribute

to these gene expression changes, ABA, methyl-jasmonate and ethylene were supplied to plants and quantitative RT-PCR used to measure transcript levels. Additionally, more than 1 kb of genomic DNA upstream of the start codons of *VvHT3*, *VvHT4*, *VvHT5* and *VvcwINV* ORFs was isolated and the sequences analysed to identify potential regulatory sequence motifs.

7.2 Materials and Methods

7.2.1 Exogenous application of ABA, ethylene and methyl jasmonate

An abscisic acid (ABA) solution containing 200 mg L^{-1} ABA and 0.05% (v/v) Tween 20 was applied by spray to the upper and lower surfaces of Cabernet Sauvignon grapevine leaves. Control leaves were sprayed with a solution containing 0.05% (v/v) Tween 20 only. Duplicate ABA and control sprayed leaves were collected at 1, 2, 4, and 6 h after spray application, snap frozen and stored at -80°C.

Ethylene was applied to grapevine leaves using a 10 mM ethephon (Ethrel, Bayer Crop Science, Australia) solution. Leaves were sprayed to run off, bagged overnight in zip-lock plastic bags and sampled 2 d post treatment. Control leaves were sprayed with distilled water only; one leaf was bagged like the ethephon sprayed leaf, while a second control leaf was not bagged. Leaves were sampled 2 d post treatment, snap frozen in liquid nitrogen and stored at -80°C.

Grapevine leaves sealed in plastic zip-lock bags were exposed to methyl jasmonate vapours generated from an ethanol bud containing 400 µL of 0.5% (v/v) methyl jasmonate. A control leaf was bagged and exposed to the ethanol bud while a second control leaf was not bagged. Leaves were sampled 2 d post treatment, snap frozen in liquid nitrogen and stored at -80°C.

Total RNA was extracted, cDNA synthesized and quantitative RT-PCR undertaken in the same manner as described in sections 2.2.12 and 2.2.13. Actin was used as the reference gene for these hormone treated comparisons. All primer sequences are described in Table 2.3.

7.2.2 Isolation of BAC DNA and direct sequencing

A *V. vinifera* cv. Cabernet Sauvignon genomic bacterial artificial chromosome (BAC) library (Barker et al., 2005) was screened by PCR with the primers used for quantitative RT-PCR to identify BACs containing the genes *VvHT3*, *VvHT4*, *VvHT5* and *VvcwINV*.

The buffers used in the procedure below were from a QIAprep Spin Miniprep Kit (Qiagen). After confirmation, positive BAC DNA was prepared from 7.5 ml of overnight culture grown in LB containing 34 ng ml^{-1} of chloramphenicol. Cultures were centrifuged for 6 min at 5,000 *g* to pellet bacteria, resuspended in 350 µl buffer P1 (Qiagen) and then 350 µl buffer P2 (Qiagen) was added. The lysate was incubated for 5 min at room temperature before 350 µl buffer P3 (Qiagen) was added, and this mixture was incubated on ice for five min. To remove cell debris and bacterial genomic DNA, the mixture was centrifuged at 15,000 *g* for 15 min, the supernatant collected and transferred to a new tube and one ml isopropanol added to precipitate DNA. After centrifugation at 15,000 *g* for 15 min, the supernatant was discarded and the DNA pellet dried under vacuum before being resuspended in 500 µl TE buffer. The DNA was phenol extracted with an equal volume of (25:24:1) phenol:chloroform:isoamyl alcohol followed by centrifugation at 15,000 rcf for 10 min. The aqueous phase was collected, ethanol precipitated using 50 µl 3 M sodium acetate and 1 ml cold absolute ethanol, and then incubated at -20°C for 1 h. BAC

DNA was pelleted by centrifugation at 15,000 *g* for 15 min, the pellet washed with 1 ml 70% ethanol, air dried under vacuum and then resuspended in 20 µl TE buffer.

BAC DNA was sequenced using 8 µl BigDye terminator V3.1 (Applied Biosystems, Foster City, California), 0.25 µM sequencing primer (Table 2.2) and 4 µl of BAC DNA in a total volume of 20 µl. Thermal cycling was performed using 80 cycles of 94°C for 30 s, 55°C for 30 s, 68°C for 4 min. BAC sequencing primers were designed to produce approximately 100 bp overlap with the previous sequencing run to allow unambiguous alignment of sequences. Each run yielded approximately 500 bp of good quality sequence and each was aligned manually using Genedoc (www.psc.edu/biomed/genedoc).

7.2.3 Promoter analysis

Promoter sequences were submitted to the PLACE database (Higo et al., 1999) to identify and map potential regulatory motifs. The PLACE database is served at: http://www.dna.affrc.go.jp/PLACE/signalscan.html.

7.2.4 Quantitative RT-PCR analysis of ABA biosynthetic genes

Gene specific primers for zeaxanthin epoxidase (*VvZEP*) and 9-cis-epoxycarotenoid dioxygenase (*VvNCED1*) were kindly supplied by Dr Jim Speirs, CSIRO Plant Industry, Adelaide. The expression of these genes was measured in the powdery and downy mildew infected, and wounded samples described in sections 5.3.1 and 5.3.2. Quantitative RT-PCR was carried out as described in section 5.2.6 using actin as the control gene for normalization. The un-normalized expression of actin in ABA-treated leaves is shown in Appenidx 2, Figure A2.7.

7.2.5 Measurement of bulk leaf ABA concentration

ABA analysis was kindly performed by Ms Suzanne Maffei, CSIRO Plant Industry Adelaide, using the method described by Soar et al. (2004). Powdery mildew infected and healthy control Chardonnay leaves were sampled 10 days after inoculation, ground under liquid nitrogen and store at -80°C until analysed.

7.3 Results

7.3.1 Expression of VvHTs and invertases in grapevine leaves exogenously supplied with ethylene and methyl jasmonate

Ethylene and jasmonate dependant pathways regulate many defence genes induced in response to pathogen attack in grapevine and other plants (Jacobs et al., 1999; Zimmerli et al., 2004). These chemicals were exogenously supplied to grapevine leaves to determine if the pathogen and wound induced genes *VvHT5* and *VvcwINV,* or the pathogen repressed genes *VvGIN1*, are regulated by these hormones. Expression of the previously reported ethylene-responsive thaumatin-like gene *VvTL2* (Jacobs et al., 1999; homologous to *VvOSM1*, Loulkakis, 1997) was also monitored in ethylene and methyl jasmonate treated leaves as a positive control.

Leaves were bagged overnight to facilitate hormone treatment and in general, this had no significant effect on the expression of the genes investigated. In both ethylene and methyl jasmonate treated leaves, *VvTl2* transcript levels were more than 3.5 fold higher than levels in control samples (Fig. 7.1). *VvHT5* was slightly induced by both treatments but by less than 2 fold relative to control samples. *VvcwINV* expression increased by approximately 2.5 fold in ethylene treated leaves and by approximately 2 fold in jasmonate supplied samples, while *VvGIN1* expression did not significantly respond to these treatments.

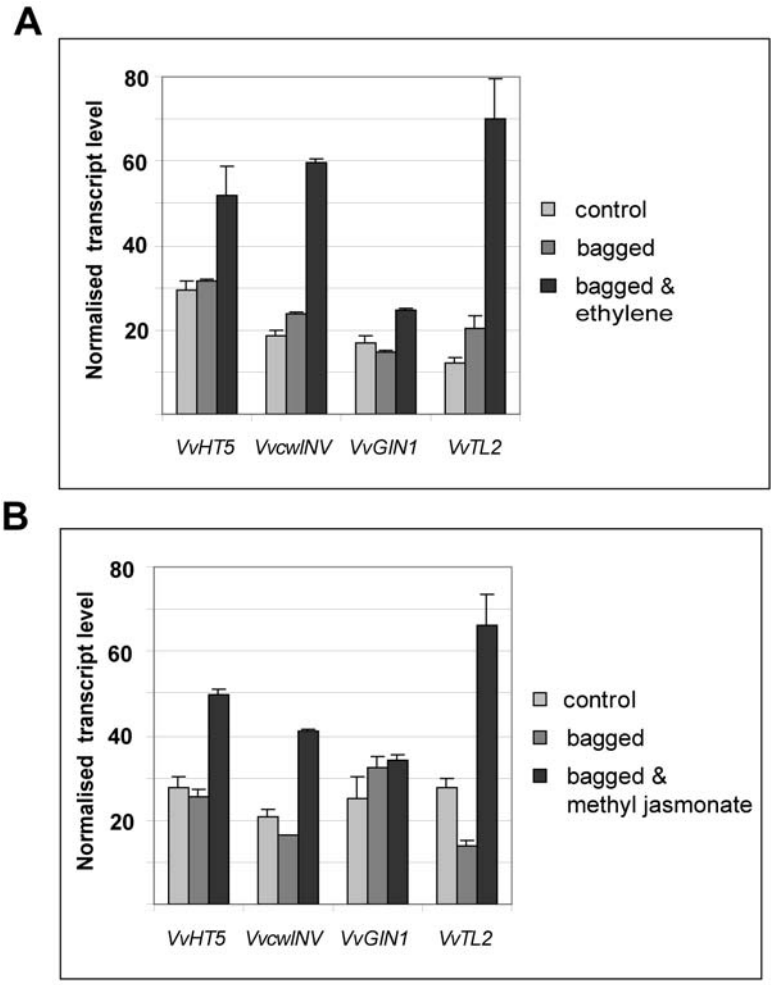

Figure 7.1. Quantitative RT-PCR analysis of *VvHT5*, *VvcwINV*, *VvGIN1* and *VvTL2* expression in leaves treated with ethylene (A) and methyl jasmonate (B). All values are relative to the expression of actin. Data analysed using the method of Muller *et al*. (2002). Data are the mean of a single sample tested in triplicate. Primer sequences are in Table 2.3.

7.3.2 Expression of VvHTs and invertases in grapevine leaves exogenously supplied with ABA

ABA application led to the specific induction of *VvHT1* and *VvHT5* expression in Cabernet Sauvignon leaves (Fig. 7.2 A). *VvHT1* transcript levels increased between 2 and 3 fold in ABA treated leaves relative to control leaves sprayed with the 0.05% Tween solution within 4-6 h after application. Some increase in *VvHT1* transcript levels were also observed in the control samples

suggesting this gene may be diurnally regulated, or alternatively, that the control treatment up-regulated expression of *VvHT1*.

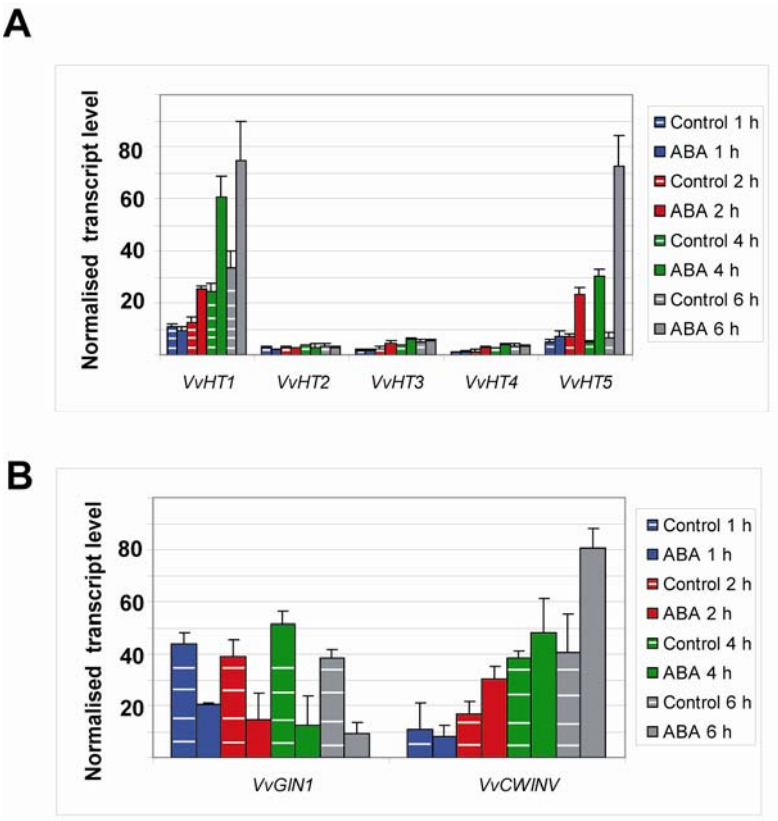

Figure 7.2. Quantitative RT-PCR analysis of VvHTs (A) and invertases (B) in ABA (200 mg/L) sprayed Cabernet Sauvignon leaves. All values are relative to the expression of actin in each sample, and the analysis performed allows comparison of expression level of genes within each figure (Muller et al., 2002). Data are the mean of biological replicates tested in triplicate. Primer sequences are in Table 2.3.

VvHT5 expression was elevated approximately 3 fold within 2 h of ABA treatment, relative to control leaves, and continued to increase until the final sampling point at 6 h where *VvHT5* expression was induced approximately 10 fold, compared to controls. In contrast, no significant induction of *VvHT2*, *VvHT3* and *VvHT4* was observed in response to ABA application (Fig. 7.2 A).

Expression of cytoplasmic invertase *VvGIN1* and the apoplasmic invertase *VvcwINV* were also measured in the ABA treated Cabernet Sauvignon leaves (Fig 7.2 B). *VvGIN1* transcript levels declined to approximately 50% of the control

leaves within 1 h of ABA treatment and continued to decline over the next 5 h. In the 4-6 h ABA treated samples, *VvGIN1* was expressed approximately 4 fold less than the control samples. Like *VvHT1*, *VvcwINV* expression increased in control leaves during the sampling period suggesting this gene may also be diurnally regulated or affected by the control treatment. Relative to the controls, ABA application caused a slight increase in *VvcwINV* expression resulting in a 2 fold increase in expression above the control sample, 6 h after treatment.

7.3.3 Promoter analysis

To identify potential regulatory elements that may mediate the induction of *VvHT5* and *VvcwINV* in response to powdery mildew infection and wounding, promoters of these genes were isolated. Approximately 55,680 clones from a Cabernet Sauvignon genomic BAC library, representing 9.4 copies of the haploid grapevine genome (Barker et al., 2005) were screened, and BACs containing the desired regions were identified. More than 1 kbp of genomic sequence upstream of the ORFs of *VvHT3*, *VvHT4*, *VvHT5* and *VvcwINV* was sequenced from isolated BAC DNA and these sequences were analysed for potential regulatory elements, together with the previously reported promoters of *VvHT1* (AJ001062; Fillion et al., 1999), *AtSTP4* (AB025631; Truernit et al., 1996) and *AtβFRUCT1* (AB028610), using the PLACE database. The promoter analysis identified an abundance of sequence elements commonly found in the 5' non-coding regions of plant genes that are known to be involved in transcriptional regulation.

The upstream genomic sequences of *VvHT3*, *VvHT4*, *VvHT5* and *VvcwINV* all contain motifs characteristic of the various Hogness (TATA) box sequences found in plant promoters (O'Shea-Greenfield and Smale, 1992). The location of the

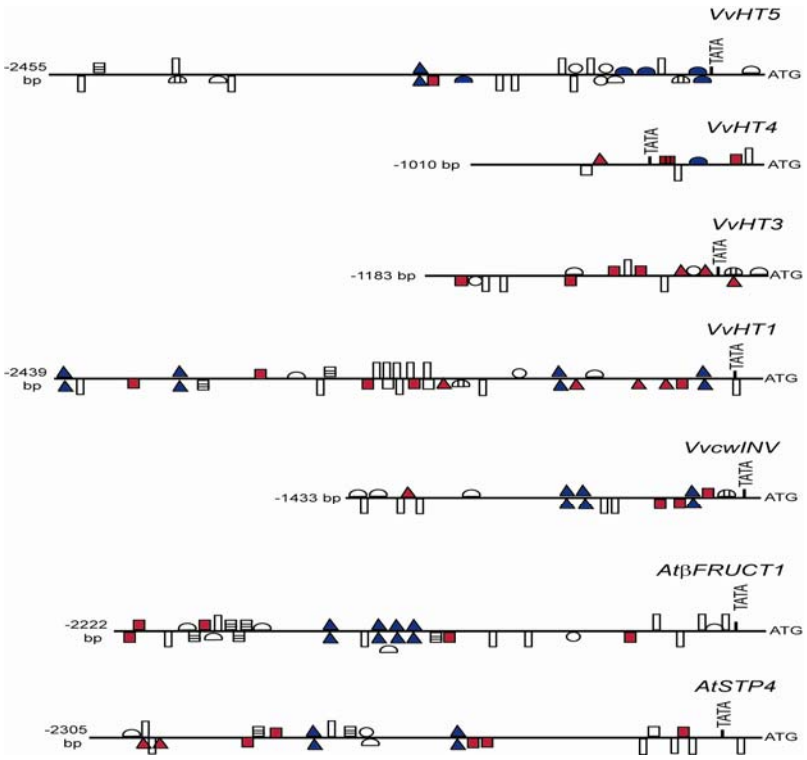

Figure 7.3. Location of regulatory elements found in promoters of grapevine and *A. thaliana* HTs and cwINVs. PLACE database (Higo et al., 1999) was used to identify regulatory motifs. *VvHT5, VvHT4, VvHT3* and *VvcwINV* promoters were isolated and sequenced from a Cabernet Sauvignon genomic BAC library (Barker et al., 2005). Accession numbers of other sequences used are: *VvHT1* (AJ001062), *AtSTP4* (AB025631), *AtβFRUCT1* (AB028610). Explanations of motifs are given below.

- Myc recognition motifs, CATGTG (Tran et al., 2004) or CACATG (Abe et al., 1997). Drought & ABA response.
- ABRE of four types: YACGTGGC (Choi et al., 2000); ACGTSSSC (Marcotte et al., 1989); CCACGTGG (Pla et al., 1993); ACGTGKC (Hatori et al., 2002). ABA response to drought and salinity.
- Pyrimidine box TTTTTTCC, (Cercos and Gomez-Cadenas, 1999). GA & ABA induction.
- EIX motif, TAAAATAT, (Matarasso et al., 2005). Ethylene induction in response to fungal elicitor.
- GARE, TAACAAR (Ogawa et al., 2003). Gibberellin response element.
- ARF, ACTTTA (Baumann et al., 1999) or TGTCTC (Hagen and Guilfoyle, 2002). Auxin regulated expression.
- SURE1 & 2, AATAGAAAA or AATACTAAT (Grierson et al., 1994). Sucrose responsive elements 1 & 2.
- GT1 binding motif, GAAAAA, (Park et al., 2004). Rapid response to pathogen attack and salinity.
- GA-down regulated motif, ACGTGTC (Ogawa et al., 2003). GA negative response element.
- Pyrimidine box, CCTTTT (Morita et al., 1998). Sugar repression.
- S1F box, ATGGTA (Zhou et al., 1992). Negative regulator of transcription.

TATA motif closest to the predicted start codon of each ORF is indicated in Figure 7.3. The TATA motifs and locations were: *VvHT3* (TTATTTT; -260), *VvHT4* (TTATTT;-416), *VvHT5* (TATATAA; -232) and *VvcwINV* (TTATTT; -157).

Numerous motifs associated with stress response and hormonal regulation were identified in the promoters of pathogen and wound responsive grapevine genes. Of particular interest is the observation that the *VvHT5* promoter contained five ABA responsive elements (ABRE) of four closely related types: C/TACGTGGC; ACGTG/CG/CC; CCACGTGG; ACGTGG/TC, whereas ABREs were absent or identified once only in other promoters. A group of drought and salinity induced *trans*-acting factors belonging to the bZIP class of proteins interact with ABREs and mediate the ABA-dependant induction of stress responsive genes (Kang et al., 2002). Numerous MYC (CATGTG) or MYB (CACATG) binding sites were identified in the promoters of *VvHT1* and *VvcwINV*, and also in the promoters of the pathogen induced *A. thaliana* genes *AtSTP4* and *AtβFRUCT1*. Drought, salinity and ABA-induced members of NAC-domain, MYC and MYB classes of transcription factors from *A. thaliana* bind at these sequences and promote expression of downstream genes (Abe et al., 1997; Tran et al., 2004).

A GT1(GAAAAA) motif in the promoter of a calcium calmodulin gene from soybean was recently identified as the *cis*-element that mediates the rapid induction of this gene in response to pathogen attack and salinity (Park et al., 2004) and GT1 *trans*-factors are rapidly induced by pathogen infection and salinity (Park et al., 2004; Wang et al. 2004). Although numerous GT1 *cis*-elements were found within the promoters of the pathogen and wound induced genes, this motif was also identified in the promoter regions of the "non-responsive" genes *VvHT3* and *VvHT4*.

Various other *cis*-elements associated with ethylene, gibberellin and auxin induction were also identified within the promoter regions (Fig. 7.3), but there was no obvious relationship between the presence of these motifs and the response of the downstream gene to pathogen infection. Of these elements, the most interesting in terms of stress induction is a cluster of three EIX sequences (TAAAATAT) found in the *VvHT5* promoter. The EIX sequence is essential for fungal elicitor-induced and ethylene-dependant induction of the tomato *Acs* gene (Matarasso et al., 2005).

Interestingly, the frequency of regulatory elements associated with transcriptional repression was found to be very low in the *VvHT5* promoter relative to the promoter sequences of the others genes examined. A pyrimidine box sequence (CCTTTT) associated with sugar repression occurs more than 3 times within the first 1,400 bp of *VvHT3*, *VvHT1* and *VvcwINV*, but occurs only once in *VvHT5*. Another negative element, S1F (ATGGTA), was not observed in *VvHT5* but is present in most of the other promoters analysed. The S1F sequence is able to repress activity of cauliflower mosaic virus 35 S promoter, and is associated with regulation of a chloroplast associated gene from spinach (Zhou et al., 1992).

7.3.4 Induction of ABA biosynthetic genes in mildew infected and wounded grapevine leaves

The powdery mildew inducible gene *VvHT5* is highly responsive to ABA (Fig. 7.2) and analysis of the *VvHT5* promoter identified the presence of numerous ABRE elements. It was therefore of interest to investigate whether ABA might regulate the powdery mildew/wound response of *VvHT5*. The ABA biosynthetic pathway is generally considered to contain two rate limiting steps (Seo and Koshiba, 2002). The first is the conversion of zeaxanthin to violaxanthin catalysed by

zeaxanthin epoxidase for which a single gene has been isolated from grapevine (*VvZEP1*; Refer to Fig. 7.4). The expression of *VvZEP1* is repressed by water stress (Soar et al., 2004). The second limiting step is the conversion of the epoxy-carotenoids violaxanthin and neoxanthin to xanthoxin, which is a precursor of ABA, catalysed by 9-cis-epoxycarotenoid dioxygenase (NCED). In grapevine, two NCED genes have been isolated: *VvNCED1* is the most highly expressed of the two and its expression is induced by water stress (Soar et al., 2004). *VvNCED2* is not stress induced but may be developmentally regulated as transcript levels tend to increase during leaf development (Soar et al., 2004).

To investigate if ABA biosynthetic genes are induced by mildew infection or wounding, the expression of *VvNCED1* and *VvZEP* was measured in powdery and downy mildew infected samples and wounded leaves. In powdery mildew infected Chardonnay and Cabernet Sauvignon leaves, *VvNCED1* transcript levels were approximately 2-3 fold higher than the appropriate control samples respectively, however *VvZEP* expression was not significantly altered (Fig. 7.5). In the downy mildew infected leaves, *NCED1* expression was induced more than 10 fold relative to controls while *ZEP* expression was repressed approximately 5 fold.

Wounding caused a very rapid, but transient increase in *VvNCED1* expression (Fig. 7.6). Within 1 h after wounding, *VvNCED1* was induced approximately 8 fold relative to unwounded control leaves. This level of expression was sustained until 2 h after wounding, after which time *VvNCED1* transcript levels declined towards control levels. In contrast, *VvZEP* expression tended to decline in response to wounding, but by a smaller amount. *VvZEP* expression remained at approximately half the control level 2-8 h after wounding and returned to normal levels by 24 h.

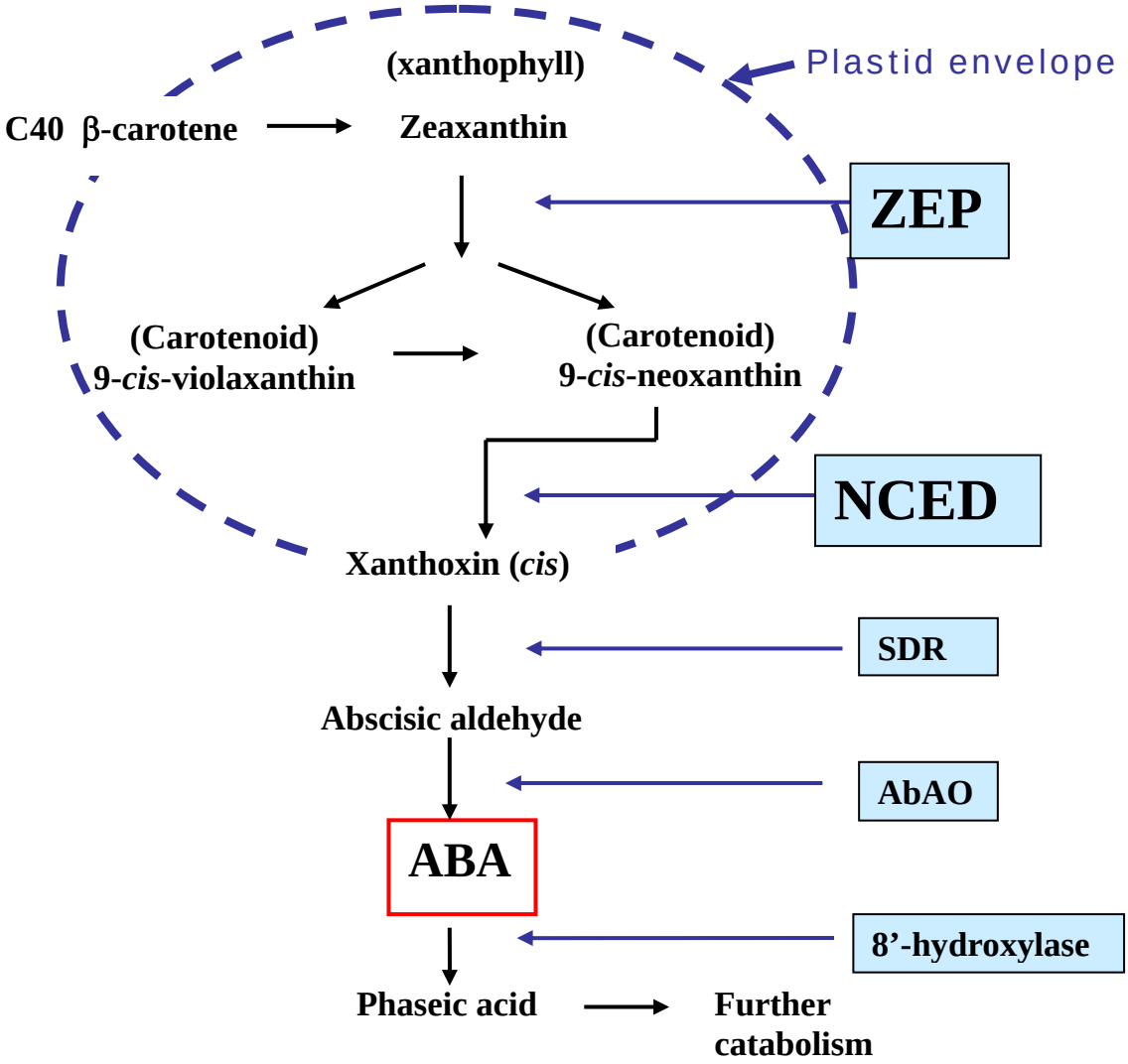

Figure 7.4. Stylised diagram representing a simplified version of the ABA biosynthetic pathway. Enzymes are contained within blue boxes, compound names are given in black text only, ABA is boxed in red. The diagram was produced by Dr Jim Speirs, CSIRO Plant Industry, Adelaide, and modified further. ZEP, zeaxanthin epoxidase; NCED, 9-cis-epoxycarotenoid dioxygenase; SDR, short-chain alcohol dehydrogenase; AbaO, abscisic aldehyde oxidase.

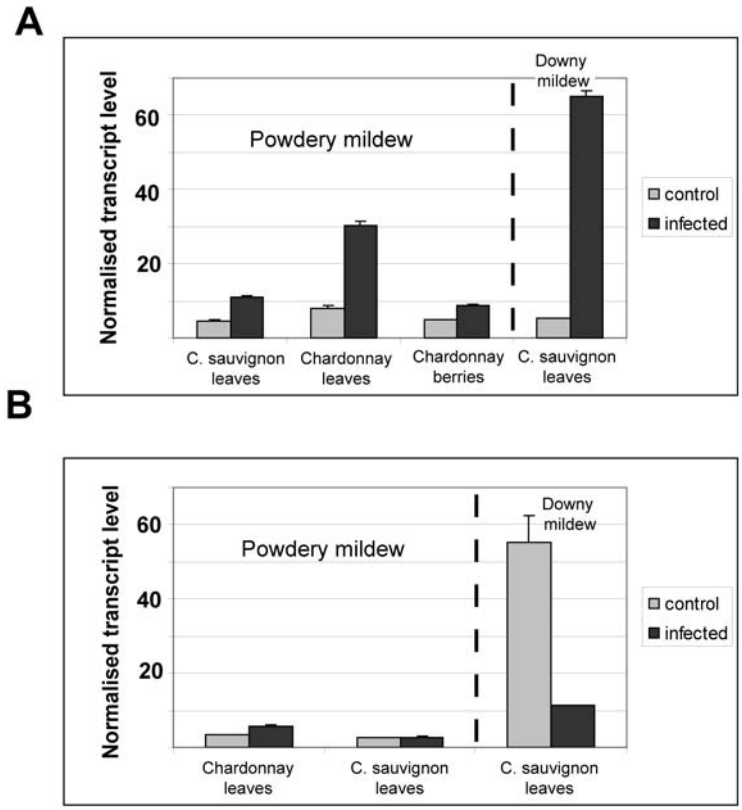

Figure 7.5. Quantitative RT-PCR analysis of VvNCED1 (A) and VvZEP1 (B) expression in powdery mildew and downy mildew infected samples. All values are relative to the expression of actin. Data analysed using the method of Muller et al. (2002). Data are the mean of one sample tested in triplicate. Primer sequences are in Table 2.3.

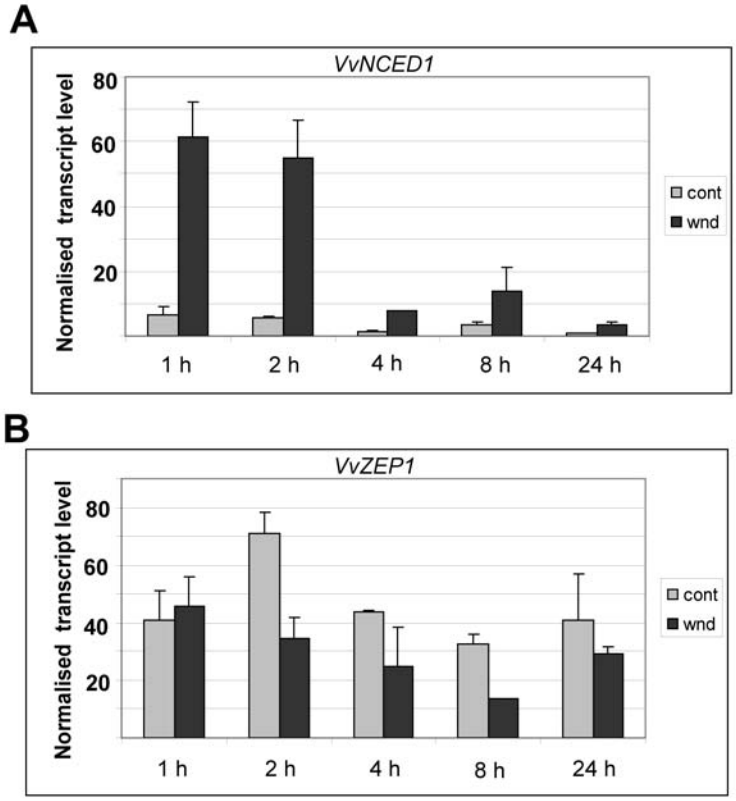

Figure 7.6. Quantitative RT-PCR analysis of *VvNCED1* (A) and *VvZEP1* (B) expression in wounded and control leaves. All values are relative to the expression of actin. Data analysed using the method of Muller et al. (2002). Data are the mean of biological replicates tested in triplicate. cont = control, wnd = wounded. Primer sequences are in Table 2.3.

7.3.5 ABA concentration in powdery mildew infected grapevine leaves

The concentration of ABA in powdery mildew infected (10 days after inoculation) and healthy (control) Chardonnay leaves was measured using gas chromatography and mass spectrometry as described (Soar et al., 2004). There was no statistically significant difference in ABA concentration between infected and healthy leaves although ABA concentration tended to be slightly higher in infected samples (Fig. 7.7)

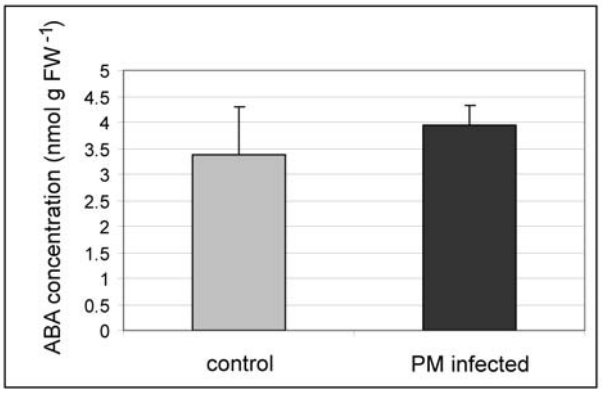

Figure 7.7. Bulk-leaf ABA concentration of glasshouse-grown powdery mildew infected and control Chardonnay leaves. Leaves were collected 10 days after inoculation. Data are means of biological replicates tested in triplicate. Error bars are one standard deviation. ABA concnetration determined using the method of Soar *et al.* (2004).

7.4 Discussion

In addition to regulating various aspects of plant development, plant growth regulators, or hormones, initiate adaptive responses to exogenous cues from both the biotic and abiotic environments. To identify pathways that may be involved in the induction of *VvHT5* and *VvcwINV* in response to powdery mildew infection (Fig. 5.1 and Fig 5.3), downy mildew infection (Fig. 5.6) and wounding (Fig. 5.7), ethylene, methyl jasmonate and ABA were exogenously supplied to grapevine leaves. Ethylene and methyl jasmonate application increased transcript levels of the thaumatin-like gene *VvTl2*, consistent with the observations of Jacobs *et al*. (1999) where expression of grapevine pathogenesis-related proteins *VvTl2*, *VvGlub* and *VvChi4* was elevated by powdery mildew infection and ethylene treatment. These hormones also marginally increased transcript levels of *VvHT5* and *VvcwINV* (Fig. 7.1), however these changes were far smaller than those elicited by pathogen infection (Fig. 5.1 and Fig 5.3) or wounding (Fig. 5.7). Furthermore, *VvGIN1* expression was not changed by either treatment (Fig. 7.1) whereas powder mildew infection strongly down-regulated expression of this gene. Taken together, these

results suggest that ethylene and jasmonate regulated pathways may not be responsible for the induction of *VvHT5* and *VvcwINV* observed during pathogen infection and wounding.

Exogenous application of ABA resulted in elevated transcript levels of *VvHT1* and *VvHT5*, but did not change the levels of *VvHT2*, *VVHT3* and *VvHT4* transcripts (Fig. 7.2 A). Specific induction of *VvHT1* and *VvHT5* was also observed in response to powdery mildew infection (Fig. 5.1) and wounding (Fig. 5.7 A), suggesting ABA-dependant pathways may contribute to the induction of these genes in response to stress stimuli. Transcript levels of *VvHT1* were previously reported to increase in grape cell cultures supplied with ABA (Çakir et al., 2003). The current study supports and extends this observation by showing that *in vivo* expression of *VvHT1* is enhanced by exogenously supplied ABA. Significantly, ABA application also enhanced cell wall invertase *VvcwINV* expression and repressed vacuolar invertase *VvGIN1* expression, again reflecting the changes in transcript levels elicited by powdery mildew infection (Fig 5.2) and wounding (Fig. 5.7 B). VvcwINV enzyme activity in grape berries and avocado is increased by ABA (Richings et al., 2000; Pan et al., 2005), and the promoter of a tomato cwINV *Lin6* is activated by ABA (Roitsch et al., 2003). In contrast to the down regulation of *VvGIN1* in response to ABA, expression of *IVR2*, a vacuolar invertase from maize, was found to be enhanced by water stress and ABA application (Kim et al., 2000; Trouverie et al., 2003). However, it should be noted that expression of other maize invertase genes did not increase in response to ABA application. Furthermore, transcript levels of a vINV from wheat declined in response to drought (Koonjul et al., 2004) indicating that individual invertase family members are differentially regulated by this hormone (Trouverie et al., 2003).

Genetic screens, mainly in *A. thaliana*, have demonstrated that there is significant overlap between sugar and ABA signalling pathways. For example, characterisation of the sugar response mutants *gin1*, *gin5* and *gin6* revealed that they are allelic to ABA response mutants *aba2*, *aba3* and *aba4* respectively (Arenas-Huertero et al., 2000; Cheng et al., 2002). Furthermore, glucose positively regulates the expression of ABA biosynthetic genes such as *ABA2* from *A. thaliana*, suggesting a direct link between sugar signalling and ABA biosynthesis (Cheng et al., 2002). In grapevine, Çakir *et al*. (2003) demonstrated that *VvMSA1*, an ASR (for ABA, stress and ripening-induced) homologue, interacts with the promoter of *VvHT1* and activates transcription of this gene. Additionally, in grape cell cultures, expression of *VvMSA1* is elevated by the addition of sucrose and ABA to the growth media, suggesting *VvMAS1* may be a link between sugar and ABA signalling pathways in grapevine (Çakir et al., 2003).

Consistent with the finding that ABA application elevated transcript levels of *VvHT5*, *VvHT1* and *VvcwINV*, analysis of the promoter regions of these genes identified ABA response motifs. For example, the *VvHT5* promoter contains five ABRE motifs. In *A. thaliana* and maize, ABA and stress-responsive genes are regulated by ABREs which are bound by a specific group of ABA, drought and salinity-induced bZIP transcription factors called ABFs (Busk and Pages, 1998; Choi et al., 2000). Other bZIP proteins closely related to ABFs, such as ABI5, are involved in developmental processes such as seed germination that are also regulated by ABA (Kim et al., 2002). GRIP 55 is a grapevine bZIP homologue that is most highly expressed in post véraison berries between 8 and 14 weeks after flowering, in correlation with maximal grape berry ABA concentrations (Davies and Robinson, 2000; Wheeler and Davies, manuscript in preparation). Consistent with

VvHT5 being ABA-regulated in leaves, transcript levels of *VvHT5* increased in berries at approximately 12 weeks after flowering (Fig. 6.3), when ABA concentration is relatively high, suggesting that GRIP 55 could also regulate *VvHT5* in ripening berries.

In contrast to *VvHT5*, the promoters of *VvHT1* and *VvcwINV* contain MYB and MYC motifs. These sequences are targets of MYB, MYC and NAC-domain transcription factors that regulate stress-induced genes in *A. thaliana* in response to abiotic stimuli, also via ABA-dependant pathways (Abe et al., 1997; Tran et al., 2004). The functional behaviour of *VvHT1* and *VvcwINV* promoters appears significantly different to the *VvHT5* promoter because expression of *VvHT1* and *VvcwINV* was elevated by a lesser amount than *VvHT5* by ABA treatment (Fig. 7.2), by powdery mildew infection (Fig. 5.1) and wounding (Fig. 5.7). This suggests that these genes may be controlled by different regulatory factors and pathways that may all involve the participation of ABA. Additionally, other pathogen and stress-associated motifs such as GT1 (Park et al., 2004; Wang et al. 2004) or EIX (Matarasso et al., 2005) may also contribute to these pathogen and wound-associated responses. Functional investigation of the *VvHT1*, *VvcwINV* and *VvHT5* promoters through promoter deletion experiments would enable the determination of the exact regions that drive gene expression in response to stress stimuli and ABA treatment and therefore establish if common regulatory motifs are in control.

While ABA is an important mediator of responses to abiotic stresses such as drought and salinity (Zhu, 2002), a role in regulating responses to biotic stimuli is also supported. For example, McDonald and Cahill (1999) showed that ABA application mediated the establishment of a compatible interaction between a usually incompatible soybean cultivar and the oomycete *P. sojae*. Furthermore, ABA

addition to *A. thaliana* plants induced susceptibility to a usually avirulent strain of *P. syringae*, while *aba1-1 A. thaliana* lines, which are ABA-deficient, displayed reduced susceptibility to virulent strains of *P. parasitica* (Mohr and Cahill, 2003). These studies provide cogent examples in support of the idea that endogenous ABA concentrations contribute to the formation of compatible interactions between microbial pathogens and plant hosts. This contribution may function by suppression of defence responses (McDonald and Cahill, 1999; Audenaert et al., 2002) or via other as yet unidentified mechanisms. In terms of obligate biotrophic pathogens that derive carbohydrate and other nutrients from plant hosts, the ABA-responsive grapevine genes identified in the current study may contribute to the formation of carbohydrate sink metabolism and subsequently allow pathogens access to additional carbohydrate. Alternatively, supplementary carbohydrate would provide more energy for defence or stress responses. Whether these responses are beneficial or detrimental to pathogen infection has not been demonstrated.

Expression of the ABA biosynthetic gene *VvNCED1* was found to be elevated by pathogen infection (Fig 7.5) and wounding (Fig. 7.6), while consistent with the findings of Soar *et al*. (2004), *VvZEP* expression was unchanged or tended to be repressed by these treatments. However, preliminary attempts to determine bulk leaf ABA levels in powdery mildew infected grape leaves did not indicate any significant differences between infected and control tissues (Fig. 7.7). Soar *et al*. (2004) observed increased transcript levels of *VvNCED1* in water stressed leaves and observed higher bulk leaf ABA concentrations in stressed tissue compared with controls. However, the level of *VvNCED1* expression did not always correlate with bulk leaf ABA concentrations, suggesting other regulatory mechanisms including changes in ABA compartmentation and differential cell-specific concentrations may

be important. Consistent with this idea, apoplasmic ABA concentrations rise rapidly within minutes after drought stress is imposed, indicating that ABA release from stores is more likely than additional biosynthesis via a transcriptionally-regulated enzymatic pathway (Hartung et al., 1997).

Chapter 8 – Summary and concluding remarks

Powdery mildew is the single most important disease of grapevine worldwide and is currently managed via the widespread application of anti-fungal chemicals (Montgomery and Hansen, 2000). Particularly in mild weather conditions where the pathogen tends to grow particularly well, outright crop loss can occur without the use of fungicides (Savocchia et al., 2004). However, liberal use of fungicides has abetted the development of pathogen resistance to these chemicals, which unfortunately no longer offer good control in some viticultural regions (Erickson and Wilcox, 1997; Savocchia et al., 2004).

Traditional plant breeding strategies have used disease resistance loci to develop pathogen resistant cultivars (Larkin et al., 1995). Such an approach is currently being employed to locate and eventually introduce resistance determinants from a North American grapevine into commercially important European species (Barker et al., 2005). However, in the majority of cases, such resistance genes are usually only effective against a single, or at most, a few races of a given pathogen species. Therefore, more recent breeding strategies have attempted to pyramid multiple resistance genes to confer more durable disease resistance (Hulbert et al., 2001).

Alternative sources of powdery mildew resistance could be engineered via identification of host genes that contribute to susceptible pathogen interactions: these genes could be targets for modification to engineer resistance via reduced susceptibility (Vogel and Somerville 2000). In this study, grapevine metabolic genes have been investigated using microarray and quantitative RT-PCR analysis, to determine if any are differentially expressed in powdery mildew infected tissues,

and therefore, may play a role in nutrient, and in particular carbohydrate, delivery to the site of pathogen infection.

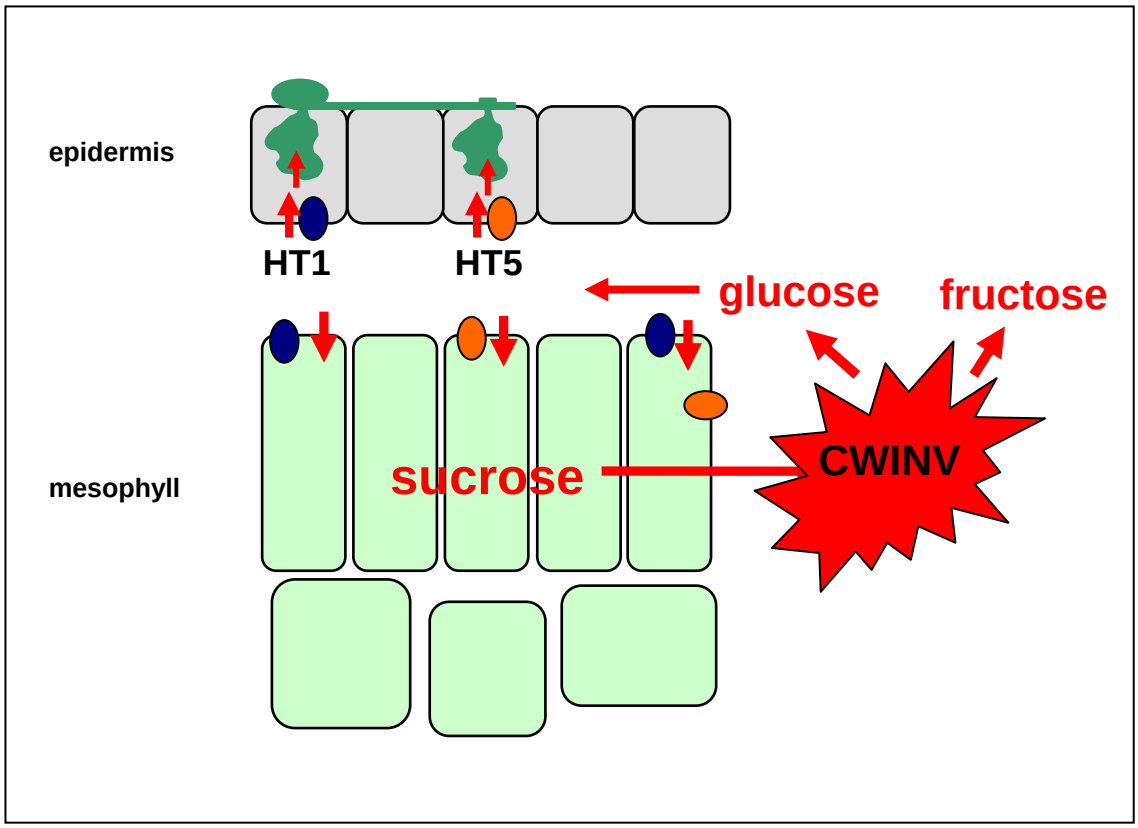

Figure 8.1. Powdery mildew infection induces sink metabolism by elevation of cwINV expression and activity, and by up-regulation of monosaccharide transporter gene expression (HT1 and HT5). Increased cwINV activity will promote apoplasmic phloem unloading and reduce phloem loading, while monosaccharide transporters would provide additional sugar uptake capacity. These genes are not induced specifically in powdery mildew infected cells but may be expressed throughout the mesophyll and in cells outside of infected regions.

The results of this study indicate that powdery mildew infection of grapevine may stimulates the formation of carbohydrate sink metabolism via the induction of cell wall invertase gene *VvcwINV* and specific members of the monosaccharide transporter gene family, *VvHT1* and *VvHT5*, to increase hexose delivery to infected epidermal cells (Refer to Fig. 8.1; Brem et al., 1988). However, this response does not appear to be powdery mildew specific because infection by downy mildew and wounding elicited similar gene expression changes indicating it may be a general response to stress. Putative ABA-responsive regulatory elements were identified in

the promoter regions of these stress-induced genes, and exogenous application of ABA elicited similar gene expression changes to those observed in response to stress. This suggests that ABA may be a participant in the pathways that regulate expression of these genes.

Clearly, an important question in determining the likelihood of success of a powdery mildew resistance strategy based on down-regulation of these host genes is whether the observed induction of sink metabolism is beneficial to the pathogen or the host. The powdery mildew pathogen may enjoy better access to carbohydrate as a result of this host response and may exploit the change in metabolism for its nutritional benefit. If this is the case, then modification of this response may be a potential means to reduce susceptibility to powdery mildew infection. However, it is also possible that the additional carbohydrate supply may be utilised by the host to energise defence and repair mechanisms to cope with infection or wounding (Truernit et al., 1996), which suggests that carbohydrate delivery may be an important aspect of this adaptive response.

Cell wall invertase activity regulates apoplasmic phloem unloading of sucrose (Patrick et al, 2000). Due to elevated *VvcwINV* expression and activity in powdery mildew infected grapevine tissues, this pathway appears to be enhanced, consistent with observations from other pathogen infected plants (Fotopoulos et al., 2003; Roitsch et al., 2003). Thus, could down-regulation of *VvcwINV* lead to increased resistance to powdery mildew without negatively impacting on grapevine growth and development? Antisense inhibition of a pollen-specific cwINV from tobacco induced male sterility, presumably due to a reduction in apoplasmic carbohydrate delivery to this sink organ (Goetz et al., 2001). Furthermore, ectopic expression of an invertase inhibitor reduced hexose concentrations of sweet potato

tubers without detrimental effects on starch content or quality (Greiner et al., 1999). As a novel powdery mildew control strategy, a powdery mildew inducible promoter, such as the *VvHT5* promoter, could be used to drive ectopic expression of an invertase inhibitor or RNA-interference molecule. Initial experiments to determine key powdery mildew responsive regions in the *VvHT5* promoter would be an essential prelude to this approach, and if the responsive sequences are specifically mapped, potential negative traits associated with the transgene may be avoided.

In addition to a reduction in sink metabolism, inhibition of cwINV expression or activity may also induce senescence. Lara *et al*. (2004) elegantly demonstrated that cwINV activity is required for cytokinin-induced delayed senescence, suggesting that apoplasmic carbohydrate delivery may override programmed cell death pathways. If carbohydrate supply to powdery mildew infected regions could be restricted, the apparent stability of the pathogen-host association may be undermined via induction of host programmed cell death pathways.

Modification of metabolic genes, as described above, may reduce susceptibility to powdery mildew infection, however, considering that these genes are not expressed exclusively in powdery mildew infected tissue, new more specific targets should be identified. Microarray analysis using the Affymetrix *V. vinifera* oligo array would allow expression analysis of 14,000 grapevine transcripts, which is 10 times more than screened with the array employed in this study. To increase the likelihood of identifying genes that are induced specifically by powdery mildew infection, microarray comparisons should also be made between powdery mildew infected and wounded tissue.

As described in the General Introduction, Vogel and Somerville (2000) identified *A. thaliana* genes that contribute to powdery mildew susceptibility. Most of these *pmr* loci cloned to date encode genes involved in some aspect of host cell wall synthesis and/or modification (Vogel et al., 2002; Nishimura et al., 2003; Vogel et al., 2004). In light of these observations, identification of grapevine genes that mediate structural changes induced by powdery mildew infection may provide better targets to engineer resistance than the metabolic genes identified in this study. The identification and analysis of grapevine homologues of the *A. thaliana PMR* genes is a direct route to identify putative susceptibility genes that could be down-regulated using RNA interference-techniques to reduce susceptibility to powdery mildew.

The potential of developing novel resistance strategies against powdery mildew through the targeting of "susceptibility" genes is supported by the *A. thaliana pmr* mutants. Furthermore, due to the nature of biotrophic pathogens, susceptibility genes, rather than typical disease resistance determinants, have the added advantage that they are not race-specific and are therefore likely to provide durable resistance in the field.

Reference list

Abe, H., Yamaguchi-Shinozaki, K., Urao, T., Iwasaki, T., Hosokawa, D., and Shinozaki, K. (1997). Role of Arabidopsis MYC and MYB Homologs in Drought- and Abscisic Acid-Regulated Gene Expression. *Plant Cell* **9,** 1859-1868.

Abood, J. K., and Losel, D. M. (2003). Changes in carbohydrate composition of cucumber leaves during the development of powdery mildew infection. *Plant Pathology* **52,** 256-265.

Aked, J., and Hall, J. L. (1993). The uptake of glucose, fructose and sucrose into pea powdery mildew (*Erysiphe pisi* DC) from the apoplast of pea leaves. *New Phytologist* **123,** 277-282.

Angra, R., and Mandahar, C. L. (1991). Pathogenesis of barley leaves by *Helminthosporium teres*I: green island formation and the possible involvement of cytokinins. *Mycopathologia* **114,** 21-27.

Arenas-Huertero, F., Arroyo, A., Zhou, L., Sheen, J., and Leon, P. (2000). Analysis of Arabidopsis glucose insensitive mutants, *gin5* and *gin6*, reveals a central role of the plant hormone ABA in the regulation of plant vegetative development by sugar. *Genes and Development* **14,** 2085-2096.

Audenaert, K., De Meyer, G. B., and Hofte, M. M. (2002). Abscisic Acid Determines Basal Susceptibility of Tomato to Botrytis cinerea and Suppresses Salicylic Acid-Dependent Signaling Mechanisms. *Plant Physiology* **128,** 491-501.

Ayliffe, M. A., Roberts, J. K., Mitchell, H. J., Zhang, R., Lawrence, G. J., Ellis, J. G., and Pryor, T. J. (2002). A Plant Gene Up-Regulated at Rust Infection Sites. *Plant Physiology* **129,** 169-180.

Baiges, I., Schaffner, A. R., and Mas, A. (2001). Eight cDNA encoding putative aquaporins in *Vitis* hybrid Richter-110 and their differential expression. *Journal of Experimental Botany* **52,** 1949-1951.

Balibrea Lara, M. E., Gonzalez Garcia, M.-C., Fatima, T., Ehness, R., Lee, T. K., Proels, R., Tanner, W., and Roitsch, T. (2004). Extracellular Invertase Is an Essential Component of Cytokinin-Mediated Delay of Senescence. *Plant Cell* **16,** 1276-1287.

Bannai, H., Tamada, Y., Maruyama, O., Nakai, K., and Miyano, S. (2002). Extensive feature detection of N-terminal protein sorting signals. *Bioinformatics* **18,** 298-305.

Barker, C. L., Donald, T., Pauquet, J., Ratnaparkhe, M. B., Bouquet, A., Adam-Blondon, A. F., Thomas, M. R., and Dry, I. B. (2005). Genetic and physical mapping of the grapevine powdery mildew resistance gene, Run1, using a bacterial artificial chromosome library. *Theoretical and Applied Genetics* **111,** 370-377.

Barth, I., Meyer, S., and Sauer, N. (2003). PmSUC3: Characterization of a SUT2/SUC3-type sucrose transporter from Plantago major. *Plant Cell* **15,** 1375-1385.

Bendtsen, J. D., Nielsen, H., Heijne, G., and Brunak, S. (2004). Improved prediction of signal peptides: SignalP 3.0. *Journal of Molecular Biology* **340**, 783-795.

Benhamou, N., Grenier, J., and Chrispeels, M. J. (1991). Accumulation of beta - fructosidase in the cell walls of tomato roots following infection by a fungal wilt pathogen. *Plant Physiology* **97,** 739-750.

Bird, D. M. (2004). Signaling between nematodes and plants *Current Opinion in Plant Biology* **7,** 372.

Blackman, L. M., and Overall, R. L. (2001). Structure and function of plasmodesmata. *Australian Journal of Plant Physiology* **28,** 709-727.

Bondada, B. R., Matthews, M. A., and Shackel, K. A. (2005). Functional xylem in the post-veraison grape berry. *Journal of Experimental Botany* **56,** 2949-2957.

Bouarab, K., Melton, R., Peart, J., Baulcombe, D., and Osbourn, A. (2002). A saponin-detoxifying enzyme mediates suppression of plant defences. *Nature* **418,** 889-892.

Boubals, D. (1961) Study of the causes of resistance of vines to powdery mildew of grapevine - *Uncinula necator*, and the mode of hereditary transmission. *Anu. Amélior. Plantes* **11**, 401-500

Boursiac, Y., Chen, S., Luu, D.-T., Sorieul, M., van den Dries, N., and Maurel, C. (2005). Early effects of salinity on water transport in *Arabidopsis* roots. Molecular and Cellular Features of Aquaporin Expression. *Plant Physiology* **139,** 790-805.

Boyd, L. A., Smith, P. H., and Brown, J. K. M. (1994). Molecular and cellular expression of quantitative resistance in barley to powdery mildew. *Physiological and Molecular Plant Pathology* **45,** 47-58.

Brem, S., Rast, D. M., and Ruffner, H. P. (1986). Partitioning of photosynthate in leaves of *Vitis vinifera* infected with *Uncinula necator* or *Plasmopora viticola*. *Physiological and Molecular Plant Pathology* **29,** 285-291.

Bruggmann, R., Abderhalden, O., Reymond, P., and Dudler, R. (2005). Analysis of epidermis- and mesophyll-specific transcript accumulationin powdery mildew-inoculated wheat leaves. *Plant Molecular Biology* **58,** 247.

Burkle, L., Hibberd, J. M., Quick, W. P., Kuhn, C., Hirner, B., and Frommer, W. B. (1998). The H^+-sucrose cotransporter *NtSUT1* is essential for sugar export from tobacco leaves. *Plant Physiology* **118,** 59-68.

Busk, P. K., and Pagès, M. (1998). Regulation of abscisic acid-induced transcription. *Plant Molecular Biology* **37,** 425-435.

Butters, J. A., Burrell, M. M., and Hollomon, S. W. (1985). Purine metabolism in barley powdery mildew and its host. *Physiological Plant Pathology* **27,** 65-74.

Buttner, M., and Sauer, N. (2000). Monosaccharide transporters in plants: structure, function and physiology. *Biochimica et Biophysica Acta* **1465,** 263-274.

Buttner, M., Truernit, E., Baier, K., Scholz-Starke, J., Sontheim, M., Lauterbach, C., Huss, V. A. R., and Sauer, N. (2000). AtSTP3, a green leaf-specific, low affinity monosaccharide -H^+ symporter of *Arabadopsis thaliana*. *Plant Cell and Environment* **23,** 175-184.

Çakir, B., Agasse, A., Gaillard, C., Saumonneau, A., Delrot, S., and Atanassova, R. (2003). A grape ASR protein involved in sugar and abscisic acid signalling. *Plant Cell* **15,** 2165-2180.

Carpaneto, A., Geiger, D., Bamberg, E., Sauer, N., Fromm, J., and Hedrich, R. (2005). Phloem-localized, proton-coupled sucrose carrier ZmSUT1 mediates sucrose efflux under the control of the sucrose gradient and the proton motive force. *Journal of Biological Chemistry* **280,** 21437-21443.

Cheng, W.-H., Endo, A., Zhou, L., Penney, J., Chen, H.-C., Arroyo, A., Leon, P., Nambara, E., Asami, T., Seo, M., Koshiba, T., and Sheen, J. (2002). A unique Short-Chain Dehydrogenase/Reductase in *Arabidopsis* glucose signaling and abscisic acid biosynthesis and functions. *Plant Cell* **14,** 2723-2743.

Cheong, Y. H., Chang, H.-S., Gupta, R., Wang, X., Zhu, T., and Luan, S. (2002). Transcriptional profiling reveals novel interactions between wounding, pathogen, abiotic stress, and hormonal responses in *Arabidopsis*. *Plant Physiology* **129,** 661-677.

Choi, H., Hong, J., Ha, J., Kang, J., and Kim, S. (2000). ABFs, a family of ABA-responsive element binding factors. *Journal of Biological Chemistry* **275,** 1723-1730.

Chou, H.-M., Bundock, N., Rolfe, S. A., and Scholes, J. D. (2000). Infection of *Arabidopsis thaliana* leaves with *Albugo candida* (white blister rust) causes a reprogramming of host metabolism. *Molecular Plant Pathology* **1,** 99-113.

Clark, J. I. M., and Hall, J. L. (1998). Solute transport into healthy and powdery mildew-infected leaves of pea and uptake by powdery mildew mycelium. *New Phytologist* **140,** 261-269.

Coglan, S. E., and Walters, D. R. (1990). Polyamine metabolism in 'green-islands' on powdery mildew-infected barley leaves: possible interactiosn with senescence. *New Phytologist* **116,** 417-424.

Cooper, S. J., and Ashby, A. M. (1998). Comparison of cytokinin and cytokinin-O-glucoside cleaving [beta]-glucosidase production *in vitro* by *Venturia inaequalis* and other phytopathogenic fungi with differing modes of nutrition *in planta*. *Physiological and Molecular Plant Pathology* **53,** 61-72.

Davies, C., Boss, P. K., and Robinson, S. P. (1997). Treatment of grape berries, a nonclimacteric fruit with a synthetic auxin, retards ripening and alters the expression of developmentally regulated genes. *Plant Physiology* **115,** 1155-1161.

Davies, C., and Robinson, S. P. (1996). Sugar accumulation in grape berries. *Plant Physiology* **111,** 275-283.

Davies, C., Wolf, T., and Robinson, S. P. (1999). Three putative sucrose transporters are differentially expressed in grapevine tissue. *Plant Science* **147,** 93-100.

De Coninck, B., Le Roy, K., Francis, I., Clerens, S., Vergauwen, R., Halliday, A. M., Smith, S. M., Van Laere, A., and Van Den Ende, W. I. M. (2005). Arabidopsis AtcwINV3 and 6 are not invertases but are fructan exohydrolases (FEHs) with different substrate specificities. *Plant Cell and Environment* **28,** 432-443.

DiDonato, R. J. J., Roberts, L. A., Sanderson, T., Eisley, R. B., and Walker, E. L. (2004). *Arabidopsis Yellow Stripe-Like2* (YSL2): a metal-regulated gene encoding a plasma membrane transporter of niciotianamine-metal complexes. *Plant Journal* **39,** 403-414.

Doke, N. (1975). Prevention of the hypersensitive reaction of potato cells to infection with an incompatible race of *Phytophthora infestans* by constituents of the zoospores. *Physiological and Molecular Plant Pathology* **7,** 1-7.

Donald, T. M., Pellerone, F., Adam-Blondon, A. F., Bouquet, A., Thomas, M. R., and Dry, I. B. (2002). Identification of resistance gene analogs linked to a powdery mildew resistance locus in grapevine. *Theoretical and Applied Genetics* **104**(4)**,** 610-618.

Dorhout, R., Kollofell, C., and Gommers, F.J. (1992). Alteration of distribution of regions with high net proton extrusion in tomato roots infected with *Meloidogyne incognita. Physiological and Molecular Plant Pathology* **40,** 153-162.

Dreier, L. P., Hunter, J. J., and Ruffner, H. P. (1998). Invertase activity, grape berry development and cell compartmentation. *Plant Physiology and Biochemistry (Paris)* **36,** 865-872.

Ehneß, R., and Roitsch, T. (1997). Co-ordinated induction of mRNAs for extracellular invertase and a glucose transporter in *Chenopodium rubrum* by cytokinins. *The Plant Journal* **11,** 539-548.

Emanuelsson, O., Nielsen, H., and von Heijne, G. (1999). ChloroP, a neural network-based method for predicting chloroplast transit peptides and their cleavage sites. *Protein Science* **8,** 978-984.

Erickson, E. O., and Wilcox, W. F. (1997). Distributions of sensitivities to three sterol demethylation inhibitor fungicides among populations of *Uncinula necator* sensitive and resistant to triadimefon. *Phytopathology* **87,** 784-791.

Famiani, F., Walker, R. P., Tecsi, L., Chen, Z.-H., Proietti, P., and Leegood, R. C. (2000). Am immunohistochemical study of the compartmentation of metabolism

during the development of grape (*Vitis vinifera* L.) berries. *Journal of Experimental Botany* **51,** 675-683.

Felsenstein, J. (1989). PHYLIP - Phylogeny Inference Package (Version 3.2). *Cladistics* **5,** 164-166.

Ficke, A., Gadoury, D.M. & Seem, R.C. (2002). Ontogenic resistance and plant disease management: a case study of grape powdery mildew. *Phytopathology* **92,** 671-675.

Fillion, L., Ageorges, A., Picaud, S., Coutos-Thevenot, P., Lemoine, R., Romieu, C., and Delrot, S. (1999). Cloning and expression of a hexose transporter gene expressed during the ripening of grape berry. *Plant Physiology* **120,** 1083-1093.

Fischer, W. N., Andre, B., Rentsch, D., Krolkiewicz, S., Tegeder, M., Breitkreuz, K., and Frommer, W. B. (1998). Amino acid transport in plants. *Trends in Plant Science* **3,** 188-195.

Fotopoulos, V., Gilbert, M. J., Pittman, J. K., Marvier, A. C., Buchanon, A. J., Sauer, N., Hall, J. L., and Williams, L. E. (2003). The monosaccharide transporter gene, *AtSTP4*, and the cell wall invertase, *AtBfruct1*, are induced in *Arabidopsis* during infection with the fungal biotroph *Erysiphe cichoracearum*. *Plant Physiology* **132,** 821-829.

Fric, F., and Wolf, G. (1994). Hydrolytic enzymes of ungerminated and germinated conidia of *Erysiphe graminis* DC f.sp. hordei Marchal. *Journal of Phytopathology* **140,** 1-10.

Frohman, A., Dush, M. K., and Martin, G. R. (1988). Rapid production of full-length cDNAs from rare transcripts: amplification using a single gene-specific oligonucleotide primer. *Proceedings of the National Academy of Sciences. U.S.A.* **85,** 8998-9002.

Gear, M. L., McPhillips, M.L., Patrick, J.W., and McCurdy, D.W. (2000). Hexose transporters of tomato: molecular cloning, expression analysis and functional characterisation. *Plant Molecular Biology* **44,** 687-697.

Gleave, A. P. (1992). A versatile binary vector system with a T-DNA organisational structure conducive to efficient integration of cloned DNA into the plant genome. *Plant Molecular Biology* **20,** 1203-1207.

Goes da Silva, F., Iandolino, A., Al-Kayal, F., Bohlmann, M. C., Cushman, M. A., Lim, H., Ergul, A., Figueroa, R., Kabuloglu, E. K., Osborne, C., Rowe, J., Tattersall, E., Leslie, A., Xu, J., Baek, J., Cramer, G. R., Cushman, J. C., and Cook, D. R. (2005). Characterizing the Grape Transcriptome. Analysis of expressed sequence tags from multiple *Vitis* species and development of a compendium of gene expression during berry development. *Plant Physiology* **139,** 574-597.

Goetz, M., Godt, D.E., and Roitsch, T. (2000). Tissue-specific induction of the mRNA for an extracellular invertase isoenzyme of tomato by brassinosteroids suggests a role for steroid hormones in assimilate partitioning. *Plant Journal* **22,** 515-522.

Goetz, M., Godt, D. E., Guivarc'h, A., Kahmann, U., Chriqui, D., and Roitsch, T. (2001). Induction of male sterility in plants by metabolic engineering of the carbohydrate supply. *Proceedings of the National Academy of Sciences. U.S.A.* **98,** 6522-6527.

Green, J. R., Carver, T. L. W. and Gurr, S. J. (2002). The formation and function of infection and feeding structures. In: Belanger, R. R., Bushenll, W. R., Dik, A. J., Carver, T. L. W. eds. *The Powdery Mildews. A comprehensive Treatis.* American Phytopathological Society, Minnesota USA, pp. 66-82.

Green, J. R., Pain, N.A., Cannell, M.E., Jones, G.L., Leckie, C.P., McCready, S., Mendgen, K., Mitchell, A.J., Callow, J.A., and O'Connell, R.J. (1994). Analysis of differentiation and development of the specialized infection structures formed by biotrophic fungal plant pathogens using monoclonal antibodies. *Canadian Journal of Botany* **73,** S408-S417.

Greenspan, M. D., Shackel, K. A., and Matthews, M. A. (1994). Developmental changes in the diurnal water budget of the grape berry exposed to water deficits. *Plant Cell and Environment* **17,** 811-820.

Greiner, S., Rausch, T., Sonnewald, U., and Herbers, K. (1999). Ectopic expression of a tobacco invertase inhibitor homolog prevents cold-induced sweetening of potato tubers. *Nature Biotechnology* **17,** 708-711.

Hahn, M., and Mendgen, K. (1997). Characterisation of in planta-induced rust genes isolated from a haustorium-specific cDNA library. *Molecular Plant-Microbe Interactions* **10,** 427-437.

Hahn, M., and Mendgen, K. (2001). Signal and nutrinet exchange at biotrophic plant-fungus interphaces. *Current Opinion in Plant Biology* **4,** 322-327.

Hahn, M., Neef, U., Struck, C., Gottfert, M., and Mendgen, K. (1997). A putative amino acid transporter is specifically expressed in haustoria of the rust fungus *Uromyces fabae*. *Molecular Plant-Microbe Interactions* **10,** 438-445.

Hall, J. L., and Williams, L. E. (2000). Assimilate transport and partitioning in fungal biotrophic interactions. *Australian Journal of Plant Physiology* **27,** 549-560.

Hammond-Kosack, K. E., and Jones, J. D. G. (1996). Resistance Gene-Dependent Plant Defence Responses. *The Plant Cell* **8,** 1773-1791.

Hammes, U. Z., Schachtman, D. P., Berg, R. H., Nielsen, E., Koch, W., McIntyre, L. M., and Taylor, C. G. (2005). Nematode-induced changes of transporter gene expression in Arabidopsis roots. *Molecular Plant-Microbe Interactions* **18**(12)**,** 1247-1257.

Harrison, M. J. (1996). A sugar transporter from *Medicago truncatula:*altered expression pattern in roots during vesicular-arbuscular (VA) mycorrhizal associations. *Plant Journal* **9,** 491-503.

Harrison, M. J. (1999). Biotrophic interfaces and nutrient transport in plant/fungal symbioses. *Journal of Experimental Botany* **50,** 1013-1022.

Harrison, M. J., Dewbre, G.R., and Liu, J. (2002). A phosphate transporter from *Medicago truncatula* involved in the acquisition of phospahte released by Arbuscular Mycorrhizal fungi. *Plant Cell* **14,** 2413-2429.

Hartung, W., Wilkinson, S., and Davies, W. (1998). Factors that regulate abscisic acid concentrations at the primary site of action at the guard cell. *Journal of Experimental Botany* **49,** 361-367.

Haupt, S., Duncan, G. H., Holzberg, S., and Oparka, K. J. (2001). Evidence for symplastic phloem unloading in sink leaves of barley. *Plant Physiology* **125,** 209-218.

Heath, M. C. (1976). Signalling between pathogenic rust fungi and resistant or susceptible host plants. *Annals of Botany* **80,** 713-720.

Heath, M. C. (1994). Signal exchange between higher plants and rust fungi. *Canadian Journal of Botany* **73,** s616-s623.

Heath, M. C. (2000). Nonhost resistance and nonspecific plant defences. *Current Opinion in Plant Biology* **3,** 315.

Hewitt, H. G., and Ayres, P. G. (1976). Effect of infection by *Microsphaera alphitoides* (powdery mildew) on carbohydrate levels and translocation in seedlings of *Quercus robur*. *New Phytologist* **77,** 379-390.

Higo, K., Ugawa, Y., Iwamoto, M., and Korenaga, T. (1999). Plant cis-acting regulatory DNA elements (PLACE) database: 1999. *Nucleic Acids Research* **27,** 297-300.

Holmes, D. S., and Quigley, M. (1981). A rapid boiling method for the preparation of bacterial plasmids. *Analytical Biochemistry* **114,** 193-197.

Hoth, S., Ikeda, Y., Morgante, M., Wang, X., Zuo, J., Hanafey, M. K., Gaasterland, T., Tingey, S. V., and Chua, N.-H. (2003). Monitoring genome-wide changes in gene expression in response to endogenous cytokinin reveals targets in *Arabidopsis thaliana*. *FEBS Letters* **554,** 373-380.

Hoth, S., Schneidereit, A., Lauterbach, C., Scholz-Starke, J., and Sauer, N. (2005). Nematode infection triggers the de novo formation of unloading phloem that allows macromolecular trafficking of green fluorescent protein into syncytia. *Plant Physiology* **138,** 383-392.

Howard, R. J., Ferrari, M. A., Roach, D. H., and Money, N. P. (1991). Penetration of hard substrates by a fungus employing enormous turgor pressures. *Proceedings of the National Academy of Sciences. U.S.A.* **88,** 11281-11284.

Hulbert, S. H., Webb, C. A., Smith, S. M., and Sun, Q. (2001). Resistance Gene Complexes : Evolution and Utilization. *Annual Review of Phytopathology* **39,** 285-312.

Hwang, B. K., and Heitefuss, R. (1986). Sugar composition and acid invertase activity in spring barley plants in relation to adult-plant resistance to powdery mildew. *Phytopathology* **76,** 365-369.

Jackson, S. A., Walters, D. R., and Baldwin, B. C. (1995). Lysine biosynthesis in powdery mildew-infected barley. *Aspects of Applied Biology* **42,** 169-176.

Jacobs, A. K., Dry, I. B. and Robinson, S. P. (1999). Induction of different pathogenesis-related cDNAs in grapevine infected with powdery mildew and treated with ethephon. *Plant Pathology* **48,** 325-336.

Jameson, P. (2000). Cytokinins and auxins in plant-pathogen interactions- an overview. *Plant Growth Regulation* **32,** 369-380.

Jang, J. Y., Kim, D. G., Kim, Y. O., Kim, J. S., and Kang, H. (2004). An expression analysis of a gene family encoding plasma membrane aquaporins in response to abiotic stresses in *Arabidopsis thaliana*. *Plant Molecular Biology* **54,** 713.

Jansen, C., Korell, M., Eckey, C., Biedenkopf, D., and Kogel, K.-H. (2005). Identification and transcriptional analysis of powdery mildew-induced barley genes. *Plant Scie*nce **168,** 373.

Jindal, S., Arora, Y. K., and Bajaj, K. L. (1979). Effect of infection by *Sphaerotheca fuliginea* (powdery mildew) on amino acids and sugars in leaves of muskmelon (*Cucumis melo* L.). *Plant Biochemical Journal* **6,** 115-123.

Kamoun, S., van West, P., Vleeshouwers, V. G. A. A., de Groot, K. E., and Govers, F. (1998). Resistance of *Nicotiana benthamiana* to *Phytophthora infestans* is mediated by the recognition of the elicitor protein INF1. *Plant Cell* **10,** 1413-1426.

Kang, J., Choi, H., Im, M., and Kim, S. (2002). *Arabidopsis* basic leucine zipper proteins that mediate stress-responsive abscisic acid signaling. *Plant Cell* **14,** 343-357.

Kim, J.-Y., Mahe, A., Brangeon, J., and Prioul, J.-L. (2000). A Maize Vacuolar Invertase, IVR2, Is Induced by Water Stress. Organ/Tissue Specificity and Diurnal Modulation of Expression. *Plant Physiology* **124,** 71-84.

Kim, S. Y., Ma, J., Perret, P., Li, Z., and Thomas, T. L. (2002). *Arabidopsis* ABI5 subfamily members have distinct DNA-binding and transcriptional activities. *Plant Physiology* **130,** 688-697.

Koch, K. (2004). Sucrose metabolism: regulatory mechanisms and pivotal roles in sugar sensing and development. *Current Opinion in Plant Biology* **7,** 235-246.

Koh, S., Andre, A., Edwards, H., Ehrhardt, D., and Somerville, S. (2005). *Arabidopsis thaliana* subcellular responses to compatible *Erysiphe cichoracearum* infections. *Plant Journal* **44,** 516-529.

Koltai, H., Dhandaydham, M., Opperman, C., Thomas, J., and Bird, D. (2001). Overlapping plant signal transduction pathways induced by a parasitic nematode and a rhizobial endosymbiont. *Molecular Plant-Microbe Interactions* **10,** 1168-1177.

Koonjul, P. K., Minhas, J. S., Nunes, C., Sheoran, I. S., and Saini, H. S. (2005). Selective transcriptional down-regulation of anther invertases precedes the failure of pollen development in water-stressed wheat. *Journal of Experimental Botany* **56,** 179-190.

Krogh, A., Larsson, B., von Heijne, G., and Sonnhammer, E. L. L. (2001). Predicting transmembrane protein topology with a hidden markov model: application to complete genomes. *Journal of Molecular Biology* **305,** 567-580.

Laloi, C., Mestres-Ortega, D., Marco, Y., Meyer, Y., and Reichheld, J.-P. (2004). The *Arabidopsis* cytosolic Thioredoxin H5 gene induction by Oxidative Stress and its W-Box-mediated response to pathogen elicitor. *Plant Physiology* **134,** 1006-1016.

Lalonde, S., Boles, E., Hellmann, H., Barker, L., Patrick, J.W., Frommer, W.B., and Ward, J.M. (1999). The dual function of sugar carriers: transport and sugar sensing. *Plant Cell* **11,** 707-726.

Lara, M. E. B., Garcia, M.-C. G., Fatima, T., Ehneb, R., Lee, T. K., Proels, R., Tanner, W., and Roitsch, T. (2004). Extracellualr invertase is an essential component of cytokinin-mediated delay of senescence. *Plant Cell* **16,** 1276-1287.

Larkin, P. J., Banks, P. M., and Chen, X. (1995). Registration of six genetic stocks of wheat with rust and BYDV resistance: Z1, Z2, Z3, Z4, Z5, and Z6 disomic addition lines with *Thinopyrum intermedium* chromosomes. *Crop Science* **35,** 604.

Leckie, C. P., Callow, J.A. and Green, J.R. (1995). Reorganisation of the endoplasmic reticulum in pea leaf epidermal cells infected by the powdery mildew fungus *Erysiphe pisi. New Phytologist* **131,** 211-221.

Lohar, D. P., Schaff, J. E., Laskey, J. G., Kieber, J. J., Bilyeu, K. D., and Bird, D. M. (2004). Cytokinins play opposite roles in lateral root formation, and nematode and Rhizobial symbioses. *Plant Journal* **38,** 203-214.

Long, S. R. (1996). Rhizobium symbiosis: Nod factors in perspective. *Plant Cell* **8,** 1885-1898.

Ma, F., and Peterson, C. A. (2000). Plasmodesmata in onion (Allium cepa L.) roots: a study enabled by improved fixation and embedding techniques. *Protoplasma* **211,** 103-115.

Mackie, A. J., Roberts, A.M., Callow, J.A. and Green, J.R. (1991). Molecular differentiation in pea powdery-mildew haustoria. *Planta* **183,** 399-408.

Manners, J. M., and Gay, J. L. (1982). Accumulation of systemic fungicides and other solutes by haustorial complexes isolated from Pisum sativum infected with *Erysiphe pisi*. *Pesticide Science* **13,** 195-203.

Matarasso, N., Schuster, S., and Avni, A. (2005). A novel plant Cysteine Protease has a dual function as a regulator of 1-Aminocyclopropane-1-Carboxylic Acid Synthase gene expression. *Plant Cell* **17,** 1205-1216.

Mathesius, U., Bayliss, C., Weinman, J. J., Schlaman, H. R. M., Spaink, H. P., Rolfe, B. G., McCully, M. E., and Djordjevic, M. A. (1998). Flavonoids synthesized in cortical cells during nodule initiation are early developmental markers in white clover. *Molecular Plant-Microbe Interactions* **11,** 1223-1232.

McDonald, K. L., and Cahill, D. M. (1999). Influence of Abscisic Acid and the Abscisic Acid Biosynthesis Inhibitor, Norflurazon, on interactions between *Phytophthora sojae* and Soybean (*Glycine max*). *European Journal of Plant Pathology* **105,** 651-658.

Mendgen, K., and Hahn, M. (2002). Plant infection and the establishment of fungal biotrophy. *Trends in Plant Science* **1016,** 1360-1385.

Mendgen, K., and Naas, P. (1988). The activity of powdery-mildew haustoria after feeding the host cells with different sugars, as measured with a potentiometric cyanine dye. *Planta* **174,** 283-288.

Meyer, S., Lauterbach, C., Niedermeier, M., Barth, I., Sjolund, R. D., and Sauer, N. (2004). Wounding enhances expression of *AtSUC3*, a sucrose transporter from *Arabidopsis* sieve elements and sink tissues. *Plant Physiology* **134,** 684-693.

Mhiri, C., Morel, J. B., Vernhettes, S., Casacuberta, J. M., Lucas, H., and Grandbastien, M. A. (1997). The promoter of the tobacco Tnt1 retrotransposon is induced by wounding and by abiotic stress. *Plant Molecular Biology* **33,** 257-266.

Miao, G. H., and Verma, D. P. S. (1993). Soybean nodulin-26 gene encoding a channel protein is expressed only in the infected cells of nodules and is regulated differently in roots of homologous and heterologous plants. *Plant Cell* **5,** 781-794.

Mohr, P. G., and Cahill, D. M. (2003). Abscisic acid influences the susceptibility of *Arabidopsis thaliana* to *Pseudomonas syringae* pv. tomato and *Peronospora parasitica. Functional Plant Biology* **30,** 461-469.

Muller, P. Y., Jarovjak, H., Miserez, A. R., and Dobbie, Z. (2002). Processing of Gene Expression Data Generated by Quantitative Real-time RT-PCR. *Biotechniques* **32,** 1372-1379.

Montgomery, R., and Hansen, J.-P. (2000). Plant protection in the EU - consumption of plant protection products in the European Union: data 1992-1996. *ISBN 92-894-0437-x.*

Mumberg, D., Muller, R., and Funk, M. (1994). Regulatable promoters of *Saccharomyces cerevisiae:* comparison of transcriptional activity and their use for heterologous expresion. *Nucleic Acids Research* **22,** 5767-5788.

Murdoch, L. J., Kobayashi, I. & Hardham, A.R. (1998). Production and characterisation of monoclonal antibodies to cell wall components of the flax rust fungus. *European Journal of Plant Pathology* **104,** 331-346.

Murphy, A. M., Pryce-Jones, E., Johnstone, K., and Ashby, A. M. (1997). Comparison of cytokinin production *in vitro* by *Pyrenopeziza brassicae* with other plant pathogens. *Physiological and Molecular Plant Pathology* **50,** 53-65.

Murray, A. J., and Ayres, P. G. (1986). Infection with powdery mildew can enhance the accumulation of proline and glycinebetaine by salt stressed barley seedlings. *Physiological and Molecular Pathology* **29,** 271-277.

Nakai, K., and Horton, P. (1999). PSORT: a program for detecting the sorting signals of proteins and predicting their subcellular localization. *Trends in Biochemical Science* **24,** 34-35.

Nishimura, M. T., Stein, M., Hou, B. H., Vogel, J. P., Edwards, H., and Somerville, S. C. (2003). Loss of a callose synthase results in salicylic acid-dependent disease resistance. *Science* **301,** 969-972.

Oldroyd, G. E. D. (2001). Dissecting Symbiosis: Developments in Nod Factor Signal Transduction. *Annals of Botony* **87,** 709-718.

Opperman, C. H., Taylor, C. G., and Conkling, M. A. (1994). Root-Knot Nematode-directed expression of a plant root-specific gene. *Science* **263,** 221-223.

O'Shea-Greenfield, A., and Smale, S. T. (1992). Roles of TATA and initiator elements in determining the start site location and direction of RNA polymerase II transcription. *Journal of Biological Chemistry* **267,** 1391-1402.

Ough, C. S., and Berg, H. W. (1979). Powdery mildew sensory effect on wine. *American Journal of Enology and Viticulture* **30,** 321.

Papadopoulou, K., Melton, R. E., Leggett, M., Daniels, M. J., and Osbourn, A. E. (1999). Compromised disease resistance in saponin-deficient plants. *Proceedings of the National Academy of Sciences. U.S.A.* **96,** 12923-12928.

Park, H. C., Kim, M. L., Kang, Y. H., Jeon, J. M., Yoo, J. H., Kim, M. C., Park, C. Y., Jeong, J. C., Moon, B. C., Lee, J. H., Yoon, H. W., Lee, S.-H., Chung, W. S., Lim, C. O., Lee, S. Y., Hong, J. C., and Cho, M. J. (2004). Pathogen- and NaCl-induced expression of the SCaM-4 promoter is mediated in part by a GT-1 Box that interacts with a GT-1-like Transcription factor. *Plant Physiology* **135,** 2150-2161.

Park, K.-J., and Kanehisa, M. (2003). Prediction of protein subcellular locations by support vector machines using compositions of amino acids and amino acid pairs. *Bioinformatics* **19,** 1656-1663.

Patrick, J. W. (1997). Phloem unloading: sieve element unloading and post-sieve element transport. *Annual Review of Plant Physiology and Plant Molecular Biology* **48,** 191-222.

Patrick, J. W., Zhang, W., Tyerman, S.D., Offler, C.E., and Walker, N.A. (2001). Role of membrane transport in phloem translocation of assimilates and water. *Australian Journal of Plant Physiology* **28,** 695-707.

Perfect, S. E., and Green, J. R. (2001). Infection structures of biotrophic and hemibiotrophic fungal plant pathogens. *Molecular Plant Pathology* **2,** 101-108.

Pryce-Jones, E., Carver, T., and Gurr, S. J. (1999). The roles of cellulase enzymes and mechanical force in host penetration by *Erysiphe graminis* f.sp. hordei. *Physiologyogical and Molecular Plant Pathology* **55,** 175-182.

Rae, A. L., Bonfante-Fasolo, P., and Brewin, N. J. (1992). Structure and growth of infection threads in the legume symbiosis with *Rhizobium leguminosarum*. *Plant Journal* **2,** 385-395.

Ramonell, K., Berrocal-Lobo, M., Koh, S., Wan, J. R., Edwards, H., Stacey, G., and Somerville, S. (2005). Loss-of-function mutations in chitin responsive genes show increased susceptibility to the powdery mildew pathogen *Erysiphe cichoracearum*. *Plant Physiology* **138,** 1027-1036.

Rezaian, M. A., and Krake, L. R. (1987). Nucleic acid extraction and virus detection in grapevine. *Journal of Virology Methods* **17,** 277-285.

Richings, E. W., Cripps, R. F., and Cowan, A. K. (2000). Factors affecting 'Hass' avocado fruit size: carbohydrate, abscisic acid and isoprenoid metabolism in normal and phenotypically small fruit. *Physiologia Plantarum* **109,** 81-89.

Roberts, A. M., Mackie, A.J., Hathaway, V., Callow, J.A. and Green, J.R. (1993). Molecular differentiation in the extrahaustorial membrane of pea powdery mildew haustoria at early and late stages of development. *Physiological and Molecular Plant Pathology* **43,** 147-160.

Roberts, J. K., and Pryor, A. (1995). Isolation of a flax (*Linum usitatissimum*) gene induced during susceptible infection by flax rust (*Melampsora lini*). *Plant Journal* **8,** 1-8.

Roitsch, T. (1999). Source-sink regulation by sugar and stress. *Current Opinion in Plant Biology* **2,** 198-206.

Roitsch, T., Balibrea, M. E., Hofmann, M., Proels, R., and Sinha, A. K. (2003). Extracellular invertase: key metabolic enzyme and PR protein. *Journal of Experimental Botany* **54,** 513-524.

Roitsch, T., and Ehneß, R. (2000). Regulation of source/sink relations by cytokinins. *Plant Growth Regulation* **32,** 359-367.

Rose, T., Schultz, E., Henikoff, J., Pietrokovski, S., and Henikoff, S. (1998). Consensu-degenerate hybrid oligonucleotide primers for amplification of distantly-related sequences. *Nucleic Acids Research* **26,** 1628-1635.

Roussel, H., Bruns, S., Gianinazzi-Pearson, V., Hahlbrock, K. & Franken, P. (1997). Induction of a membrane intrinsic protein-encoding mRNA in arbuscular mycorrhiza and elicitor-stimulated cell suspension cultures of parsley. *Plant Science* **126,** 203-210.

Ruffner, H. P., Adler, S., and Rast, D.M. (1990). Soluble and wall associated forms of invertase in *Vitis vinifera*. *Phytochemistry* **29,** 2083-2086.

Ruffner, H. P., Hurlimann, M., and Skrivan, R. (1995). Soluble invertase from grape berries: purification, deglycosylation and antibody specificity. *Plant Physiology and Biochemistry (Paris)* **33,** 25-31.

Rumbolz, J., Kassemeyer, H.-H., Steinmetz, V., Deising, H. B., Mendgen, K., Mathys, D., Wirtz, S., and Guggenheim, R. (2000). Differentiation of infection structures of the powdery mildew fungus *Uncinula necator* and adhesion to the host cuticle. *Canadian Journal of botany* **78,** 409-421.

Rushton, P. J., Reinstadler, A., Lipka, V., Lippok, B. and Somssich, I.E. (2002). Synthetic plant promoters containing defined regulatory elements provide novel insights into pathogen- and wound-induced signalling. *The Plant Cell* **14,** 749-762.

Sambrook, J., and Russell, D. W. (2001). Molecular Cloning. A Laboratory Manual. Cold Spring Harbor Laboratory press, Cold Spring Harbor, New York, USA.

Sarr, J.-E., Sommerer, N., Bergoin, A., Rossignol, M., Albagnac, G., and Romieu, C. (2004). Grape berry biochemistry revisited upon proteomic analysis of the mesocarp. *Proteomics* **4,** 201-215.

Sauer, N., Friedlander, K., and Graml-Wicke, U. (1990). Primary structure, genomic organization and heterologous expression of a glucose transporter from *Arabidopsis thaliana*. *EMBO Journal* **9,** 3045-3050.

Sauer, N., and Stadler, R. (1993). A sink-specific H^+/monosaccharide co-transporter from *Nicotiana tabacum*: cloning and heterologous expression in baker's yeast. *Plant journal* **4,** 601-610.

Savocchia, S., Stummer, B. E., Wicks, T. J., Heeswijck, R. v., and Scott, E. S. (2004). Reduced sensitivity of *Uncinula necator* to sterol demethylation inhibiting fungicides in southern Australian vineyards. *Australasian Plant Pathology* **33,** 465-473.

Schenk, P. M., Kazan, K., Wilson, I., Anderson, J.P., Richmond, T., Somerville, S.C. & Manners, J.M. (2000). Coordinated plant defence responses in *Arabidopsis* revealed by microarray analysis. *Proceedings of the National Academy of Sciences. U.S.A.* **97,** 11655-11660.

Schneidereit, A., Scholz-Starke, J., Sauer, N., and Buttner, M. (2005). *AtSTP11*, a pollen tube-specific monosaccharide transporter in *Arabidopsis*. *Planta* **221,** 48-55.

Scholes, J. D., Lee, P. J., Horton, P., and Lewis, D. H. (1994). Invertase: understanding changes in the photosynthetic and carbohydrate metabolism of barley leaves infected with powdery mildew. *New Phytologist* **126,** 213-222.

Scholz-Starke, J., Buttner, M., and Sauer, N. (2003). AtSTP6, a new pollen-specific H+-monosaccharide symporter from Arabidopsis. *Plant Physiology* **131**(1)**,** 70-77.

Scott, E. (1998). Mildews: what they are and how they survive in the vineyard. *Australian Viticulture* **2,** 5-15.

Seo, M., and Koshiba, T. (2002). Complex regulation of ABA biosynthesis in plants. *Trends in Plant Science* **7,** 41.

Shahmuradov, I. A., Gammerman, A. J., Hancock, J. M., Bramley, P. M., and Solovyev, V. V. (2003). PlantProm: a database of plant promoter sequences. *Nucleic Acids Research* **31,** 114-117.

Shakya, R., and Sturm, A. (1998). Characterization of source- and sink-specific sucrose/H^+ symporters from carrot. *Plant Physiology* **118,** 1473-1480.

Sherson, S. M., Hemmann, G., Wallace, G., Forbes, S., Germain, V., Stadler, R., Bechtold, N., Sauer, N., and Smith, S. M. (2000). Monosaccharide/proton symporter *AtSTP1* plays a major role in uptake and response of *Arabidopsis* seeds and seedlings to sugars. *Plant Journal* **24,** 849-857.

Soar, C. J., Speirs, J., Maffei, S. M., and Loveys, B. R. (2004). Gradients in stomatal conductance, xylem sap ABA and bulk leaf ABA along canes of *Vitis vinifera* cv. Shiraz: molecular and physiological studies investigating their source. *Functional Plant Biology* **31,** 659-669.

Sohn, J., Voegele, R.T., Mendgen, K., and Hahn, M. (2000). High level activation of Vitamin B1 biosynthesis genes in haustoria of the rust fungus *Uromyces fabae*. *Molecular Plant-Microbe Interactions* **13,** 629-636.

Storr, T., and Hall, J. L. (1992). The effect of infection by *Erysiphe pisi* DC on acid and alkaline invertase activities and aspects of starch biochemistry in leaves of *Pisum sativum* L. *New Phytologist* **121,** 535-543.

Struck, C., Hahn, M., and Mendgen, K. (1996). Plasma membrane H^+-ATPase activity in spores, germ tubes, and haustoria of the rust fungus *Uromyces viciae-fabae*. *Fungal Genetics and Biology* **20,** 30-35.

Stummer, B. E., Francis, I. L., Zanker, T., Lattey, K. A., and Scott, E. S. (2005). Effects of powdery mildew on the sensory properties and composition of Chardonnay juice and wine when grape sugar ripeness is standardised. *Australian Journal of Grape and Wine Research* **11,** 66-76.

Sturm, A., and Chrispeels, M. J. (1990). cDNA cloning of carrot extracellular *β*-fructosidase and its expression in response to wounding and bacterial infection. *Plant Cell* **2,** 1107-1119.

Sutton, P. N., Henry, M. J., and Hall, J. L. (1999). Glucose, not sucrose, is transported from wheat to wheat powdery mildew. *Planta* **208,** 426-430.

Tang, G.-Q., Luscher, M., and Sturm, A. (1999). Antisense repression of vacuolar and cell wall invertase in transgenic carrot alters early plant development and sucrose partitioning. *Plant Cell* **11,** 177-189.

Tang, X., Rolfe, S. A., and Scholes, J. D. (1996). The effect of *Albugo candida* (white blister rust) on the photosynthetic and carbohydrate metabolism of leaves of *Arabidopsis thaliana*. *Plant Cell and Environment* **19,** 967-975.

Terrier, N., Glissant, D., Grimplet, J., Barrieu, F., Abbal, P., Couture, C., Ageorges, A., Atanassova, R., Léon, C. l., Renaudin, J.-P., Dédaldéchamp, F., Romieu, C., Delrot, S., and Hamdi, S. (2005). Isogene specific oligo arrays reveal multifaceted changes in gene expression during grape berry (*Vitis vinifera*) development. *Planta* **222,** 832-847.

Thompson J.D., Higgins, D.G., and Gibson, T.J. (1994). CLUSTAL W: improving the sensitivity of progressive multiple sequence alignment through sequence weighting, position-specific gap penalties and weight matrix choice. *Nucleic Acids Research* **22,** 4673-4680.

Toyofuku, K., Kasahara, M., and Yamaguchi, J. (2000). Characterization and expression of monosaccharide transporters (*OsMSTs*) in Rice. *Plant and Cell Physiology.* **41,** 940-947.

Tran, L.-S. P., Nakashima, K., Sakuma, Y., Simpson, S. D., Fujita, Y., Maruyama, K., Fujita, M., Seki, M., Shinozaki, K., and Yamaguchi-Shinozaki, K. (2004). Isolation and functional analysis of *Arabidopsis* stress-inducible NAC transcription factors that bind to a Drought-responsive cis-element in the early responsive to dehydration stress 1 promoter. *Plant Cell* **16,** 2481-2498.

Trouverie, J., Thevenot, C., Rocher, J.-P., Sotta, B., and Prioul, J.-L. (2003). The role of abscisic acid in the response of a specific vacuolar invertase to water stress in the adult maize leaf. *Journal of Experimental Botany* **54,** 2177-2186.

Truernit, E., Schmid, J., Epple, P., Illig, J., and Sauer, N. (1996). The sink-specific and stress-regulated *Arabadopsis STP4* gene: enhanced expression of a gene encodinga monosaccharide transporter by wounding, elicitors and pathogen challenge. *Plant Cell* **8,** 2169-2182.

Tsiamis, G., Mansfield, J. W., Hockenhull, R., Jackson, R. W., Sesma, A., Athanassopoulos, E., Bennett, M. A., Stevens, C., Vivian, A., Taylor, J. D., and Murillo, J. (2000). Cultivar-specific avirulence and virulence functions assigned to avrPphF in *Pseudomonas syringae* pv. phaseolicola, the cause of bean halo-blight disease. *EMBO Journal* **19,** 3204-3214.

Tsuba, M., Katagiri, C., Takeuchi, Y., Takada, Y., and Yamaoka, N. (2002). Chemical factors of the leaf surface involved in the morphogenesis of *Blumeria graminis. Physiological and Molecular Plant Pathology* **60,** 51-57.

Tymowska-Lalanne, Z. K., M. (1998). Expression of the *Arabadopsis thaliana* invertase gene family. *Planta* **207,** 259-265.

Vasil'ev, A. E. (1999). Primary and secondary plasmodesmata: Their frequencies in shoot apical meristem and leaf. *Izvestiya Akademii Nauk Seriya Biologicheskaya* **4,** 497-500.

Vasse, J., Billy, F., and Truchet, G. (1993). Abortion of infection during the *Rhizobium meliloti*-alfalfa symbiotic interaction is accompanied by a hypersensitive reaction. *Plant Journal* **4,** 555-566.

Vignault, C., Vachaud, M., Cakir, B., Glissant, D., Dedaldechamp, F., Buttner, M., Atanassova, R., Fleurat-Lessard, P., Lemoine, R., and Delrot, S. (2005). *VvHT1* encodes a monosaccharide transporter expressed in the conducting complex of the grape berry phloem. *Journal of Experimental Botony* **56,** 1409-1418.

Voegele, R. T., Hahn, M., Lohaus, G., Link, T., Heiser, I., and Mendgen, K. (2005). Possible roles for mannitol and mannitol dehydrogenase in the biotrophic plant pathogen *Uromyces fabae*. *Plant Physiology* **137,** 190-198.

Voegele, R. T., Struck, C., Hahn, M. and Mendgen, K. (2001). The role of haustoria in sugar supply during infection of broad bean by the rust fungus *Uromyces fabae*. *Proceedings of the National Academy of Sciences. U.S.A.* **98,** 8133-8138.

Vogel, J., and Somerville, S. (2000). Isolation and characterisation of powdery mildew-resistant *Arabidopsis* mutants. *Proceedings of the National Academy of Sciences. U.S.A.* **97,** 1897-1902.

Vogel, J. P., Raab, T. K., Schiff, C., and Somerville, S. C. (2002). *PMR6*, a pectate lyase-like gene required for powdery mildew susceptibility in *Arabidopsis*. *Plant Cell* **14,** 2095-2106.

Vogel, J. P., Raab, T. K., Somerville, C. R., and Somerville, S. C. (2004). Mutations in *PMR5* result in powdery mildew resistance and altered cell wall composition. *Plant Journal* **40,** 968-978.

Walters, D. R., and Wylie, M. A. (1986). Polyamines in discreet regions of barley leaves infected with the powdery mildew fungus, *Erysiphe graminis. Physiologia Plantarum* **67,** 630-633.

Wang, R., Hong, G., and Han, B. (2004). Transcript abundance of rml1, encoding a putative GT1-like factor in rice, is up-regulated by *Magnaporthe grisea* and down-regulated by light. *Gene* **324,** 105-115.

Waters, B. M., Blevins, D. G., and Eide, D. J. (2002). Characterisation of *FRO1*, a pea ferric-chelate reductase invovled in root iron acquisition. *Plant Physiology* **129,** 85-94.

Wei, Y. D., Zhang, Z.G., Anderson, C.H., Schmelzer, E., Gregersen, P.L., Collinge, D.B., Smedegarrd-Petersen, V., Thordal-Christensen, H., Wei, Y.D., and Zhang, Z.G. (1998). An epidermal/papillae-specific oxalate oxidase-like protein in the defence response of barley attacked by the powdery mildew fungus. *Plant Molecular Biology* **36,** 101-112.

Weig, A., Franz, J., Sauer, N., and Komor, E. (1994). Isolation of a family of cDNA clones from *Ricinus communis* L. with close homology to the hexose carriers. *Journal of Plant Physiologyy* **143,** 178-183.

Werner, M., Uehlein, N., Proksch, P., and Kaldenhoff, R. (2001). Characterisation of two tomato aquaporins and expression during the incompatible interaction of tomato with the plant parasite *Cuscuta reflexa*. *Planta* **213,** 550-555.

Wieczorke, R., Krampe, S., Weierstall, T., Freidel, K., Hollenberg, C. P., and Boles, E. (1999). Concurrent knock-out of at least 20 transporter genes is required to block uptake of hexoses in *Saccharomyces cerevisiae*. *FEBS Letters* **464,** 123-128.

Will, A., Caspari, T., and Tanner, W. (1994). KM Mutants of the *Chlorella* Monosaccharide/H^+ Cotransporter randomly generated by PCR. *Proceedings of the National Academy of Sciences. U.S.A.* **91,** 10163-10167.

Wirsel, S. G., Voegele, R. T., and Mengen, K. W. (2001). Differential regulation of gene expression in the obligate biotrphic interaction of *Uromyces fabae* with its host *Vicia faba*. *Molecular Plant-Microbe Interactions* **14,** 1319-1326.

Woods, A. M., and Gay, J.L. (1983). Evidence for a neckband deliminating structural and physiological regions of the host plasma membrane associated with haustoria of *Albugo candida*. *Physiological Plant Pathology* **23,** 73-88.

Wright, D. P., Baldwin, B. C., Shephard, M. C., and Scholes, J. D. (1995). Source-sink relationships in wheat leaves infected with powdery mildew. I. Alterations in carbohydrate metabolism. *Physiological and Molecular Plant Pathology* **47,** 237-253.

Zhang, L.-Y., Peng, Y.-B., Pelleschi-Travier, S., Fan, Y., Lu, Y.-F., Lu, Y.-M., Gao, X.-P., Shen, Y.-Y., Delrot, S., and Zhang, D.-P. (2004). Evidence for apoplasmic phloem unloading in developing Apple fruit. *Plant Physiology* **135,** 574-586.

Zhou, D. X., Li, Y. F., Rocipon, M., and Mache, R. (1992). Sequence-specific interaction between S1F, a spinach nuclear factor, and a negative cis-element conserved in plastid-related genes. *Journal of Biological Chemistry* **267,** 23515-23519.

Zhu, C., Schraut, D., Hartung, W., and Schaffner, A. R. (2005). Differential responses of maize *MIP* genes to salt stress and ABA. *Journal of Experimental Botony* **56,** 2971-2981.

Zhu, J. K. (2002). Salt and drought stress signal transduction in plants. *Annual Review of Plant Biology* **53,** 247-273.

Zimmerli, L., Stein, M., Lipka, V., Schulze-Lefert, P., and Somerville, S. (2004). Host and non-host pathogens elicit different jasmonate/ethylene responses in *Arabidopsis*. *Plant Journal* **40,** 633-646.

Appendix 1- sequences isolated during this project

Novel sequences amplified from powdery mildew infected leaf cDNA, using degenerate and subsequent RACE PCR, are listed below, along with promoter sequences isolated from a Cabernet Sauvignon BAC library. cDNA sequences are given first, followed by the predicted amino acid and promoter sequences. Putative start and stop codons are indicated in green and red type, respectively.

VvHT3 (Genbank accession number AY538259)

Full length cDNA

AAGGAGAAGAAGGTCTTAGTCATTTTCCTTGGTGTCTCAACTGTGTTGGGAGAGGAGGAAGAAGAGGA
ACTATGGAGGTGGGAGATGGGTCTTTTGCTCCTGTAGGTGTGTCCAAGCAGAGGGCAGACCAGTACAA
AGGCAGGCTCACTACTTATGTGGTCGTTGCTTGCCTTGTTGCTGCTGTTGGGGGTGCAATTTTCGGCT
ATGACATTGGGGTTTCAGGAGGCGTGACATCAATGGATACATTTCTTGAAAAATTCTTCCACACAGTC
TATTTAAAGAAGAGGCGGGCCGAAGAAGACCACTACTGCAAGTACAATGACCAAGGCCTTGCAGCATT
TACCTCTTCCCTCTACCTTGCTGGTTTGGTTGCGTCCATTGTGGCATCGCCTATTACAAGGAAGTATG
GGCGTCGAGCAAGTATAGTATGTGGTGGGATCAGCTTTCTTATTGGAGCTGCCCTAAATGCTGCAGCT
GTGAACTTGGCGATGCTTCTTTCGGGTCGGATCATGCTTGGTATTGGCATTGGATTTGGCGATCAGGC
AGTGCCACTATATTTGTCAGAGATGGCGCCGGCCCATCTCCGAGGAGCCCTGAACATGATGTTTCAGT
TAGCAACTACGACGGGGATCTTCACAGCAAACATGATCAATTACGGAACTGCAAAGCTCCCCTCATGG
GGATGGAGGCTGTCATTGGGCCTGGCTGCATTACCAACTATCTTAATGACAGTGGGAGGCCTATTTCT
TCCTGAGACTCCCAACAGTCTAATCGAACGGGGATCAAGGGAGAAAGGGAGACGAGTCCTAGAAAGAA
TCAGAGGTACCAACGAAGTTGATGCAGAGTTTGAAGACATTGTGGATGCTAGTGAGCCTGCAAACTCA
ATCAAGCATCCTTTCAGAAACATCCTTGAGAGAAGGAACAGGCCACAGCTGGTTATGGCAATCTGCAT
GCCAGCTTTCCAGATCCTCAACGGCATCAATTCTATTCTCTTCTATGCCCCAGTTCTGTTTCAGACCA
TGGGATTTGGAAATGCTACTCTCTACTCGTCCGCTTTGACAGGGGCCGTTCTTGTTTTATCCACAGTG
GTTTCAATCGGATTGGTGGATAGATTGGGTAGAAGAGTTTTATTGATTTCTGGGGGAATCCAAATGGT
CTTATGTCAGGTGACAGTTGCCATAATCCTGGGGGTCAAGTTCGGAAGCAATGACGAGCTCTCGAAAG
GCTACTCAGTATTGGTGGTGATTGTGATCTGCCTCTTTGTTATAGCATTCGGATGGTCGTGGGGGCCA
CTTGGGTGGACAGTTCCAAGTGAGATATTCCCACTGGAGACCCGATCAGCAGGACAGAGCATAACAGT
GGCTGTGAACCTCCTGTTCACCTTCATAATAGCTCAGTGTTTCCTTTCCATGCTTTGTTCTTTCAAGC
ATGGAATTTTCCTCTTTTTTGCTGGGTGGATTGTTATCATGACCCTCTTCGTATACTTCTTCCTACCT
GAAACAAAGGGAGTTCCCATTGAAGAAATGATATTCGTGTGGAAGAAGCATTGGTTCTGGAAGAGGAT
GGTGCCTGGGACTCCAGATGTTGACGACATCGACGGCCTGGGAAGCCATTCAATGGAGTCAGGTGAAA
AGACAAAGCTAGGCAGCTGAGCTTAATTCTTCCGATTTCGGTGAACTTCAAATAATCCATGTAGCATA
TGGCAAGCCAGGCTCCTATCATGAGCCAATAATTAGT

Predicted amino acid sequence

MEVGDGSFAPVGVSKQRADQYKGRLTTYVVVACLVAAVGGAIFGYDIGVSGGVTSMDTFLEKFFHTVY
LKKRRAEEDHYCKYNDQGLAAFTSSLYLAGLVASIVASPITRKYGRRASIVCGGISFLIGAALNAAAV
NLAMLLSGRIMLGIGIGFGDQAVPLYLSEMAPAHLRGALNMMFQLATTTGIFTANMINYGTAKLPSWG
WRLSLGLAALPTILMTVGGLFLPETPNSLIERGSREKGRRVLERIRGTNEVDAEFEDIVDASEPANSI
KHPFRNILERRNRPQLVMAICMPAFQILNGINSILFYAPVLFQTMGFGATLYSSALTGAVLVLSTVVS
IGLVDRLGRRVLLISGGIQMVLCQVTVAIILGVKFGSNDELSKGYSVLVVIVICLFVIAFGWSWGPLG
WTVPSEIFPLETRSAGQSITVAVNLLFTFIIAQCFLSMLCSFKHGIFLFFAGWIVIMTLFVYFFLPET
KGVPIEEMIFVWKKHWFWKRMVPGTPDVDDIDGLGSHSMESGEKTKLGS

Promoter

GATCTTCTCATACCCCCATTATAGCCACAAGATAAAATACCAAAATTTTCAAATACAATATCATCTCT
TTACCACTGCATTGGTGATGGGGCTGAGTGATGATAGTGAATTATTTGGCTTCAATGTAGAGAGTGGG
GCCTGATAAAAGGACTCTGTTTTTGTTTTTGATTTGGCACTGAATTATTTTATGTCTGGAAGATTCAT
TGGTGTTGATGGTGCACAGAGATGGTGACTCTCAACAAGTTGAGGAAAATTACAGCCAAGTACTATAA
AATATTCATACACCTTCATGCATTATATTTGGTTTGGTGACAAAGTCCTCTTGCCTTTCTTTATTAAA
CAAAAAGAGAAAATAAAAATGAAGATTTGGTTGTGGTTAAAATGAAATTATGGGGAGTTTTTCAAAGT
ATTGGTGTCATTCCACTGGGTGTATTTATGGAAGGGAGACTAAGCAAAGTCAATAATAATAAACTGTC
ACTGCGAAAAAAGGGTTGTCTCTGACNATTTCTGAGATGTTTTGGATTATAGGGGGGTGGGACTTNAG
TGTGATGAGCCCACCATCCATGACTACGGAGGAATGCAGACATAGCAGATAAGAAATGGAATCCAGAA
ACTGAAGCAAATCCCANATAAACTTCCAACAGGAAAGAACAAGCCAAGTGGGTGAAGAAAAGACAGAG
GGGGAAAAGCGTTGAAAGGCCCATTAACCTTTTTAAGGGTCTCTCTCTTTCTGTTTNTCTTCTTGCCT
TTTCAAGCGTCTCCAAAACCACCCAAAACCATTTTTTTTTAAATGGAAGTTTTTTCTTGGATGGTAAC
TTTCTTGGGTGCCAAAAACAGAGCAAGCCTTCCGATTGTTTTCATGGTAATTTAATCCCTTCCTTGAT
TTAAAGCAAGGATTTTTTTTCCTTAAATAATTGTTGTCCTGTATCAAATATTTTATCCATTTGTTGTC
GATGAAGACTGGTAACTGATTACGATAGGTCAGCCCCTCATTATTAAAAGCTAATACCATTGTTGATT
TTCTCTTCACTTCAGTTGAGAATTACAAAAACCTTGAGTGGGGAACCTCTCTGTTTCTCCTTGTAAAC
CGCCCTTGGATTGAATTCTCAAGGAGAAGAAGGTCTTAGTCATTTTCCAAGGTGTCTCAACTGTGTTG
GGAGAGGAGGAAGAAGAGGAACTATG

VvHT4 (Genbank accession number AY538260)

Full length cDNA

TCCTCTCTATCCTTTTCTCTCTTCAGAGCCATGGCAGTGGGAATTGCAGTAACAAGCCATGGTGGGCA
CTACAATGGAAGAATAACCCTATTTGTGGTTCTATCTTGTATGATGGCTGGCATGGGAGGAGTCATTT
TTGGATATGATATTGGAATTTCAGGCGGGGTGACCTCAATGGATTCATTTCTAAAGAAATTCTTCCCG
GAGGTGTACAAGAGGATGAAAGAAGACACCAAGATTAGCAACTACTGCAAATTTGACAGTCAATTGTT
GACCTCATTCACATCCTCCCTGTATATTGCTGGCCTTGTTGCTTCCTTTGTTGCTTCTTGGATCACTA
AAAAGTTCGGGCGCAAGCCAACCATCCTTGCTGGAGGGGCTGCCTTTCTCATCGGATCAGCACTAGGT
GGTGCCGCCTTCAATGTCTATATGGTTATATTAGGCCGGATTTTGCTTGGCGTTGGCGTTGGTTTTGC
AAACCAGGCAGTGCCACTTTACCTGTCCGAAATGGCTCCACCAAGATACAGAGGGGCAATCAACAATG
GCTTTCAATTCAGCATTGGCGTTGGGGCTCTATCAGCTAACCTTATTAACTTTGGCACTGAAAAAATC
AAAGGCGGTTGGGGCTGGCGAGTTTCTCTAGCATTGGCTGCAGTTCCGGCTTCAATCCTCACCCTAGG
GGCACTTTTTCTCCCAGAAACCCCCAATAGCTTAATCCAACGAAGCAAAGACTATGGAAAGGCTGAGC
TGATGTTGCAGCGTGTTCGAGGCACAAACGATGTCCAAGCAGAACTTGATGATCTGGTAAAAGCAAGC
TCCCTAGCAAAAACCATCAATGACCCGTTCAAGAAAATCTTGCAAAGGAAATATAGGCCTCAACTTGT
TATGGCAATCGCTATACCATTCTTTCAGCAAGTAACGGGAATCAATGTCATTGCATTTTATGCTCCCG
TACTTTTCCGGGCAATTGGATTAGGTGTGAGTGCATCCCTCCTGTCAGCAGTTGTGACCGGCGTAGTT
GGTATGGCCTCCACCTTCATCTCAATGCTCATAGTAGATAAACTCGGCCGAAGAGTTCTTTTCTTAGT
CGGGGGAATACAAATGCTGGTCTCACAAATTATGGTAGGAGGAATATTGGCAGCTGAGCTTGGTGATC
ATGGTGGGGTGAGCAAAGTGTACGCTTTTCTGGTTCTGCTTTTGATTTGTGTTTATGTCGCTGGGTTC
GGGTGGTCCTGGGGTCCATTGGGATGGTTGGTTCCAAGCGAGATTTTCCCACTCGAGATTCGATCAGC
TGGGCAAAGCATCACAGTGGCAGTCAGCTTTATCTTCACTTTCATTGTAGCTCAAACATTTTTATCTA
TGCTCTGCCATTTCAAGTCTGGGATTTTCTTCTTTTTTGGGGGTTGGGTGGTGTTGATGACTGCATTC
GTGTATTATTTGCTGCCAGAGACTAAGAGCATTCCCATTGAACAGATGGACAGAGTCTGGAAGGAGCA
TTGGTTTTGGAAGAGAATTGTGGTTGAAAAGCTCAGCAACCCTAAAATGGAGACAGCCTAAAGATTCA
ATACAAATCTCAACAGCATCCTCCTCTAAGGAAAAACTGTTAATGCATGCATTCATATACAGTTTCTA
AATTTAGTGGTTGCTAGACCTTAACTGCTTGTTTAGTTCTGTTGAGCCAAAGATCCAGAAGGCAGCCT
TTCATGCACTACAAGAATGAGCTAGCAGTCATAGAAACAATGATCGTAAATTGCCCGAAAAAAAAAAA
AAAAAAAAA

Predicted amino acid sequence

MAVGIAVTSHGGHYNGRITLFVVLSCMMAGMGGVIFGYDIGISGGVTSMDSFLKKFFPEVYKRMKEDT
KISNYCKFDSQLLTSFTSSLYIAGLVASFVASWITKKFGRKPTILAGGAAFLIGSALGGAAFNVYMVI

LGRILLGVGVGFANQAVPLYLSEMAPPRYRGAINNGFQFSIGVGALSANLINFGTEKIKGGWGWRVSL
ALAAVPASILTLGALFLPETPNSLIQRSKDYGKAELMLQRVRGTNDVQAELDDLVKASSLAKTINDPF
KKILQRKYRPQLVMAIAIPFFQQVTGINVIAFYAPVLFRAIGLGVSASLLSAVVTGVVGMASTFISML
IVDKLGRRVLFLVGGIQMLVSQIMVGGILAAELGDHGGVSKVYAFLVLLLICVYVAGFGWSWGPLGWL
VPSEIFPLEIRSAGQSITVAVSFIFTFIVAQTFLSMLCHFKSGIFFFFGGWVVLMTAFVYYLLPETKS
IPIEQMDRVWKEHWFWKRIVVEKLSNPKMETA

Promoter

TGGGATATTTGATGANATATTTTNTAATATAAGGAAAAATAAGGTGGAGAGAAGTAAAAAAATAANGT
CAAGAGAAGGATATTCGGGGAAANAAAAAAATTTATTTANTTANTTATTTTTNCTAATTNACANATTT
CTCTAAATAGTTGTTTTCATATTTCCTTAANTATAAATTGTTCTTTTTAATTAAAAAAATTAAAATAA
TTTTATATTCTAAACTTATTTTTAATTTATTACATATAAATATATATTATATAATATATAACAATAAT
AATAATAATAAAAATATGAAAACAAAAGTTCAAGAATGGGACAGATTAAGGTAATTTCTTTTTTTTTT
TTAAAAAAAAAATTACAAACTAACAATAAAGATTCTTCAAACTTTTACAAGTAGTATAGATTATTGTA
AAAGTTGATCATATAATGACAAAATCTCTTTTTTTTTTTTCTATTTAATTTTAGCAATGGTATAAATG
CGATTTTGTTTCCAAGATTCTATTGAATCACAAATTGGCCGTAACCTTATCATGACCCAATTTAAAGG
GCTTCTCTTTTTTATTTCCATTTTAAAAAATATTTAAGATCTCTTGCTGGTGAAAATTCAAAATTTGG
TCCAATAATTGAGCAAGAGTCAACAAGGATCCCTTCGTTTATTAAATATTCCTTTAACGAGAGATTCT
CTTTCTTTGTTCAGACTTCAGACGGAAGCAATTGATTGGTCCAGTTTGAATCTATCGTATTACGTGTC
TGATAGTGGAAGCCCATGATACTCTAAAGCTCCAACCCCAATGTTCACCTCCACATGCCCCATATAAC
TCCAAATTCACAGCAAAGTACGAAAAGTTTTTATTACTTTTTTATAGTGAACATGTCCTAGCATAGAC
GGCCATATTCACCAGTCAAGAAAGACTGCTTCTCTCTCATCTTCATTTTATCTTCCACTCTTTGTCAT
CATATCTGATTCCACAGGATTTCTCTCCTATCCTTTTCTCTCTTCAGAGCCATG

VvHT5 (Genbank accession number AY538261)

Full length cDNA

TTGAGGCCGAAGCGACATTGATAAGGTTTTTAGGAGTTTGTAGGTGGTGACATCATGCCTGCTGGAGG
ATTCGCGGCCCCGTCGGCCGGTGGCGACTTTGAAGCCAAGATCACTCCTATCGTTATCATTTCTTGCA
TCATGGCCGCCACCGGCGGCCTCATGTTCGGCTACGACGTTGGCGTTTCTGGGGGTGTGACGTCGATG
GACCCATTCTTGAAGAAATTTTTTCCGGTAGTATATAGGAAGCAGCATGAGGAGCTGGAGAGCAATTA
CTGCAAGTACGACAACCAAGGGCTACAGCTGTTCACGTCGTCTCTATATCTTGCGGGCTTGACCTCCA
CTTTCTTCGCATCATACACAACCAGAAGTTTTGGTCGTAAGGCAACCATGCTTATTGCTGGGATTTTC
TTCATTGTGGGAGTGGTGCTTAATACCGCTGCCCAAGATCTAGCTATGCTCATCATTGGGAGGATCCT
TTTGGGCTGTGGCGTCGGTTTCGCTAATCAGGCTGTTCCACTGTTCTTATCGGAGATAGCACCTACAA
GAATACGTGGAGGACTAAACATACTGTTCCAACTTAACGTCACTATTGGCATACTTTTTGCTAACCTC
GTCAATTACGGCACTGCCAAAATCAAAGGGGGATGGGGATGGAGGGTATCATTGGGGTTGGCTGGGAT
TCCTGCGGTCCTCCTAACTGTGGGGTCTCTCTTGGTGGTGGACACCCCTAACAGCCTTATCGAGCGTG
GTCGCTTGGAAGAAGGAAAGGCAGTTCTCAGAAAGATAAGGGGCACTGACAAGATTGAACCAGAATAT
CAGGAGCTTCTTGAGGCAAGTCGTGTGGCTAAATTAGTGAAGCACCCCTTTAGGAATCTAATGCAGCG
CAGAAACCGACCCCAGCTGATCATTGCTGTGGCCTTGCAGATCTTCCAGCAATTCACAGGCATCAATG
CAATCATGTTTTATGCTCCAGTCCTGTTCGACACTTTGGGATTTGGTAGTGATGCGTCCCTCTACTCA
GCTGTCATAACGGGGGCTGTTAATGTTCTCTCAACCCTCGTGTCCGTCTACTCTGTCGACAAAGTAGG
CCGTCGATTGCTCTTGCTGGAAGCTGGCGTCCAGATGTTCTTCTCTCAAGTGGTAATTGCAATCATAC
TAGGCATCAAAGTCAAAGATCACTCCAACAATCTCCACACTGGCTATGCAGTCCTAGTAGTGGTCTTG
GTGTGCACTTTTGTGGCCGGCTTTGCATGGTCTTGGGGGCCACTCGGTTGGCTCATTCCAAGTGAGAC
CTTCCCACTGGAGACCCGATCAGCAGGGCAGAGTGTGACTGTTTGTGTGAACCTGCTCTTCACTTTTG
TCATAGCACAGTCCTTCCTTTCCATGCTTTGCCATTTAAAGTATGGCATCTTCCTTTTCTTCTCCGGC
TGGGTCTTCATCATGTCCTTCTTTGTGCTCTTTTTGCTCCCGGAGACCAAAAACATTCCAATTGAGGA
AATGACAGAGAGGGTGTGGAAGAAGCATTGGTTGTGGAAGAGATTCATGGATGACCATGTGGAGGGCT
TCCCTGTTTTTGGTTATAATGATGAAGAAACTGTTGTTAATGGAAGTGACAAAAAGAGAGATGGGTAC
GGCAATGGATTCGATCCTTCTTCCCAATTATAAGATTAGTGGTGTATGGGGAGGGAAAGAAAAGACAT
CACTAGATAAATGAATAGCTAAAAATAGTTTGATATGCCCCTTGTTGCTTACCATTTGTTTTCACTAG
TTCTATGGTATTTGATACCTTACCCCTATATGATGAATCCCCCTGTATATGTGTTCTTGTGCCCATGT

CGGTCCATGTATGACTCAGAATTATGAAAAAAAATAAAGAGATTATTGGAATTCAAAAAAAAAAAAAA
AAAAA

Predicted amino acid sequence

MPAGGFAAPSAGGDFEAKITPIVIISCIMAATGGLMFGYDVGVSGGVTSMDPFLKKFFPVVYRKQHEE
LESNYCKYDNQGLQLFTSSLYLAGLTSTFFASYTTRSFGRKATMLIAGIFFIVGVVLNTAAQDLAMLI
IGRILLGCGVGFANQAVPLFLSEIAPTRIRGGLNILFQLNVTIGILFANLVNYGTAKIKGGWGWRVSL
GLAGIPAVLLTVGSLLVVDTPNSLIERGRLEEGKAVLRKIRGTDKIEPEYQELLEASRVAKLVKHPFR
NLMQRRNRPQLIIAVALQIFQQFTGINAIMFYAPVLFDTLGFGSDASLYSAVITGAVNVLSTLVSVYS
VDKVGRRLLLLEAGVQMFFSQVVIAIILGIKVKDHSNNLHTGYAVLVVVLVCTFVAGFAWSWGPLGWL
IPSETFPLETRSAGQSVTVCVNLLFTFVIAQSFLSMLCHLKYGIFLFFSGWVFIMSFFVLFLLPETKN
IPIEEMTERVWKKHWLWKRFMDDHVEGFPVFGYNDEETVVNGSDKKRDGYGNGFDPSSQL

Promoter

CATCTTGACCTTGGGTTAGGATTGTNGACGTGGATTAAGAGAGGTCGACTTCTCAATTTCTTCNCCTT
GGAGTGGGCCAAGGAGCAAGGGTTGACCCAAAATGGCTTCACAAAAAACCTACACAACTGTAGGCATG
GTGGGCTGAGGCCTAATCCCATTGTTTACATTTGATACGTGATGGAAAACTCTTAACCAATGTCGGAT
AAACTTACAAGATAACAAAATAACCACCACATCCTGGTGCCAATCAATTCCCAAGAAATAGGACACGA
GCAAAATATTGGATCAATATTCATTAAAAAAATGAAATGTTTTCCAATTTGTAAATTAATTCCCGTGG
TGTTTGTATTTGAAAAGTAATTAATTTTTAATACAGTTTTAAAATAGAAGATTATTGTTATAAGAAAA
AAAGTGAGAGTATTTTAATAAAAAAATTAATATTTTTTAAGCTATAAAATTGTGAAAATTAGATTGAT
AAATTAGGATTGTTTTATCTATTTTAGTTGAATGACCTTAAAATATTTTAAGGTTATGTTTGGTGTTA
GGAAAATATTAAGGAAAAAAAAAATTAAGGGTAGTTTGGCTTAAAAAAGATTTAAAGTTGTTAGAAAA
TTGTTTCCTTATAATTTTTTTTCTTTTTTTTAAAATATTTTCAGGAAACAAAGTATAATATAAGAAAA
ATTATTTTCTTGTATTTGATTGTATTATGAATAAAACTATGAAAGGAAATAAAAATAATTTATTAATT
TTAAATAATTTTTTTTTTTTAAATCTATCTATTTTTTCTGACATTTTTTTCTTCCAGATGCATAGCTG
CCGCCATTTATGATCGAAACCCAAGCTATCACGAGCCCATCTATGAACTCCTAGAAAGTGGAAAGTGG
AAAGTGGAAATTAAGATAAGGTGAAAGGAGTCGACTCAAATCTGTGGCTGCCGGAGTCCAACAACATT
GCTTTTCCTGTGAATGGCGAAAGGTTTTGGGCCAGTAGTACTCTTTTGATTTTCATCCTTATCCATTG
ACGACACGAACTTGGATTTTCCAAACCCTAAATCGAGAGAGTGGTGGTCAAAGTTGGTGTCCCCGATA
TTACAAGCCAACTCACGCCCACACGTTCGTATTGAATGATCTCGCCTCCTAAACCCTCGTTAATTTCT
TAAAAAAATCAAAGTGTTAATTCTCGATGCCATCAACTCTGACTTTGAGGTTGTAAAATACAAAAGCA
TGAGATTCCAAATATAAAGCATTTTTTTTACTAGGATATATACATAGCAGAAGGTCAATCTTTTGACG
TTGAATTTTCCACGGTTGTTGTGGGCCCCTGACTTTCCATGGCAGCCAGTTGATATGATCACATGATT
CAGACGAAAGGCAACAAAAGGTTTTGTTGTTGGATTCTATTCACTTATCAATTTTGCATTGATTTTTA
CTTTTTTTTTTTTTTTTTTTTTTTGTCCATAATTTTTGATGATTGGGTTTGGGTGGAGGAAATGATTT
ATGAGTAGACTAGGAGCATTAGAGGGGCTCCGATTCCGAGTATGGTGGAATTGGGAGTGAAAAGATGG
TCGTAGGCCCAATAATTATCTGCCCACGTCCATTTATGGCCGTCGTGAAATGCATGTTGCAAATGGTC
GTAGGCCCAATAATTATCTGCCCACATCCATTTATAGCCTTCGTGAAATGGATGTTGCAACCAAGCTC
ACTAAAATGATTTCTCATAATTATTTAAATAAATTATTTTTAAAAAAAATTGCAACATCATCAAATCC
CGTAAAATGACAATATTAAGATCTTCGAATCAACTTAAAGTATTCTTGTAACGATAATGATATATGAT
GGTTTTTTTTCTGAGAAAGTTATTTTTTATTTTTTATTTAAATAATAATAATAATAATAGAAGCGTGG
ACTTATACGGTATCAGAACAAAACTCAGTGAAAGTGGGAAAGTTGGCAAGTACTTTCTACTTGGTTTT
GATTACAATAACGAACCTGGAAATGCGCACGTGGCATTATTAGAAGAGGTACAATTGTACAAATAATC
ATCATCCATACACGCCTCTTTGGGTTATGTTCTTACGACGTGGCATTTGGTGAACCCCCTGGCACTGG
CGCACCCACCGTCCATGTTCCCATTTTGCTTCGGAAATGGGCCCCATTATGACGCGAAGGGGGAAAAA
ACGTTGGCTTGACTAAGCAGCCGTCGATGAAGAACATCGGGTTCATGGTTGCCACGTGGATATATCCT
GGTGGTCATCCTATTACATCATCCATTTCGTACTTCGTGCTCCTCTCCCTACTCTCCTCTATATATAC
ACTCGCTCCGGATGGTCTTTTTCCAACTCTCTCTGCCTAGTGTCTCTTCTTCTTCTTCTTCTTCTT
TCTGCTCTTTCTGCTGCTTGAGGCCGAAGCGACATTGATAAGGTTTTTAGGAGTTTGTAGGTGGTGAC
ATCATG

VvcwINV (Genbank accession number AY538262)

Full length cDNA

CACAAAGCCATCATGGCCACCTCTTCTCATGGCCTATTAGGGTTCTTCTTCTCTCGGTTCTTGGGCCA
TGGCTTTGTGCCCCTTGAAGCCTCCCCACCAAGTCTACATCCCACCTCCAAAATCAGTCTCCCCTCTT
CTTTAAAAACCCACCAGCCTTACAGAACTGGATATCATTTCCAGCCTCGCAAGAACTGGATGAATGAT
CCTAATGGGCCTATGATCTACAAGGGGCTCTACCATTTCTTCTATCAATACAATCCCCATGGTGCAGT
TTGGGGAAACATAGTGTGGGCACATTCCACATCAACCGATCTTGTCAACTGGACTCCTCATAAATATG
CCATTTCCCCATCCCAGCCAGCTGATATCAATGGCTGCTGGTCAGGTTCAGCAACCATCCTGCCAAAC
GGCAAGCCAGTGATTCTCTATACTGGTATCGATCCACAGAACAAGCAAGTTCAGAACATGGCTGTGCC
CAAAAATCTCTCTGACCCCTTCCTTCTAGAATGGACTAAGCTCTCTCAGAACCCTCTAATGGAACCTA
CTACCATCAACAGCATCAATGCTAGCTCATTCAGAGACCCTACGACTGCTTGGCAGGGCACTGATGGA
AGATGGAGGGTGATAATTGGAAGCAAAATAAAGCGAAAAGGATTAGCAATTTTGTATAGGAGCAAAGA
TTTTGTCCGCTGGACTAAAGCACAACACCCGTTACATTCAGGGAAGAATACTGGAATGTGGGAGTGTC
CAGACTTTTTTCCAGTATCTATCAACAGCTCTACGGGTGTAGATACATCATCGATAAGTAAAACCCTT
AAATATGTTCTTAAATTGAGCTTGGATGATACTAAGCATGACTACTACACGATTGGAAGCTACAACCG
TGAGAAGGATACCTATGTCCCAGATAAGGGGTCTGTGGATAATGACTCAGGCTTAAGATATGATTATG
GCAAGTTTTATGCTTCAAAAACCTTCTTTGACAACGCTAAGAACCGAAGAATCTTGTGGGGTTGGATC
AACGAATCATCTAGTGTGGAGCACGATATCGAGAAGGGATGGTCTGGAGTTCAGGCAATTCCAAGGAA
TGTTTGGCTGGACAAGTCTGGGAAACAGTTACTGCAATGGCCGATTGCAGAGATTGAAAAACAACGGA
TTAAACCGGGGCATATGTCTAGCAGAGAGCTGAAGGGAGGATCAAAGGTTGAAGTTGGTGGAATAACA
GCATCACAGGCAGATGTGGAGATATCGTTTAAGATATCAGACTTTAAGAAAGCAGAGGTTTTTGACGA
AAGCTGGAGTAATCCACAGCTGCTGTGCAGTCAAAGGGGTGCATCAGTAAAAGGTGGGCTAGGGCCAT
TTGGACTAATGGTGCTGGCTTCAAAGGGCATGGAAGAATACACAGCAGTTTTCTTTAGAATTTTCAAA
CGTCAGACCAAATATGTGGTGCTCATGTGCAGTGACCAAAGCAGGTCGTCTTTAGATAATGATAATGA
TAAGACCACGTATGGGGCATTTTTGGACGTGGATCCTGTCCATGAGAAGCTGTCACTAAGGAGTTTGA
TTGATCACTCAATAGTGGAGAGCTTTGGAGGAGGTGGAAAGGTTTGCATAACAGCTAGGGTTTATCCT
ACATTGGCTATTGACGGTGAAGCCCACTTGTATGCCTTCAACAAAGGAACTGGGAGTGTAGGGATGAC
AACACTGAGAGCTTGGAGCATGAAGAAAGCTAAAATCAATTGAAGGAAACAATCCTAGAGATGTATGT
AGAGTTGTGAGTGAAGAGCCAGGCTTTTGCAAATTTATCTTCTTCTATGGATTTGTACTAGAAGTCTG
CAGCAAATCCTCTTATGTAATTCATGTCAGTTTCTTTTGTTACCTAGCTGGAATCAATTCAAAGTTAG
TACAATATAAGAGAATAATTCCTGAAAAAAAAAA

Predicted amino acid sequence

MATSSHGLLGFFFSRFLGHGFVPLEASPPSLHPTSKISLPSSLKTHQPYRTGYHFQPRKNWMNDPNGP
MIYKGLYHFFYQYNPHGAVWGNIVWAHSTSTDLVNWTPHKYAISPSQPADINGCWSGSATILPNGKPV
ILYTGIDPQNKQVQNMAVPKNLSDPFLLEWTKLSQNPLMEPTTINSINASSFRDPTTAWQGTDGRWRV
IIGSKIKRKGLAILYRSKDFVRWTKAQHPLHSGKNTGMWECPDFFPVSINSSTGVDTSSISKTLKYVL
KLSLDDTKHDYYTIGSYNREKDTYVPDKGSVDNDSGLRYDYGKFYASKTFFDNAKNRRILWGWINESS
SVEHDIEKGWSGVQAIPRNVWLDKSGKQLLQWPIAEIEKQRIKPGHMSSRELKGGSKVEVGGITASQA
DVEISFKISDFKKAEVFDESWSNPQLLCSQRGASVKGGLGPFGLMVLASKGMEEYTAVFFRIFKRQTK
YVVLMCSDQSRSSLDNDNDKTTYGAFLDVDPVHEKLSLRSLIDHSIVESFGGGGKVCITARVYPTLAI
DGEAHLYAFNKGTGSVGMTTLRAWSMKKAKIN

Promoter

AAAANNATNNTGAGAANNCCCCCCNCCCCCTTCCCATTTGTCTCTCTCTCTCTCTCTCTCTCTCTCAT
CTTTTTGGGGGAGAAATCTCAAAGAGACTTTAGTCAAATTTAGAANTCAAATTAGTAATGGTTTTAAA
CAGGACAATTAAGTATTAGGTCAAAGGTATCCAGCCAATCTTTGAGTGTCCATAGTTAGGCTCATTAA
TGTGTTCATTTTTGACGATTAATTGATTCGACAAGTTAATTATTATATCCTCATTAGGGGTTTCAATT
TTCCATATAAATGGTAATCGACATATAACTTTTCATACAATCAAAATTGTATCTATCTTATTTGTCCA
ATACAATTAATGTTTGCATCAAAAGCATTTCTTGACTAATTGTAGATTTTTTTTTTAAAGTCAACAAA
GTTCAAATTTAAATTTTTACGTATTTTCTTAATAAAACTATCATTCTTATAAGATTAGTTTATATTTG
TTGATATCAATATATTCAAAACTGACAAATTTTCCAAGATTCCTCTGTTTCATTCTTTATTTTTTTTT
TCTTCTTATTGTTCAATATGTCATTTTTAGGCATTTTTTTCTTTTTACTTTTATTTCTCGGATCTCTA
ATGAATTAGAGATAAAAATCATATAACACAATGTTAAGATTCCTTATCCATGAATAGAAATAACCCAC

TTGGATTTTGAAATTTAATATCGACAAAACATAATAAATTAAAAAATTATAATCTACATATTAATTTC
TATAAGTAGATTTATTTAAAATCCCATTGCAAATTAAATATTAATTATAAATTGGCCACATCTTATCA
CATGATTCACATGGCACACTTGCAGTCTTTATTTCTAATAAGTAATTATTATAGATGTTTAATTTGCT
ATCATATCAAAATTTTTGTTTGACTCATTTAAAGCATTCAAAAATGAAATTATGACACTAATAAAAGA
GATAAGAAATATAAGATCATAAGACATCAATGCAAAGGAACAGTACCTTATCTATATCTGAGTGGATT
TTCTTTCCATATGATATGGAAAAGGAGCTTTTTGGCCAATCCCAAAATCAACTTTTATTTATTTTATT
ATTATTATTAAAATAAAATTTAGCTAAAGAAAAGGAACCACATGGCCATTGGGGGTGGTCCAAGGGAA
GTTGCCTACACACTTCCCCCGCCTTTTTCTTTGTCTTTTCTAAATATTCAACCATCCCCATATATTGA
CTTCCATTGATACAGAACCCCTCGAATTTTCTATGGCACTTCTCCTCTCCAAAAACACTTTTTTTCCT
GATTTTTTGTGGGGAAAAGAAATAATAAAAAAATGAAAGTAAAAAACCTCATTGGTGACTTTTCCCAT
CACCCAAAATCCTTCACTATAAATAGGACACTCTGGCCTAAGGCTCTCTCCTCATTCCCACAAAGCCA
TCATG

ProT degenerate clone (not submitted to Genbank)

Partial cDNA

TACTCCGGTACCATTATGGTGCCCCTTGGTTGGGCTGGTGGTGTGATTGGTTTTCTTTTAGCCGCAGG
AATATCACTTTATGCAAATTCTCTCGTTGCCAAGCTCCATGAATTTGGTGGAAAGAGACATATTAGAT
ACAGAGATCTTGCAGGATATATATATGGTAAGAAAGCATATACTCTGACTTGGGCTTTGCAATATGTA
AATCTTTTCATGATTAATACTGGATATCTCATTTTGGCAGGTCAGGCTCTGAAGGCTGTCTATGTTCT
TTTTAGGGATGATGGTGGCATGAAGCTCCCATACTTTATTGCGATTGGAGGCTTTGTATGTGCCATCT
TCGCCATAGGAATCCCACACTTGTCAGCTCTAGGGATTTGGCTGGGTTTTTCGACATGCTTGAGTCTA
ATATATATTGTTACAGCATTTGTGCTGTCACTTACAGATGGAATTAAAGCTCCATCTAGGGATTACAG
CATCCCAGGAACAGAAGCAAGCAAGGTCTTCAGTATTATAGGGGCAGCTGCTAATCTTGTTTTTGCAT
TCAACACAGGAATGCTTCCTGAGATACAGGCAACTATTAGACAACCTGTGGTTAAGAATATGATGAAA
GCTCTCTACTTCCAATTTACTGCTGGAATTCTACCACTGTATGCTGTTGTTTTTATGGGGTATTGGGC
TTATGGATCAACAACATCAACCTATTTGCTCAATAGTGTCTCTGGTCCAGTTTGGGGTTAAGACAATG
GCAAATCTTGCTGCCTTCCTGCNAACGGTTATTGCTTTGCATATATTCGCTTCCCCA

Predicted amino acid sequence

YSGTIMVPLGWAGGVIGFLLAAGISLYANSLVAKLHEFGGKRHIRYRDLAGYIYGKKAYTLTWALQYV
NLFMINTGYLILAGQALKAVYVLFRDDGGMKLPYFIAIGGFVCAIFAIGIPHLSALGIWLGFSTCLSL
IYIVTAFVLSLTDGIKAPSRDYSIPGTEASKVFSIIGAAANLVFAFNTGMLPEIQATIRQPVVKNMMK
ALYFQFTAGILPLYAVVFMGYWAYGSTTSTYLLNSVSGPVWG*DNGKSCCLPANGYCFAYIRFP

AAP degenerate clone (not submitted to Genbank)

Partial cDNA

GTTACCGGAAAGAGGAACTATACTTATATGGATGTTGTGAGAGCCAACTTAGGAGGTATGAAGGTTCA
GCTGTGTGGGATCGCTCAATATGGAAATCTCATAGGGGTCACGATCGGATACACAATCACGGCTTCTA
TCAGTATGGTTGCCGTACGACGGTCAAACTGTTACCACAAGCACGGCCATCAGGCGAAGTGCAACCCG
TCAGACTACCCTCACATGATCATCTTCGCTTGCATCCAGATCGTTCTGAGCCAAATACCAAACTTTCA
CAAGCTGTCATGGCTCTCTATTCTCGCAGCTGTCATGTCTTTCAGTTATGCCTCTATAGGCATCGGAC
TCTCCATTGCCAGGGTTGCAGGAGGGGCGCATGCAAGGACAACGTTAACAGGAAGGACAGTTGGAGTG
GACTTGTCAAGCTCAGAGAAGGTTTGGAGAACCTTCGAGTCCATCGGAAATATTGCTTTTGCTTACGC
ATACTCCACCGTCCTCGTC

Predicted amino acid sequence

```
VTGKRNYTYMDVVRANLGGMKVQLCGIAQYGNLIGVTIGYTITASISMVAVRRSNCYHKHGHQAKCNP
SDYPHMIIFACIQIVLSQIPNFHKLSWLSILAAVMSFSYASIGIGLSIARVAGGAHARTTLTGRTVGV
DLSSSEKVWRTFESIGNIAFAYAYSTVLV
```

Appendix 2- Expression of control genes

In Chapters 5, 6 and 7, quantitative RT-PCR was used to measure expression of sugar transport and invertase genes in a range of tissues. To normalise expression between samples, actin and ubiquitin expression was used. The level of actin expression was found to be more stable than ubiquitin in pathogen infected and wounded samples and was the reference gene used in these comparisons, however in the grape developmental series ubiquitin was more stable than actin and was used to normalise these samples. In the following Figures, the "cycling threshold" (CT) of the reference genes is shown. The CT is the cycle number at which the maximal rate of product amplification was observed and therefore, a low CT value represents a highly expressed gene and a high CT value indicates a gene expressed at a low level. In summary, the standard deviation across the samples compared was between 0.1 and 0.66, indicating that expression of the selected reference genes was relatively stable and differed by significantly less than a factor of 2 (ie. a CT difference of 1 would indicate 1 PCR cycle difference which in the exponential phase of amplification is one doubling of PCR product or a two-fold increase).

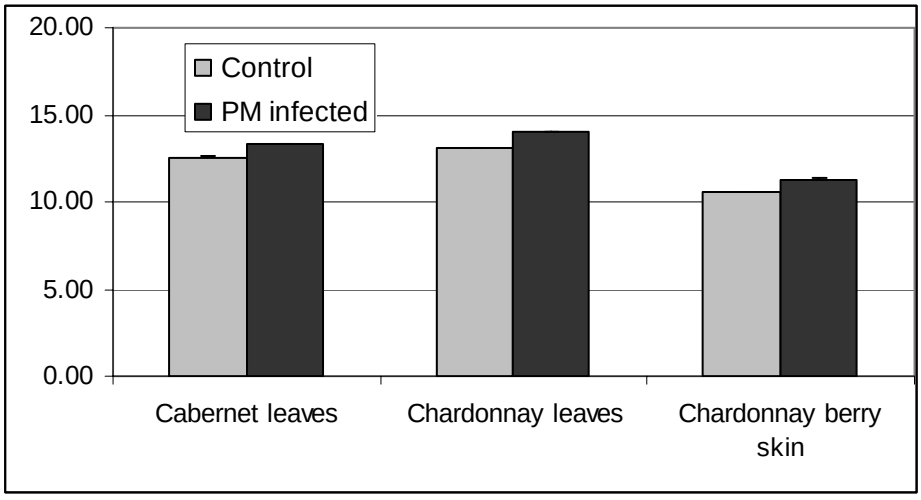

Figure A2.1. Actin expression in control and powdery mildew infected Cabernet Sauvignon and Chardonnay leaves, and Chardonnay berry skins. The standard deviations of the CTs compared was: Cabernet Sauvignon leaves: 0.556, Chardonnay leaves: 0.641, Chardonnay berry skin: 0.542.

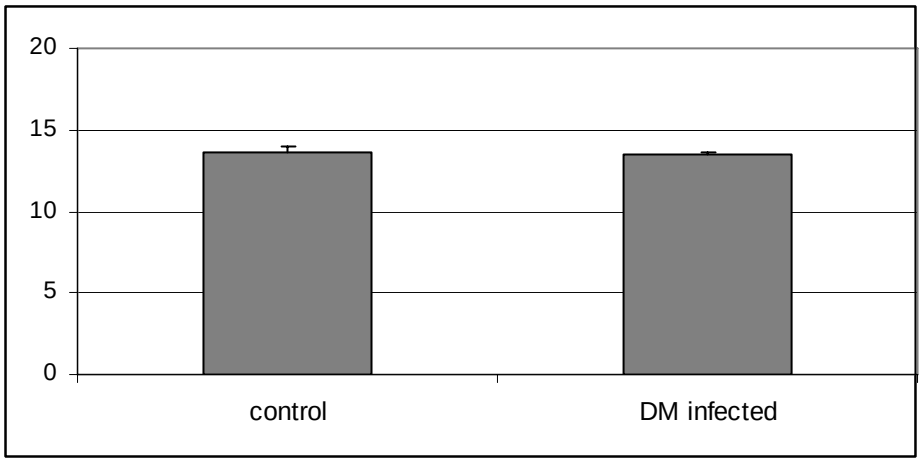

Figure A2.2. Actin expression in healthy control and downy mildew infected Cabernet Sauvignon leaves. The standard deviation of the CTs compared was 0.113.

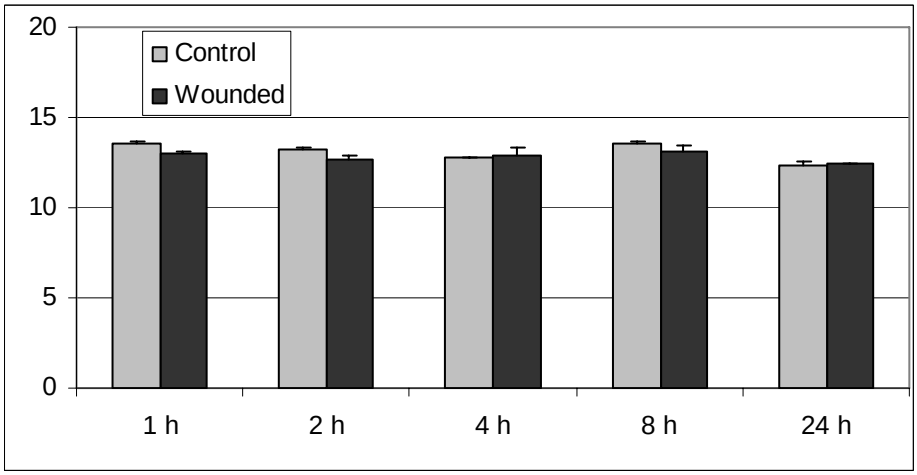

Figure A2.3. Actin expression in healthy control and wounded Cabernet Sauvignon leaves. The standard deviation of the CTs compared was 0.423.

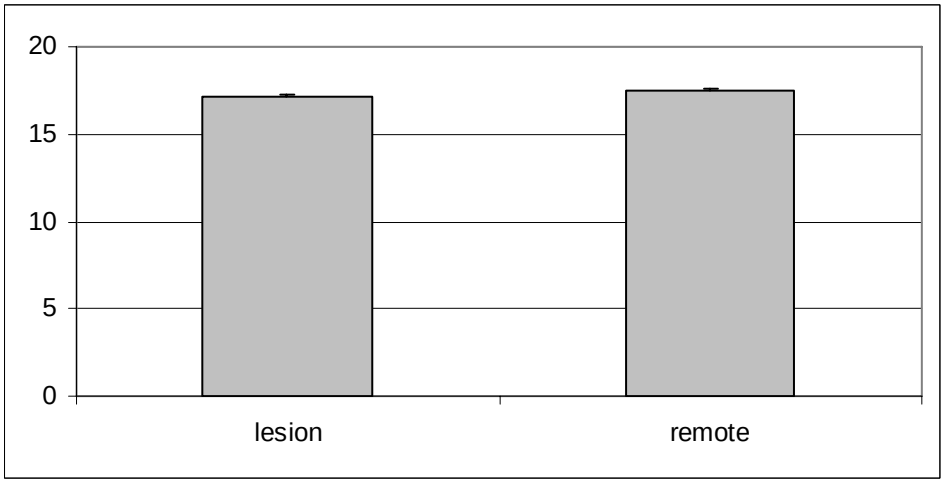

Figure A2.4. Actin expression in discreet powdery mildew infected regions and non-infected areas of the same leaves. The standard deviation of the CTs compared was 0.213.

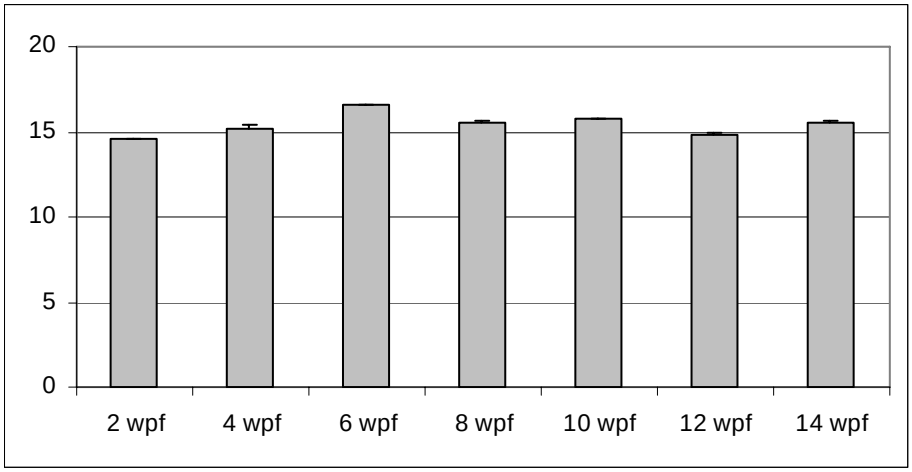

Figure A2.5. Ubiquitin expression in ripening Cabernet Sauvignon berry pulp cells. The standard deviation of the CTs compared was 0.647.

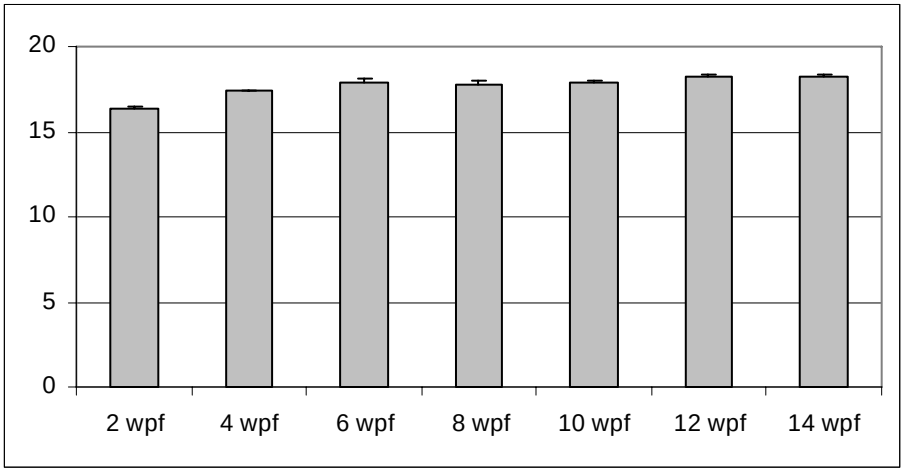

Figure A2.6. Ubiquitin expression in ripening Shiraz berry pulp cells. The standard deviation of the CTs compared was 0.652.

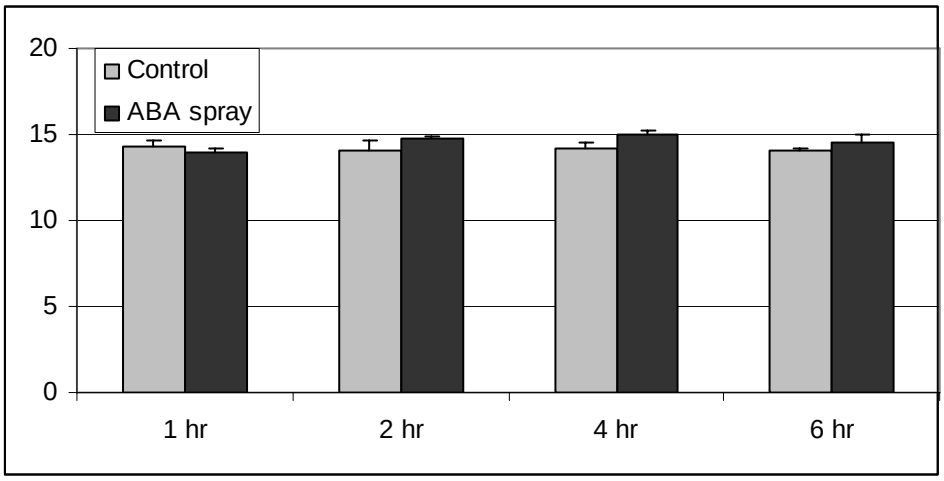

Figure A2.7. Actin expression control and ABA-sparyed leaves. The standard deviation of the CTs compared was 0.471.

Appendix 3 page numbers do not follow-on correctly in this digital copy and they do not correspond with the print copies.

Appendix 3- List of cDNAs on grape berry microarray

List of cDNAs on microarray screened in Section 3.3.1.

Block	Row	Column	ID	Name	Description
4	1	13	1	p1a1	UBIQUITIN-CONJUGATING ENZYME E2-21 KDA (UBIQUITIN-PROTE
5	15	4	2	p1a2	zinc-finger protein Lsd1 - Arabidopsis thaliana >gi|1872521|gb|AAC4966
4	1	12	3	p1a3	SULFITE REDUCTASE (FERREDOXIN) >gi|7432743|pir||S74718 sulfite
5	15	5	4	p1a4	(AE003464) CG13579 gene product [Drosophila melanogaster]
4	1	11	5	p1a5	(AC011020) unknown protein [Arabidopsis thaliana]
5	15	6	6	p1a6	hypothetical protein T18B16.130 - Arabidopsis thaliana >gi|2828291|eml
4	1	10	7	p1a9	hypothetical protein T18B16.130 - Arabidopsis thaliana >gi|2828291|eml
5	15	7	8	p1a10	(AB026646) gb|AAF26109.1~gene_id:MIG5.8~similar to unknown protei
4	1	9	9	p1a11	mipC protein - common ice plant >gi|1657948|gb|AAB18227.1| (U73466
5	15	8	10	p1a12	(AC026234) Contains similarity to a prolyl 4-hydroxylase alpha subunit p
4	1	8	11	p1b2	(AC007071) unknown protein [Arabidopsis thaliana]
5	15	9	12	p1b3	(AF121355) peroxiredoxin TPx1 [Arabidopsis thaliana] >gi|6227022|gb|A
8	1	13	13	p1b4	(AF156776) lysophosphatidic acid acyltransferase-delta [Homo sapiens]
1	15	4	14	p1b5	adenylate translocator brittle-1 homolog F8B4.100 - Arabidopsis thaliana
8	1	12	15	p1b7	(AL161946) light-inducible protein ATLS1 [Arabidopsis thaliana]
1	15	5	16	p1b8	(AL022198) putative protein kinase [Arabidopsis thaliana] >gi|7269998|e
8	1	11	17	p1b10	(AB026646) gb|AAF26109.1~gene_id:MIG5.8~similar to unknown protei
1	15	6	18	p1b11	mipC protein - common ice plant >gi|1657948|gb|AAB18227.1| (U73466
8	1	10	19	p1b12	(AL161491) hypothetical protein [Arabidopsis thaliana]
1	15	7	20	p1c1	(AF250236) 2C-methyl-D-erythritol 2,4-cyclodiphosphate synthase [Cath
8	1	9	21	p1c2	(AC011661) T23J18.15 [Arabidopsis thaliana]
1	15	8	22	p1c3	
8	1	8	23	p1c4	40S RIBOSOMAL PROTEIN S15 >gi|7440527|pir||T03388 probable ribo
1	15	9	24	p1c5	hypothetical protein APE2320 - Aeropyrum pernix (strain K1) >gi|510602
3	1	13	25	p1c6	(AC006577) F15I1.20 [Arabidopsis thaliana]
6	15	4	26	p1c7	
3	1	12	27	p1c8	probable cinnamyl-alcohol dehydrogenase (EC 1.1.1.195) CPRD14 - co
6	15	5	28	p1c9	(AC016041) F27J15.9 [Arabidopsis thaliana]
3	1	11	29	p1c10	HISTONE DEACETYLASE (HD) >gi|2318131|gb|AAB66486.1| (AF0148.
6	15	6	30	p1c11	(AF108896) GTP-binding protein [Capsicum annuum]
3	1	10	31	p1d1	(AB025624) contains similarity to putative receptor-like protein kinase~g
6	15	7	32	p1d2	(AC010657) T5E21.8 [Arabidopsis thaliana]
3	1	9	33	p1d3	(Z70524) PDR5-like ABC transporter [Spirodela polyrrhiza]
6	15	8	34	p1d4	(AB027455) anthocyanin 5-O-glucosyltransferase [Petunia x hybrida]
3	1	8	35	p1d5	(AL138651) ADP-ribosylation factor-like protein [Arabidopsis thaliana]
6	15	9	36	p1d6	(AF221856) heat-shock protein 80 [Euphorbia esula]
7	1	13	37	p1d7	VACUOLAR PROCESSING ENZYME PRECURSOR (VPE) >gi|107656.
2	15	4	38	p1d8	(AC009325) unknown protein [Arabidopsis thaliana]
7	1	12	39	p1d12	
2	15	5	40	p1e1	POLYPHENOL OXIDASE PRECURSOR (PPO) (CATECHOL OXIDASE
7	1	11	41	p1e2	(AC011663) unknown protein [Arabidopsis thaliana]
2	15	6	42	p1e3	hypothetical protein F28P10.20 - Arabidopsis thaliana >gi|4678293|emb|
7	1	10	43	p1e4	pathogenesis-related protein F20M13.220 - Arabidopsis thaliana >gi|446
2	15	7	44	p1e5	LEUCYL-TRNA SYNTHETASE (LEUCINE--TRNA LIGASE) (LEURS) >g
7	1	9	45	p1e6	(AF171676) envelope glycoprotein [Porcine reproductive and respiratory
2	15	8	46	p1e7	Zinc finger protein 68 >gi|4514561|dbj|BAA75468.1| (AB024005) KRAB-
7	1	8	47	p1e8	(AF029980) A37 [Arabidopsis thaliana] >gi|4103954|gb|AAD01898.1| (A
2	15	9	48	p1e9	PHOTOSYSTEM I REACTION CENTRE SUBUNIT II PRECURSOR (PH
2	1	13	49	p1e11	hypothetical protein F17A8.20 - Arabidopsis thaliana >gi|4538897|emb|C
7	15	4	50	p1e12	(AC009526) Putative histidine decarboxylase [Arabidopsis thaliana]
2	1	12	51	p1f1	
7	15	5	52	p1f2	(AF085279) hypothetical EIF-2-Alpha [Arabidopsis thaliana]
2	1	11	53	p1f3	ribosomal protein L32, cytosolic - Arabidopsis thaliana >gi|5816996|emb
7	15	6	54	p1f4	(AC004450) 3-isopropylmalate dehydratase, small subunit [Arabidopsis
2	1	10	55	p1f5	CYTOCHROME P450 85 (DWARF PROTEIN) >gi|7430727|pir||T07859
7	15	7	56	p1f6	lipopolysaccharide biosynthesis-related protein homolog - Lyme disease
2	1	9	57	p1f7	
7	15	8	58	p1f8	(AB022223) kinase-like protein [Arabidopsis thaliana]
2	1	8	59	p1f9	(AF054584) gastric mucin [Sus scrofa domestica]
7	15	9	60	p1f10	(AC005496) unknown protein [Arabidopsis thaliana]
6	1	13	61	p1f11	(AF180143) ubiquitin carrier protein 4 [Glycine max]

Block	Row	Column	ID	Name	Description
3	15	4	62	p1g1	(L76926) putative zinc finger protein [Arabidopsis thaliana]
6	1	12	63	p1g2	(AL132965) 60S RIBOSOMAL PROTEIN-like [Arabidopsis thaliana]
3	15	5	64	p1g3	(AC009918) unknown protein [Arabidopsis thaliana] >gi|9502172|gb|AAF
6	1	11	65	p1g4	hypothetical protein F17A8.160 - Arabidopsis thaliana >gi|4538911|emb|
3	15	6	66	p1g5	(AF002109) putative nematode-resistance protein [Arabidopsis thaliana]
6	1	10	67	p1g6	(AL137898) putative protein [Arabidopsis thaliana]
3	15	7	68	p1g7	(AL138652) putative protein [Arabidopsis thaliana]
6	1	9	69	p1g9	hypothetical protein F19B15.190 - Arabidopsis thaliana >gi|4972062|eml
3	15	8	70	p1g11	(AC024208) Hypothetical protein Y75B7B.1 [Caenorhabditis elegans]
6	1	8	71	p1g12	
3	15	9	72	p1h1	(AL163002) laccase precursor-like [Arabidopsis thaliana]
1	1	13	73	p1h2	(AC002343) unknown protein [Arabidopsis thaliana]
8	15	4	74	p1h3	
1	1	12	75	p1h5	(U07597) delta-9 stearoyl-acyl carrier protein desaturase precursor [Thu
8	15	5	76	p1h6	(AJ249331) heat shock protein 70 [Cucumis sativus]
1	1	11	77	p1h7	(AF206324) putative DNA binding protein [Arabidopsis thaliana] >gi|776
8	15	6	78	p1h8	(AF109215) TibA [Escherichia coli]
1	1	10	79	p1h9	(AF139499) unknown [Prunus armeniaca]
8	15	7	80	p1h12	(AC010796) putative alanine aminotransferase [Arabidopsis thaliana] >g
1	1	9	81	p3a1	(AF233883) AALP protein [Arabidopsis thaliana]
8	15	8	82	p3a2	(AF164610) Gag protein [Homo sapiens]
1	1	8	83	p3a3	(AF007784) LTCOR11 [Lavatera thuringiaca]
8	15	9	84	p3a4	(AC007017) unknown protein [Arabidopsis thaliana]
5	1	13	85	p3a6	(AC005169) putative CCCH-type zinc finger protein [Arabidopsis thalian
4	15	4	86	p3a7	(AL132763) hypothetical protein L4768.05 [Leishmania major]
5	1	12	87	p3a9	(AF161180) high molecular weight heat shock protein [Malus x domestic
4	15	5	88	p3a10	(AJ237985) putative ripening-related protein [Vitis vinifera]
5	1	11	89	p3a11	26S proteasome regulatory subunit S5A - common ice plant >gi|320204
4	15	6	90	p3b1	60S RIBOSOMAL PROTEIN L23A (L25) >gi|1084424|pir||S48026 ribosc
5	1	10	91	p3b2	(Y14071) HMG protein [Arabidopsis thaliana] >gi|3068715|gb|AAC1441
4	15	7	92	p3b3	(AC006550) Similar to gb|U70015 lysosomal trafficking regulator from M
5	1	9	93	p3b4	(U12823) hemolysin [Acanthamoeba polyphaga]
4	15	8	94	p3b5	
5	1	8	95	p3b8	(AC012328) unknown protein [Arabidopsis thaliana]
4	15	9	96	p3b9	(AL163818) cytokinin oxidase-like protein [Arabidopsis thaliana]
4	1	7	97	p3b10	ZEAXANTHIN EPOXIDASE PRECURSOR >gi|7489081|pir||T07754 zea
5	15	10	98	p3b12	(AC006234) unknown protein [Arabidopsis thaliana]
4	1	6	99	p3c1	hypothetical protein MJ1282 - Methanococcus jannaschii >gi|1591919|gl
5	15	11	100	p3c2	CHAPERONIN CPN60-2, MITOCHONDRIAL PRECURSOR (HSP60-2)
4	1	5	101	p3c4	(AJ000691) heat shock protein 17.4 [Quercus suber]
5	15	12	102	p3c6	PHOTOSYSTEM II 22 KD PROTEIN PRECURSOR >gi|282837|pir||S26
13	15	13	103	p3c7	hypothetical protein ZK488.9 - Caenorhabditis elegans >gi|2384936|gb|A
5	15	13	104	p3c8	G-box-binding protein TAF-2 - common tobacco >gi|728626|emb|CAA8
4	1	3	105	p3c9	(AF188998) S-adenosylmethionine decarboxylase [Ipomoea batatas]
5	14	1	106	p3c10	hypothetical protein F20M13.250 - Arabidopsis thaliana >gi|4467156|em
4	1	2	107	p3c11	(AC025416) F5O11.29 [Arabidopsis thaliana]
5	14	2	108	p3c12	(AC016972) putative ribose 5-phosphate isomerase [Arabidopsis thalian
8	1	7	109	p3d2	(AF259801) eIF4E [Lycopersicon esculentum]
1	15	10	110	p3d3	EUKARYOTIC INITIATION FACTOR 4A (EIF-4A) >gi|542153|pir||S3835
8	1	6	111	p3d4	(Y09314) Rab2-like protein [Arabidopsis thaliana] >gi|5281023|emb|CAE
1	15	11	112	p3d5	hypothetical protein F17K2.16 - Arabidopsis thaliana >gi|2979553|gb|AA
8	1	5	113	p3d6	(AB023038) cytochrome P450 [Arabidopsis thaliana]
1	15	12	114	p3d7	REV3 (yeast homolog)-like, catalytic subunit of DNA polymerase zeta >g
8	1	4	115	p3d8	(AE003549) CG6590 gene product [Drosophila melanogaster]
1	15	13	116	p3d9	cytokinin-induced proline rich protein - southern Asian dodder >gi|43732
8	1	3	117	p3d10	hypothetical protein F59E12.9 - Caenorhabditis elegans >gi|2088843|gb
1	14	1	118	p3d11	CTP synthetase homolog >gi|1654186|gb|AAB17729.1| (U49385) CTP s
8	1	2	119	p3d12	(AJ277744) protein phosphatase 2C (PP2C) [Fagus sylvatica]
1	14	2	120	p3e4	(AJ276420) 68 kDa protein [Cicer arietinum]
3	1	7	121	p3e5	(AE003635) CG6618 gene product [Drosophila melanogaster]
6	15	10	122	p3e6	(U39531) bindin [Echinometra mathaei]
3	1	6	123	p3e8	
6	15	11	124	p3e9	(AC004667) unknown protein [Arabidopsis thaliana]
3	1	5	125	p3e10	hypothetical protein T09D3.3 - Caenorhabditis elegans >gi|1458250|gb|A
6	15	12	126	p3e11	(AF230372) fatty acid hydroperoxide lyase [Lycopersicon esculentum]
3	1	4	127	p3e12	60S RIBOSOMAL PROTEIN L9 (GIBBERELLIN-REGULATED PROTEI
6	15	13	128	p3f1	(AJ242970) BTF3b-like factor [Arabidopsis thaliana]

Block	Row	Column	ID	Name	Description
3	1	3	129	p3f2	(AF093631) Rieske Fe-S precursor protein [Oryza sativa]
6	14	1	130	p3f3	60S ACIDIC RIBOSOMAL PROTEIN P2 >gi|551267|emb|CAA55047.1|
3	1	2	131	p3f4	
6	14	2	132	p3f5	(AF136539) YABBY2 [Arabidopsis thaliana]
7	1	7	133	p3f6	hypothetical protein T29H11.70 - Arabidopsis thaliana >gi|4678347|emb
2	15	10	134	p3f7	hypothetical protein R1 - potato >gi|3287270|emb|CAA70725.1| (Y0953
7	1	6	135	p3f8	(AC009853) hypothetical protein [Arabidopsis thaliana]
2	15	11	136	p3f11	(AL161574) putative protein [Arabidopsis thaliana]
7	1	5	137	p3f12	(AP001297) nucleotide sugar epimerase-like protein [Arabidopsis thaliar
2	15	12	138	p3g1	(D84069) anti-HLA-DR antibody heavy chain (IgG2a) [Mus musculus]
7	1	4	139	p3g2	(AP001307) disease resistance response protein-like [Arabidopsis thalia
2	15	13	140	p3g3	(AF007215) stress-induced cysteine proteinase [Lavatera thuringiaca]
7	1	3	141	p3g4	(AB020754) contains similarity to nuclear movement protein nudC~gene
2	14	1	142	p3g5	(AC009400) hypothetical protein [Arabidopsis thaliana]
7	1	2	143	p3g6	(AC018907) putative RING zinc finger protein [Arabidopsis thaliana]
2	14	2	144	p3g7	TUBULIN BETA-1 CHAIN (BETA-1 TUBULIN) >gi|1490665|gb|AAB643(
2	1	7	145	p3g10	hypothetical protein - Arabidopsis thaliana >gi|2245005|emb|CAB10425.
7	15	10	146	p3g11	HYPOTHETICAL 35.0 KDA PROTEIN STKORF319 >gi|1732028|gb|AA
2	1	6	147	p3g12	proline-rich protein precursor - upland cotton >gi|2829206|gb|AAC00500
7	15	11	148	p3h1	hypothetical protein c0113 - Sulfolobus solfataricus >gi|1707743|emb|C/
2	1	5	149	p3h3	(AC009999) Contains similarity to a basic endochitinase from Arabidopi
7	15	12	150	p3h4	
2	1	4	151	p3h5	(AJ250667) copper/zinc-superoxide dismutase [Ananas comosus]
7	15	13	152	p3h6	(AB012640) light harvesting chlorophyll a/b-binding protein [Nicotiana sy
2	1	3	153	p3h7	(AC008153) putative UDP-glucuronosyltransferase, 5' partial [Arabidops
7	14	1	154	p3h8	(Y13178) multicatalytic endopeptidase [Arabidopsis thaliana]
2	1	2	155	p3h9	(AL132975) methionyl-tRNA synthetase (AtcpMetRS) [Arabidopsis thalia
7	14	2	156	p3h10	(AC068197) F16A14.23 [Arabidopsis thaliana]
6	1	7	157	p3h11	(AC002304) F14J16.9 [Arabidopsis thaliana]
3	15	10	158	p3h12	
6	1	6	159	p4a1	(AB024032) gene_id:K9P8.4~pir||T04010~strong similarity to unknown p
3	15	11	160	p4a2	glycine-rich RNA-binding protein - garden pea >gi|1778374|gb|AAB7141
6	1	5	161	p4a4	hypothetical protein SPCC569.06 - fission yeast (Schizosaccharomyces
3	15	12	162	p4a5	(AB016888) arm repeat containing protein [Arabidopsis thaliana]
6	1	4	163	p4a6	(AC001645) Myb-related transcription activator (MybSt1) isolog [Arabido
3	15	13	164	p4a7	(AC006550) Belongs to the PF|01027 Uncharacterized protein family UF
6	1	3	165	p4a8	(AF162150) COP1-interacting protein CIP8 [Arabidopsis thaliana] >gi|88
3	14	1	166	p4a9	hypothetical protein - Arabidopsis thaliana >gi|2244965|emb|CAB10386.
6	1	2	167	p4a11	hypothetical protein F23E12.120 - Arabidopsis thaliana >gi|3080418|eml
3	14	2	168	p4b2	(AL161503) UV-damaged DNA binding factor-like protein [Arabidopsis th
1	1	7	169	p4b3	(AF213695) FH protein NFH1 [Nicotiana tabacum]
8	15	10	170	p4b4	protein kinase homolog T14N5.13 - Arabidopsis thaliana >gi|3540207|gb
1	1	6	171	p4b5	(AB023043) contains similarity to NRK-related kinase~gene_id:MWC10.
8	15	11	172	p4b7	(AB009050) gene_id:MDF20.5~unknown protein [Arabidopsis thaliana]
1	1	5	173	p4b9	(U15933) ascorbate peroxidase [Nicotiana tabacum]
8	15	12	174	p4b11	(AL365234) putative protein [Arabidopsis thaliana]
1	1	4	175	p4b12	60S RIBOSOMAL PROTEIN L5 >gi|1881380|dbj|BAA19415.1| (AB0015
8	15	13	176	p4c1	hypothetical protein SENU1, senescence up-regulated - tomato (fragme
1	1	3	177	p4c2	hypothetical protein F12L6.11 - Arabidopsis thaliana >gi|3355474|gb|AA
8	14	1	178	p4c3	(AC025416) F5O11.4 [Arabidopsis thaliana]
1	1	2	179	p4c4	(AJ130885) xyloglucan endotransglycosylase 1 [Fagus sylvatica]
8	14	2	180	p4c5	(AL132970) putative protein [Arabidopsis thaliana]
5	1	7	181	p4c7	(AL132971) RING finger-like protein [Arabidopsis thaliana]
4	15	10	182	p4c9	(AF262934) ubiquitin conjugating protein [Avicennia marina]
5	1	6	183	p4c10	(AC002329) unknown protein [Arabidopsis thaliana]
4	15	11	184	p4c11	(X61287) Type I (26 kD) CP29 polypeptide [Lycopersicon esculentum]
5	1	5	185	p4c12	(X94995) naringenin-chalcone synthase [Juglans nigra x Juglans regia]
4	15	12	186	p4d1	(AB019228) serine/threonine protein kinase [Arabidopsis thaliana]
5	1	4	187	p4d2	(AC007519) F16N3.2 [Arabidopsis thaliana]
4	15	13	188	p4d3	(Z97187) swiss cheese protein [Drosophila melanogaster]
5	1	3	189	p4d4	transmembrane protein (63kD), endoplasmic reticulum/Golgi intermedia
4	14	1	190	p4d5	non-functional folate binding protein >gi|2565196|gb|AAB81938.1| (AF0(
5	1	2	191	p4d7	(AC007583) F24B9.20 [Arabidopsis thaliana]
4	14	2	192	p4d9	(AB023036) contains similarity to endo-1,3-1,4-beta-D-glucanase~gene_
4	1	1	193	p4d10	proton pump interactor - Arabidopsis thaliana >gi|4972075|emb|CAB438
5	14	3	194	p4d11	(U89702) DNA polymerase alpha [Pleurotricha lanceolata]
4	2	13	195	p4e1	(AC006300) unknown protein [Arabidopsis thaliana]

Block	Row	Column	ID	Name	Description
5	14	4	196	p4e2	(AB008848) Csf-3 [Cucumis sativus]
4	2	12	197	p4e3	chalcone isomerase (EC 5.5.1.6) - apple tree (fragment) >gi|19587|emb|
5	14	5	198	p4e4	hypothetical protein T5L19.200 - Arabidopsis thaliana >gi|4539010|emb|
4	2	11	199	p4e5	(Z99707) putative protein [Arabidopsis thaliana] >gi|7270657|emb|CAB8
5	14	6	200	p4e6	(AB010700) MAP protein kinase [Arabidopsis thaliana]
4	2	10	201	p4e8	hypothetical protein F17I5.110 - Arabidopsis thaliana >gi|3297816|emb|(
5	14	7	202	p4e9	18.2 KD CLASS I HEAT SHOCK PROTEIN >gi|99979|pir||S16247 heat :
4	2	9	203	p4e10	(AC008148) Unknown protein [Arabidopsis thaliana]
5	14	8	204	p4e11	(AC006418) hypothetical protein [Arabidopsis thaliana]
8	1	1	205	p4e12	(AP002030) gene_id:K16F4.10~pir||T00468~similar to unknown protein
1	14	3	206	p4f1	(AC000103) F21J9.12 [Arabidopsis thaliana]
8	2	13	207	p4f2	THAUMATIN-LIKE PROTEIN PRECURSOR >gi|2129751|pir||S71175 th
1	14	4	208	p4f3	(AC007504) Putative BURP domain containing protein [Arabidopsis thali
8	2	12	209	p4f4	(AF261139) dehydration-induced protein ERD15 [Lycopersicon esculent
1	14	5	210	p4f6	
8	2	11	211	p4f9	(U64905) ATFP2 [Arabidopsis thaliana]
1	14	6	212	p4f10	AMINOMETHYLTRANSFERASE PRECURSOR (GLYCINE CLEAVAGE
8	2	10	213	p4f11	(AB033601) polyubiquitin [Cucumis melo]
1	14	7	214	p4f12	NONSPECIFIC LIPID-TRANSFER PROTEIN PRECURSOR (LTP) (NSL
8	2	9	215	p4g1	(AL133314) arm repeat containing protein homolog [Arabidopsis thaliana
1	14	8	216	p4g3	(AC019018) putative lipase [Arabidopsis thaliana]
3	1	1	217	p4g5	(AC003105) putative receptor-like protein kinase [Arabidopsis thaliana]
6	14	3	218	p4g6	(AC010795) putative RING zinc finger protein [Arabidopsis thaliana]
3	2	13	219	p4g8	hypothetical protein 3 - potato transposon Tst1 >gi|21433|emb|CAA3661
6	14	4	220	p4g9	
3	2	12	221	p4g10	(AB022220) contains similarity to diaminopimelate decarboxylase~gene
6	14	5	222	p4g11	(AC000132) F21M12.20 gene product [Arabidopsis thaliana]
3	2	11	223	p4h1	(AF007784) LTCOR11 [Lavatera thuringiaca]
6	14	6	224	p4h2	(AJ006764) putative deoxycytidylate deaminase [Cicer arietinum]
3	2	10	225	p4h3	(AB006698) ornithine aminotransferase [Arabidopsis thaliana]
6	14	7	226	p4h4	(AJ000762) MADS-box protein [Malus domestica]
3	2	9	227	p4h5	SERINE HYDROXYMETHYLTRANSFERASE, MITOCHONDRIAL PRE(
6	14	8	228	p4h6	(AL162973) protein kinase-like [Arabidopsis thaliana]
7	1	1	229	p4h8	(AE003996) sugar-phosphate dehydrogenase [Xylella fastidiosa]
2	14	3	230	p4h9	(AF182039) ammonium transporter [Arabidopsis thaliana]
7	2	13	231	p4h11	
2	14	4	232	p4h12	(AC004667) hypothetical protein [Arabidopsis thaliana]
7	2	12	233	p5a1	(AB042856) 60S ribosomal protein L27a [Panax ginseng]
2	14	5	234	p5a2	PHOSPHOLIPASE D PRECURSOR (PLD) (CHOLINE PHOSPHATASE
7	2	11	235	p5a3	hypothetical protein - Arabidopsis thaliana >gi|2244882|emb|CAB10303.
2	14	6	236	p5a4	hypothetical protein T5L19.200 - Arabidopsis thaliana >gi|4539010|emb|
7	2	10	237	p5a5	(AF239701) sterol delta7 reductase [Arabidopsis thaliana] >gi|9454565|g
2	14	7	238	p5a7	(AC012562) hypothetical protein [Arabidopsis thaliana]
7	2	9	239	p5a8	(AF031487) bZIP transcription factor [Nicotiana tabacum]
2	14	8	240	p5a9	probable cinnamyl-alcohol dehydrogenase (EC 1.1.1.195) - apple tree >g
2	1	1	241	p5a10	IgE-dependent histamine-releasing factor homolog - alfalfa (fragment) >g
7	14	3	242	p5a11	(AL109787) putative protein [Arabidopsis thaliana] >gi|7269979|emb|CA
2	2	13	243	p5a12	TRIOSEPHOSPHATE ISOMERASE, CHLOROPLAST PRECURSOR (T
7	14	4	244	p5b1	(AB016893) gene_id:MYH9.3~pir||S75332~similar to unknown protein [A
2	2	12	245	p5b3	H+-transporting ATPase (EC 3.6.1.35) chain E, vacuolar - Arabidopsis th
7	14	5	246	p5b4	(U66264) ubiquitin [Nicotiana tabacum]
2	2	11	247	p5b5	(AL138652) protein kinase-like protein [Arabidopsis thaliana]
7	14	6	248	p5b6	(AP001299) gene_id:F4B12.1~unknown protein [Arabidopsis thaliana]
2	2	10	249	p5b7	(AF021810) putative sucrose transporter [Vitis vinifera]
7	14	7	250	p5b9	(D63137) Beta-tubulin [Zinnia elegans]
2	2	9	251	p5b10	(AL163527) putative protein [Arabidopsis thaliana]
7	14	8	252	p5b11	(AC006569) putative NADH-ubiquinone oxireductase [Arabidopsis thalia
6	1	1	253	p5b12	probable ubiquitin - kidney bean >gi|1684855|gb|AAB36545.1| (U77939)
3	14	3	254	p5c1	(AC006917) F10B6.34 [Arabidopsis thaliana]
6	2	13	255	p5c3	(AC012188) Contains similarity to a Receptor-like Protein Kinase 5 Prec
3	14	4	256	p5c4	
6	2	12	257	p5c5	(AF068722) MADS-box protein MADS3 [Nicotiana sylvestris]
3	14	5	258	p5c6	(U93872) ORF 06, major ssDNA binding protein homolog [Kaposi's sarc
6	2	11	259	p5c7	
3	14	6	260	p5c8	NADH-UBIQUINONE OXIDOREDUCTASE CHAIN 5 >gi|1078745|pir||S!
6	2	10	261	p5c9	(AL162691) transporter-like protein [Arabidopsis thaliana]
3	14	7	262	p5c10	probable Rieske iron-sulfur protein L73G19.30 - Arabidopsis thaliana >g

Block	Row	Column	ID	Name	Description
6	2	9	263	p5d1	(AL163812) putative protein [Arabidopsis thaliana]
3	14	8	264	p5d2	eukaryotic release factor 3 homolog - castor bean (fragment) >gi|107972
1	1	1	265	p5d3	small heat-shock protein class I, 18.6K - common sunflower >gi|123589
8	14	3	266	p5d4	(AF223358) triose phosphate/phosphate translocator precursor [Mesem
1	2	13	267	p5d5	chlorophyll a/b-binding protein - garden pea >gi|20671|emb|CAA49149.1
8	14	4	268	p5d6	(AB006698) gene_id:MCL19.23~pir||T04534~strong similarity to unknow
1	2	12	269	p5d7	(U25628) stigma-specific arabinogalactan-protein precursor [Nicotiana a
8	14	5	270	p5d8	homeotic protein - common sunflower >gi|349379|gb|AAA63765.1| (L22
1	2	11	271	p5d9	cryptogene protein G4 - Leishmania tarentolae (strain LEM125)
8	14	6	272	p5d10	(U81805) GDP-D-mannose-4,6-dehydratase [Arabidopsis thaliana]
1	2	10	273	p5d12	hypothetical protein T20B5.2 - Arabidopsis thaliana >gi|2623296|gb|AAE
8	14	7	274	p5e1	ribonucleoprotein homolog F21B7.26 - Arabidopsis thaliana
1	2	9	275	p5e2	
8	14	8	276	p5e3	(AC023673) F21D18.18 [Arabidopsis thaliana]
5	1	1	277	p5e4	
4	14	3	278	p5e6	hypothetical protein slr2121 - Synechocystis sp. (strain PCC 6803) >gi|1
5	2	13	279	p5e8	(AC011001) putative signal peptidase [Arabidopsis thaliana]
4	14	4	280	p5e9	(AB004067) KN-BJ2 [Bothrops jararaca]
5	2	12	281	p5e10	ct565 hypothetical protein - Chlamydia pneumoniae (strain CWL029) >g
4	14	5	282	p5e11	ELONGATION FACTOR G, CHLOROPLAST PRECURSOR (EF-G)
5	2	11	283	p5e12	(AB022217) 60S ribosome protein L19-like [Arabidopsis thaliana]
4	14	6	284	p5f1	cytochrome P450 homolog F23K16.110 - Arabidopsis thaliana >gi|5042
5	2	10	285	p5f2	proline-rich protein BstNI subfamily 4 >gi|131005|sp|P10163|PRP4_HUM
4	14	7	286	p5f6	
5	2	9	287	p5f7	TU12B1-TY protein >gi|7384771|dbj|BAA93053.1| (AB032773) TU12B1-
4	14	8	288	p5f8	CALNEXIN HOMOLOG PRECURSOR >gi|7441504|pir||T06415 calnexir
4	2	8	289	p5f9	HYPOTHETICAL PROTEIN HI1671 >gi|1074892|pir||I64039 hypothetica
5	14	9	290	p5f10	(AC011437) hypothetical protein [Arabidopsis thaliana]
4	2	7	291	p5f11	(AC002339) hypothetical protein [Arabidopsis thaliana]
5	14	10	292	p5g1	(AF271660) putative aquaporin TIP3 [Vitis berlandieri x Vitis rupestris]
4	2	6	293	p5g2	(AF123508) Nt-iaa28 deduced protein [Nicotiana tabacum]
5	14	11	294	p5g3	H+-transporting ATPase (EC 3.6.1.35) T17F15.180 - Arabidopsis thaliar
4	2	5	295	p5g4	hypothetical protein F9D16.290 - Arabidopsis thaliana >gi|4454051|emb
5	14	12	296	p5g5	(AC023912) hypothetical protein [Arabidopsis thaliana]
4	2	4	297	p5g6	(AB024031) protein kinase ATN1-like protein [Arabidopsis thaliana]
5	14	13	298	p5g7	(U93872) ORF 73, contains large complex repeat CR 73 [Kaposi's sarcc
4	2	3	299	p5g8	hypothetical protein A_IG002N01.18 - Arabidopsis thaliana >gi|2191138
5	13	1	300	p5g9	(AF190474) bdn1 [Boea crassifolia]
8	2	8	301	p5g10	
1	14	9	302	p5g11	hypothetical protein F27B13.90 - Arabidopsis thaliana >gi|4914409|emb|
8	2	7	303	p5g12	(AC009853) unknown protein [Arabidopsis thaliana]
1	14	10	304	p5h1	RIBULOSE BISPHOSPHATE CARBOXYLASE/OXYGENASE ACTIVAS
8	2	6	305	p5h3	78 KD GLUCOSE-REGULATED PROTEIN HOMOLOG PRECURSOR (
1	14	11	306	p5h4	(AP001389) ESTs AU077873(S1878),D40121(S1878) correspond to a r
8	2	5	307	p5h5	
1	14	12	308	p5h6	METABOTROPIC GLUTAMATE RECEPTOR 1 >gi|1850987|gb|AAB48(
8	2	4	309	p5h7	non-functional folate binding protein >gi|2565196|gb|AAB81938.1| (AF0(
1	14	13	310	p5h8	
8	2	3	311	p5h9	(AC013483) unknown protein [Arabidopsis thaliana]
1	13	1	312	p5h10	hypothetical protein - Arabidopsis thaliana >gi|2244908|emb|CAB10329.
3	2	8	313	p6a1	(AB015477) 40S ribosomal protein S3 [Arabidopsis thaliana]
6	14	9	314	p6a2	GLUTAMINE SYNTHETASE CYTOSOLIC ISOZYME 2 (GLUTAMATE--
3	2	7	315	p6a3	ketol-acid reductoisomerase (EC 1.1.1.86) - Arabidopsis thaliana >gi|40
6	14	10	316	p6a6	(AF145647) BcDNA.GH08312 [Drosophila melanogaster] >gi|7301992|g
3	2	6	317	p6a7	(AC021640) unknown protein [Arabidopsis thaliana]
6	14	11	318	p6a8	(AC007767) Strong similarity to heat shock factor protein HSF from Lyc
3	2	5	319	p6a9	PROTEASOME COMPONENT C8 (MACROPAIN SUBUNIT C8) (MULT
6	14	12	320	p6a10	von Hippel-Lindau binding protein 1; VHL binding protein-1 >gi|3212112|
3	2	4	321	p6a11	hypothetical protein C25G6.1 - Caenorhabditis elegans >gi|1086717|gb|
6	14	13	322	p6a12	HISTIDINE-RICH, METAL BINDING POLYPEPTIDE >gi|7465222|pir||C
3	2	3	323	p6b2	(AL353994) putative protein [Arabidopsis thaliana]
6	13	1	324	p6b4	hypothetical protein F10M23.190 - Arabidopsis thaliana >gi|4455208|em
7	2	8	325	p6b5	
2	14	9	326	p6b6	(AC009322) Hypothetical protein [Arabidopsis thaliana] >gi|6453851|gb|
7	2	7	327	p6b7	(AL162971) 60S ribosomal protein-like [Arabidopsis thaliana]
2	14	10	328	p6b9	VACUOLAR ATP SYNTHASE SUBUNIT B ISOFORM 2 (V-ATPASE B
7	2	6	329	p6b10	

Block	Row	Column	ID	Name	Description
2	14	11	330	p6b12	(AF053302) putative transcriptional co-activator [Arabidopsis thaliana]
7	2	5	331	p6c1	(AL137701) hypothetical protein [Homo sapiens]
2	14	12	332	p6c2	(AC005990) Contains repeated region with similarity to gb|U43627 exter
7	2	4	333	p6c3	(D26086) zinc-finger protein [Petunia x hybrida]
2	14	13	334	p6c5	hypothetical protein M01E5.5b - Caenorhabditis elegans >gi|3878631|en
7	2	3	335	p6c7	TUBULIN BETA-6 CHAIN >gi|320187|pir||JQ1590 tubulin beta-6 chain -
2	13	1	336	p6c8	proline-rich protein F26K10.180 - Arabidopsis thaliana >gi|7269684|emb
2	2	8	337	p6c9	
7	14	9	338	p6c10	1-AMINOCYCLOPROPANE-1-CARBOXYLATE OXIDASE (ACC OXIDA
2	2	7	339	p6c11	(AC008148) Unknown protein [Arabidopsis thaliana]
7	14	10	340	p6c12	(AC009177) unknown protein [Arabidopsis thaliana]
2	2	6	341	p6d1	
7	14	11	342	p6d2	SODIUM/CALCIUM EXCHANGER 3 PRECURSOR (NA+/CA2+-EXCHA
2	2	5	343	p6d3	(AC006551) Similar to LeOPT1 [Lycopersicon esculentum] [Arabidopsis
7	14	12	344	p6d4	vacuolar invertase 2, GIN2 [Vitis vinifera=grape berries, Sultana, berries
2	2	4	345	p6d5	(AC009243) F28K19.27 [Arabidopsis thaliana]beta-1,4-xylosidase
7	14	13	346	p6d6	(AC006284) unknown protein [Arabidopsis thaliana]
2	2	3	347	p6d7	(U32474) putative heat shock protein [Treponema phagedenis]
7	13	1	348	p6d8	(AB024035) gb|AAD55473.1~gene_id:MHM17.18~similar to unknown pr
6	2	8	349	p6d9	transforming protein (clone 210) - human >gi|2135854|pir||S57875 oncoc
3	14	9	350	p6e1	subtilisin-like proteinase (EC 3.4.21.-) 1 - tomato >gi|1771160|emb|CAA
6	2	7	351	p6e2	(AF138264) papain-like cysteine proteinase isoform I [Ipomoea batatas]
3	14	10	352	p6e4	(AJ002594) subtilisin-like protease [Plasmodium falciparum]
6	2	6	353	p6e5	(AB020749) emb|CAB68144.1~gene_id:MRC8.17~similar to unknown p
3	14	11	354	p6e6	(AF194416) MAP kinase homolog [Oryza sativa]
6	2	5	355	p6e7	RNA REPLICATION PROTEIN (156 KD PROTEIN) (ORF 1) [CONTAIN
3	14	12	356	p6e9	(AL359782) hypothetical protein, CHR1.200. [Trypanosoma brucei]
6	2	4	357	p6e11	(AC007070) hypothetical protein [Arabidopsis thaliana]
3	14	13	358	p6e12	TUBULIN BETA-2 CHAIN (BETA-2 TUBULIN) >gi|4415992|gb|AAD201
6	2	3	359	p6f2	probable na+/h+ antiporte PAB1518 - Pyrococcus abyssi (strain Orsay)
3	13	1	360	p6f3	CYTOCHROME P450 51 (CYPL1) (P450-L1A1) (OBTUSIFOLIOL 14-AL
11	2	8	361	p6f5	(AF200972) sulfite oxidase [Arabidopsis thaliana]
8	14	9	362	p6f6	(AC008075) Similar to gb|AF023472 peptide transporter from Hordeum
1	2	7	363	p6f7	37 KD INNER ENVELOPE MEMBRANE PROTEIN, CHLOROPLAST PI
8	14	10	364	p6f8	probable cadmium-transporting ATPase - soybean >gi|2565259|gb|AAB
1	2	6	365	p6f9	(AC010657) T5E21.11 [Arabidopsis thaliana]
8	14	11	366	p6f10	(AC002334) putative synaptobrevin [Arabidopsis thaliana]
1	2	5	367	p6f11	UTP--GLUCOSE-1-PHOSPHATE URIDYLYLTRANSFERASE (UDP-GL
8	14	12	368	p6f12	MITOCHONDRIAL FORMATE DEHYDROGENASE PRECURSOR (NAI
1	2	4	369	p6g1	
8	14	13	370	p6g2	conserved hypothetical protein - Thermotoga maritima (strain MSB8) >g
1	2	3	371	p6g3	unspecific monooxygenase (EC 1.14.14.1) - common tobacco >gi|1545E
8	13	1	372	p6g5	hypothetical protein ykrT - Bacillus subtilis >gi|2633727|emb|CAB13229.
5	2	8	373	p6g7	(Y16328) putative cyclic nucleotide-regulated ion channel [Arabidopsis tl
4	14	9	374	p6g9	(AJ251646) beta-1,3 glucanase [Pisum sativum]
5	2	7	375	p6g11	(AC005916) Strong similarity to gb|Y18349 U2 snRNP auxiliary factor, s
4	14	10	376	p6g12	(AP002044) DNA-damage-repair/toleration protein-like; disease resistan
5	2	6	377	p6h2	(AB019229) serine protease-like protein [Arabidopsis thaliana]
4	14	11	378	p6h3	(AB016885) protein kinase-like protein [Arabidopsis thaliana]
5	2	5	379	p6h4	(Y16832) alpha-1,3-mannosyl-glycoprotein beta-1,2-N-acetylglucosamin
4	14	12	380	p6h6	(AF119716) dMi-2 protein [Drosophila melanogaster]
5	2	4	381	p6h7	INITIATION FACTOR 5A-2 (EIF-5A) (EIF-4D) >gi|100278|pir||S21059 tra
4	14	13	382	p6h8	(U89841) diadenosine 5',5'''-P1,P4-tetraphosphate hydrolase [Lupinus a
5	2	3	383	p6h9	(AL163527) ABC transporter-like protein [Arabidopsis thaliana]
4	13	1	384	p6h10	(AF109693) allergen-like protein BRSn20 [Sambucus nigra]
4	2	2	385	p6h11	mannose-1-phosphate guanylyltransferase (EC 2.7.7.13) - Arabidopsis t
5	12	13	386	p6h12	(AC006233) hypothetical protein [Arabidopsis thaliana]
4	2	1	387	p10a1	L1439.3 [Leishmania major] >gi|7460183|pir||T02851 probable membrar
5	11	1	388	p10a4	PHOTOSYSTEM II REACTION CENTER W PROTEIN PRECURSOR (I
4	3	13	389	p10a5	(AJ243904) SF1 protein [Drosophila melanogaster]
5	11	2	390	p10a6	(AC002339) unknown protein [Arabidopsis thaliana]
4	3	12	391	p10a7	
5	11	3	392	p10a9	(AC007197) dynamin-like protein [Arabidopsis thaliana]
4	3	11	393	p10a10	(AJ238754) phenylalanine-ammonia lyase [Citrus clementina x Citrus re
5	11	4	394	p10a11	(AC034106) Contains similarity to RING-H2 finger protein RHG1a (partia
4	3	10	395	p10a12	membrane protein, peroxisomal [imported] - Arabidopsis thaliana >gi|39
5	11	5	396	p10b1	(AC006193) Similar to Flavonol 3-O-Glucosyltransferase [Arabidopsis th

Block	Row	Column	ID	Name	Description
8	2	2	397	p10b2	(D84126) leptin receptor(short cytoplasmic form) [Rattus norvegicus]
1	12	13	398	p10b3	(AC009243) F28K19.27 [Arabidopsis thaliana]
8	2	1	399	p10b7	neurofilament triplet H1 protein - rabbit (fragment) >gi|601930|gb|AAA57
1	11	1	400	p10b9	(Y11138) shows weak homology to C. elegans cosmid C33A12 ORF an
8	3	13	401	p10b10	(Y12599) histone H1 [Apium graveolens]
1	11	2	402	p10b11	(AB023038) cytochrome P450 [Arabidopsis thaliana]
8	3	12	403	p10b12	
1	11	3	404	p10c2	
8	3	11	405	p10c5	(AF174481) gonadotropin-releasing hormone receptor [Typhlonectes na
1	11	4	406	p10c10	(AF239675) amphotropic murine leukemia virus receptor [Cricetulus gris
8	3	10	407	p10c11	(AC006585) putative steroid-binding protein [Arabidopsis thaliana]
1	11	5	408	p10d1	probable serine/threonine protein kinase (EC 2.7.1.-) - rice (fragment) >g
3	2	2	409	p10d2	multicatalytic endopeptidase complex (EC 3.4.99.46) iota chain - soybea
6	12	13	410	p10d4	subtilisin-like proteinase (EC 3.4.21.-), nodule-specific - Arabidopsis thal
3	2	1	411	p10d5	(AF061282) patatin-like protein [Sorghum bicolor]
6	11	1	412	p10d6	CARNITINE O-ACETYLTRANSFERASE PRECURSOR (CARNITINE A
3	3	13	413	p10d8	hypothetical protein F7A7.110 - Arabidopsis thaliana >gi|7327818|emb|C
6	11	2	414	p10d10	conserved hypothetical protein CP1049 [imported] - Chlamydophila pneu
3	3	12	415	p10d11	(AF220204) unknown [Malus x domestica]
6	11	3	416	p10e1	(AC009999) Contains similarity to an unknown protein from Arabidopsis
3	3	11	417	p10e2	HYPOTHETICAL PROTEIN MJ1177 >gi|2128709|pir||A64447 hypothetic
6	11	4	418	p10e3	
3	3	10	419	p10e4	(AC007233) putative beta-1,3-glucanase [Arabidopsis thaliana]
6	11	5	420	p10e6	hypothetical protein F22I13.200 - Arabidopsis thaliana >gi|4539351|emb
7	2	2	421	p10e7	
2	12	13	422	p10e8	(L03424) beta-D-galactosidase [Bacillus circulans]
7	2	1	423	p10e11	(AP000836) ESTs AU068544(C30430),C98487(E0325),D23445(C2825)
2	11	1	424	p10e12	CATALASE ISOZYME 1 >gi|1084411|pir||S48650 catalase (EC 1.11.1.6
7	3	13	425	p10f1	(AB028611) non-LTR retroelement reverse transcriptase-like protein [Ar
2	11	2	426	p10f2	
7	3	12	427	p10f4	(U89839) ADP/ATP translocator [Lycopersicon esculentum]
2	11	3	428	p10f5	(AF082030) senescence-associated protein 5 [Hemerocallis hybrid cultiv
7	3	11	429	p10f6	(AB020749) cytosolic chaperonin, delta-subunit [Arabidopsis thaliana]
2	11	4	430	p10f9	
7	3	10	431	p10f11	proline-rich protein PRB3M (null) - human (fragment)
2	11	5	432	p10f12	dipeptide abc transporter, dipeptide-binding protein PAB0092 - Pyrococ
2	2	2	433	p10g1	TRANSLATIONALLY CONTROLLED TUMOR PROTEIN HOMOLOG (T
7	12	13	434	p10g5	proline-rich protein, 14K - kidney bean >gi|1420885|gb|AAC49369.1| (U3
2	2	1	435	p10g6	chlorophyll a/b-binding protein type II precursor, photosystem I - garden
7	11	1	436	p10g8	UBIQUITIN-CONJUGATING ENZYME E2-17 KD (UBIQUITIN-PROTEIN
2	3	13	437	p10g9	(AC005397) hypothetical protein [Arabidopsis thaliana]
7	11	2	438	p10g10	hypothetical protein T30N20_130 - Arabidopsis thaliana >gi|8979720|em
2	3	12	439	p10g12	CATALASE >gi|7433025|pir||T10902 catalase (EC 1.11.1.6) - mung bea
7	11	3	440	p10h1	ENOLASE (2-PHOSPHOGLYCERATE DEHYDRATASE) (2-PHOSPHO
2	3	11	441	p10h2	ENDOGLUCANASE A PRECURSOR (ENDO-1,4-BETA-GLUCANASE)
7	11	4	442	p10h3	(AJ012693) basic blue copper protein [Cicer arietinum]
2	3	10	443	p10h4	Rieske [2Fe-2S] iron-sulfur protein tic55 - garden pea >gi|2764524|emb|
7	11	5	444	p10h5	chaperonine 60K alpha chain - rape (fragment)
6	2	2	445	p10h6	(AC023912) acetyl-coA dehydrogenase, putative [Arabidopsis thaliana]
3	12	13	446	p10h8	
6	2	1	447	p10h9	dnaK-type molecular chaperone hsp70 - alfalfa (fragment) >gi|1430887|e
3	11	1	448	p10h10	(AB037743) KIAA1322 protein [Homo sapiens]
6	3	13	449	p10h11	
3	11	2	450	p10h12	AMV259 [Amsacta moorei entomopoxvirus] >gi|9944782|gb|AAG02965.
6	3	12	451	p11a1	hypothetical protein T13E15.7 - Arabidopsis thaliana >gi|2344892|gb|AA
3	11	3	452	p11a2	(AC012395) putative 60S ribosomal protein L13A [Arabidopsis thaliana]
6	3	11	453	p11a3	(AC008263) ESTs gb|T75898, gb|R65457, gb|AA597517 and gb|AA597
3	11	4	454	p11a5	(AC008148) Hypothetical protein [Arabidopsis thaliana]
6	3	10	455	p11a6	(AB026639) emb|CAB16809.1~gene_id:K21L13.17~similar to unknown
3	11	5	456	p11a7	
1	2	2	457	p11a8	acyl carrier protein - swamp oak >gi|1838961|emb|CAA71885.1| (Y1099
8	12	13	458	p11a9	(AB007648) succinyl-CoA synthetase, alpha subunit [Arabidopsis thaliar
1	2	1	459	p11a12	(AB025606) contains similarity to GTPase activating protein~gene_id:F6
8	11	1	460	p11b2	acetyl-CoA C-acyltransferase (EC 2.3.1.16) precursor, glyoxysomal - rap
1	3	13	461	p11b3	(AJ299059) cytosolic malate dehydrogenase [Cicer arietinum]
8	11	2	462	p11b4	similar to microsomal glutathione S-transferase 1 (H. sapiens) [Homo sa
1	3	12	463	p11b5	ribosomal protein L5, organellar - Arabidopsis thaliana >gi|2191128|gb|A

Block	Row	Column	ID	Name	Description
8	11	3	464	p11b6	(AB010071) gene_id:MCO15.7~pir||T04808~strong similarity to unknowr
1	3	11	465	p11b8	(AF141642) putative aquaporin PIP2-1 [Vitis berlandieri x Vitis rupestris]
8	11	4	466	p11b10	SPERMIDINE SYNTHASE (PUTRESCINE AMINOPROPYLTRANSFER
1	3	10	467	p11b11	(AF075580) protein phosphatase-2C; PP2C [Mesembryanthemum cryst.
8	11	5	468	p11c1	
5	2	2	469	p11c2	hypothetical protein T25B15.140 - Arabidopsis thaliana >gi|10045570|en
4	12	13	470	p11c4	VP39=CAPSID=AcMNPV orf89 [Bombyx mori nuclear polyhedrosis viru:
5	2	1	471	p11c8	(AF002109) unknown protein [Arabidopsis thaliana] >gi|3158394|gb|AAC
4	11	1	472	p11c9	hypothetical protein A_IG005I10.24 - Arabidopsis thaliana >gi|2252843|g
5	3	13	473	p11c11	
4	11	2	474	p11d2	hypothetical protein T13J8.210 - Arabidopsis thaliana >gi|4455369|emb|
5	3	12	475	p11d3	(AC007651) Hypothetical Protein [Arabidopsis thaliana]
4	11	3	476	p11d4	(AF200322) putative glycine-rich RNA binding protein 3 [Catharanthus rc
5	3	11	477	p11d5	(AB018587) ZmGR1a [Zea mays]
4	11	4	478	p11d8	(AB047607) hypothetical protein [Macaca fascicularis]
5	3	10	479	p11d9	(AJ277086) protein phosphatase 2C [Nicotiana tabacum]
4	11	5	480	p11d10	40S RIBOSOMAL PROTEIN SA (P40) >gi|3204099|emb|CAA07226.1| (
4	3	9	481	p11d12	(AC002130) F1N21.10 [Arabidopsis thaliana]
5	11	6	482	p11e1	(AF187853) putative multispanning membrane protein [Populus x canes
4	3	8	483	p11e2	fat protein - Synechocystis sp. (strain PCC 6803) >gi|1652190|dbj|BAA1
5	11	7	484	p11e3	(AC009513) Strong similarity to gb|AF155333 NADP-specific isocitrate c
4	3	7	485	p11e4	(AJ005345) hypothetical protein [Cicer arietinum]
5	11	8	486	p11e5	(AC022455) unknown protein; 69948-68670 [Arabidopsis thaliana]
4	3	6	487	p11e6	(AB005232) gene_id:MBG8.14~pir||T04825~strong similarity to unknowr
5	11	9	488	p11e7	probable carboxyl-terminal proteinase - Arabidopsis thaliana >gi|224510
4	3	5	489	p11e8	hypothetical protein F1P2.170 - Arabidopsis thaliana >gi|6522545|emb|C
5	11	10	490	p11e10	(AF187853) putative multispanning membrane protein [Populus x canes
4	3	4	491	p11e12	(AF210249) sugar epimerase BlmG [Streptomyces verticillus]
5	11	11	492	p11f1	(AF154424) putative beta-galactosidase [Lycopersicon esculentum]
8	3	9	493	p11f2	(AC022287) unknown protein [Arabidopsis thaliana]
1	11	6	494	p11f3	protein-arginine deiminase (EC 3.5.3.15) 2 - mouse (fragment)
8	3	8	495	p11f4	(AB025102) protoporphyrinogen IX oxidase [Glycine max]
1	11	7	496	p11f5	(AC009243) F28K19.2 [Arabidopsis thaliana]
8	3	7	497	p11f6	probable protein phosphatase 2A B regulatory chain 55K - rice >gi|3421·
1	11	8	498	p11f8	serine-type carboxypeptidase II-like protein - Arabidopsis thaliana >gi|83
8	3	6	499	p11f9	(AB020742) anthranilate N-hydroxycinnamoyl/benzoyltransferase-like pr
1	11	9	500	p11f10	(AC011623) unknown protein [Arabidopsis thaliana]
8	3	5	501	p11f11	40S RIBOSOMAL PROTEIN S18 >gi|480908|pir||S37496 ribosomal prot
1	11	10	502	p11f12	(AF071477) isoflavone reductase related protein [Pyrus communis]
8	3	4	503	p11g3	hypothetical protein F9G14.50 - Arabidopsis thaliana >gi|7413549|emb|(
1	11	11	504	p11g4	uracil transporter-like protein - Arabidopsis thaliana >gi|7378642|emb|CA
3	3	9	505	p11g5	hypothetical protein - Madagascar periwinkle >gi|407410|emb|CAA8152(
6	11	6	506	p11g6	(L33973) agamous protein [Petunia integrifolia]
3	3	8	507	p11g7	(AC012395) putative RING zinc finger protein [Arabidopsis thaliana]
6	11	7	508	p11g8	RNA-binding protein RNP1 precursor - kidney bean >gi|558629|emb|CA.
3	3	7	509	p11g9	
6	11	8	510	p11g11	(AF194174) alcohol dehydrogenase 2 [Vitis vinifera]
3	3	6	511	p11h1	
6	11	9	512	p11h2	(Z97342) putative serine protease-like protein [Arabidopsis thaliana] >gi|
3	3	5	513	p11h3	(AC026875) T6D22.2 [Arabidopsis thaliana]
6	11	10	514	p11h4	(AC009999) Contains similarity to a basic endochitinase from Arabidopis
3	3	4	515	p11h5	(AC007232) hypothetical protein [Arabidopsis thaliana]
6	11	11	516	p11h6	
7	3	9	517	p11h8	(AC006340) unknown protein [Arabidopsis thaliana]
2	11	6	518	p11h9	(AE003458) CG4046 gene product [Drosophila melanogaster]
7	3	8	519	p11h11	(AC016661) unknown protein [Arabidopsis thaliana]
2	11	7	520	p11h12	(AC006248) unknown protein [Arabidopsis thaliana]
7	3	7	521	p12a1	(AJ007578) pRIB5 protein [Ribes nigrum]
2	11	8	522	p12a2	(Y16262) neutral invertase [Daucus carota]
7	3	6	523	p12a5	hypothetical protein T09D3.3 - Caenorhabditis elegans >gi|10864483|gb
2	11	9	524	p12a7	(AC005970) putative translation initiation factor eIF-2B alpha subunit [Ar
7	3	5	525	p12a9	14-3-3-LIKE PROTEIN >gi|555974|gb|AAA85817.1| (U15036) 14-3-3-lik
2	11	10	526	p12a12	(AF200713) inwardly rectifying potassium channel Kir7.1 [Cavia porcellu
7	3	4	527	p12b1	FLORAL HOMEOTIC PROTEIN FBP2 (FLORAL BINDING PROTEIN 2)
2	11	11	528	p12b2	hypothetical protein TC0114 [imported] - Chlamydia muridarum (strain N
2	3	9	529	p12b3	
7	11	6	530	p12b4	(AC012193) unknown protein; 14107-15252 [Arabidopsis thaliana]

Block	Row	Column	ID	Name	Description
2	3	8	531	p12b5	DNA binding protein EREBP-4 - common tobacco >gi|1208497|dbj|BAA(
7	11	7	532	p12b6	(AJ007580) Mitochondrial carrier protein [Ribes nigrum]
2	3	7	533	p12b7	(AB038692) similar to the BURP domain [Vigna unguiculata]
7	11	8	534	p12b8	
2	3	6	535	p12b9	UBIQUINOL-CYTOCHROME C REDUCTASE COMPLEX 14 KDA PRO
7	11	9	536	p12b10	(Y10024) ubiquitin extension protein [Solanum tuberosum]
2	3	5	537	p12b11	(AC021666) unknown protein; 24499-21911 [Arabidopsis thaliana]
7	11	10	538	p12b12	(AJ237992) putative ripening-related bZIP protein [Vitis vinifera]
2	3	4	539	p12c1	
7	11	11	540	p12c2	TRANSLATIONALLY CONTROLLED TUMOR PROTEIN HOMOLOG (T
6	3	9	541	p12c4	Sali3-2 protein, aluminium-induced - soybean >gi|2317900|gb|AAB6636
3	11	6	542	p12c5	(AJ292768) RNA Binding Protein 47 [Nicotiana plumbaginifolia]
6	3	8	543	p12c6	(AB013395) poly(A)-binding protein II-like [Arabidopsis thaliana]
3	11	7	544	p12c7	(AJ003197) adenine nucleotide translocator [Lupinus albus]
6	3	7	545	p12c8	
3	11	8	546	p12c9	
6	3	6	547	p12d1	(AF224337) beta-1 integrin [Ictalurus punctatus]
3	11	9	548	p12d2	(AJ297951) p23 co-chaperone [Arabidopsis thaliana]
6	3	5	549	p12d3	(AJ236913) metallothionein-like protein [Elaeis guineensis]
3	11	10	550	p12d4	
6	3	4	551	p12d7	
3	11	11	552	p12d8	FERREDOXIN >gi|65744|pir||FEED ferredoxin [2Fe-2S] - European elde
1	3	9	553	p12d9	THIAZOLE BIOSYNTHETIC ENZYME PRECURSOR >gi|7446894|pir||T
8	11	6	554	p12d11	(AC079374) unknown protein [Arabidopsis thaliana]
1	3	8	555	p12d12	(AC006264) hypothetical protein [Arabidopsis thaliana]
8	11	7	556	p12e1	(AB010069) gb|AAC80624.1~gene_id:MAC9.17~strong similarity to unk
1	3	7	557	p12e2	(AE003528) CG5151 gene product [Drosophila melanogaster]
8	11	8	558	p12e3	hypothetical protein ZK6.6 - Caenorhabditis elegans >gi|3165580|gb|AA
1	3	6	559	p12e5	(AC006260) unknown protein [Arabidopsis thaliana]
8	11	9	560	p12e6	(AC018907) hypothetical protein [Arabidopsis thaliana]
1	3	5	561	p12e7	
8	11	10	562	p12e8	(AB042860) ribosomal protein L29 [Panax ginseng]
1	3	4	563	p12e9	coat protein gamma-COP homolog T4L20.30 - Arabidopsis thaliana >gi|
8	11	11	564	p12e10	(AF071893) AP2 domain containing protein [Prunus armeniaca]
5	3	9	565	p12e11	(AC011620) putative 60S ribosomal protein L18 [Arabidopsis thaliana]
4	11	6	566	p12e12	(AL353822) hypothetical protein [Neurospora crassa]
5	3	8	567	p12f1	ADP-ribosylation factor-like protein - Arabidopsis thaliana >gi|6899939|e
4	11	7	568	p12f2	glycine-rich cell wall protein EMB31 - white spruce >gi|1350526|gb|AAB(
5	3	7	569	p12f3	MLO PROTEIN HOMOLOG 1 (ATMLO-H1) >gi|7486849|pir||T01089 hyp
4	11	8	570	p12f4	HEAT SHOCK PROTEIN 101 >gi|537446|gb|AAA67927.1| (U13949) Ath
5	3	6	571	p12f5	vacuolar invertase 1, GIN1 [Vitis vinifera=grape berries, Sultana, berries
4	11	9	572	p12f6	(U64925) NTGP4 [Nicotiana tabacum]
5	3	5	573	p12f7	
4	11	10	574	p12f8	CALCIUM-DEPENDENT PROTEIN KINASE SK5 (CDPK) >gi|280393|pi
5	3	4	575	p12f9	(L39791) complement component receptor type 1 [Papio hamadryas]
4	11	11	576	p12f10	(AF212109) ATP-dependent phosphoenolpyruvate carboxykinase [Medi
4	3	3	577	p12f11	
5	11	12	578	p12f12	
4	3	2	579	p12g1	
5	11	13	580	p12g5	
4	3	1	581	p12g8	(AL034558) predicted using hexExon; MAL3P2.18 (PFC0245c), Hypothe
5	10	1	582	p12g11	
4	4	13	583	p12g12	
5	10	2	584	p12h2	hypothetical protein F15B8.20 - Arabidopsis thaliana >gi|4678268|emb|C
4	4	12	585	p12h3	(AB009053) permease 1 [Arabidopsis thaliana]
5	10	3	586	p12h5	26S PROTEASOME REGULATORY SUBUNIT S3 (NUCLEAR ANTIGE
4	4	11	587	p12h6	UDP-galactose transporter related [Homo sapiens] >gi|2136346|pir||JC5
5	10	4	588	p12h8	(AB024034) DnaJ-like protein [Arabidopsis thaliana]
8	3	3	589	p12h9	(AL137798) dJ1182A14.1 (similar to rat Espin) [Homo sapiens]
1	11	12	590	p12h10	
8	3	2	591	p12h11	(AC016795) unknown protein [Arabidopsis thaliana]
1	11	13	592	p12h12	(AF071527) putative calcium channel [Arabidopsis thaliana] >gi|426304
8	3	1	593	p13a1	sucrose synthase (EC 2.4.1.13) - soybean (fragment)
1	10	1	594	p13a2	hypothetical protein [imported] - soybean (fragment) >gi|3832528|gb|AA(
8	4	13	595	p13a3	(AB005238) gb|AAF26109.1~gene_id:MKP11.4~similar to unknown prot
1	10	2	596	p13a4	(AC011437) unknown protein [Arabidopsis thaliana]
8	4	12	597	p13a5	(AP002070) Similar to Arabidopsis thaliana low temperature and salt res

Block	Row	Column	ID	Name	Description
1	10	3	598	p13a6	
8	4	11	599	p13a10	polyubiquitin 5 - Arabidopsis thaliana >gi|17678|emb|CAA31331.1| (X12
1	10	4	600	p13a12	60S RIBOSOMAL PROTEIN L37A >gi|4741896|gb|AAD28753.1|AF127(
3	3	3	601	p13b1	36 KDA OUTER MITOCHONDRIAL MEMBRANE PROTEIN PORIN (VC
6	11	12	602	p13b7	(AF163823) endoxyloglucan transferase [Arabidopsis thaliana] >gi|9758:
3	3	2	603	p13b9	
6	11	13	604	p13b10	hypothetical protein F1C12.90 - Arabidopsis thaliana >gi|2982434|emb|(
3	3	1	605	p13c1	40S RIBOSOMAL PROTEIN S16
6	10	1	606	p13c2	hypothetical protein F16G20.180 - Arabidopsis thaliana >gi|3451073|em
3	4	13	607	p13c3	(M62431) nonstructural protein; putative helicase/protease; contains dup
6	10	2	608	p13c4	(AB020755) gene_id:MZN1.6~pir||T02484~strong similarity to unknown
3	4	12	609	p13c7	PECTINESTERASE 3 PRECURSOR (PECTIN METHYLESTERASE 3)
6	10	3	610	p13c8	
3	4	11	611	p13c9	amino acid transport protein AAP5 - Arabidopsis thaliana
6	10	4	612	p13c10	
7	3	3	613	p13c11	probable cytochrome P450, hypersensitivity-related - common tobacco >
2	11	12	614	p13c12	
7	3	2	615	p13d1	(AJ011862) flavonoid 3',5'-hydroxylase [Catharanthus roseus]
2	11	13	616	p13d2	hypothetical protein F4D11.50 - Arabidopsis thaliana >gi|3063695|emb|(
7	3	1	617	p13d3	CELL ELONGATION PROTEIN DIMINUTO >gi|7488800|pir||T06575 dw
2	10	1	618	p13d4	chlorophyll a/b-binding protein type III precursor - tomato >gi|226872|prf|
7	4	13	619	p13d5	(AC015446) Putative integral membrane protein [Arabidopsis thaliana]
2	10	2	620	p13d8	(AB007651) 60S ribosomal protein L10A [Arabidopsis thaliana]
7	4	12	621	p13d10	(AC007109) putative heat shock protein [Arabidopsis thaliana]
2	10	3	622	p13d12	cysteine proteinase (EC 3.4.22.-) - garden pea >gi|1134882|emb|CAA92
7	4	11	623	p13e1	(AF135596) Skp1 [Medicago sativa]
2	10	4	624	p13e2	hypothetical protein F28P10.120 - Arabidopsis thaliana >gi|4678303|eml
2	3	3	625	p13e4	(AC007260) lcl|prt_seq No definition line found [Arabidopsis thaliana]
7	11	12	626	p13e5	
2	3	2	627	p13e7	(D21814) ORF [Lilium longiflorum]
7	11	13	628	p13e8	ribosomal protein L11 homolog - Arabidopsis thaliana >gi|5830791|emb|
2	3	1	629	p13e9	oligo-1,6-glucosidase homolog ycdG - Bacillus subtilis >gi|2415735|dbj|E
7	10	1	630	p13e11	sperm associated antigen 1 [Homo sapiens] >gi|10863768|gb|AAG2396
2	4	13	631	p13e12	(AF090446) unknown [Zea mays]
7	10	2	632	p13f1	(AC021199) hypothetical protein; 51999-52350 [Arabidopsis thaliana]
2	4	12	633	p13f2	HMG1/2-LIKE PROTEIN >gi|1085860|pir||S40302 high mobility group pr
7	10	3	634	p13f3	3-HYDROXY-3-METHYLGLUTARYL-COENZYME A REDUCTASE 1 (H
2	4	11	635	p13f4	(AC012393) unknown protein [Arabidopsis thaliana]
7	10	4	636	p13f5	PHOTOSYSTEM II 10 KD POLYPEPTIDE PRECURSOR (PII10) >gi|32
6	3	3	637	p13f8	(AC024609) Putative GSH-dependent dehydroascorbate reductase [Ara
3	11	12	638	p13f9	lipid transfer protein precursor [imported] - upland cotton >gi|7012719|gb
6	3	2	639	p13g1	LATE EMBRYOGENESIS ABUNDANT PROTEIN LEA14-A >gi|748472
3	11	13	640	p13g2	hypothetical protein - Arabidopsis thaliana >gi|2245118|emb|CAB10540.
6	3	1	641	p13g4	(AP001518) phosphoenolpyruvate carboxykinase [Bacillus halodurans]
3	10	1	642	p13g5	(AJ299061) hypothetical protein [Cicer arietinum]
6	4	13	643	p13g6	
3	10	2	644	p13g8	(AB026643) DNA helicase-like [Arabidopsis thaliana]
6	4	12	645	p13g10	
3	10	3	646	p13g11	translocated promoter region (to activated MET oncogene); Tumor poter
6	4	11	647	p13h1	(AC006081) unknown protein [Arabidopsis thaliana]
3	10	4	648	p13h2	(AJ007579) cysteine proteinase [Ribes nigrum]
1	3	3	649	p13h3	
8	11	12	650	p13h4	(AF139470) chlorophyll a/b-binding protein CP24 precursor [Vigna radia
1	3	2	651	p13h7	(AC013483) hypothetical protein [Arabidopsis thaliana]
8	11	13	652	p13h8	probable formamidase (EC 3.5.1.49) F19F18.40 - Arabidopsis thaliana >
1	3	1	653	p13h11	(AC009519) F1N19.9 [Arabidopsis thaliana]
8	10	1	654	p13h12	(U70869) type II iodothyronine deiodinase [Fundulus heteroclitus]
1	4	13	655	p14h12	(AJ245867) photosystem I subunit XI precursor [Arabidopsis thaliana]
8	10	2	656	p12h11	(AC016795) unknown protein [Arabidopsis thaliana]
1	4	12	657	p14h9	26S proteasome regulatory subunit S5A - common ice plant >gi|320204:
8	10	3	658	p14a1	hypothetical protein T18E12.21 - Arabidopsis thaliana >gi|3548818|gb|A
1	4	11	659	p14a2	(AC011708) putative RING zinc finger protein [Arabidopsis thaliana]
8	10	4	660	p14a4	hypothetical protein L7610.6 - Leishmania major >gi|4165503|emb|CAA:
5	3	3	661	p14a5	(AF002109) hypothetical protein [Arabidopsis thaliana]
4	11	12	662	p14a8	NARINGENIN,2-OXOGLUTARATE 3-DIOXYGENASE (FLAVONONE-3-
5	3	2	663	p14a9	WD-40 REPEAT PROTEIN MSI1 >gi|2394229|gb|AAB70242.1| (AF016
4	11	13	664	p14a10	(AB011482) contains similarity to AAA-type ATPase~gene_id:MUA2.5 [A

Block	Row	Column	ID	Name	Description
5	3	1	665	p14a12	(AB026979) ten-m3 [Danio rerio]
4	10	1	666	p14b1	(AL359988) putative membrane protein [Streptomyces coelicolor A3(2)]
5	4	13	667	p14b2	rpl21 [Marchantia polymorpha] >gi|132774|sp|P06387|RK21_MARPO C
4	10	2	668	p14b3	
5	4	12	669	p14b6	nucleotide pyrophosphatase homolog T16L4.190 - Arabidopsis thaliana
4	10	3	670	p14b7	(AB035312) NADP-glyceraldehyde-3-phosphate dehydrogenase [Chlam
5	4	11	671	p14b12	(AB006703) gb|AAD10667.1~gene_id:MRH10.15~similar to unknown pr
4	10	4	672	p14c1	hypothetical protein F10M23.190 - Arabidopsis thaliana >gi|4455208|em
4	4	10	673	p14c3	(AC009519) F1N19.23 [Arabidopsis thaliana]
5	10	5	674	p14c7	(AC000132) Identical to A. thaliana AtK-1 (gb|X79279). [Arabidopsis tha
4	4	9	675	p14c8	(AC013258) putative GDP-mannose pyrophosphorylase; 64911-67597 [
5	10	6	676	p14c9	
4	4	8	677	p14c11	(AJ249330) heat shock protein 70 [Cucumis sativus]
5	10	7	678	p14d2	
4	4	7	679	p14d3	(AJ006754) hypothetical protein [Yarrowia lipolytica]
5	10	8	680	p14d4	(AB022217) translationally controlled tumor protein-like [Arabidopsis tha
4	4	6	681	p14d5	probable methylmalonate-semialdehyde dehydrogenase (acylating) (EC
5	10	9	682	p14d6	
4	4	5	683	p14d8	(AF161180) high molecular weight heat shock protein [Malus x domestic
5	10	10	684	p14d9	(AF206526) seroreactive antigen BMN1-17 [Babesia microti]
8	4	10	685	p14d10	hypothetical protein C03G6.9 - Caenorhabditis elegans >gi|1938485|gb|
1	10	5	686	p14d11	(AF325010) T21H19.30 [Arabidopsis thaliana]
8	4	9	687	p14e1	
1	10	6	688	p14e3	
8	4	8	689	p14e5	(AC003970) Similar to ATP-citrate-lyase [Arabidopsis thaliana]
1	10	7	690	p14e7	NADP-DEPENDENT MALIC ENZYME (NADP-ME) >gi|515759|gb|AAAE
8	4	7	691	p14e8	(AF137273) alpha 1 (V) collagen [Gallus gallus]
1	10	8	692	p14e9	(AC018849) putative protein kinase; 6651-4392 [Arabidopsis thaliana]
8	4	6	693	p14e10	
1	10	9	694	p14e11	(AF145386) hypersensitive reaction associated Ca2+-binding protein [P
8	4	5	695	p14e12	S-ADENOSYLMETHIONINE DECARBOXYLASE PROENZYME (ADOM
1	10	10	696	p14f1	serine protease (capsid) [Bovine herpesvirus type 1.1] >gi|1722778|sp|P
3	4	10	697	p14f2	Ca2+-transporting ATPase-like protein - Arabidopsis thaliana >gi|75733
6	10	5	698	p14f7	(AC000107) F17F8.22 [Arabidopsis thaliana]
3	4	9	699	p14f8	60S RIBOSOMAL PROTEIN L34 >gi|2119150|pir||S60476 ribosomal pro
6	10	6	700	p14f9	
3	4	8	701	p14f11	(AF324991) DL3005C [Arabidopsis thaliana]
6	10	7	702	p14f12	(AF129478) K+ transporter HAK5 [Arabidopsis thaliana]
3	4	7	703	p14g1	(AC009322) Unknown protein [Arabidopsis thaliana]
6	10	8	704	p14g3	(AJ401158) pectin methylesterase [Nicotiana tabacum]
3	4	6	705	p14g4	hypothetical protein T9J22.16 - Arabidopsis thaliana >gi|2739374|gb|AA
6	10	9	706	p14g5	hypothetical protein F25F2.2 - Caenorhabditis elegans >gi|3875769|emb
3	4	5	707	p14g6	(AE003738) CG13855 gene product [Drosophila melanogaster]
6	10	10	708	p14g7	hypothetical protein F26K9.200 - Arabidopsis thaliana >gi|7362757|emb|
7	4	10	709	p14g8	(AB018558) Gag-like protein [Bombyx mori]
2	10	5	710	p14g9	(AF271660) putative aquaporin TIP3 [Vitis berlandieri x Vitis rupestris]
7	4	9	711	p14g10	
2	10	6	712	p14g11	(AC022455) hydrophilic protein, putative; 29542-30030 [Arabidopsis thal
7	4	8	713	p14g12	(AB010692) contains similarity to chalcone-flavonone isomerase (chalcc
2	10	7	714	p14h1	(AC006248) putative RING-H2 zinc finger protein [Arabidopsis thaliana]
7	4	7	715	p14h2	
2	10	8	716	p14h3	
7	4	6	717	p14h5	TRANSCRIPTION INITIATION FACTOR IIB (TFIIB) >gi|7443551|pir||T0
2	10	9	718	p14h6	60S RIBOSOMAL PROTEIN L7 >gi|7440720|pir||T00692 ribosomal prot
7	4	5	719	p14h7	syntaxin-like protein - Arabidopsis thaliana >gi|8346545|emb|CAB93709
2	10	10	720	p14h8	(AJ132580) enolase, isoform 1 [Hevea brasiliensis]
2	4	10	721	p14h10	germin-like protein 3 - rice (fragment) >gi|2655289|gb|AAC04834.1| (AF
7	10	5	722	p14h11	
2	4	9	723	p17a2	(AF272951) microsomal oleate desaturase [Arachis duranensis]
7	10	6	724	p17a4	
2	4	8	725	p17a7	
7	10	7	726	p17a8	(AB025613) gene_id:K2I5.7~pir||T05575~similar to unknown protein [Ar
2	4	7	727	p17a9	(AP002855) hypothetical protein~similar to Arabidopsis thaliana hypothe
7	10	8	728	p17a10	hypothetical protein F23E12.210 - Arabidopsis thaliana >gi|3080427|eml
2	4	6	729	p17b1	
7	10	9	730	p17b2	cytochrome-c oxidase (EC 1.9.3.1) chain III - Trypanosoma brucei mitoc
2	4	5	731	p17b3	(AF109156) thiosulfate sulfurtransferase [Datisca glomerata]

Block	Row	Column	ID	Name	Description
7	10	10	732	p17c2	(AC007591) ESTs gb|T22508, gb|H36196 and gb|AI100134 come from
6	4	10	733	p17c3	(AB028620) gb|AAD49773.1~gene_id:MTO12.2~strong similarity to unk
3	10	5	734	p17c4	(AB007650) nodulin-like protein [Arabidopsis thaliana]
6	4	9	735	p17c8	
3	10	6	736	p17c12	(AC007651) Similar to ribokinase [Arabidopsis thaliana]
6	4	8	737	p17d3	
3	10	7	738	p17d5	(AJ271439) plasma membrane H+ ATPase [Prunus persica]
6	4	7	739	p17d8	(AC025808) F18O14.5 [Arabidopsis thaliana]
3	10	8	740	p17d9	hypothetical protein T13D8.29 - Arabidopsis thaliana >gi|3249084|gb|AA
6	4	6	741	p17e8	
3	10	9	742	p17e12	(AJ277744) protein phosphatase 2C (PP2C) [Fagus sylvatica]
6	4	5	743	p17f2	6-phosphofructo-2-kinase (EC 2.7.1.105) / fructose-2, 6-bisphosphate 2-
3	10	10	744	p17f3	hypothetical protein T18N14.30 - Arabidopsis thaliana >gi|6580147|emb
1	4	10	745	p17f5	(AC034106) Strong similarity to GER1 from Arabidopsis thaliana gb|AF0
8	10	5	746	p17f6	hypothetical protein F20D10.220 - Arabidopsis thaliana >gi|4467116|em
1	4	9	747	p17f8	plastocyanin b" - common tobacco
8	10	6	748	p17g3	
1	4	8	749	p17g11	
8	10	7	750	p17h1	(AP001300) pyruvate kinase [Arabidopsis thaliana]
1	4	7	751	p17h4	(AF209910) vacuolar sorting receptor protein [Prunus dulcis]
8	10	8	752	p17h6	(AC006569) unknown protein [Arabidopsis thaliana]
1	4	6	753	p17h8	(AL161575) putative protein [Arabidopsis thaliana] >gi|11908084|gb|AA0
8	10	9	754	p17h12	
1	4	5	755	p18a1	(AC015446) Similar to Allinase [Arabidopsis thaliana]
8	10	10	756	p18a4	lipid transfer protein precursor - upland cotton >gi|2829204|gb|AAC0049
5	4	10	757	p18a5	(AE003580) CG3304 gene product [Drosophila melanogaster]
4	10	5	758	p18a8	ribosome releasing factor (OO, TP) PFB0390w [imported] - malaria para
5	4	9	759	p18a10	
4	10	6	760	p18b1	(AF275639) cytosolic phosphoglycerate kinase [Pisum sativum]
5	4	8	761	p18b4	(AF114171) hypothetical protein [Sorghum bicolor]
4	10	7	762	p18b6	(AB011482) calmodulin-binding protein [Arabidopsis thaliana]
5	4	7	763	p18b9	(AF211539) Avr9/Cf-9 rapidly elicited protein 65 [Nicotiana tabacum]
4	10	8	764	p18b10	hypothetical protein F22K18.40 - Arabidopsis thaliana >gi|4220514|emb|
5	4	6	765	p18b11	(U32923) potassium channel homolog [Polyorchis penicillatus]
4	10	9	766	p18c1	(AC005623) unknown protein [Arabidopsis thaliana]
5	4	5	767	p18c4	UBIQUINOL-CYTOCHROME C REDUCTASE COMPLEX UBIQUINONE
4	10	10	768	p18d1	(AC005311) hypothetical protein [Arabidopsis thaliana]
4	4	4	769	p18d6	PHOSPHOGLYCERATE KINASE, CYTOSOLIC >gi|7434547|pir||T0366
5	10	11	770	p18d9	
4	4	3	771	p18d12	chlorophyll a/b-binding protein type III precursor - tomato >gi|226872|prf|
5	10	12	772	p18e3	(AL136898) hypothetical protein [Homo sapiens]
4	4	2	773	p18e6	DC6 protein [Homo sapiens] >gi|11424709|ref|XP_005156.1| DC6 protei
5	10	13	774	p18e8	phosphoenolpyruvate carboxylase (EC 4.1.1.31) 1 - upland cotton >gi|22
4	4	1	775	p18f2	HMG1/2-LIKE PROTEIN (SB11 PROTEIN) >gi|99914|pir||S22309 high r
5	9	1	776	p18f3	(AC009978) T23E18.6 [Arabidopsis thaliana]
4	5	13	777	p18f5	(AJ289866) putative aquaporin [Vitis vinifera]
5	9	2	778	p18g1	
4	5	12	779	p18g2	
5	9	3	780	p18g4	(AC011438) T23G18.10 [Arabidopsis thaliana]
8	4	4	781	p18g7	(AF128392) F15P23.2 gene product [Arabidopsis thaliana] >gi|7267413|
1	10	11	782	p18g8	hypothetical protein F7K15.80 - Arabidopsis thaliana >gi|7649363|emb|C
8	4	3	783	p18g9	
1	10	12	784	p18g10	
8	4	2	785	p18g11	
1	10	13	786	p18f3	(AC009978) T23E18.6 [Arabidopsis thaliana]
8	4	1	787	p18f4	
1	9	1	788	p18f6	
8	5	13	789	p18f8	
1	9	2	790	p18f11	
8	5	12	791	p19f1	CYTOCHROME B5 >gi|7430587|pir||T14454 cytochrome b5 - wild cabb
1	9	3	792	p19f2	(AF159229) glutathione S-transferase [Gossypium hirsutum]
3	4	4	793	p19f3	hypothetical protein T8K22.5 - Arabidopsis thaliana >gi|3184275|gb|AAC
6	10	11	794	p19f8	(AF195865) lipid transfer protein precursor [Gossypium hirsutum]
3	4	3	795	p19f9	(AC007591) Contains similarity to gb|AF014403 type-2 phosphatidic acid
6	10	12	796	p19g2	(AF237957) LMW heat shock protein [Euphorbia esula]
3	4	2	797	p19g3	amino acid permease 6 [imported] - Arabidopsis thaliana >gi|1769887|e
6	10	13	798	p19g7	(S58644) integrin beta 5 subunit [Rattus sp.]

Block	Row	Column	ID	Name	Description
3	4	1	799	p19g8	RUBISCO SUBUNIT BINDING-PROTEIN ALPHA SUBUNIT PRECURS
6	9	1	800	p19g9	(AC025417) T12C24.18 [Arabidopsis thaliana]
3	5	13	801	p19g10	(AB024024) gene_id:K15C23.10~unknown protein [Arabidopsis thaliana
6	9	2	802	p19g11	ADP,ATP carrier protein F20O9.60 - Arabidopsis thaliana >gi|2842480|e
3	5	12	803	p19h1	
6	9	3	804	p19h4	(AL161514) putative protein [Arabidopsis thaliana]
7	4	4	805	p19h5	hypothetical protein F26K9.160 - Arabidopsis thaliana >gi|7362753|emb|
2	10	11	806	p19h6	
7	4	3	807	p19h7	(AL161503) receptor protein kinase-like protein [Arabidopsis thaliana]
2	10	12	808	p19h8	(AC007190) F23N19.15 [Arabidopsis thaliana]
7	4	2	809	p19h10	hypothetical protein slr2121 - Synechocystis sp. (strain PCC 6803) >gi|1
2	10	13	810	p19h12	
7	4	1	811	p20a2	hypothetical protein F16G20.200 - Arabidopsis thaliana >gi|3451075|em
2	9	1	812	p20a3	
7	5	13	813	p20a4	(AJ278332) 12-oxophytodienoate reductase 3 [Lycopersicon esculentum
2	9	2	814	p20a6	cellulase (EC 3.2.1.4) F16B22.6 - Arabidopsis thaliana >gi|3341677|gb|A
7	5	12	815	p20a7	
2	9	3	816	p20a9	probable transcription factor - fava bean >gi|2104681|emb|CAA66481.1|
2	4	4	817	p20a10	(AB006698) gene_id:MCL19.8~pir||T27174~similar to unknown protein [
7	10	11	818	p20a11	amino acid transport protein homolog F22I13.20 - Arabidopsis thaliana >
2	4	3	819	p20b3	
7	10	12	820	p20b4	
2	4	2	821	p20b6	DEOXYURIDINE 5'-TRIPHOSPHATE NUCLEOTIDOHYDROLASE (DU
7	10	13	822	p20b7	
2	4	1	823	p20b9	(AF051735) hypothetical protein [Picea mariana]
7	9	1	824	p20b10	
2	5	13	825	p20b12	(AP001305) syringomycin biosynthesis enzyme-like protein [Arabidopsis
7	9	2	826	p20c1	hypothetical protein F1C12.120 - Arabidopsis thaliana >gi|2982437|emb
2	5	12	827	p20c3	
7	9	3	828	p20c4	
6	4	4	829	p20c5	
3	10	11	830	p20c6	(AC015450) unknown protein; 51686-53591 [Arabidopsis thaliana]
6	4	3	831	p20c8	(AC006951) putative translation initiation factor eIF-1A [Arabidopsis thal
3	10	12	832	p20c10	(AC016447) unknown protein; 73543-72303 [Arabidopsis thaliana]
6	4	2	833	p20c12	
3	10	13	834	p20d1	(U06782) L2 [Bluetongue virus]
6	4	1	835	p20d3	(AF188844) plasma membrane aquaporin [Vitis vinifera]
3	9	1	836	p20d4	(AC011810) Putative glyceraldehyde-3-phosphate dehydrogenase [Arab
6	5	13	837	p20d8	
3	9	2	838	p20d9	(AF237589) cyclin 5 [Trypanosoma cruzi]
6	5	12	839	p20d10	(AB019229) cucumisin-like serine protease; subtilisin-like protease [Arat
3	9	3	840	p20d11	probable transmembrane protein G1p [imported] - Arabidopsis thaliana >
1	4	4	841	p20d12	(X07715) protein Po (partial) (217 is 2nd base in codon) [Homo sapiens]
8	10	11	842	p20e1	(AC010924) Identical to gb|AJ002551 heat shock protein 70 from Arabid
1	4	3	843	p20e2	(AC012328) unknown protein [Arabidopsis thaliana]
8	10	12	844	p20e5	
1	4	2	845	p20e6	(AF132157) unknown [Drosophila melanogaster]
8	10	13	846	p20e7	
1	4	1	847	p20e8	RUBISCO SUBUNIT BINDING-PROTEIN BETA SUBUNIT PRECURSC
8	9	1	848	p20e9	(AB023036) contains similarity to endo-1,3-1,4-beta-D-glucanase~gene_
1	5	13	849	p20e10	
8	9	2	850	p20e11	VACUOLAR ATP SYNTHASE SUBUNIT E (V-ATPASE E SUBUNIT) (V
1	5	12	851	p20e12	CYTOCHROME P450 93A3 (P450 CP5) >gi|7430613|pir||T07119 cytoch
8	9	3	852	p20f1	(AB005233) 6-phosphogluconate dehydrogenase [Arabidopsis thaliana]
5	4	4	853	p20f4	(AJ299248) elongation factor 2 [Nicotiana tabacum]
4	10	11	854	p20f5	PROBABLE GLUTATHIONE S-TRANSFERASE PARA (AUXIN-REGUL
5	4	3	855	p20f6	(AB012248) gb|AAD25781.1~gene_id:MXI22.10~strong similarity to unk
4	10	12	856	p20f7	
5	4	2	857	p20f8	
4	10	13	858	p20f9	hypothetical protein - castor bean >gi|1621268|emb|CAB02653.1| (Z810
5	4	1	859	p20f11	(AP002818) putative peptide transporter-like protein [Oryza sativa]
4	9	1	860	p20f12	
5	5	13	861	p20g1	serine/proline-rich protein - Arabidopsis thaliana >gi|6911861|emb|CAB7
4	9	2	862	p20g2	(AF106660) mRNA binding protein precursor [Lycopersicon esculentum]
5	5	12	863	p20g3	
4	9	3	864	p20g4	hypothetical protein DKFZp564O243.1 - human (fragment) >gi|4884084|
4	5	11	961	p20g5	(AC005698) T3P18.6 [Arabidopsis thaliana]

Block	Row	Column	ID	Name	Description
5	9	4	962	p20g8	
4	5	10	963	p20g9	(AC006200) unknown protein [Arabidopsis thaliana]
5	9	5	964	p20g11	hypothetical protein F17K2.13 - Arabidopsis thaliana >gi|2979555|gb|AA
4	5	9	965	p20h2	hypothetical protein T8M16_230 - Arabidopsis thaliana >gi|9663009|emt
5	9	6	966	p20h3	(AP000815) ESTs D47452(S12946),C23573(S10086),C19173(E10057),
4	5	8	967	p20h7	
5	9	7	968	p20h8	
4	5	7	969	p20h9	(AC006836) putative nitrilase-associated protein [Arabidopsis thaliana]
5	9	8	970	p8a3	(AF195654) SCUTL2 [Vitis vinifera]
4	5	6	971	p8a4	coat protein >gi|3702790|gb|AAC62913.1| (AF026278) coat protein [grap
5	9	9	972	p8a6	(AB019235) contains similarity to embryo-specific protein 3~gene_id:MN
8	5	11	973	p8a7	(AF200185) profilin 2 [Lilium longiflorum]
1	9	4	974	p8a8	(AL353993) putative protein [Arabidopsis thaliana]
8	5	10	975	p8a9	(AJ237989) putative ripening-related protein [Vitis vinifera]
1	9	5	976	p8a10	(AF026151) beta-ketoacyl-ACP synthase IIIB [Perilla frutescens]
8	5	9	977	p8a11	(AL353995) 14-3-3-like protein AFT1 [Arabidopsis thaliana]
1	9	6	978	p8a12	(AJ276482) putative Sec23 protein [Drosophila melanogaster]
8	5	8	979	p8b2	(AL133248) 40S ribosomal protein S2 homolog [Arabidopsis thaliana]
1	9	7	980	p8b3	(AP000600) glycolate oxidase [Arabidopsis thaliana]
8	5	7	981	p8b4	EARLY NODULIN 93 (N-93) >gi|486679|pir||S34801 nodulin N93 - soybe
1	9	8	982	p8b5	vasopressin precursor [Rattus norvegicus]
8	5	6	983	p8b7	(AP000419) zinc metalloprotease (insulinase family) [Arabidopsis thaliar
1	9	9	984	p8b11	(X54876) alpha 1 type I collagen [Mus musculus]
3	5	11	985	p8c1	(AC005396) GAST1/GASA-like protein [Arabidopsis thaliana]
6	9	4	986	p8c2	(AF123393) 26S proteasome AAA-ATPase subunit RPT4a [Arabidopsis
3	5	10	987	p8c3	(AB024029) gene_id:K21L19.10~unknown protein [Arabidopsis thaliana
6	9	5	988	p8c4	ubiquitin-conjugating enzyme UBC7 - Arabidopsis thaliana >gi|992704|g
3	5	9	989	p8c5	
6	9	6	990	p8c7	(AP000419) zinc metalloprotease (insulinase family) [Arabidopsis thaliar
3	5	8	991	p8c9	
6	9	7	992	p8c10	(AC009176) unknown protein [Arabidopsis thaliana]
3	5	7	993	p8c11	
6	9	8	994	p8d2	
3	5	6	995	p8d3	(AC002292) Phosphatidylinositol 3-kinase [Arabidopsis thaliana]
6	9	9	996	p8d4	(AF073697) cysteine synthase [Oryza sativa]
7	5	11	997	p8d6	(AF051135) putative ubiquitin activating enzyme E1 [Arabidopsis thalian
2	9	4	998	p8d8	(AF216697) NADH dehydrogenase subunit 5 [Fasciola hepatica] >gi|10
7	5	10	999	p8e1	
2	9	5	1000	p8e2	(AF108140) gamete-specific homeodomain protein GSP1 [Chlamydomo
7	5	9	1001	p8e3	
2	9	6	1002	p8e5	
7	5	8	1003	p8e6	
2	9	7	1004	p8e7	(AB025000) multicatalytic endopeptidase complex [Cicer arietinum]
7	5	7	1005	p8e9	(AJ237990) putative metallothionein-like protein [Vitis vinifera]
2	9	8	1006	p8e10	
7	5	6	1007	p8e11	S-ADENOSYLMETHIONINE SYNTHETASE 1 (METHIONINE ADENOS
2	9	9	1008	p8f1	(AC004557) F17L21.10 [Arabidopsis thaliana]
2	5	11	1009	p8f2	(AP002071) Similar to Antirrhinum majus transposon Tam3 gene; transp
7	9	4	1010	p8f3	
2	5	10	1011	p8f5	(AC002291) similar to &#034tub&#034 protein gp|U82468|2072162 [Ara
7	9	5	1012	p8f8	(AC002291) similar to &#034tub&#034 protein gp|U82468|2072162 [Ara
2	5	9	1013	p8f9	(AC011620) putative protein phosphatase-2C [Arabidopsis thaliana]
7	9	6	1014	p8f10	
2	5	8	1015	p8f11	ubiquitin / ribosomal protein CEP52 - Arabidopsis thaliana >gi|166930|gb
7	9	7	1016	p8g1	(Y14432) NAD-dependent isocitrate dehydrogenase [Nicotiana tabacum
2	5	7	1017	p8g2	actin-like protein - fission yeast (Schizosaccharomyces pombe) >gi|5051
7	9	8	1018	p8g3	(AF184164) transaldolase [Lycopersicon esculentum]
2	5	6	1019	p8g4	(AJ131733) ubiquitin-conjugating enzyme E2 [Pseudotsuga menziesii]
7	9	9	1020	p8g5	protein kinase >gi|1869835|emb|CAB06773.1| (Z86099) protein kinase [
6	5	11	1021	p8g6	
3	9	4	1022	p8g7	ANTER-SPECIFIC PROLINE-RICH PROTEIN APG (PROTEIN CEX) >g
6	5	10	1023	p8g8	(AF139499) unknown [Prunus armeniaca]
3	9	5	1024	p8g9	hypothetical protein T19P19.170 - Arabidopsis thaliana >gi|3080447|eml
6	5	9	1025	p8g10	(AC011001) Hypothetical protein [Arabidopsis thaliana]
3	9	6	1026	p8g11	(U92815) heat shock protein 70 precursor [Citrullus lanatus]
6	5	8	1027	p8g12	EUKARYOTIC TRANSLATION INITIATION FACTOR 4E (EIF-4E) (EIF4
3	9	7	1028	p8h1	hypothetical protein M7J2.190 - Arabidopsis thaliana >gi|2980806|emb|C

Block	Row	Column	ID	Name	Description
6	5	7	1029	p8h2	(Z99707) putative protein [Arabidopsis thaliana] >gi|7270713|emb|CAB8
3	9	8	1030	p8h3	(AF128482) NADH dehydrogenase subunit 2 [Calotes calotes]
6	5	6	1031	p8h4	(D11443) polyprotein precursor [Hepatitis C virus] >gi|745386|prf||20162
3	9	9	1032	p8h7	(AL353819) hypothetical protein [Neurospora crassa]
1	5	11	1033	p8h8	conserved hypothetical secreted protein HP0949 - Helicobacter pylori (s
8	9	4	1034	p8h9	(AF014396) Snakin-1 [Solanum tuberosum]
1	5	10	1035	p8h10	(AB010981) photosynthetic reaction center L subunit [Erythrobacter litor
8	9	5	1036	p8h11	(AF195863) lipid transfer protein precursor [Gossypium hirsutum]
1	5	9	1037	p8h12	late-embryogenesis protein lea5 - common tobacco >gi|2981167|gb|AA(
8	9	6	1038	p15a1	
1	5	8	1039	p15a3	
8	9	7	1040	p15a4	(AJ237985) putative ripening-related protein [Vitis vinifera]
1	5	7	1041	p15a8	PROTEIN DISULFIDE ISOMERASE PRECURSOR (PDI) >gi|2146797|p
8	9	8	1042	p15a12	
1	5	6	1043	p15b2	(AF092168) signal recognition particle 54 kDa subunit precursor [Arabid
8	9	9	1044	p15b3	
5	5	11	1045	p15b4	
4	9	4	1046	p15b6	methylenetetrahydrofolate dehydrogenase (NADP+) (EC 1.5.1.5) / meth
5	5	10	1047	p15b9	
4	9	5	1048	p15b10	
5	5	9	1049	p15b11	
4	9	6	1050	p15b12	hypothetical protein F22K18.270 - Arabidopsis thaliana >gi|4220537|eml
5	5	8	1051	p15c1	(AC000132) EST gb|ATTS2829 comes from this gene. [Arabidopsis thal
4	9	7	1052	p15c2	
5	5	7	1053	p15c3	
4	9	8	1054	p15c5	(AC008017) Transcription Factor [Arabidopsis thaliana]
5	5	6	1055	p15c9	(AJ223252) UDP-glucose:protein transglucosylase [Solanum tuberosum
4	9	9	1056	p15d3	
4	5	5	1057	p15d5	
5	9	10	1058	p15d6	
4	5	4	1059	p15d7	
5	9	11	1060	p15d9	GASA4 - Arabidopsis thaliana >gi|2764941|emb|CAA66909.1| (X98255)
4	5	3	1061	p15d10	
5	9	12	1062	p15d11	(AC007202) Is a member of the PF|00171 aldehyde dehydrogenase fam
4	5	2	1063	p15d12	
5	9	13	1064	p15e2	(AB015861) photosystem I subunit PSI-L [Arabidopsis thaliana]
4	5	1	1065	p15e6	ABA stress ripening protein - common ice plant >gi|3064035|gb|AAC141
5	8	1	1066	p15e11	
4	6	13	1067	p15e12	
5	8	2	1068	p15f2	(AF298769) 40S ribosomal protein S24 [Zea mays]
8	5	5	1069	p15f3	(AB009885) wound inducive gene [Nicotiana tabacum]
1	9	10	1070	p15f12	
8	5	4	1071	p15g2	
1	9	11	1072	p15g3	CHALCONE--FLAVONONE ISOMERASE (CHALCONE ISOMERASE) :
8	5	3	1073	p15g5	
1	9	12	1074	p15g7	
8	5	2	1075	p15g10	
1	9	13	1076	p15g11	(AC006282) putative giberellin beta-hydroxylase [Arabidopsis thaliana]
8	5	1	1077	p15g12	small nuclear ribonucleoprotein T30B22.5 - Arabidopsis thaliana >gi|373
1	8	1	1078	p15h3	
8	6	13	1079	p15h4	BAX INHIBITOR-1 (BI-1) (ATBI-1) >gi|7209774|dbj|BAA89541.2| (AB02
1	8	2	1080	p15h6	
3	5	5	1081	p15h8	(AJ237995) putative ripening-related P-450 enzyme [Vitis vinifera]
6	9	10	1082	p15h10	
3	5	4	1083	p15h11	NADH-UBIQUINONE OXIDOREDUCTASE 20 KDA SUBUNIT PRECUR
6	9	11	1084	p15h12	
3	5	3	1085	p9a1	RNA dependent RNA polymerase [Leishmania RNA virus 1-1] >gi|32147
6	9	12	1086	p9a7	probable cytochrome P450 monooxygenase - maize (fragment) >gi|299
3	5	2	1087	p9a8	
6	9	13	1088	p9a9	(AB006696) emb|CAB71880.1~gene_id:MAF19.18~similar to unknown p
3	5	1	1089	p9a10	
6	8	1	1090	p9a11	
3	6	13	1091	p9b4	ribosomal protein S27 - Arabidopsis thaliana >gi|4193382|gb|AAD10029
6	8	2	1092	p9b6	(AC006743) contains similarity to Pfam family PF01391 (Collagen triple
7	5	5	1093	p9c5	protein kinase-like protein - Arabidopsis thaliana >gi|6967109|emb|CAB
2	9	10	1094	p9c12	ATP-dependent protease proteolytic subuni [Nicotiana tabacum] >gi|116
7	5	4	1095	p9d1	(AJ271079) hypothetical protein [Oenothera elata subsp. hookeri] >gi|67

Block	Row	Column	ID	Name	Description
2	9	11	1096	p9d6	(AC010924) Contains similarity to gb|AF181686 membrane protein TMS
7	5	3	1097	p9e1	
2	9	12	1098	p9e3	probable cytochrome P450 monooxygenase - maize (fragment) >gi|299
7	5	2	1099	p9e4	CYTOCHROME C1, HEME PROTEIN PRECURSOR (CLONE PC13III)
2	9	13	1100	p9e5	hypothetical protein 68B2.90 [imported] - Neurospora crassa >gi|763581
7	5	1	1101	p9e6	(AB010077) thaumatin-like protein [Arabidopsis thaliana]
2	8	1	1102	p9e7	
7	6	13	1103	p9f2	probable cytochrome P450 monooxygenase - maize (fragment) >gi|299
2	8	2	1104	p9f4	
2	5	5	1105	p9f5	(AF002109) unknown protein [Arabidopsis thaliana]
7	9	10	1106	p9f6	ribosomal protein L2 - evening primrose mitochondrion >gi|516394|emb|
2	5	4	1107	p9f7	(AC007017) putative homeodomain transcription factor [Arabidopsis tha
7	9	11	1108	p9f9	(AC009325) unknown protein [Arabidopsis thaliana]
2	5	3	1109	p9f10	(AB048248) gamma tonoplast intrinsic protein [Pyrus communis]
7	9	12	1110	p9f11	hypothetical protein APES063 - Aeropyrum pernix (strain K1) >gi|51056
2	5	2	1111	p9g5	
7	9	13	1112	p9g6	(AB015468) peptidylprolyl isomerase [Arabidopsis thaliana]
2	5	1	1113	p9g7	
7	8	1	1114	p9g10	
2	6	13	1115	p9g11	(AB022219) gb|AAF19538.1~gene_id:MKP6.24~similar to unknown prot
7	8	2	1116	p9h1	(AC006955) putative retroelement pol polyprotein [Arabidopsis thaliana]
6	5	5	1117	p9h2	(AB022222) gene_id:MUD12.5~ref|NP_009841.1~similar to unknown pr
3	9	10	1118	p9h4	PHOTOSYSTEM I REACTION CENTRE SUBUNIT II PRECURSOR (PI
6	5	4	1119	p9h5	(AC016827) putative mudrA protein [Arabidopsis thaliana]
3	9	11	1120	p9h8	(AC004077) hypothetical protein [Arabidopsis thaliana]
6	5	3	1121	p9h9	GLUCAN ENDO-1,3-BETA-GLUCOSIDASE PRECURSOR ((1->3)-BET
3	9	12	1122	p9h10	
6	5	2	1123	p9h11	polyketide synthase pksE - Mycobacterium leprae >gi|467207|gb|AAA17
3	9	13	1124	p2a1	(U20948) receptor protein kinase [Ipomoea trifida]
6	5	1	1125	p2a2	(AF195865) lipid transfer protein precursor [Gossypium hirsutum]
3	8	1	1126	p2a3	
6	6	13	1127	p2a4	
3	8	2	1128	p2a5	
1	5	5	1129	p2a11	hypothetical protein MAL3P4.14 - Plasmodium falciparum >gi|4725990|e
8	9	10	1130	p2a12	
1	5	4	1131	p2b1	(AL138647) putative protein [Arabidopsis thaliana]
8	9	11	1132	p2b2	(AC006837) transfactor-like protein [Arabidopsis thaliana]
1	5	3	1133	p2b3	ubiquitin carrier protein >gi|2501433|sp|Q16763|UBCE_HUMAN UBIQUI
8	9	12	1134	p2b6	(Y18930) dTDP-glucose 4,6-dehydratase [Sulfolobus solfataricus]
1	5	2	1135	p2b7	
8	9	13	1136	p2b8	vacuolar invertase 2, GIN2 [Vitis vinifera=grape berries, Sultana, berries
1	5	1	1137	p2b9	
8	8	1	1138	p2b12	(AF072931) chlorophyll a/b binding protein [Medicago sativa]
1	6	13	1139	p2c1	(AC006526) unknown protein [Arabidopsis thaliana]
8	8	2	1140	p2c2	pectinesterase (EC 3.1.1.11) PECS-c1 - sweet orange >gi|2098711|gb|A
5	5	5	1141	p2c3	(AC011620) putative 60S ribosomal protein L22 [Arabidopsis thaliana]
4	9	10	1142	p2c4	(AF034578) fizzy1 [Xenopus laevis]
5	5	4	1143	p2c5	(AC007258) Putative Aldo/keto reductase [Arabidopsis thaliana]
4	9	11	1144	p2c6	(AL162875) fatty acid elongase-like protein [Arabidopsis thaliana]
5	5	3	1145	p2c7	UBIQUITIN-CONJUGATING ENZYME E2-17 KD 8 (UBIQUITIN-PROTE
4	9	12	1146	p2c8	(AJ011894) cyclin D3.2 protein [Nicotiana tabacum]
5	5	2	1147	p2c10	(AF204967) histone H2A [Arabidopsis thaliana] >gi|7595339|gb|AAF644
4	9	13	1148	p2c11	hypothetical protein F6I7.20 - Arabidopsis thaliana >gi|4678260|emb|CA
5	5	1	1149	p2d1	(AF057144) signal peptidase [Arabidopsis thaliana]
4	8	1	1150	p2d5	HYPOTHETICAL 20.5 KDA PROTEIN IN CRCB-LIPA INTERGENIC RE
5	6	13	1151	p2d6	hypothetical protein ydaQ - Bacillus subtilis >gi|1881245|dbj|BAA19272.
4	8	2	1152	p2d7	
4	6	12	1153	p2d10	RER1B PROTEIN (ATRER1B) >gi|2865177|dbj|BAA24804.1| (AB01094
5	8	3	1154	p2d11	(AB012639) light harvesting chlorophyll a/b-binding protein [Nicotiana sy
4	6	11	1155	p2e1	
5	8	4	1156	p2e2	(AC008148) Unknown protein [Arabidopsis thaliana] >gi|6453883|gb|AAI
4	6	10	1157	p2e3	
5	8	5	1158	p2e5	
4	6	9	1159	p2e6	(AC020646) T32E20.29 [Arabidopsis thaliana]
5	8	6	1160	p2e7	
4	6	8	1161	p2e8	(AL049730) putative protein [Arabidopsis thaliana] >gi|7267961|emb|CA
5	8	7	1162	p2e9	

Block	Row	Column	ID	Name	Description
4	6	7	1163	p2e11	(AC016795) unknown protein [Arabidopsis thaliana]
5	8	8	1164	p2f2	(L41833) polymorphic immunodominant molecule [Theileria parva]
8	6	12	1165	p2f3	TUBULIN ALPHA CHAIN >gi|486847|pir||S36232 tubulin alpha chain - a
1	8	3	1166	p2f5	hypothetical protein F28A23.200 - Arabidopsis thaliana >gi|2911058|eml
8	6	11	1167	p2f6	(L24497) ribulose 1,5-bisphosphate carboxylase small subunit [Malus dc
1	8	4	1168	p2f7	PHOTOSYSTEM I REACTION CENTRE SUBUNIT IV PRECURSOR (P
8	6	10	1169	p2f8	(AF139466) chlorophyll a/b binding protein CP29 [Vigna radiata]
1	8	5	1170	p2f9	(AC008017) Unknown protein [Arabidopsis thaliana]
8	6	9	1171	p2f10	
1	8	6	1172	p2f11	hypothetical protein F19H22.140 - Arabidopsis thaliana >gi|4539323|eml
8	6	8	1173	p2f12	probable chlorophyll a/b-binding protein type III precursor - garden pea c
1	8	7	1174	p2g1	(Y08161) aquaporin 1 [Nicotiana tabacum]
8	6	7	1175	p2g2	(AF020709) chalcone synthase [Vitis vinifera]
1	8	8	1176	p2g3	TUBULIN BETA-7 CHAIN >gi|320188|pir||JQ1591 tubulin beta-7 chain -
3	6	12	1177	p2g4	
6	8	3	1178	p2g5	(AL160371) possible rv3532 [Leishmania major]
3	6	11	1179	p2g7	
6	8	4	1180	p2g9	
3	6	10	1181	p2g11	probable ribosomal protein L9 - rice (fragment) >gi|971282|dbj|BAA0720
6	8	5	1182	p2g12	SUBTILISIN-CHYMOTRYPSIN INHIBITOR CI-1A >gi|82381|pir||JA0181
3	6	9	1183	p2h3	hypothetical protein F17L22.80 - Arabidopsis thaliana >gi|4455270|emb|
6	8	6	1184	p2h4	probable proteinase inhibitor SE60 precursor - soybean >gi|509769|emb
3	6	8	1185	p2h5	CHALCONE SYNTHASE 1 (NARINGENIN-CHALCONE SYNTHASE 1)
6	8	7	1186	p2h6	(AP000370) emb|CAA17570.1~gene_id:K15M2.13~similar to unknown p
3	6	7	1187	p2h7	(AC026875) T6D22.7 [Arabidopsis thaliana]
6	8	8	1188	p2h8	(AL132966) splicing factor-like protein [Arabidopsis thaliana]
7	6	12	1189	p2h9	(AC021640) putative phosphatidate phosphohydrolase [Arabidopsis thal
2	8	3	1190	p2h10	ATP SYNTHASE B' CHAIN PRECURSOR (SUBUNIT II) >gi|479533|pir|
7	6	11	1191	p2h11	(D85027) integral membrane protein [Thermus sp. A4]
2	8	4	1192	p2h12	
7	6	10	1193	p7a1	hypothetical protein T19F6.120 - Arabidopsis thaliana >gi|2262104|gb|A
2	8	5	1194	p7a2	(AL365234) embryonic abundant protein-like [Arabidopsis thaliana]
7	6	9	1195	p7a3	(AF065555) envelope glycoprotein; gp120 [Human immunodeficiency vi
2	8	6	1196	p7a5	PHOTOSYSTEM II 5 KD PROTEIN PRECURSOR (PSII-T) (LIGHT-RE(
7	6	8	1197	p7a6	(AC020646) T32E20.27 [Arabidopsis thaliana]
2	8	7	1198	p7a7	
7	6	7	1199	p7a8	(AE003614) CG13770 gene product [Drosophila melanogaster]
2	8	8	1200	p7a9	(AF228877) unknown [Strongylocentrotus purpuratus]
2	6	12	1201	p7a10	(AB018119) dolichyl-di-phosphooligosaccharide-protein glycotransferase
7	8	3	1202	p7a12	HOMEOBOX PROTEIN GSH-2 >gi|2143479|pir||I57039 genomic screen
2	6	11	1203	p7b1	(AJ245866) photosystem I subunit X precursor [Arabidopsis thaliana]
7	8	4	1204	p7b2	cell proliferation antigen Ki-67 - mouse >gi|1177528|emb|CAA58026.1| (
2	6	10	1205	p7b3	(AF112440) ribosomal protein S26 [Pisum sativum]
7	8	5	1206	p7b4	(AL356014) putative protein [Arabidopsis thaliana]
2	6	9	1207	p7b6	(AC007169) putative glyoxalase II [Arabidopsis thaliana]
7	8	6	1208	p7b7	(AB021790) metallothionein-like protein [Pyrus pyrifolia]
2	6	8	1209	p7c3	
7	8	7	1210	p7c5	(U79114) auxin-binding protein ABP19 [Prunus persica]
2	6	7	1211	p7c11	urPAB protein precursor - Peptostreptococcus magnus >gi|854371|emb|
7	8	8	1212	p7c12	
6	6	12	1213	p7d1	(AL161574) RIBOSOMAL PROTEIN S30 homolog [Arabidopsis thaliana
3	8	3	1214	p7d2	hypothetical protein PH1964 - Pyrococcus horikoshii >gi|3258408|dbj|BA
6	6	11	1215	p7d3	transcription activator of D-serine dehydratase - Escherichia coli >gi|145
3	8	4	1216	p7d4	hypothetical protein F22D6.5 - Caenorhabditis elegans >gi|3876247|emb
6	6	10	1217	p7d6	peroxidase (EC 1.11.1.7) 2, cationic - soybean >gi|3982596|gb|AAC834(
3	8	5	1218	p7d7	proline-rich proteoglycan 2 precursor, parotid - rat >gi|310200|gb|AAA03
6	6	9	1219	p7d8	60S RIBOSOMAL PROTEIN L27A >gi|2129719|pir||S71256 ribosomal p
3	8	6	1220	p7d9	(AF139468) photosystem I reaction center subunit III [Vigna radiata]
6	6	8	1221	p7e1	(AB026647) emb|CAB71043.1~gene_id:MJL12.8~similar to unknown pr
3	8	7	1222	p7e2	(AB028132) Dof zinc finger protein [Oryza sativa]
6	6	7	1223	p7e3	ADR11-2 protein - soybean (fragment) >gi|296443|emb|CAA49341.1| (X
3	8	8	1224	p7e5	glycine-rich protein - common sainfoin >gi|2565429|gb|AAB82000.1| (AF
1	6	12	1225	p7e6	(AL034558) predicted using hexExon; MAL3P2.8 (PFC0195w), Hypothe
8	8	3	1226	p7e7	(AB012243) gene_id:MIJ24.6~ref|NP_013897.1~similar to unknown prot
1	6	11	1227	p7f2	hypothetical protein 937 - citrus tatter leaf virus (fragment) >gi|563955|dl
8	8	4	1228	p7f3	PEPTIDYL-PROLYL CIS-TRANS ISOMERASE (PPIASE) (ROTAMASE
1	6	10	1229	p7f6	histone H4 (TH091) - wheat >gi|170747|gb|AAA34292.1| (M12277) histo

Block	Row	Column	ID	Name	Description
8	8	5	1230	p7f8	(AB011483) gene_id:MUF9.9~unknown protein [Arabidopsis thaliana]
1	6	9	1231	p7f9	(AC015986) putative receptor kinase [Arabidopsis thaliana]
8	8	6	1232	p7f10	MYOSIN HEAVY CHAIN, NONMUSCLE TYPE A (CELLULAR MYOSIN
1	6	8	1233	p7f11	
8	8	7	1234	p7f12	hypothetical protein T27I1.4 - Arabidopsis thaliana >gi|3540181|gb|AAC:
1	6	7	1235	p7g1	(AF109693) allergen-like protein BRSn20 [Sambucus nigra]
8	8	8	1236	p7g2	(AL132969) peroxiredoxin-like protein [Arabidopsis thaliana]
5	6	12	1237	p7g3	hypothetical protein F22K18.300 - Arabidopsis thaliana >gi|4220540|eml
4	8	3	1238	p7g5	(AC024202) contains similarity to Escherichia ecoli hypothetical protein
5	6	11	1239	p7g8	histone H3 - garden pea >gi|82610|pir||S00373 histone H3 - wheat
4	8	4	1240	p7g12	translation elongation factor EF-Tu precursor, mitochondrial - Arabidops
5	6	10	1241	p7h3	(Y00759) 20 kDa protein (AA 1-212) [Spinacia oleracea]
4	8	5	1242	p7h4	
5	6	9	1243	p7h5	(AF155232) extensin [Pisum sativum]
4	8	6	1244	p7h6	(AJ133439) GRIP1 protein [Homo sapiens]
5	6	8	1245	p7h9	(AF039662) ferredoxin-like protein [Capsicum annuum]
4	8	7	1246	p7h11	(AF248055) proline-rich protein [Glycine max]
5	6	7	1247	p7h12	
4	8	8	1248	p1f3	ribosomal protein L32, cytosolic - Arabidopsis thaliana >gi|5816996|emb
4	6	6	1249	p1a2	zinc-finger protein Lsd1 - Arabidopsis thaliana >gi|1872521|gb|AAC4966
5	13	2	1250	p1a9	50S RIBOSOMAL PROTEIN L27, CHLOROPLAST PRECURSOR (CL2
4	6	5	1251	p1a10	(AB026646) gb|AAF26109.1~gene_id:MIG5.8~similar to unknown protei
5	13	3	1252	p1b3	(AF121355) peroxiredoxin TPx1 [Arabidopsis thaliana] >gi|6227022|gb|A
4	6	4	1253	p1b5	adenylate translocator brittle-1 homolog F8B4.100 - Arabidopsis thaliana
5	13	4	1254	p1b10	(AB026646) gb|AAF26109.1~gene_id:MIG5.8~similar to unknown protei
4	6	3	1255	p1b11	mipC protein - common ice plant >gi|1657948|gb|AAB18227.1| (U73466
5	13	5	1256	p1c5	hypothetical protein APE2320 - Aeropyrum pernix (strain K1) >gi|510602
4	6	2	1257	p1e1	POLYPHENOL OXIDASE PRECURSOR (PPO) (CATECHOL OXIDASE
5	13	6	1258	p1e11	hypothetical protein F17A8.20 - Arabidopsis thaliana >gi|4538897|emb|C
4	6	1	1259	p1f2	(AF085279) hypothetical EIF-2-Alpha [Arabidopsis thaliana]
5	13	7	1260	p1f8	(AB022223) kinase-like protein [Arabidopsis thaliana]
8	6	6	1261	p1g2	(AL132965) 60S RIBOSOMAL PROTEIN-like [Arabidopsis thaliana]
1	13	2	1262	p1g3	(AC009918) unknown protein [Arabidopsis thaliana] >gi|9502172|gb|AAF
8	6	5	1263	p1g7	(AL138652) putative protein [Arabidopsis thaliana]
1	13	3	1264	p1g9	hypothetical protein F19B15.190 - Arabidopsis thaliana >gi|4972062|eml
8	6	4	1265	p1h2	(AC002343) unknown protein [Arabidopsis thaliana]
1	13	4	1266	p1h7	(AF206324) putative DNA binding protein [Arabidopsis thaliana] >gi|776
8	6	3	1267	p1h9	(AF139499) unknown [Prunus armeniaca]
1	13	5	1268	p3b10	ZEAXANTHIN EPOXIDASE PRECURSOR >gi|7489081|pir||T07754 zea
8	6	2	1269	p3c10	hypothetical protein F20M13.250 - Arabidopsis thaliana >gi|4467156|em
1	13	6	1270	p3d4	(Y09314) Rab2-like protein [Arabidopsis thaliana] >gi|5281023|emb|CAE
8	6	1	1271	p3e4	(AJ276420) 68 kDa protein [Cicer arietinum]
1	13	7	1272	p3e5	(AE003635) CG6618 gene product [Drosophila melanogaster]
3	6	6	1273	p3e9	(AC004667) unknown protein [Arabidopsis thaliana]
6	13	2	1274	p3f5	(AF136539) YABBY2 [Arabidopsis thaliana]
3	6	5	1275	p3h1	hypothetical protein c0113 - Sulfolobus solfataricus >gi|1707743|emb|C/
6	13	3	1276	p3h4	
3	6	4	1277	p4b2	(AL161503) UV-damaged DNA binding factor-like protein [Arabidopsis th
6	13	4	1278	p4c4	(AJ130885) xyloglucan endotransglycosylase 1 [Fagus sylvatica]
3	6	3	1279	p4c10	(AC002329) unknown protein [Arabidopsis thaliana]
6	13	5	1280	p4d1	(AB019228) serine/threonine protein kinase [Arabidopsis thaliana]
3	6	2	1281	p4d5	non-functional folate binding protein >gi|2565196|gb|AAB81938.1| (AF0(
6	13	6	1282	p4d10	proton pump interactor - Arabidopsis thaliana >gi|4972075|emb|CAB438
3	6	1	1283	p4e2	(AB008848) Csf-3 [Cucumis sativus]
6	13	7	1284	p4e3	chalcone isomerase (EC 5.5.1.6) - apple tree (fragment) >gi|19587|emb|
7	6	6	1285	p4e12	(AP002030) gene_id:K16F4.10~pir||T00468~similar to unknown protein
2	13	2	1286	p4g1	(AL133314) arm repeat containing protein homolog [Arabidopsis thaliana
7	6	5	1287	p4g10	(AB022220) contains similarity to diaminopimelate decarboxylase~gene
2	13	3	1288	p4h6	(AL162973) protein kinase-like [Arabidopsis thaliana]
7	6	4	1289	p5a4	hypothetical protein T5L19.200 - Arabidopsis thaliana >gi|4539010|emb|
2	13	4	1290	p5a7	(AC012562) hypothetical protein [Arabidopsis thaliana]
7	6	3	1291	p5a11	(AL109787) putative protein [Arabidopsis thaliana] >gi|7269979|emb|CA
2	13	5	1292	p5d9	cryptogene protein G4 - Leishmania tarentolae (strain LEM125)
7	6	2	1293	p5f1	cytochrome P450 homolog F23K16.110 - Arabidopsis thaliana >gi|5042
2	13	6	1294	p5f6	
7	6	1	1295	p5f9	HYPOTHETICAL PROTEIN HI1671 >gi|1074892|pir||I64039 hypothetica
2	13	7	1296	p5g7	(U93872) ORF 73, contains large complex repeat CR 73 [Kaposi's sarcc

Block	Row	Column	ID	Name	Description
2	6	6	1297	p5g10	
7	13	2	1298	p5h5	
2	6	5	1299	p5h6	METABOTROPIC GLUTAMATE RECEPTOR 1 >gi|1850987|gb|AAB48(
7	13	3	1300	p5h8	
2	6	4	1301	p6a6	(AF145647) BcDNA.GH08312 [Drosophila melanogaster] >gi|7301992|g
7	13	4	1302	p6a7	(AC021640) unknown protein [Arabidopsis thaliana]
2	6	3	1303	p6b6	(AC009322) Hypothetical protein [Arabidopsis thaliana] >gi|6453851|gb|
7	13	5	1304	p6c10	1-AMINOCYCLOPROPANE-1-CARBOXYLATE OXIDASE (ACC OXIDA
2	6	2	1305	p6d7	(U32474) putative heat shock protein [Treponema phagedenis]
7	13	6	1306	p6d8	(AB024035) gb|AAD55473.1~gene_id:MHM17.18~similar to unknown pr
2	6	1	1307	p6e2	(AF138264) papain-like cysteine proteinase isoform I [Ipomoea batatas]
7	13	7	1308	p6e9	(AL359782) hypothetical protein, CHR1.200. [Trypanosoma brucei]
6	6	6	1309	p6f11	UTP--GLUCOSE-1-PHOSPHATE URIDYLYLTRANSFERASE (UDP-GL
3	13	2	1310	p6f12	MITOCHONDRIAL FORMATE DEHYDROGENASE PRECURSOR (NAI
6	6	5	1311	p6g1	
3	13	3	1312	p6g2	conserved hypothetical protein - Thermotoga maritima (strain MSB8) >g
6	6	4	1313	p6g5	hypothetical protein ykrT - Bacillus subtilis >gi|2633727|emb|CAB13229.
3	13	4	1314	p6g11	(AC005916) Strong similarity to gb|Y18349 U2 snRNP auxiliary factor, s
6	6	3	1315	p6h2	(AB019229) serine protease-like protein [Arabidopsis thaliana]
3	13	5	1316	p10a9	(AC007197) dynamin-like protein [Arabidopsis thaliana]
6	6	2	1317	p10c2	
3	13	6	1318	p10d4	subtilisin-like proteinase (EC 3.4.21.-), nodule-specific - Arabidopsis thal
6	6	1	1319	p10d10	conserved hypothetical protein CP1049 [imported] - Chlamydophila pneı
3	13	7	1320	p10e3	
1	6	6	1321	p10g5	proline-rich protein, 14K - kidney bean >gi|1420885|gb|AAC49369.1| (U3
8	13	2	1322	p10h11	
1	6	5	1323	p10h12	AMV259 [Amsacta moorei entomopoxvirus] >gi|9944782|gb|AAG02965.
8	13	3	1324	p11a6	(AB026639) emb|CAB16809.1~gene_id:K21L13.17~similar to unknown
1	6	4	1325	p11d9	(AJ277086) protein phosphatase 2C [Nicotiana tabacum]
8	13	4	1326	p11d12	(AC002130) F1N21.10 [Arabidopsis thaliana]
1	6	3	1327	p11e8	hypothetical protein F1P2.170 - Arabidopsis thaliana >gi|6522545|emb|C
8	13	5	1328	p11g9	
1	6	2	1329	p11g11	(AF194174) alcohol dehydrogenase 2 [Vitis vinifera]
8	13	6	1330	p12b10	(Y10024) ubiquitin extension protein [Solanum tuberosum]
1	6	1	1331	p12d1	(AF224337) beta-1 integrin [Ictalurus punctatus]
8	13	7	1332	p12e8	(AB042860) ribosomal protein L29 [Panax ginseng]
5	6	6	1333	p12e10	(AF071893) AP2 domain containing protein [Prunus armeniaca]
4	13	2	1334	p12e12	(AL353822) hypothetical protein [Neurospora crassa]
5	6	5	1335	p12f1	ADP-ribosylation factor-like protein - Arabidopsis thaliana >gi|6899939|e
4	13	3	1336	p12f6	(U64925) NTGP4 [Nicotiana tabacum]
5	6	4	1337	p12f12	
4	13	4	1338	p12h5	26S PROTEASOME REGULATORY SUBUNIT S3 (NUCLEAR ANTIGE
5	6	3	1339	p13c12	
4	13	5	1340	p13e1	(AF135596) Skp1 [Medicago sativa]
5	6	2	1341	p13e4	(AC007260) lcl|prt_seq No definition line found [Arabidopsis thaliana]
4	13	6	1342	p13e12	(AF090446) unknown [Zea mays]
5	6	1	1343	p13g5	(AJ299061) hypothetical protein [Cicer arietinum]
4	13	7	1344	p13h3	
4	7	13	1345	p14a1	hypothetical protein T18E12.21 - Arabidopsis thaliana >gi|3548818|gb|A
5	13	8	1346	p14b12	(AB006703) gb|AAD10667.1~gene_id:MRH10.15~similar to unknown pr
4	7	12	1347	p14c9	
5	13	9	1348	p14d5	probable methylmalonate-semialdehyde dehydrogenase (acylating) (EC
4	7	11	1349	p14g11	(AC022455) hydrophilic protein, putative; 29542-30030 [Arabidopsis thal
5	13	10	1350	p17b1	
4	7	10	1351	p17b2	cytochrome-c oxidase (EC 1.9.3.1) chain III - Trypanosoma brucei mitoc
5	13	11	1352	p17c8	
4	7	9	1353	p17d5	(AJ271439) plasma membrane H+ ATPase [Prunus persica]
5	13	12	1354	p17h1	(AP001300) pyruvate kinase [Arabidopsis thaliana]
4	7	8	1355	p18b1	(AF275639) cytosolic phosphoglycerate kinase [Pisum sativum]
5	13	13	1356	p18d1	(AC005311) hypothetical protein [Arabidopsis thaliana]
8	7	13	1357	p18d6	PHOSPHOGLYCERATE KINASE, CYTOSOLIC >gi|7434547|pir||T0366
1	13	8	1358	p18d9	
8	7	12	1359	p18d12	chlorophyll a/b-binding protein type III precursor - tomato >gi|226872|prf|
1	13	9	1360	p18g4	(AC011438) T23G18.10 [Arabidopsis thaliana]
8	7	11	1361	p18f3	(AC009978) T23E18.6 [Arabidopsis thaliana]
1	13	10	1362	p18f4	
8	7	10	1363	p19g10	(AB024024) gene_id:K15C23.10~unknown protein [Arabidopsis thaliana

Block	Row	Column	ID	Name	Description
1	13	11	1364	p19h4	(AL161514) putative protein [Arabidopsis thaliana]
8	7	9	1365	p19h8	(AC007190) F23N19.15 [Arabidopsis thaliana]
1	13	12	1366	p20h9	(AC006836) putative nitrilase-associated protein [Arabidopsis thaliana]
8	7	8	1367	p20a6	cellulase (EC 3.2.1.4) F16B22.6 - Arabidopsis thaliana >gi|3341677|gb|A
1	13	13	1368	p20b3	
3	7	13	1369	p20b12	(AP001305) syringomycin biosynthesis enzyme-like protein [Arabidopsis
6	13	8	1370	p20c3	
3	7	12	1371	p20c8	(AC006951) putative translation initiation factor eIF-1A [Arabidopsis thal
6	13	9	1372	p20f1	(AB005233) 6-phosphogluconate dehydrogenase [Arabidopsis thaliana]
3	7	11	1373	p20f5	PROBABLE GLUTATHIONE S-TRANSFERASE PARA (AUXIN-REGUL
6	13	10	1374	p20f8	
3	7	10	1375	p20f11	(AP002818) putative peptide transporter-like protein [Oryza sativa]
6	13	11	1376	p20g5	(AC005698) T3P18.6 [Arabidopsis thaliana]
3	7	9	1377	p20h2	hypothetical protein T8M16_230 - Arabidopsis thaliana >gi|9663009|emb
6	13	12	1378	p8c5	
3	7	8	1379	p8c11	
6	13	13	1380	p8d4	(AF073697) cysteine synthase [Oryza sativa]
7	7	13	1381	p8e10	
2	13	8	1382	p8f2	(AP002071) Similar to Antirrhinum majus transposon Tam3 gene; transp
7	7	12	1383	p8g10	(AC011001) Hypothetical protein [Arabidopsis thaliana]
2	13	9	1384	p15b3	
7	7	11	1385	p15b4	
2	13	10	1386	p15b12	hypothetical protein F22K18.270 - Arabidopsis thaliana >gi|4220537|emb
7	7	10	1387	p15d5	
2	13	11	1388	p15f3	(AB009885) wound inducive gene [Nicotiana tabacum]
7	7	9	1389	p15g12	small nuclear ribonucleoprotein T30B22.5 - Arabidopsis thaliana >gi|373
2	13	12	1390	p2b7	
7	7	8	1391	p2f10	
2	13	13	1392	p2f12	probable chlorophyll a/b-binding protein type III precursor - garden pea c
2	7	13	1393	p2g7	
7	13	8	1394	p2g11	probable ribosomal protein L9 - rice (fragment) >gi|971282|dbj|BAA0720
2	7	12	1395	p2g12	SUBTILISIN-CHYMOTRYPSIN INHIBITOR CI-1A >gi|82381|pir||JA0181
7	13	9	1396	p2h7	(AC026875) T6D22.7 [Arabidopsis thaliana]
2	7	11	1397	p7c12	
7	13	10	1398	p7f10	MYOSIN HEAVY CHAIN, NONMUSCLE TYPE A (CELLULAR MYOSIN
2	7	10	1399	p7g3	hypothetical protein F22K18.300 - Arabidopsis thaliana >gi|4220540|emb
7	13	11	1400	p20a4	(AJ278332) 12-oxophytodienoate reductase 3 [Lycopersicon esculentum
2	7	9	1401	pNCED	NCED cDNA
7	13	12	1402	pAbAO	Abscisic aldehyde Oxidase
2	7	8	1403	pVvTTG G2	pVvTTG G2
7	13	13	1404	pVvTTGlike B1	pVvTTGlike B1
6	7	13	1405	pVvP5CS	pyrroline-5carboxylate synthetase Genbank No. AJ0056865
3	13	8	1406	pVvTL1	thaumatin-like protein Genbank No. AF003007
6	7	12	1407	pVvPR-4A	VVPR-4A cDNA PR-4 type protein Genbank No. AF061329
3	13	9	1408	pHTPR12A	flavonoid-3'-hydroxylase
6	7	11	1409	pHTPR2C	SAM transferase
3	13	10	1410	pHTPR7C	chalcone isomerase
6	7	10	1411	pHTPR8C	Unknown
3	13	11	1412	pPRL-7	Prl-7 cDNA
6	7	9	1413	pPRL-4	Prl-4 cDNA
3	13	12	1414	pPRL-13	Prl-13 cDNA
6	7	8	1415	pPRL-5	Prl-5 cDNA
3	13	13	1416	pGlg-19	PR2-type basic glucanase (VvGlua) Accession No. U68144
1	7	13	1417	pGlg-20	PR2-type basic glucanase (VvGlub) Accession No. AF053750
8	13	8	1418	pGlg-32	PR2-type glucanase (VvGluc) Accession No. U73709
1	7	12	1419	pGLC-5	chitinase (VvChi1a) Accession No. Z54234
8	13	9	1420	pGLC-32	PR3-type ClassI basic chitinase (VvChi1b) Accession No. AF053341
1	7	11	1421	pVvChit3	PR3-type ClassIII basic chitinase (VvChi3) Accession No. Z68123
8	13	10	1422	pVvOsmo-1	PR5-type Thaumatin-like protein (VvTL2) Accession No. Y109920
1	7	10	1423	pMlo-L5	Barley Mlo homolog
8	13	11	1424	pL8	14-3-3 Like protein
1	7	9	1425	pMig-3	PREG-like protein Accession No. AF051226
8	13	12	1426	pMig-5	ACC oxidase Accession No. Q08507
1	7	8	1427	pMig-8	proton-pump interactor Accession No. AE001032
8	13	13	1428	pMig-11	translation initation factor Accession No. P24922
5	7	13	1429	pStSy	Stilbene synthase
4	13	8	1430	p1F-15	Germin-like gene (VvGLP1)

Block	Row	Column	ID	Name	Description
5	7	12	1431	p2Fb-5	Germin-like gene (VvGLP2)
4	13	9	1432	p3F-12	Germin-like gene (VvGLP3)
5	7	11	1433	p1F-7	Germin-like gene (VvGLP4)
4	13	10	1434	pHsp70E6	Heat shock ptn 71
5	7	10	1435	pHsp70A1	Heat shock ptn 70
4	13	11	1436	pHsp70A4	Heat shock ptn 70
5	7	9	1437	pMig-10	Heat shock ptn 70
4	13	12	1438	pHsc18F5	Heat shock ptn 18kd
5	7	8	1439	pHsp18M1	Heat shock ptn 18kd
4	13	13	1440	pG21	Grip 21 (11A1)
4	7	7	1441	pG13	Grip 13 (25a1)
5	12	1	1442	pG55	Grip 55 (29A)
4	7	6	1443	pG58	Grip58 (46B)
5	12	2	1444	pG61	Grip 61 (17C)
4	7	5	1445	pG32	Grip 32 (21A1)
5	12	3	1446	pSuc11	vvSuc11 (1/1B21)
4	7	4	1447	pSuc12	VvSuc12 (1/2 2P1A)
5	12	4	1448	pPL	Pectate lyase (PEC10-1-T7)
4	7	3	1449	pGst	Gst
5	12	5	1450	pPec61	Glycine rich (PEC6-1)
4	7	2	1451	pExp1	Expansin 1 (Exp1-5)
5	12	6	1452	pExp2	Expansin2 (p6-2-6)E10
8	7	7	1453	pExp3	Expansin 3 (Exp3-4)
1	12	1	1454	pExp4	Expansin 4 (Exp4-3)
8	7	6	1455	pExp6	Expansin6 (C30L1)E7
1	12	2	1456	pVvMADS1	pVvMADS1
8	7	5	1457	pVvMADS2	pVvMADS2
1	12	3	1458	pVvMADS3	pVvMADS3
8	7	4	1459	pVvLFY1	pVvLFY1
1	12	4	1460	pVvTFL1	pVvTFL1
8	7	3	1461	pVvGAI1	pVvGAI1
1	12	5	1462	pVvGA20	pVvGA20
8	7	2	1463	pVvMYB1	pVvMYB1
1	12	6	1464	pVvMYB2	pVvMYB2
3	7	7	1465	pcontrol1	B.thuringiensis cry1Ac, U89872
6	12	1	1466	pcontrol2	Phophinothricin acetyl transferase X17220
3	7	6	1467	pcontrol3	Green Fluorescent protein, AF078810
6	12	2	1468	pcontrol4	Globin, NM_000518
3	7	5	1469	pcontrol5	Beta-glucuronidase (uidA), A00196
6	12	3	1470	pcontrol6	Hydromycin, K01193
3	7	4	1471	pcontrol7	Luciferase, X65316
6	12	4	1472	pcontrol8	Kanamycin, V00618
3	7	3	1473	pcontrol9	B-cell receptor, AF126021
6	12	5	1474	pcontrol10	Insert 250bp PCR fragment from Ndo DNA using IW3D12/IW5C4
3	7	2	1475	pcontrol11	Insulin-like growth factor
6	12	6	1476	pcontrol12	Myosin heavy chain, X13988